
**Proceedings for the 25th Annual Conference
of the Society for Astronomical Sciences**



Symposium on Telescope Science

Editors:
Brian D. Warner
Jerry Foote
David A. Kenyon
Dale Mais

May 23-25, 2006
Northwoods Resort, Big Bear Lake, CA

Reprints of Papers

Distribution of reprints of papers by any author of a given paper, either before or after the publication of the proceedings is allowed under the following guidelines.

1. Papers published in these proceedings are the property of SAS, which becomes the exclusive copyright holder upon acceptance of the paper for publication.
2. Any reprint must clearly carry the copyright notice and publication information for the proceedings.
3. The reprint must appear in full. It may not be distributed in part.
4. The distribution to a third party is for the sole private use of that person.
5. Under NO circumstances may any part or the whole of the reprint be published or redistributed without express written permission of the Society for Astronomical Sciences. This includes, but is not limited to, posting on the web or inclusion in an article, promotional material, or commercial advertisement distributed by any means.
6. Limited excerpts may be used in a review of the reprint as long as the inclusion of the excerpts is NOT used to make or imply an endorsement of any product or service.
7. Under no circumstances may anyone other than the author of a paper distribute a reprint without the express written permission of all authors of the paper and the Society for Astronomical Sciences.

Photocopying

Single photocopies of single articles may be made for personal use as allowed under national copyright laws. Permission of SAS and payment of a fee are required for all other photocopying.

Disclaimer

The acceptance of a paper for the SAS proceedings can not be used to imply or infer an endorsement by the Society for Astronomical Sciences of any product or method mentioned in the paper.

© 2006 Society for Astronomical Sciences, Inc.
All Rights Reserved

Published by the Society for Astronomical Sciences, Inc.

First printed: May 2006

ISBN: 0-9714693-5-0

Table of Contents

PREFACE	7
CONFERENCE SPONSORS	9
<i>Submitted Papers</i>	<i>11</i>
SINGLE CHANNEL UBV AND JH BAND PHOTOMETRY OF EPSILON AURIGAE <i>JEFFREY L. HOPKINS, ROBERT E. STENCEL</i>	13
LONG-PERIOD ECLIPSING BINARY SYSTEM EPSILON AURIGAE ECLIPSE CAMPAIGN <i>GENE A. LUCAS, JEFFREY L. HOPKINS, ROBERT E. STENCEL</i>	25
THREE YEARS OF MIRA VARIABLE PHOTOMETRY: WHAT HAS BEEN LEARNED? <i>DALE E. MAIS, DAVID RICHARDS, ROBERT E. STENCEL</i>	31
UNC-CHAPEL HILL'S GAMMA-RAY BURST FOLLOW-UP PROGRAMS <i>DR. DANIEL E. REICHART</i>	39
THE INTERNATIONAL VARIABLE STAR INDEX (VSX) <i>CHRISTOPHER L. WATSON, ARNE A. HENDEN, AARON PRICE</i>	47
CCD PHOTOMETRY FROM A SMALL OBSERVATORY IN A LARGE CITY <i>JENNIE MCCORMICK</i>	57
FAINT CV MONITORING AT CBA PRETORIA <i>L. A. G. BERTO MONARD</i>	63
CLEANING UP THE GCVS ECLIPSING BINARY LISTINGS: STRATEGIES AND TOOLS TO MAXIMIZE SUCCESS <i>TOM KRAJCI</i>	71
THE DETECTION OF THE WZ SGE-TYPE NATURE OF THE DWARF NOVAE ASAS 023322-1047.0 AND ASAS 102522-1542.4 BY THE CENTER FOR BACKYARD ASTROPHYSICS <i>TONNY VANMUNSTER, TOM KRAJCI, BERTO MONARD, LEWIS M. COOK, PIERRE DE PONTIÈRE, DAVID BOYD, TIM R. CRAWFORD, MICHAEL J. ARMSTRONG, DIEGO RODRIGUEZ</i>	77
A COMPACT, OFF-THE-SHELF, LOW-COST DUAL CHANNEL PHOTOMETER <i>THOMAS C. SMITH, RUSSELL M. GENET, CHRISTINE L. HEATHER</i>	87
EXTRASOLAR PLANETS AND THE RACE TO UNCOVER THE FIRST HABITABLE TERRESTRIAL PLANET <i>AARON WOLF, GREGORY LAUGHLIN</i>	91

DETECTING EXOPLANETS BY GRAVITATIONAL MICROLENSING USING A SMALL TELESCOPE <i>GRANT CHRISTIE</i>	97
SINGLE CHANNEL UBV PHOTOMETRY OF LONG PERIOD ECLIPSING BINARY VV CEPHEI <i>JEFFREY L. HOPKINS, PHILIP D. BENNETT</i>	105
COLLABORATIVE RESEARCH OPPORTUNITIES WITH THE GLOBAL NETWORK OF ASTRONOMICAL TELESCOPES (GNAT): VARIABLE STAR RESEARCH <i>E.R. CRAINE, R.A. TUCKER, A.L. KRAUS, R.B. CULVER, M.S. GIAMPAPA</i>	111
RECENT ASTEROID LIGHTCURVE STUDIES AT THE PALMER DIVIDE OBSERVATORY <i>BRIAN D. WARNER</i>	117
FOLLOW-UP DATA FOR LARGE PHOTOMETRIC SURVEYS <i>MIKKO KAASALAINEN</i>	125
MONITORING CHANGES IN ECLIPSING BINARY ORBITS <i>LEE F. SNYDER, JOHN LAPHAM</i>	129
ANALYSIS OF GSC 2475-1587 AND GSC 841-277: TWO ECLIPSING BINARY STARS FOUND DURING ASTEROID LIGHTCURVE OBSERVATIONS <i>ROBERT D. STEPHENS, BRIAN D. WARNER</i>	141
SWITCHING TO INFRARED! A NEW METHOD FOR NON-PROFESSIONAL IMAGING IN THE MID-IR <i>THOMAS G. KAYE</i>	151
GROUND IMAGING FOR SOLAR SAIL ORBIT DETERMINATION: A PROOF OF CONCEPT <i>JOHN E. HOOT, MARK S. WHORTON</i>	157
<i>Abstracts Only</i>	<i>166</i>
SUPERHUMPS IN CATAclysmic VARIABLES <i>JOE PATTERSON</i>	168
ARECIBO AND GOLDSTONE RADAR IMAGING OF NEAR-EARTH AND MAIN-BELT ASTEROIDS IN 2005 <i>LANCE A. M. BENNER</i>	169
RADAR IMAGES AND SHAPE MODELS OF ASTEROIDS 10115 (1992 SK), 23187 (2000 PN9), AND 29075 (1950 DA) <i>M.W. BUSCH, S.J. OSTRO, L.A.M BENNER, J.D. GIORGINI</i>	170

Poster Papers **172**

THE DISCOVERY AND INITIAL CHARACTERIZATION OF A NEW ECLIPSING BINARY WITH PECULIAR PROPERTIES <i>DALE E. MAIS, DAVID RICHARDS</i>	174
AN AMATEUR ASTRONOMER'S GROWTH INTO SCIENCE <i>CINDY FOOTE</i>	180
SERENDIPITOUS DISCOVERY OF VARIABLE STARS WHILE GATHERING ASTEROID LIGHTCURVES <i>BOB BUCHHEIM</i>	184
OBSERVING VISUAL DOUBLE STARS WITH A CCD CAMERA AT THE PALMER DIVIDE OBSERVATORY <i>BRIAN D. WARNER</i>	188
MAGNET LOADER FOR SCHMIDT-CASSEGRAIN MIRROR FLOP REDUCTION <i>GARY A. VANDER HAAGEN</i>	192

Preface

It's said that "time flies when you're having fun." It seems not that long ago that the Symposium on Telescope Science started. This year we reach the milestone of our Silver Anniversary, 25 years. So long and yet so soon. It must mean we're having LOTS of fun.

Things certainly have changed during our first quarter century, except maybe some of Lee Snyder's jokes. Some things never change – nor should they. We've gone from photometry using Photomultiplier Tubes (PMT) to CCD cameras and, as a review of these proceedings shows, back a little to PMT work. Automated telescopes were a dream. Now they are common. What an astronomer can do with his modest backyard telescope and CCD camera under good conditions rivals and even surpasses what the 200-inch at Palomar did with film during its halcyon days.

The Symposium has been under the auspices of different groups and flags in its time, but is now guided, as it has been since 2003, by the steady hands of the Society for Astronomical Sciences. SAS, as it's known for short, is a non-profit corporation exempt under I.R.S. Code Section 501(c)(3).

The Symposium has been held in Southern California since 1982 but it wasn't always in its current home in Big Bear Lake, California. Previously it's been held in other locations, including Lake Arrowhead. The timing and location of the meeting is not by chance. It's meant to be a lead-in to one of the biggest star parties in the world, the annual RTMC Astronomy Expo, held just "up the road" the weekend following the Symposium. After nearly a week of cameras, and telescopes, and stars (Oh! My!), those wanting their fill of astronomy leave more than satisfied.

Through the three days of the Symposium on Telescope Science, the Society hopes to foster new friendships and new collaborations among amateur and professional astronomers. Our goals are the personal scientific advancement of Society members, the development of the amateur-professional community, and promoting research that increases our understanding of the Universe.

It takes many people to have a successful conference, starting with the Conference Committee. This year the committee members are:

Lee Snyder	Robert Stephens
Robert Gill	Dave Kenyon
Dale Mais	Brian D. Warner
Jerry Foote	

There are many others involved in a successful conference. The editors take time to note the many volunteers who put in considerable time and resources. We also thank the staff and management of the Northwoods Resort in Big Bear Lake, CA, for their efforts at accommodating the Society and our activities.

Membership dues alone do not cover the costs of the Society and annual conference. We owe a great debt of gratitude to our corporate sponsors: Sky and Telescope, Software Bisque, Santa Barbara Instruments Group, and Apogee Instruments, Inc.

Finally, there would be no conference without our speakers and poster presenters. We thank them for making the time to prepare and present the results of their research.

Brian D. Warner
 Jerry Foote
 Dale Mais
 Dave Kenyon

Conference Sponsors

The conference organizers thank the following companies for their significant contributions and financial support. Without them, this conference would not be possible.



Apogee Instruments, Inc.

Manufactures of astronomical and scientific imaging cameras

<http://www.ccd.com>



Santa Barbara Instruments Group

Makers of astronomical instrumentation

<http://www.sbig.com>



Sky Publishing Corporation

Publishers of Sky and Telescope Magazine

<http://skyandtelescope.com>



Software Bisque

Developers of TheSky Astronomy Software and the Paramount Telescope Mount

<http://www.bisque.com>

Submitted Papers

Single Channel UBV and JH Band Photometry of Epsilon Aurigae

*Jeffrey L. Hopkins
Hopkins Phoenix Observatory
7812 West Clayton Drive
Phoenix, Arizona 85033-2439
phxjeff@hposoft.com*

*Robert E. Stencel
University of Denver
Denver, Colorado
rstencel@du.edu*

Abstract

Epsilon Aurigae is the longest known eclipsing binary star system, with a 27.1 year period. The next eclipse begins in 2009. While many observatories make observations during the eclipse, few have maintained an observing program between eclipses. As seen with the last eclipse, there are some very interesting pre- and post-eclipse light variations. There is evidence for periodic variations between eclipses, possibly pulsations of the primary F star. The Hopkins Phoenix Observatory made single channel UBV photon counting observations during the last eclipse and for several years thereafter. In 2003 a concentrated observing effort was resumed and recently infrared bands J and H have been added. The intent of these observations is to provide out-of-eclipse data on the system in preparation for the 2009–2011 eclipse. This paper will summarize current activity, present out-of-eclipse data, and provide analysis of the data. © 2006 Society for Astronomical Sciences.

1. Introduction

The Hopkins Phoenix Observatory has been observing Epsilon Aurigae in the UBV bands since early 1982 including detailed coverage during the 1982-1984 eclipse [1]. Observations continued through 1988 and resumed in the fall of 2003 [2]. At the end of 2005 infrared bands J and H were added to the observing program. This work complements new spectroscopy and space infrared observations now underway, to be reported elsewhere.

1.1. Epsilon Aurigae (HR1605)

Epsilon Aurigae ($V_{\max} = 2.99$) is the longest period eclipsing binary known with a period of 27.1 years. The next eclipse is due in 2009. The exact na-

ture of this system is still not fully resolved. With such a long period the actual eclipse would be expected to be short, but is just the opposite – lasting nearly 2 years. This means the eclipsing body is gigantic – by some estimates more than 2,000 solar radii, making it a contender for the largest object known. What is even more intriguing is that during the middle of the eclipse there is an eclipse brightening. There appears to be a hole in the center of this object. To add to the mystery the secondary object does not appear to have a spectrum of its own. Only the primary star's spectrum can be seen. During the eclipse the system's light is reduced the same at all wavelengths. It is as if there is a giant neutral density filter with a hole in the middle passing in front of the primary star.

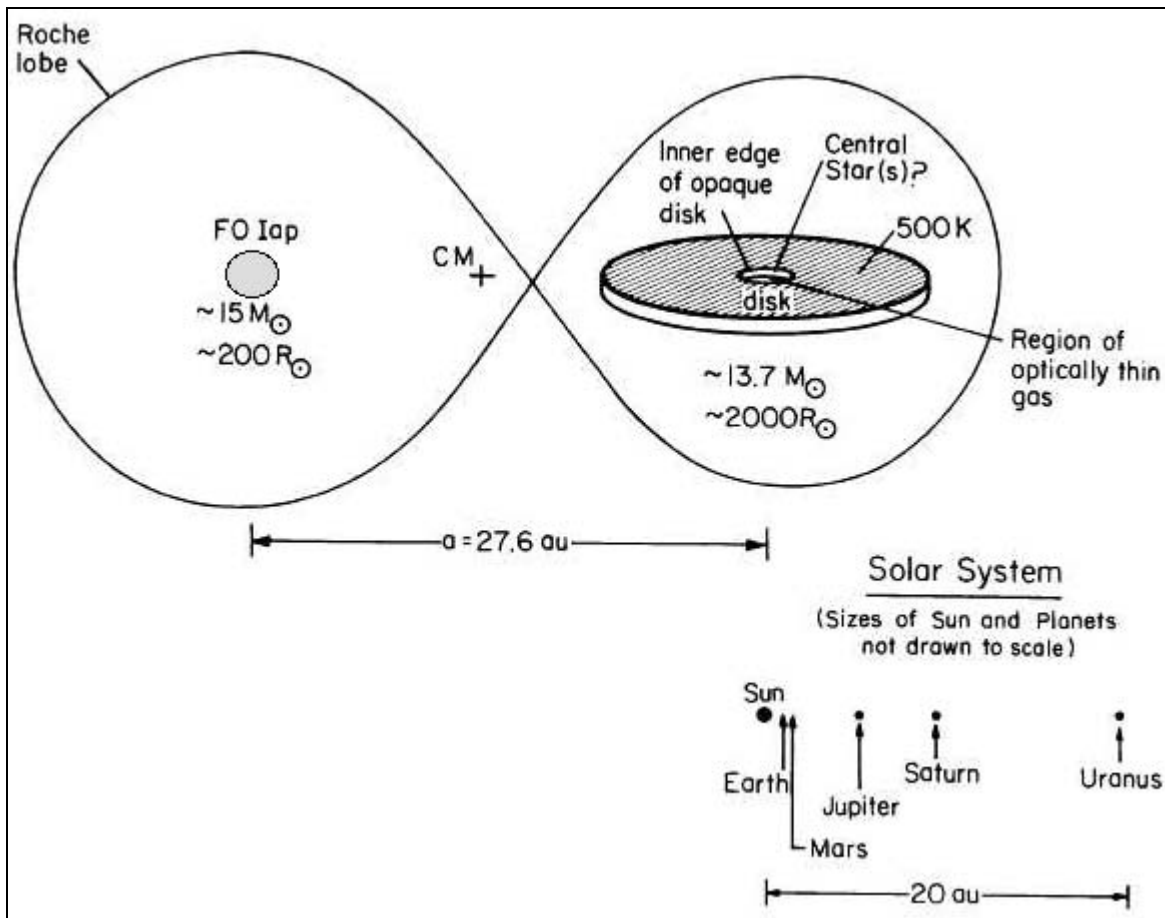


Figure 1 Epsilon Aurigae System Schematic (Carroll et. al.1991 Ap. J. 367: 278)

2. Hopkins Phoenix Observatory Photometry Equipment

2.1. UBV Photometry Equipment

The UBV photometry used an HPO photon counting photometer with a 1P21 photomultiplier tube with standard filters and 8" Celestron Schmidt Cassegrain C-8 telescope. For improved tracking the C-8 has been adapted to a Meade LX-90 fork mount. In the fall of 2004 a Meade 8" LX-90 was to replace the C-8. It was discovered that the LX-90 OTA produced 50% fewer counts in the U band than the C-8. Since the C-8 OTA is fine, it was decided to just adapt it to the newer LX-90 mount. The system has been calibrated using standard stars.

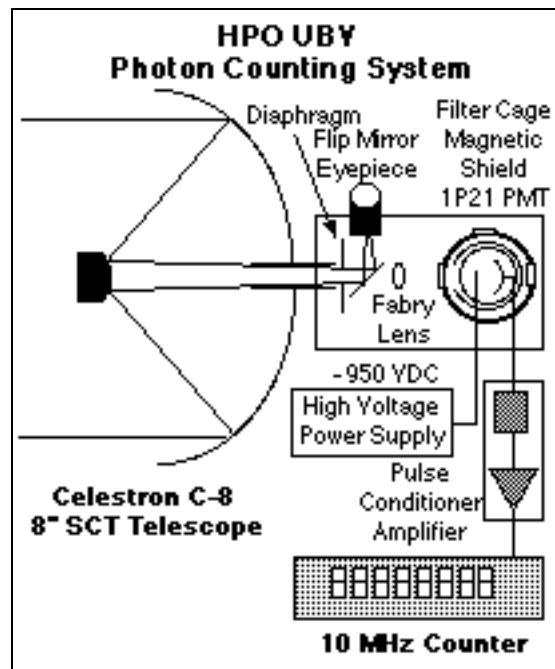


Figure 2. HPO UBV Photon Counting System



Figure 3. HPO UBV Equipment

tor is -40 degrees. The photometer is mounted on a Meade 12" LX200GPS telescope (see Figure 6). The system is auto guided with an Orion 80 mm f/11.4 guide telescope attached to the LX200 and uses a Meade Deep Sky Imager Pro CCD camera and AutoStar software for the guiding. Because of the small detector area, precise centering of the star is essential for consistent readings. It was found near impossible to do without the auto guiding. If continued observational data do not provide a better data spread, the 0.3 mm detector may need to be replaced with the large 1.0 mm detector.

Filter Specifications:

J Band - Central Wavelength 1250 nm

FWHM 200 nm

H Band - Central Wavelength 1650 nm

FWHM 300 nm

Photodiode Specification:

Hamamatsu G5851-203 PIN Diode

Active area 0.3 mm with two-stage thermoelectric cooler (maximum cooling to -40 degrees F)

Spectral sensitivity: 1000 nm to 2100 nm, peaking at about 1900 nm.



Figure 4. UBV Equipment Detail

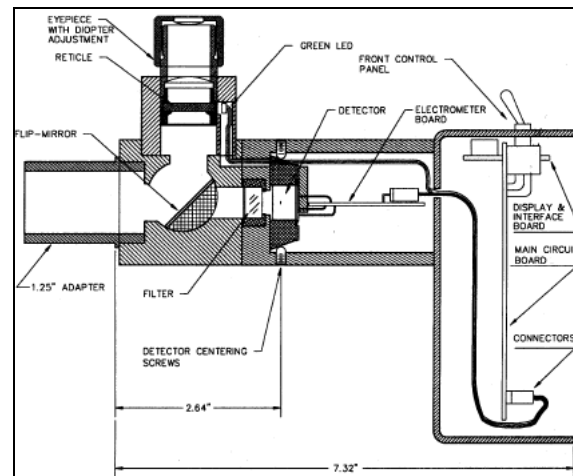


Figure 5. SSP-4 Cross-sectional View

2. 2. JH Photometry Equipment

JH photometry was done using an Optec SSP-4 (see Figure 5) solid state photometer with a 0.3 mm InGaAs 2-stage thermoelectric cooled photodiode detector. Normal operating temperature for the detec-

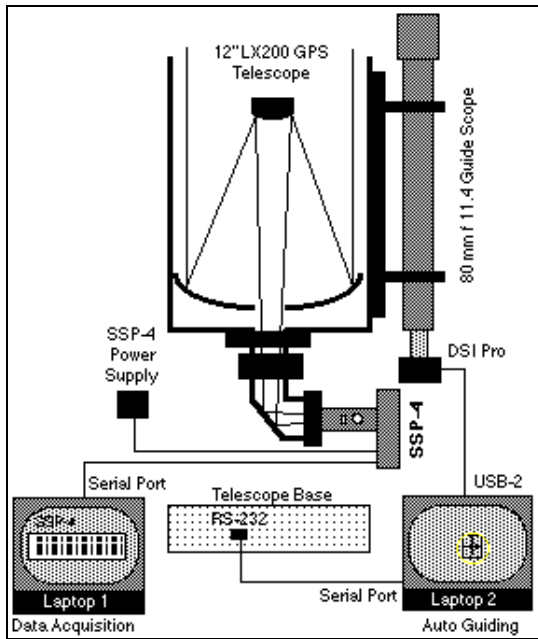


Figure 6. HPO JH Band Photometry System Block Diagram



Figure 7. HPO JH Equipment



Figure 8. JH Equipment Detail

3. Hopkins Phoenix Observatory Observations

While the Hopkins Phoenix Observatory has been observing Epsilon Aurigae in the UBV bands since the early 1980's including through the last eclipse, infrared J and H band observations have only been recently added to the program due to the availability of the Optec SSP-4.

Typical observations of a star, which include both the UBV and JH band observations, consisted of 3-10 second readings of each star (star + sky) in each band followed by 1-10 second reading of the sky adjacent to the star in each band. Because of the poor signal-to-noise ratio in the JH bands, 3-10 second readings of the sky in each filter were done instead of the single sky reading as with the UBV photometry. A gain of 100 was used for the JH readings.

All observations were made using differential photometry with the sequence of comparison, program, comparison, program, comparison and comparison star as the last star measured. Initial data reduction adjusted for dead time for the photon counting data, for counts per second and adjusted to unity gain for the J and H band data.

A database program developed with FileMaker Pro was used to reduce and archive the data.

Data reduction procedure consisted of:

1. Three consecutive 10-second star observations for each band entered.
2. Corresponding sky data entered.
3. Data averaged.
4. Sky readings subtracted.
5. This constitutes one set of readings for each star.
6. Comparison star has 4 sets.
7. Program star has 3 sets.
8. Air mass of each the observations was calculated.
9. The air mass for the middle observation was used as the air mass for the final data point. Data were then transferred into another part of the database program, converted to magnitude data and adjusted for extinction and color coefficients.
10. Three differential readings were then calculated referenced to the comparison star.
11. Three resulting values for each band were then averaged and a standard deviation determined as an indication of the data spread.

The results were then normalized to the comparison star's published value. The resulting reduced data were then archived.

Typical UBV data have standard deviations of better than 0.01 magnitudes and often approach 0.001 magnitudes and better. The J and H band data have a

less favorable signal to noise ratio and typical standard deviations are 0.2 magnitudes.

Observing seasons for Epsilon Aurigae at the latitude of the Hopkins Phoenix Observatory (33 degrees north) begins late summer and runs through April. However, because of the weather extreme in the summer in Phoenix, Arizona, summer observations are limited due both to seasonal storm activity and observatory temperatures that can exceed 100 degrees F at midnight.

3.1. Sample Data

A complete set of UBV data from the fall of 2003 through the current season as well as 1980's data is available from HPO. Recent JH infrared and corresponding temporal UBV data for 2006 are shown in Tables 1 and 2.

The comparison star used for both UBV and JH data was Lambda Aurigae (HR1729). Lambda Aurigae magnitudes used were:

$$\begin{aligned} U &= 5.46 & J &= 3.62 \\ B &= 5.34 & H &= 3.33 \\ V &= 4.71 \end{aligned}$$

HPO JH Infrared Data

JD	X	J	#	SD	H	#	SD	(J - H)
March 2006								
2453811.66	1.3489	1.777	3	0.040	1.525	3	0.139	0.253
2453808.62	1.1519	1.728	3	0.044	1.403	3	0.055	0.325
2453807.62	1.1626	1.921	2	0.074	1.524	2	0.140	0.397
2453802.59	1.0394	1.830	3	0.267	1.399	3	0.502	0.430
2453799.59	1.0339	1.695	3	0.234	1.279	3	0.345	0.416
2453798.61	1.0479	1.909	3	0.204	1.601	3	0.347	0.307
2453797.59	1.0314	1.858	3	0.169	1.222	3	0.289	0.636
February 2006								
2453790.59	1.0189	1.719	3	0.145	1.301	3	0.225	0.418
2453788.59	1.0171	1.824	3	0.099	1.572	3	0.120	0.251
2453786.59	1.0167	1.826	3	0.010	1.420	3	0.086	0.406
2453784.65	1.0574	1.895	3	0.032	1.597	3	0.139	0.297
2453781.62	1.0218	1.632	3	0.103	1.109	3	0.051	0.523
2453780.58	1.0217	1.983	3	0.352	1.790	3	0.033	0.193
2453779.62	1.0196	1.886	3	0.012	1.762	3	0.108	0.124
2453777.62	1.0189	1.740	3	0.375	1.432	3	0.921	0.307
January 2006								
2453767.68	1.0327	1.850	3	0.023	1.565	3	0.042	0.285
2453766.65	1.0168	1.770	3	0.140	1.356	3	0.253	0.414
2453763.67	1.0243	1.832	3	0.122	1.483	3	0.156	0.349
2453759.63	1.0288	1.853	3	0.021	1.409	3	0.095	0.443
2453758.67	1.0187	1.883	3	0.093	1.615	3	0.155	0.238
2453756.68	1.0193	1.783	3	0.024	1.443	3	0.097	0.340
2453742.70	1.0202	1.705	1		1.476	1		0.228
2453741.70	1.0173	1.843	3	0.377	1.526	3	0.737	0.317
December 2005								
2453734.60	1.2297	1.760	3	0.062	1.483	3	0.286	0.277

Table 1 Epsilon Aurigae JH Band Photometric Data

HPO UBV Data

JD	X	V	#	SD	B	#	SD	U	#	SD	B - V	U - B
March 2006												
2453818.63	1.2055	3.011	3	0.004	3.590	3	0.007	3.712	3	0.007	0.579	0.122
2453815.61	1.1206	3.009	3	0.002	3.581	3	0.002	3.697	3	0.005	0.572	0.116
2453813.61	1.1026	3.013	3	0.001	3.582	3	0.002	3.700	3	0.005	0.570	0.118
2453812.62	1.1059	3.005	3	0.005	3.575	3	0.002	3.693	3	0.004	0.570	0.118
2453811.63	1.1376	3.005	3	0.004	3.572	3	0.005	3.692	3	0.004	0.566	0.121
2453810.72	1.6232	3.004	3	0.002	3.588	3	0.005	3.662	3	0.010	0.584	0.075
2453808.61	1.0665	3.014	3	0.003	3.588	3	0.005	3.705	3	0.003	0.575	0.116
2453807.60	1.0579	3.015	3	0.003	3.579	3	0.004	3.701	3	0.007	0.565	0.122
2453802.64	1.1006	3.025	3	0.003	3.587	3	0.007	3.703	3	0.006	0.562	0.116
2453799.65	1.1156	3.023	3	0.004	3.596	3	0.003	3.717	3	0.001	0.574	0.121
2453798.65	1.1026	3.029	3	0.004	3.609	3	0.012	3.720	3	0.008	0.579	0.111
2453797.64	1.0811	3.026	3	0.016	3.595	3	0.021	3.691	3	0.049	0.569	0.097
February 2006												
2453791.68	1.1289	3.045	3	0.003	3.638	3	0.004	3.748	3	0.010	0.583	0.120
2453790.64	1.0511	3.047	3	0.008	3.618	3	0.005	3.757	3	0.009	0.571	0.139
2453788.63	1.0331	3.060	3	0.003	3.633	3	0.005	3.763	3	0.005	0.573	0.130
2453786.63	1.0232	3.067	3	0.002	3.647	3	0.001	3.786	3	0.004	0.580	0.139
2453784.71	1.1682	3.077	3	0.007	3.651	3	0.001	3.784	3	0.005	0.575	0.133
2453781.67	1.0536	3.089	3	0.001	3.669	3	0.005	3.812	3	0.007	0.580	0.143
2453780.63	1.0196	3.083	3	0.006	3.653	3	0.009	3.801	3	0.010	0.570	0.148
2453779.68	1.0578	3.092	3	0.007	3.670	3	0.004	3.810	3	0.006	0.578	0.140
2453777.69	1.0644	3.061	3	0.002	3.672	3	0.004	3.798	3	0.009	0.581	.126
January 2006												
2453767.66	1.0165	3.086	3	0.002	3.658	3	0.003	3.788	3	0.004	0.572	0.130
2453766.72	1.0760	3.082	3	0.004	3.652	3	0.011	3.778	3	0.003	0.570	0.126
2453763.72	1.0568	3.061	3	0.005	3.603	3	0.006	3.743	3	0.013	0.542	0.140
2453758.73	1.0433	3.057	3	0.002	3.611	3	0.003	3.729	3	0.003	0.554	0.118
2453759.68	1.0167	3.070	3	0.014	3.624	3	0.012	3.745	3	0.014	0.554	0.121
2453757.72	1.0358	3.060	3	0.007	3.617	3	0.006	3.725	3	0.003	0.557	0.108
2453756.74	1.0553	3.043	3	0.005	3.598	3	0.008	3.707	3	0.001	0.555	0.109
2453752.71	1.0205	3.033	3	0.003	3.581	3	0.001	3.691	3	0.009	0.548	0.110
2453751.73	1.0276	3.020	3	0.006	3.567	3	0.010	3.673	3	0.010	0.547	0.106
2453746.72	1.0172	3.017	3	0.010	3.567	3	0.003	3.673	3	0.005	0.550	0.106
2453745.72	1.0171	3.011	3	0.003	3.558	3	0.007	3.657	3	0.008	0.547	0.099
2453744.73	1.0175	3.009	3	0.005	3.554	3	0.009	3.666	3	0.007	0.545	0.112
2453742.74	1.0214	3.018	3	0.002	3.560	3	0.002	3.662	3	0.005	0.542	0.102
2453741.69	1.0354	3.020	3	0.006	3.567	3	0.006	3.670	3	0.006	0.547	0.103
2453740.73	1.0166	3.021	3	0.002	3.568	3	0.010	3.661	3	0.003	0.547	0.093
December 2005												
2453734.73	1.0200	3.022	3	0.005	3.587	3	0.006	3.705	3	0.000	0.565	0.008

Table 2 Epsilon Aurigae UBV Band Photometric Data

3. 2. Data Plots

Plots of V data for the 2004/2005 and 2005/2006 observing seasons are shown in Figures 9 and 10 respectively.

A frequency domain plot is shown in Figure 15 using V data from the year 2003 - 2006 (as of April 2006). The plots were generated using Persano Light Curve and Period Analysis Software [4]. A major period is shown at 66.2006 days.

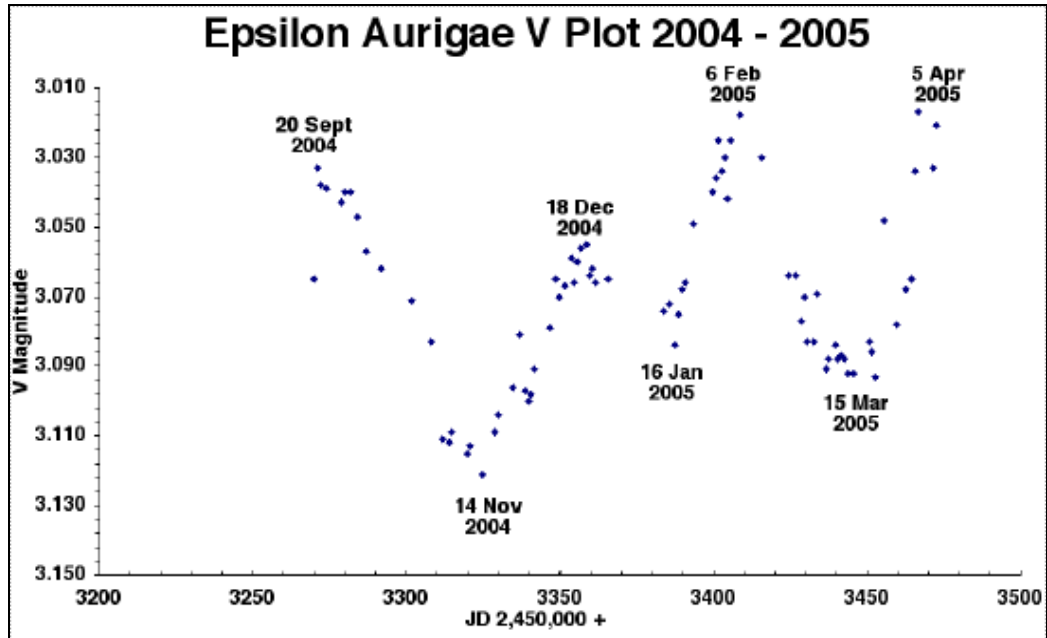


Figure 9 V Band Data Plot for the 2004 - 2005 Observing Season

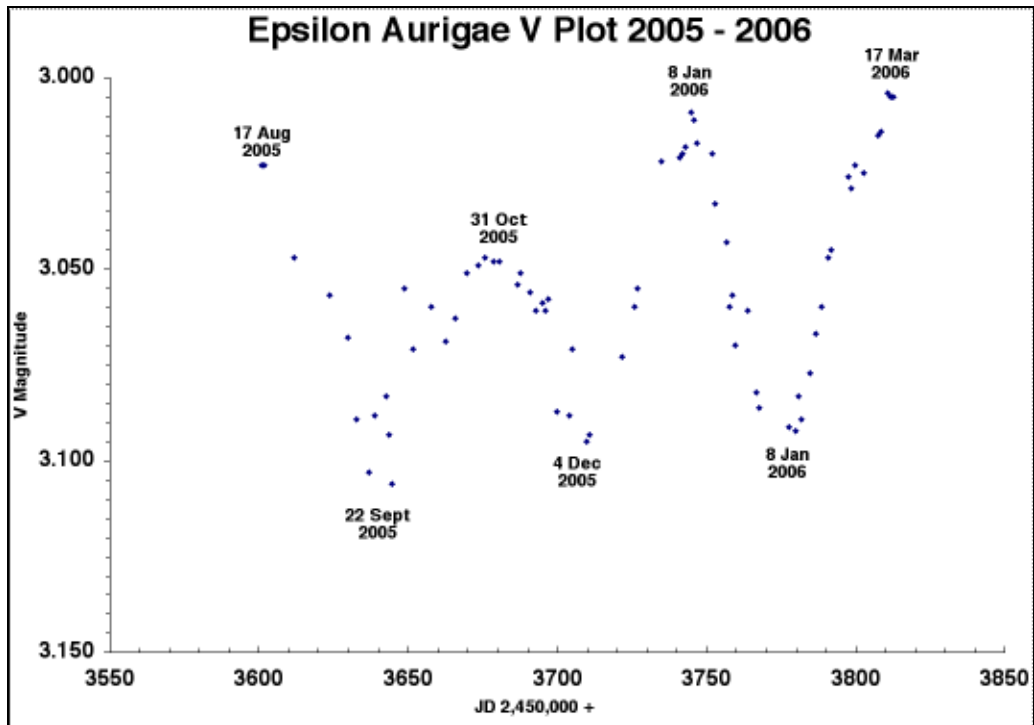


Figure 10 V Band Data Plot for the 2005 - 2006 Observing Season. A set detailed plots for V and B - V data that correspond to the recent JH data acquisition are shown in Figures 11 and 12. This covers the period JD 2,453734 through 2,453818.

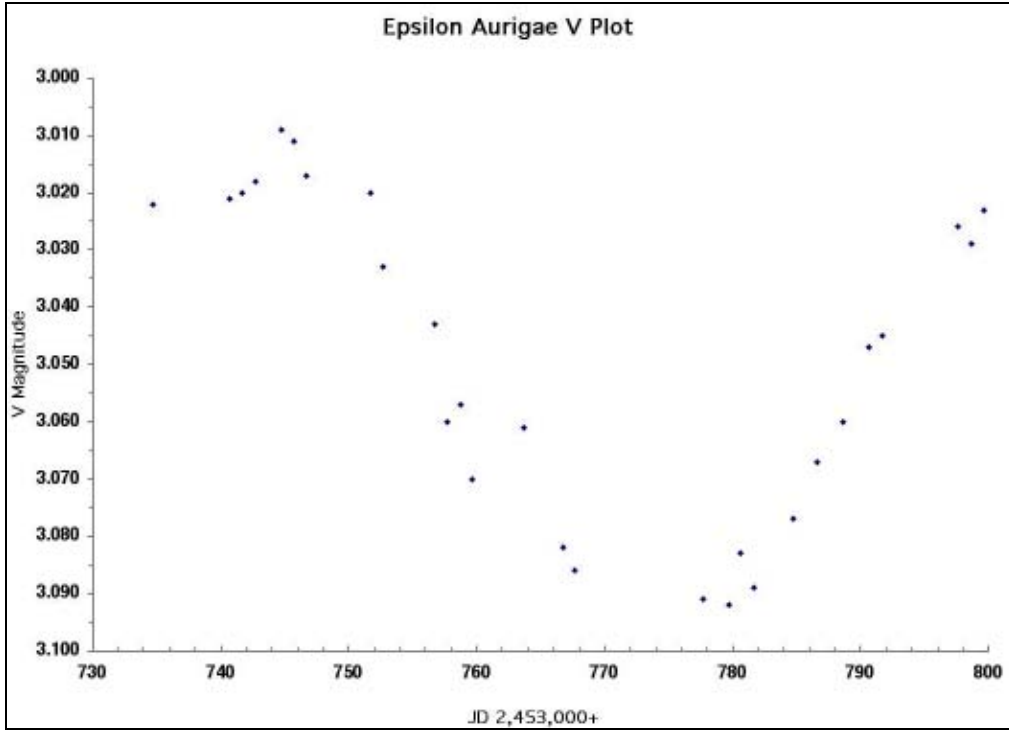


Figure 11 V Band Data Plot

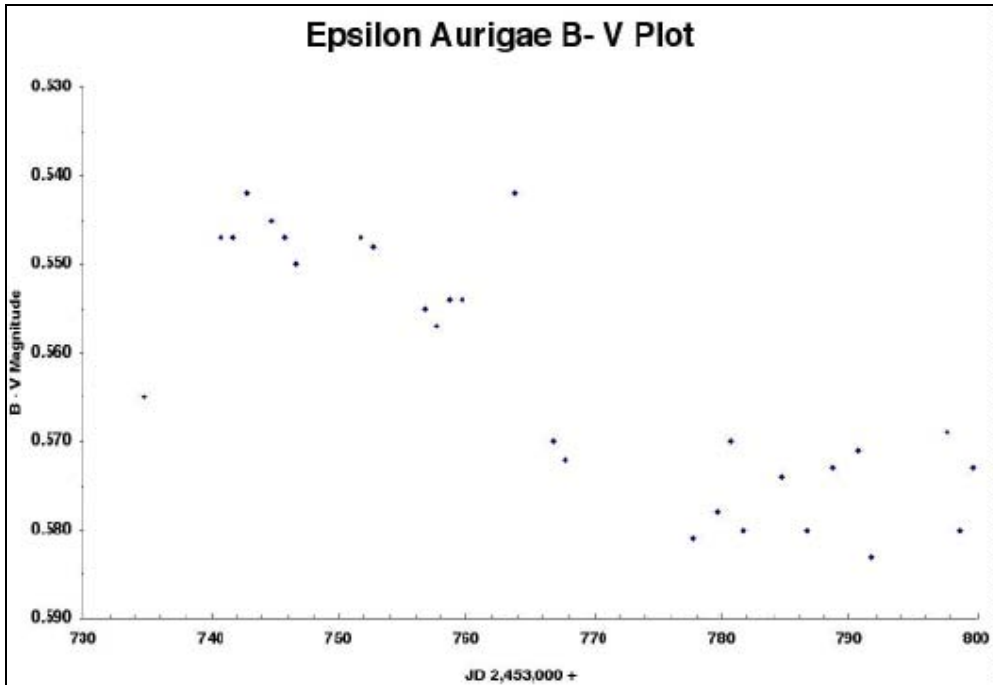


Figure 12. B- V Data Plot. A set detailed plots for JH data t shown in Figures 13 and 14. This covers the period JD 2,453734 through 2,453811.

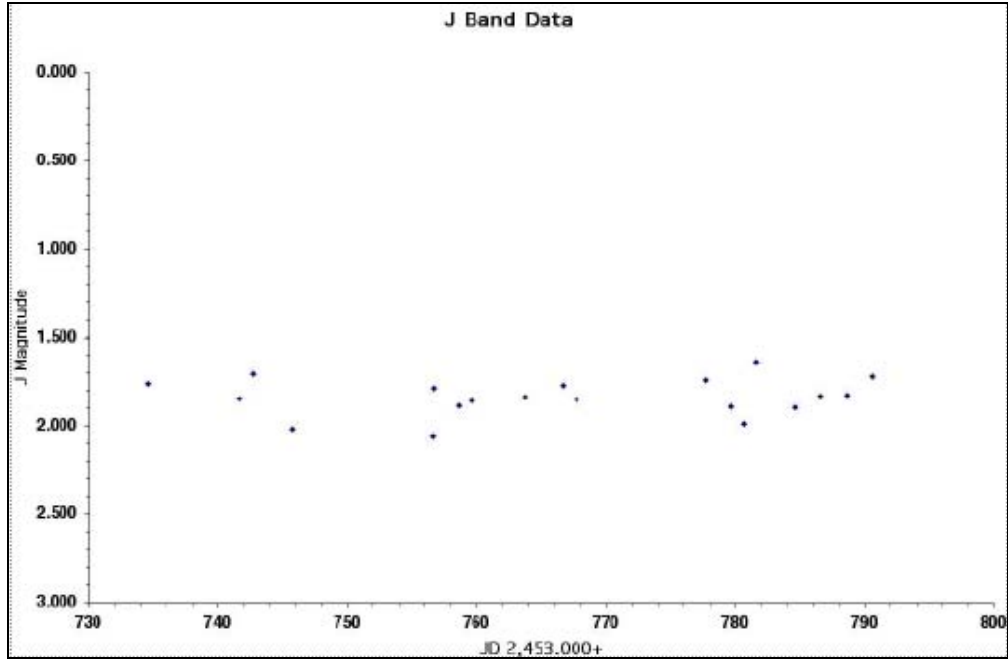


Figure 13 J Band Data Plot

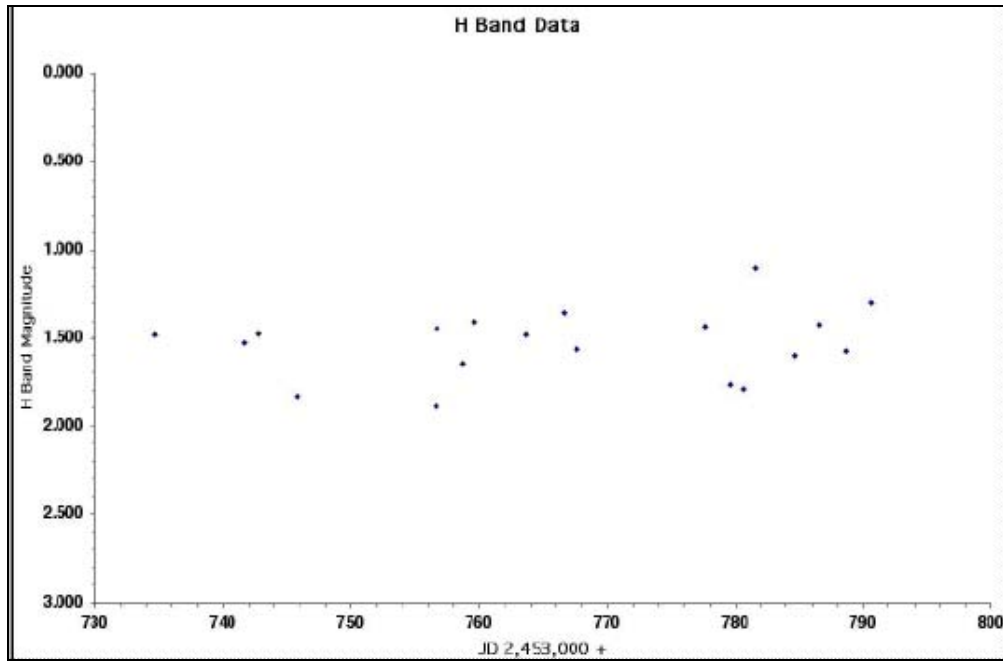


Figure 14 H Band Data Plot

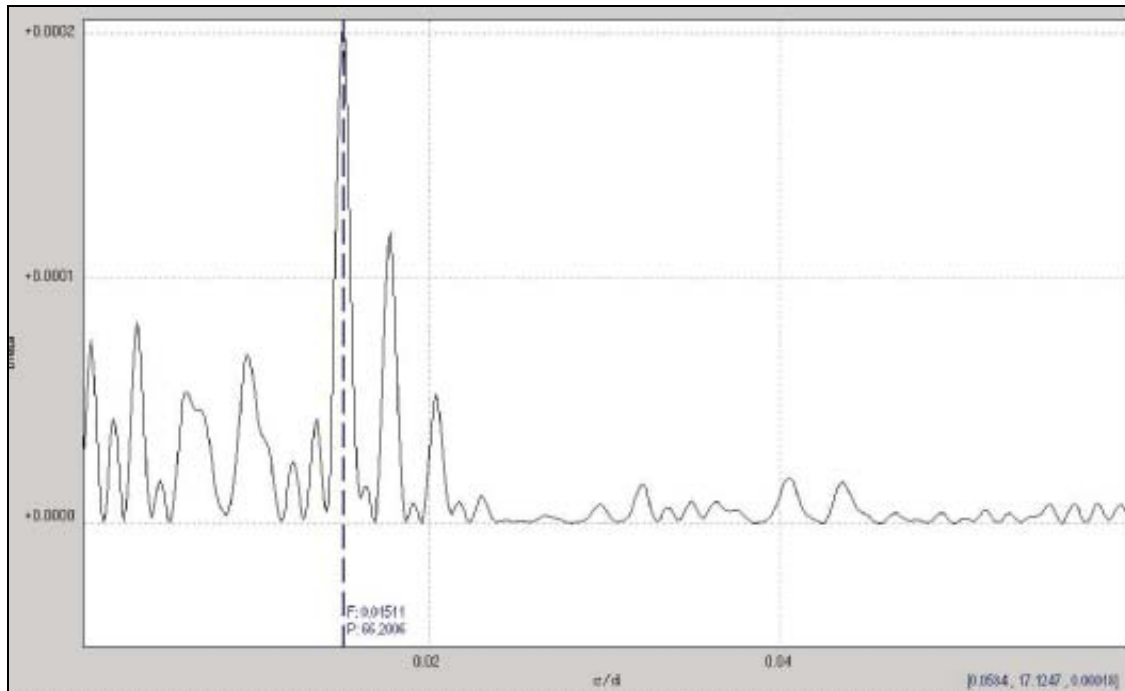


Figure 15 A Frequency Domain Plot of the V data for 2003 - 2006 * Cursor is at 66.2006 days

4. Analysis

From the photometry presented here, we can provide the following statements. The mean V magnitude was 3.05 with a variation range of 0.132 magnitude and a basic period of 66.2 days (see Figure 15). The pulsations appear to show a step like action starting lower, the next step higher and finally a highest step (see Figures 9, 10 and 11). A couple of more seasons of observations should show this in better detail.

Mean B magnitude is 3.625 with a variation of 0.175 magnitude and similar period (see Figure 12). Mean U band is 3.725 with a variation of 0.35 magnitude and similar period (see Figure 13). The B-V and U-B colors range from 0.54 to 0.58 magnitude and 0.10 to 0.14 magnitude respectively, corresponding to F8 supergiant colors [3] (see Figures 14 and 15). These colors are significantly redder than the canonical F0 I spectral type assigned Epsilon Aurigae [5] and may represent spectral evolution during the 20th century. For comparison, see the Hopkins web report for post-eclipse UB and color values [1986-88] [6].

We are fortunate to be receiving contributed data from observers following the optical spectrum [especially H-alpha, L. Schanne and D. Mais], the near infrared spectrum [MIMIR, D. Clemens and R. Stencel] and far infrared data [Spitzer infrared space telescope, R. Stencel et al]. Correlations of the strength of the hydrogen recombination emission

lines, seen in these spectra, with the optical variation will be closely studied.

5. Conclusions

Photometry will continue in the UB and V bands with IR bands to be added. Data in the JH bands will also continue with hopes of being able to get more consistent data using a larger detector with the SSP-4. Partners in monitoring the coming eclipse are welcome to join in.

6. Acknowledgments

The Hopkins Phoenix Observatory wishes to thank Dr. Stencel for his help and encouragement for this project. This research also was supported in part by an astronomy bequest from William Herschel Womble to the University of Denver.

7. References

- [1] Stencel R., ed., *The 1982- 84 Eclipse of Epsilon Aurigae*, NASA Conf. Publ. 2384, NASA, Washington, D.C. [copies available on request to rstencel@du.edu]
- [2] Hopkins, J.L., Stencel, R.E., *Out-of-Eclipse UVB Variations of epsilon Aurigae, FOIap+?*, Poster Paper [107.05], AAS Meeting January 2005.
- [3] deJager and Nieuwenhuijzen 1987 *Astron. Astrophys.* 177: 217.
- [4] <http://users.skynet.be/fa079980/peranso/index.htm>
- [5] Carroll et al. 1991 *Astrophys. J.* 367: 278.
- [6] <http://www.hposoft.com/Astro/PEP/EAur82-88.html>

Long-Period Eclipsing Binary System Epsilon Aurigae Eclipse Campaign

Gene A. Lucas
15640 East Cholla Drive
Fountain Hills, Arizona 85268
geneluca@ix.netcom.com

Jeffrey L. Hopkins
Hopkins Phoenix Observatory
7812 West Clayton drive
Phoenix, Arizona 85033-2439
phxjeff@hposoft.com

Robert E. Stencel
University of Denver
Denver, Colorado
rstencel@du.edu

Abstract

Epsilon Aurigae ($V_{\max} = 2.99$) is an eclipsing binary star system with the longest orbital period known (27.1 years or 9,886 days). The next eclipse of this unique object is due summer 2009. With such a long orbital period, the actual eclipse might be expected to be short, but is just the opposite, lasting nearly 2 years (ca. 714 days). To a first approximation, this indicates the eclipsing body is of gigantic proportions, on the order of 2,000 solar radii. The exact nature of Eps Aur is still not fully resolved. A successful observing campaign was organized during the last eclipse, 1982-1984. Amateur and professional astronomers around the world contributed photometry, polarimetry, and spectroscopy data. Despite the strong effort, some questions still remain. Efforts have begun for a new eclipse campaign in 2009-2011. Out-of-eclipse observations are being made. A dedicated web site has been set up as a focal point. © 2006 Society for Astronomical Sciences.

1. Introduction and Background

Epsilon Aurigae, nominally a 3rd-magnitude naked-eye star in the northern sky, holds a secret that has defied complete understanding for more than 185 years. Every 27.1 years, the primary F star undergoes a diminution of its light for the extraordinary period of about 714 days. A cold, non-luminous obscuring body passes across our line of sight, reducing the light of the primary by one-half, or about 0.8 magnitude. The secondary object is never seen – the light of the primary star is diminished equally at all visible wavelengths, while no spectrum of the secondary is noted. From the length of the eclipse, the estimated size of the secondary is truly gigantic – more than 2,000 solar radii. Because of the length of time between eclipses, the chance to study this object comes only once or twice in an average scientific career. So each cycle brings a new generation of observers, with more sophisticated techniques.

2. History – Observational Timeline

The history of Epsilon Aurigae can be divided into several observational eras: 19th Century – Visual Observations; Early to mid 20th Century – Ground-Based Observations; and Late 20th Century to Present – Ground and Space-Based Observations.

2.1. 19th Century – Discovery and Visual Observations

The light variation of Epsilon Aurigae was evidently first noted by J. Fritsch, a German observer, in 1821. He sent his observations to other observers, but they apparently attracted little notice until the 1840s, when a second eclipse cycle was observed. Subsequently, through the next cycle, occurring in the 1870s, the star was carefully watched. Apart from the three long eclipses, the star showed no significant out-of-eclipse variation visually. The main features of

the eclipse cycle were established, those being a slow decline by about 0.8 magnitude over 190 days, steady light during the total phase for about 330 days, and then a slow recovery to original brightness over 190 days. It was also established that the two-year eclipse cycle repeated at intervals of 27.1 years. An attempt to classify the star with other known long-period or Algol-type variables lead to more questions than answers. Markwick (1904) in Britain was the last of this era to report visual observations; his plot of light intensity over the period 1888-1904 is shown for comparison in Figure 1a against other, modern light curves. Unfortunately, he missed most of the important eclipse features.

2. 2. Early 20th Century – Ground-Based Instrumentation and Observations

Beginning with the 1900-1902 eclipse, with the availability of photographic and spectroscopic equipment, more was learned. Spectroscopic studies were initiated at Yerkes Observatory and in Germany where H. Vogel used the well-equipped facilities he had established at the Potsdam Observatory. Vogel determined he had detected Doppler-shifted spectral lines and confidently announced that Epsilon Aurigae was a spectroscopic binary. He set his colleague, H. Ludendorff, to work on the problem, who examined all the available observations in a 1904 report. Other workers began to make spectroscopic, and later, photoelectric observations. After the 1928-30 eclipse cycle, C.M. Huffer (1932) and M. Güssow (1936) published extensive reports. Güssow published a detailed light curve, Fig. 1b, based on photoelectric observations by her, J. Stebbins, and C.M. Huffer (Reddy 1982).

Otto Struve, beginning his studies of eclipsing binaries in 1924, observed Epsilon Aurigae spectroscopically. In 1937 he and his colleagues at Yerkes announced a model that postulated a very large, semi-transparent secondary star (the "I" star) passing in front of the F primary (Kuiper, Struve, and Ström-gren, 1937). The gasses of this object were supposed to be subject to intense ionizing radiation from the F primary, producing an atmospheric layer that would attenuate the light from the primary equally at all wavelengths, in accordance with ground-based observations. This model came in for criticism almost immediately, as the radiation from the primary would be insufficient to produce the necessary depth of opacity. As further evidence built, Struve discussed the spectroscopic data extensively (Struve 1953, 1956). Later models were modified to include clouds or rings since, in order to maintain equal opacity at visible wavelengths, the material had to be larger solid particles, not gas or fine dust.

For the 1955-57 eclipse cycle, F. B. Wood and his associates at Flower and Cook Observatory of the University of Pennsylvania organized an international cooperative observing campaign under the auspices of IAU Commission 42. Ten bulletins were published and distributed to interested observers as the eclipse progressed. Observations were also reported for another long-period eclipsing binary, VV CEP. Wood's student L. Fredrick published a comprehensive report in 1960.

In 1962, O. Struve stated, "*The history of the eclipsing binary Epsilon Aurigae is, in many respects, the history of astrophysics since the beginning of the 20th century.*" During the 1960s and 1970s, astronomers such as M. Hack, S. Huang, and Z. Kopal extended the existing models and suggested new ones. The proposed models underwent many changes and adjustments as new information became available through the middle years of the century. Sahade and Wood (1978) published a review of the 1928-30 and 1955-57 results, giving a 1970 comparison light curve by Glyndenkerne, Fig. 1c, along with a good review of the known data.

2. 3. Late 20th Century to Present – Ground- and Space-Based Observations

By the late 1970s, both new ground-based and space-based techniques and instrumentation became available. The space satellite resources enabled observations to be made at Infrared and Ultraviolet (IR and UV) wavelengths not available to ground-based observatories. Leading up to and during the 1982-84 eclipse cycle, popular level articles were published by F. J. Reddy (1982) and D. Darling (1983) that outlined the leading theories and models.

For the 1982-84 Epsilon Aurigae eclipse, the fledgling International Amateur-Professional Photoelectric Photometry (IAPPP) organization, headed by Dr. Douglas Hall of Vanderbilt University, established a cooperative international observing program. Initially, the Campaign Newsletter editor for photoelectric photometry was Russ Genet and then Jeff Hopkins of Hopkins Phoenix Observatory took responsibility. Dr. Robert Stencel, of NASA Headquarters (later at Denver University), was the editor for spectroscopy, polarimetry, and space-based observations. Altogether, 13 Newsletters were published and sent to interested observers around the world. Up-to-the-minute results and data were included in each newsletter, published about every quarter. (Hopkins 1984, 1985, 1987.)

After the eclipse ended, a NASA-sponsored Conference held in Tucson, Arizona in 1985 was attended by more than 50 people (Fig. 2 and 3) and included many interesting papers (Stencel 1985). A

composite 1982-4 light curve from Hopkins Phoenix Observatory is shown in Fig. 1d. Other review articles were published by M. Hack (1984), R. Chapman

(1985), K. Crosswell (1985) and A. MacRobert (1985, 1988).

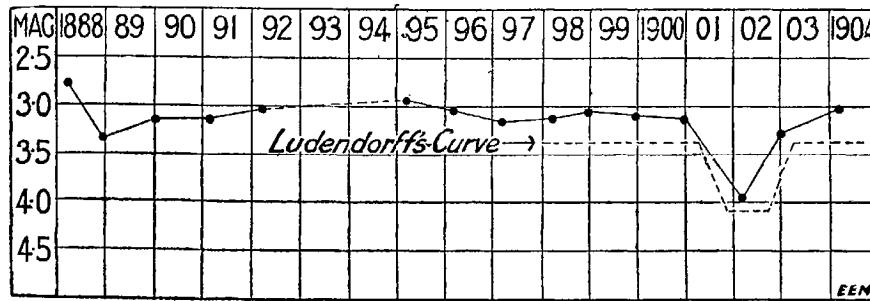


Figure 1. 1888–1904 (JD 2,410,600 to JD 2,415,600) Ref: Markwick, MNRAS Vol. 64 (1904) p. 85. (Visual observations).

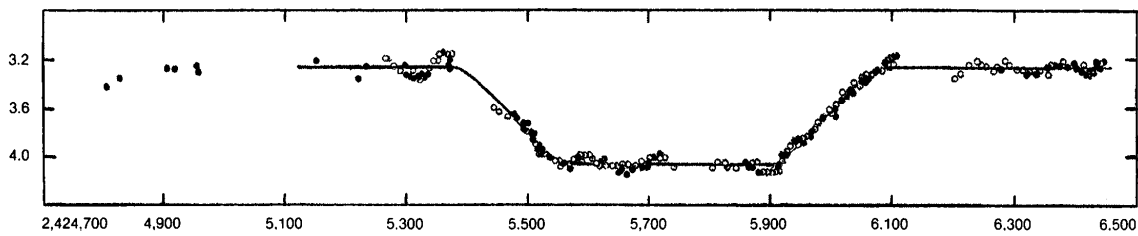


Figure 1b. 1928-30 ECLIPSE – JD 2,424,700 to JD 2,426,500) Ref: Reddy, Sky & Telescope May 1982 p. 460. (Data from Güssow, Stebbins, and Huffer).

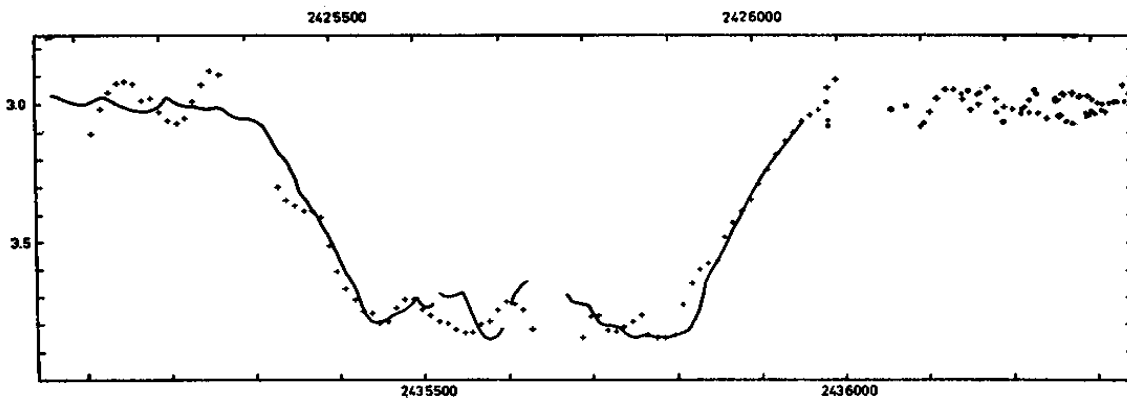


Figure 1c. 1928-30 and 1955-57 ECLIPSES JD 2,425,500 to 2,426,000 (+) and JD 2,435,500 to 2,436,000 (smooth curve + dots) Ref: Sahade and Wood, *Interacting Binary Stars* (1978), p. 153. (Data from Glyndenkerne 1970).

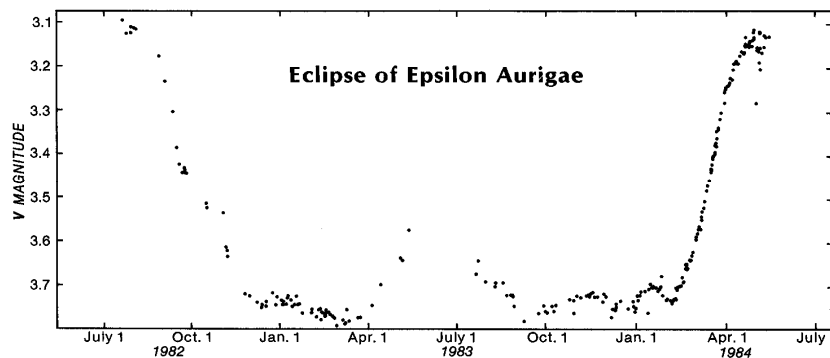


Figure 1d. Epsilon Aurigae Light Curves 1982-1984.

2. 4. The 1990s and Beyond

Since the last eclipse cycle, sporadic observations of the Epsilon Aurigae system have been accomplished with space-based instruments by various groups of observers, including a new generation of Infrared instruments and the Hubble Space Telescope. The space-borne observations, while encouraging, are not easy to analyze. While at least one group has confidently declared the “mystery” of Epsilon Aurigae has been “solved”, yet more work needs to be accomplished to wring out the details and confirm the latest models.

Ground-based observers have continued to monitor the small-amplitude, ~ 0.2 mag, fluctuations of the primary star. A renewed effort was started at the Hopkins Phoenix Observatory beginning in the fall of 2003 to obtain out-of-eclipse UB V photometry data. During the winter of 2005/2006, J and H band infrared observations were added. Multiple periods have been determined (Hopkins 2006).



Figure 2. 1985 AAS Meeting in Tucson, Arizona. (Epsilon Aurigae took top billing over the Hubble Space Telescope.)



Figure 3. Group Photo – Tucson 1985 Conference Attendees.

3. Prospects For The 2009-11 Eclipse

J. Hopkins and R. Stencel have posted predicted event times for the upcoming 2009-11 Epsilon Aurigae eclipse cycle on their respective web pages (see the Web Resources list below). Plans are being drawn for a coordinated observing campaign, and a dedicated web site is to be announced shortly. The focus for the upcoming campaign will be on electronic dissemination of campaign information via e-mail and the web pages. Guidelines for observations, report forms, etc. are being developed and will be posted. Amateur observers in particular need to be aware of proper observing procedures, use of the standard comparison star (Lambda Aurigae), and use of stan-

dard filters. While continuous coverage of observations is desirable, the emphasis will be on quality of observations, rather than quantity. Epsilon Aurigae is a nearly ideal object for visual observers, small telescopes, and CCD cameras, because it is bright, has a long observing season, and a leisurely pace of events. It is an excellent target for training and developing measurement skills. Along with times of ingress and egress during the eclipse cycle, perhaps the most important observations will help refine our knowledge of the mid-eclipse brightening and how it changes cycle to cycle. The mid-eclipse occurs during summer months, when Auriga is low in the sky, adding to the challenge.

3.1. Photoelectric Photometry Recommendations

Amateur astronomers with modest observing equipment and backyard observatories have a unique opportunity to make a valuable contribution during the upcoming campaign. Concentrated photometry in the ultraviolet (UV) through infrared (IR) bands is encouraged. Observations from multiple observatories are encouraged, particularly from higher latitude locations. Overlapping data will help provide more complete coverage of the star system, including before and during the ingress, mid-eclipse, egress, and post-eclipse phases. Coverage of the mid-eclipse period is especially desirable.

It is very important that filter photometry is properly accomplished and the observer's photometric system is properly calibrated to provide color-corrected data. Uncalibrated data will not be useful. The photometer system must be calibrated and the color transformation coefficients determined and used in the data reduction. While single-channel photometry may be easiest, CCD photometry is also encouraged. For best accuracy, differential photometry should be performed. Due to the star's brightness and the angular distance from the commonly used comparison star, CCD photometry may be difficult.

Practice before the eclipse period is suggested to refine observing techniques and at the same time produce valuable data. Observers can try measuring Deneb (Alpha Cygni) during the summer seasons. Single-channel photometry is ideal for this. In addition to photomultiplier tube (PMT) UVB photometry, the solid-state Optec SSP-3 photometer unit can provide BVRI data, and the Optec SSP-4 unit can provide Infrared J and H band photometry. If making observations with in the J and H bands with the SSP-4, a telescope of at least 12-inch (30 cm) aperture is recommended, otherwise the signal-to-noise ratio will be too low. For PMT (UBV) and SSP-3 (BVRI) photometry, an 8-inch (20 cm) aperture telescope is more than adequate. Again, calibrated data is required.

4. Web Resources

Anyone interested in contributing photometric data for Epsilon Aurigae should view the Epsilon Aurigae web sites and contact Jeff Hopkins at phxjeff@hposoft.com.

Hopkins Phoenix Observatory (HPO) pages:
<http://www.hposoft.com/Astro/PEP/EpsilonAurigae.html>

Dr. Robert Stencel (U. of Denver) web pages:
<http://www.du.edu/~rstencel/epsaur.htm>

5. Acknowledgments – Research Notes

The idea for this paper grew out of a talk on “Serious Astronomy” presented by Jeff Hopkins to the Saguaro Astronomy Club (SAC), Phoenix Arizona (Hopkins 2005). The lead author (Lucas) discovered there are close to 300 published articles relating to this fascinating object. Only a few of the most interesting are cited here.

The majority of the references cited herein are available on the Internet. Research for this article made use of the SIMBAD astronomical database, and the NASA Astrophysics Data Services (NASA-ADS) web resources. A few journal articles were retrieved using the facilities of the Noble Science Library, Arizona State University, Tempe, Arizona, and the Burton Barr Central Public Library, Phoenix, Arizona. Jeff Hopkins supplied archive copies of the 1982-84 Epsilon Aurigae Eclipse Campaign Newsletters, and Dr. Robert Stencel supplied a copy of the NASA 1985 Conference Proceedings. These last materials are being scanned and will be made available electronically on the Epsilon Aurigae web pages.

6. Conclusions

Observations of Epsilon Aurigae stretch back more than 185 years. Although successful international observing campaigns were waged during the 1950s and 1980s, the exact nature of this unique, very long period eclipsing binary system is still not fully established. Out-of-eclipse photometry is underway. Preparations have begun for a new observing campaign for the 2009-11 eclipse season. Interested amateur and professional observers are encouraged to contact the authors and visit the web pages for additional information.

7. References

- Chapman, Robert D., “Epsilon Aurigae,” *Astronomy and Space Science*, Vol. **110**, pp. 177-182, 1985.
- Croswell, Ken, “Epsilon Aurigae’s Secret Companion,” *Astronomy Magazine*, p. 60, January 1985.
- Darling, David, “Mystery Star,” *Astronomy Magazine*, pp. 66-71, August 1983.
- Fredrick, L., “Observations of Epsilon Aurigae,” *Astronomical Journal* Vol. **65**, pp. 97-100, 1960.
- Glyndenkerne, K. “The light and colour variation of Epsilon Aurigae,” *Vistas in Astronomy*, Vol. **12**, Issue 1, pp. 199-216, 1970.

- Güssow, M. “Epsilon Aurigae,” Veröffentlichungen der Universitätssternwarte zu Berlin-Babelsberg, B. **11**, H. 3, 1936.
- Hack, Margherita, “Epsilon Aurigae,” *Scientific American*, Vol. **251**, pp. 98-105, 154, October 1984.
- Hopkins, J.L., “Update on Epsilon Aurigae (May 1984),” *IAPPP Communications* **17**, pp. 22-30, 1984.
- Hopkins, J.L., “A Post Eclipse Report on Epsilon Aurigae,” *IAPPP Communications* **22**, pp. 9-13, 1985.
- Hopkins, J.L., “The 1982-84 Eclipse Campaign for Epsilon Aurigae,” *IAPPP Communications* **27**, pp. 30-40, 1987.
- Hopkins, J.L., “The Mysterious Epsilon Aurigae,” *Newsletter of the Saguaro Astronomy Club, Phoenix, AZ* February, 2005. <http://www.saguaroastro.org/content/SACNEWS/sac2005/SACnews0205.pdf>
- Hopkins, J.L. and Stencel, R.E., “Epsilon Aurigae 1982-1984 Eclipse Campaign Report,” (Abstract) *Bulletin of the American Astronomical Society*, Vol. **16**, p. 910, 1984.
- Hopkins, J., and Stencel, R.E., “Out-of-Eclipse UVB Variations of Epsilon Aurigae [FOIap+?],” Poster [107.05], American Astronomical Society Meeting, 9-13 January 2005, (Abstract) *Bulletin of the American Astronomical Society*, Vol. **36**, p. 5, 2004.
- Hopkins, J.L., and Stencel, R.E., “Single Channel UVB and JH Band Photometry of Epsilon Aurigae,” SAS 2006 Proceedings, Big Bear Lake, CA, May 2006 (in press).
- Huffer, C.M., “A Photo-Electric Study of Epsilon Aurigae,” *Astrophysical Journal*, Vol. **76**, pp. 1-8, July 1932.
- Kuiper, G., Struve, O., and Strömgren, B., “The Interpretation of Epsilon Aurigae,” *Astrophysical Journal*, Vol. **86**, p. 570-612, 1937.
- Ludendorff, H., “Untersuchungen über den Lichtwechsel von Epsilon Aurigae,” *Astronomische Nachrichten* No. 3918, Vol. **164**, pp. 81-116, 1904.
- MacRobert, A., “The Puzzle of Epsilon Aurigae,” *Sky and Telescope Magazine*, Vol. **70**, pp. 527-529, December 1985.
- MacRobert, A., “Epsilon Aurigae: Puzzle Solved?,” *Sky and Telescope Magazine*, Vol. **75**, p. 15, January 1988.
- Markwick, E. E., “Note on the Variability of Epsilon Aurigae,” *Monthly Notices Royal Astronomical Society*, Vol. **64**, pp. 83-89, 1904.
- Reddy, F.J., “The Mystery of Epsilon Aurigae,” *Sky and Telescope Magazine*, Vol. **63**, pp. 460-462, May 1982.
- Sahade, J. and Wood, F.B., “Interacting Binary Stars,” Pergamon Press, NY. ISBN 0-08-021656-0. pp. 152-157, 1978.
- Stencel, R., ed., “1982-84 Eclipse of Epsilon Aurigae, Summary of a Working Meeting Held in Tucson, Arizona January 16-17, 1985,” NASA Conference Publ. 2384, NASA, Washington, D.C. 1985.
- Struve, O., “The Coming Eclipse of Epsilon Aurigae,” *Sky & Telescope Magazine*, pp. 99-101, February 1953.
- Struve, O., “Epsilon Aurigae,” *Publications of Astronomical Society of the Pacific*, Vol. **68**, pp. 27-37, 1956.
- Struve, O. and Zebergs, V., “Astronomy of the 20th Century,” MacMillan Co., NY. LCC 62-21206, pp. 305-312, 1962.

Three Years of Mira Variable Photometry: What Has Been Learned?

Dale E. Mais
Palomar Community College
dmais@ligand.com

David Richards
Aberdeen & District Astronomical Society
david@richweb.f9.co.uk

Robert E. Stencel
Dept. Physics & Astronomy
University of Denver
rstencdel@du.edu

Abstract

The subject of micro-variability among Mira stars has received increased attention since DeLaverny et al. (1998) reported short-term brightness variations in 15 percent of the 250 Mira or Long Period Variable stars surveyed using the broadband 340 to 890 nm “Hp” filter on the HIPPARCOS satellite. The abrupt variations reported ranged 0.2 to 1.1 magnitudes, on time-scales between 2 to 100 hours, with a preponderance found nearer Mira minimum light phases. However, the HIPPARCOS sampling frequency was extremely sparse and required confirmation because of potentially important atmospheric dynamics and dust-formation physics that could be revealed. We report on Mira light curve sub-structure based on new CCD V and R band data, augmenting the known light curves of Hipparcos-selected long period variables [LPVs], and interpret same in terms of [1] interior structure, [2] atmospheric structure change, and/or [3] formation of circumstellar [CS] structure. We propose that the alleged micro-variability among Miras is a largely undersampled, transient overtone pulsation structure in the light curves. © 2006 Society for Astronomical Sciences.

1. Introduction

From European Space Agency's High Precision Parallax Collecting Satellite, HIPPARCOS (ESA, 1997) mission data, deLaverny et al. (1998) discovered a subset of variables (15 percent of the 250 Mira-type variables surveyed) that exhibited abrupt short-term photometric fluctuations within their long period cycle. All observations were made in a broadband mode, 340 to 890 nm, their so-called Hp magnitude. They reported variation in magnitude of 0.23 to 1.11 with durations of two hours up to almost six days, preferentially around minimum light phases. Instrumental causes could not be identified to produce this behavior. Most of these variations are below the level of precision possible with purely visual estimates of the sort collected by AAVSO, but may contribute to some of the scatter in visual light curves. 51 events in 39 M-type Miras were detected

with HIPPARCOS, with no similar variations found for S and C-type Miras.

These short-term variations were mostly detected when the star was fainter than $H_p = 10$ magnitude including one star at $H_p = 13$ magnitude and one at $H_p = 8.3$. For 27 of the original 39 observations, the star underwent a sudden increase in brightness. From their study, deLaverny et al. found that 85% of these short-term variations were occurring around the minimum of brightness and during the rise to the maximum, at phases ranging from 0.4 to 0.9. No correlation was found between these phases and the period of the Miras, but it does appear that brightness variations occur preferentially at spectral types later than M6 and almost never for spectral types earlier than M4. Similar results were reported by Maffei & Tosti (1995) in a photographic study of long period variables in M16 and M17, where 28 variations of 0.5 mag or more on timescales of days were found among spectral types later than M6. Schaeffer (1991)

collected reports on fourteen cases of flares on Mira type stars, with an amplitude of more than half a magnitude, a rise time of minutes, and a duration of tens of minutes. In analogy to the R CrB phenomenon, brightness variation could also be consequence of dust formation (fading) and dissipation (brightening) in front of a star's visible hemisphere. Future narrow band infrared interferometric observations will help resolve this.

Recently, Wozniak, McGowen and Vestrand (2004) reported analysis of 105,425 I-band measurements of 485 Mira-type galactic bulge variables sampled every other day, on average, over nearly 3 years as a subset of the OGLE project. They failed to find any significant evidence for micro-variability, to a limit of 0.038 I-band events per star per year. They conclude that either Hipparcos data are instrumentally challenged, or that discovery is subject to metallicity or wavelength factors that minimize detection in I-band among galactic bulge objects. In contrast, Mighell and Roederer [2004] report flickering among red giant stars in the Ursa Minor dwarf spheroidal galaxy, including detection of low-amplitude variability in faint RGB stars on 10-minute timescales! However, Melikian [1999] provides a careful analysis of the light curves for 223 Miras based on Hipparcos data, finding that 82 stars [37%] show a post-minimum hump-shaped increase in brightness on the ascending branch of the light curve. Melikian advocates that differing physical processes and perhaps stellar properties, e.g. later spectral types, longer periods and higher luminosity, differentiate behaviors among these stars.

The purpose of this report is to provide V and R-band photometry of objects related to the deLaverny et al. results, with dense temporal sampling. We find a similar lack of micro-variability as noted by Wozniak et al., but do confirm facets of the Melikian report. This suggests that these phenomena can be placed in a larger context of pulsational variations and episodic dust formation, with implications for ongoing spectroscopic and interferometric observations of mid-infrared studies of LPV stars.

2. Observations and Data Reduction

Our target list was drawn primarily from the objects listed by deLaverny et al. (1998), although limited to the northern sky. Of the 39 M type Mira's described therein, 20 are relatively bright and visible from the northern hemisphere. Because of the efficiency of automated sampling, we augmented this list with additional M type Miras and the brightest C, CS and S stars where one can obtain good signal to noise with low to moderate resolution spectroscopy on a

small telescope. These stars and associated characteristics are detailed in Table 1.

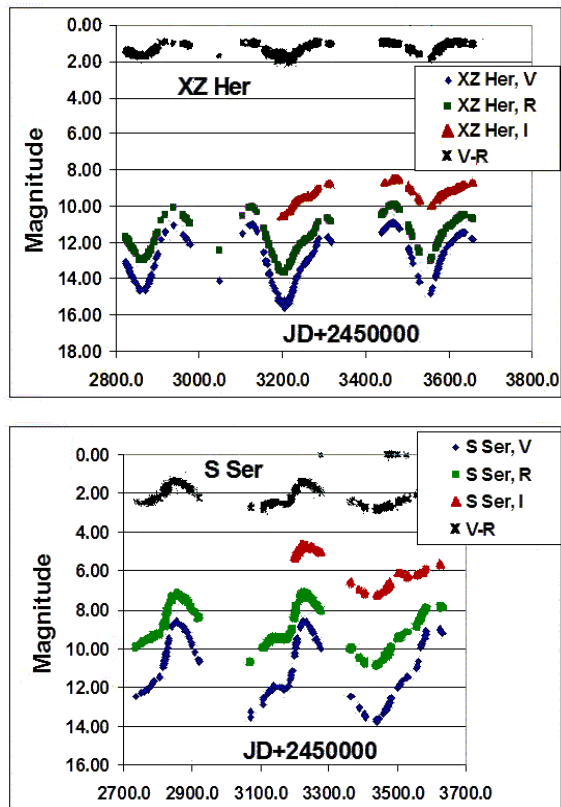


Figure 1. Dale Mais and his photometry machine co-located near Valley Center, California.

These, along with a variety of brighter S and C type stars, were also chosen. Brighter stars were chosen since they represented stars with magnitudes such that moderate resolution spectroscopy could be performed as part of the monitoring process. To accomplish this in a semi-automated manner, the telescope, camera and filter wheel are controlled by a single computer using Orchestrate software (www.bisque.com). Once the images are reduced, a script written by one of the authors (David Richards) examines the images performing an image link with TheSky software (www.bisque.com). The images obtained in this manner are stamped both with the name of the variable star, since this was how Orchestrate was instructed to find the object, and the position of the image in the sky. This allows TheSky to quickly perform the links with its USNO database.

Once the astrometric solution is accomplished, the program reads through a reference file with the pertinent data such as reference star name and magnitudes along with variable star of interest. The input file is highly flexible, stars and filter magnitudes of reference stars can be added freely as image data require. This file only needs to be created once, which is especially convenient for a set of program stars that will have continuous coverage over time. There is no need for entering magnitude information of reference stars in a repeated manner.

The results file is readily imported to spreadsheet software, where the various stars and their magnitudes can be plotted, almost in real time. This is an important aspect of this project, the ability to see changes (flare-ups) quickly and as a result respond to these changes with spectroscopic observations.



Figures 2a and 2b: Representative light curves. Additional examples can be found in Mais et al. 2005 SAS Conference Proceedings. These data will be submitted to the AAVSO archives.

Photometry was conducted with an Astrophysics 5.1-inch f/6 refractor located in rural San Diego county, California, using an ST-10XME camera and 2x2 binned pixels and the Johnson V and R filters. Images were obtained in duplicate for each band and two reference stars used per variable star for analysis. Image reduction was carried out with CCDSOFT (www.bisque.com) and Source Extractor (Bertin and Arnout, 1996) image reduction groups and specially written scripts for magnitude determinations, which allowed for rapid, nearly real time magnitudes to be found (see below).

The project has been underway since 2003 and involves a total of 96 stars, 20 M type Miras, 19 S types and the remainder C types. While there are certainly many more of these type stars, only those that had a significant part of their light curve brighter than visual magnitude 8 were considered, due to magnitude limitations in the spectroscopy part of the project. Fortunately, these stars are much brighter in the R and I bands, often by 2-4 magnitudes when compared to their V magnitudes, and many of the interesting molecular features are found in this region of the spectrum. The photometric analysis involves using two different reference stars. Their constant na-

ture is readily discerned over the time period by the horizontal slope of their light curves in both the V and R bands. After considerable effort, magnitudes are now determined at the 0.02 magnitude level. Thus any flare-ups in the range of 0.1 magnitude and brighter should be readily discerned.

Early on it was felt that semi-automating the process was the best way to proceed. The use of a precision, computer-controlled mount (Paramount, www.bisque.com) along with the suite of software by Software Bisque got the project rapidly underway. TheSky in conjunction with CCDSOFT lends itself to scripting, and a script was put together that automated the magnitude determinations.

To give an example of how this has streamlined the effort, on a typical night, initially using Orchestrate and later using a script developed by coauthor David Richards to control the telescope, camera and filter wheel, 40 stars, visible at the time, are imaged in duplicate in each of the V and R bands. This takes about 1 hour.

Reduction of the images using image reduction groups in CCDSOFT takes another 5 minutes. The script that determines the magnitudes takes about 10 minutes to churn its way through all the images. Within another 20 minutes, the data, via spreadsheet, has been added to each variable star's growing light curve. Thus in less than 2 hours all of the program stars have been observed and their results tallied. Until more of program stars rotate into view, one is free to pursue spectroscopic examination of the program stars, establishing baseline observations. Another portion of this effort included standardizing the reference stars in each of the fields using the Landolt standards (Landolt, 1983). Once this is done all previous and subsequent observations of the variable stars will have their magnitudes expressed in absolute Johnson-Cousins magnitudes.

3. Results & Analysis

3.1. Evidence for Flares?

Three years of monitoring of 96 Mira-like variables, including all the northern objects included in the Hipparcos report [deLaverny et al. 1998] has yielded minimal evidence for flare-like changes in V or R band. Best cases include 0.2 and 0.3 magnitude increases near minimum light in RR Boo. This object was reported by Guenther and Henson [2001] to have shown a one-time 0.8 mag flare. Other marginal cases in our data include CE Lyr, X CrB and DH Lac. In the case of CE Lyr, the proximity of a faint stellar companion could contribute to jumps in automated photometry as the variable changes around minimum. Otherwise, most variables show smooth light varia-

tion with no hint of flare-like fluctuations at a level of 0.01 mag.

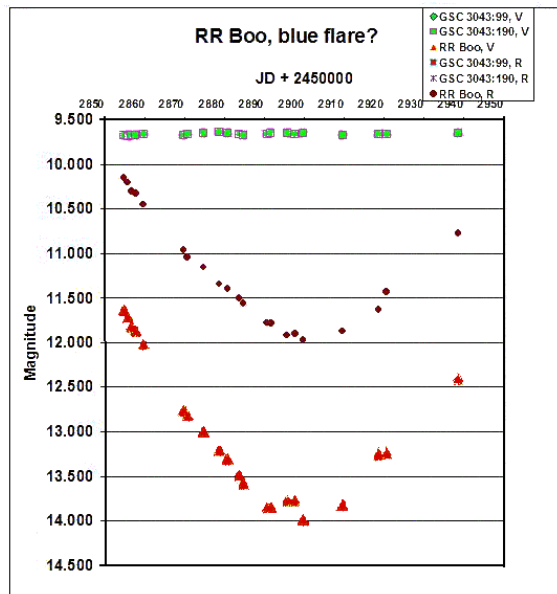


Figure 3a. variation near minimum light, RR Boo

3. 2. Light Curve “Bump” Phenomena

In contrast to high-frequency events like flares [hours or days], examining the light curves for the stars observed between 2003 and 2006 revealed persistent low frequency changes on timescales of weeks. Following the discussion of these by Melikian [1999], we label these “bumps” in the Mira light curves. Good examples of this are seen in the light curves of RT Boo, R CMi, X CrB, U Cyg, XZ Her [Fig.2a], S Ser [Fig.2b], RU Her, U Cyg and R Lyn. Some of these are seen in visual light curves compiled by AAVSO and AEFOV, but others are seen at levels below the ~0.1 mag precision typical of visual observations. This is one of the important benefits of high precision photometry. Most light curve bumps are non-recurring and seem to appear after especially deep minimum light. The correlation of bumps with Mira properties deserves further attention. A few extremes in our sample are noted: double maxima in T Cam, S Cas, RR Her, S Cep, RS Cyg, RR Her and Y Per. Two stars show the bump feature post-maximum light: V CrB and T Dra.

3. 3. Period Determination

Period finding was performed using PerAnSo software suite by Tonny Vanmunster, [http://users.skynet.be/fa079980/peranso/index.htm], which reports best fits using the ANOVA method. Initial application shows agreement with

literature periods for most variables, within a few percent and with errors in fit of 1 to 20 days, depending on the data interval and phase coverage thus far. More work is in progress.

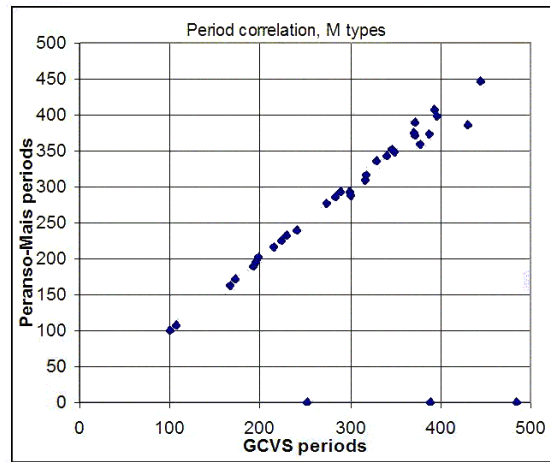


Figure 3b: correlation between M-type Miras newly derived periods and older GCVS determinations.

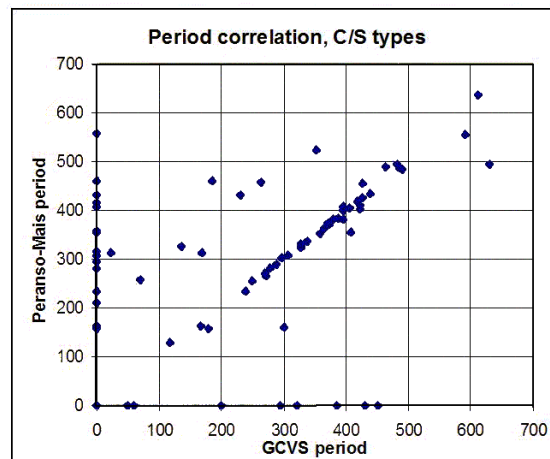


Figure 3c: correlation between C&S-type Miras newly derived periods and older GCVS determinations.

4. Conclusions

Among our conclusions based on V and R band measurements, with ~10 millimag precision, of nearly one hundred brighter Mira type stars are:

[1] Flare events are rare, and statistically similar to the OGLE result for I band monitoring of 0.038 events per star per year, with some evidence that “flares” are bluer in color;

[2] We are confirming indications of correlations between depth of minima and occurrence of a “bump” or change of slope on the ascending branch of some light curves [cf. Melikian 1999];

[3] Our coverage of approximately 3 cycles is sufficient to confirm the majority of previously published periods;

[4] We hypothesize that bump phasing and contrast varies with internal structure and opacity in analogy with similar phenomena among the “bump Cepheids” and deserves further study.

5. Acknowledgements

The authors wish to acknowledge the assistance of Thomas Bisque of Software Bisque for many useful discussions and help with the scripting, the AAVSO for its compilation of variable star visual light curves referenced in this paper, and the estate of William Herschel Womble for partial support of University of Denver astronomers participating in this effort.

6. References

Buchler, J. R., Moskalik, P., & Kovačs, G. 1990, *ApJ*, 351, 617 “A survey of Cepheid bump mode pulsations”

de Laverny, P.; Geoffroy, H.; Jorda, L.; Kopp, M. 1997 *A&AS* 122: 415 “Long-term UBVRI monitoring of 12 southern hemisphere Long Period Variables”

deLaverny, P., Mennessier, M., Mignard, F., & Mattei, J. 1998, *A & A* 330: 169, “Detection of short-term variations in Mira-type variables from HIPPARCOS photometry”

Guenther, H. D.; Henson, G. D., 2001, *BAAS* 199: 90-07 “Monitoring Select Mira Stars for Short-term Variability”

Hawkins, G., Mattei, J. & Foster, G. 2001 *PASP* 113:501, “R Centauri: An Unusual Mira Variable in a He-Shell Flash”

Maffei, P. and Tosti, G. 1995 *AJ* 109: 2652, “Rapid Variations in Long Period Variables”

Marsikova, V. 1997 *JAAVSO* 27: 141, “Fast Variations of the Mean brightness and Light Curve Parameters of the Carbon Mira-Type Star S Cep”

Melikian, N. 1999 *Astrophysics* 42: 408, “Classification of light curves of Mira variables”

Mighell, K. and Roederer, I. 2004 *ApJ* 617: L41 “Flickering Red Giants in the Ursa Minor Dwarf

Spheroidal Galaxy: Detection of Low-Amplitude Variability in Faint Red Giant Branch Stars on 10 Minute Timescales” & San Diego AAS poster 54.18

Schaefer, B. 1991, *ApJ*. 366: L39, “Flares on Mira stars?”

Stencel, R., Phillips, A., Jurgenson, C. and Ostrowski-Fukuda, T. 2002 DC-AAS poster 92.19 “Efforts to Verify Microvariability among Hipparcos-selected AGB Stars”

Teets, W. and Henson, G. 2004 Atlanta-AAS poster 8.03 “Multiple Wavelength Monitoring of Mira Stars for microvariability”

Vardya, M. 1988 *A&AS* 73:181, “Classification of Mira variables based on visual light curve shape”

Wozniak, P., McGowan, K. and Vestrand, W. 2004 *ApJ* 610:1038 “Limits on I-band Microvariability of Galactic Bulge Mira variables” [< 0.038 I-band events per star per year]

7. Tables

Table 1a: M type Mira Stars monitored

Star*	Sp.Type,	Vmax	Period, Epoch*	Period, Epoch* GCVS IV	Notes Anova/ Peranso
SV And**	M5e	7.7	316.21, 42887	308.64, 52892.3	
R Boo	M3e	6.2	223.40, 44518	224.22, 53465.3	
RR Boo**	M2e	8.3	194.70, 43047	194.74, 53197.7	
RT Boo**	M6.5e	8.3	273.86, 42722	276.12, 53225.5	
W Cnc	M6.5e	7.4	393.22, 43896	406.36, 53336.8	
R CVn	M5.5e	6.5	328.53, 43586	335.14, 53425.5	
V CVn	M4e	6.5	191.89, 43929	189.21, 53210.1	
R Cas	M6e	4.7	430.46, 44463	385.8, 53533.9	dP/dt?
T Cas	M6e	6.9	444.83, 44160	447.18, 53289.3	
V Cas	M5e	6.9	228.83, 44605	232.71, 53285.6	
T Cep	M5.5e	5.2	388.14, 44177	372.67, 53287.2	
R Cet**	M4e	7.2	166.24, 43768	163.30, 53221.6	
X CrB**	M5e	8.5	241.17, 43719	240.17, 52865.3	
AM Cyg**	M6e	11.3	370.6, 30075	374.47, 53345.2	
T Eri**	M3e	7.2	252.29, 42079	--, --	
RU Her**	M6e	6.8	484.83, 44899	--, --	
SS Her**	M0e	8.5	107.36, 45209	106.44, 53245.4	
XZ Her**	M0	10.5	171.69, 33887	171.15, 52939.3	
R Hya	M6eTc	3.5	388.87, 43596	--, --	
T Hya**	M3e	6.7	298.7, 41975	292.44, 53492.1	
X Hya**	M7e	7.2	301.10, 41060	287.91, 53113.4	dP/dt?
DH Lac**	M5e	11.6	288.8, 41221	292.45, 52929.6	
R Lmi	M6.5eTc:	6.3	372.19, 45094	390.02, --	
W Lyr	M2e	7.3	197.88, 45084	201.57, 53575.0	
CE Lyr**	--	11.7	318, 25772	315.90, 53259.0	
HO Lyr**	M2e	11.4	100.4, 30584	99.75, 53235.6	
V Mon**	M5e	6.0	340.5, 44972	342.51, 53312.7	
RX Mon**	M6e	9.6	345.7, 35800	351.62, 53192.9	
Z Oph	K3ep	7.6	348.7, 42238	347.52, 53450.6	
R Peg	M6e	6.9	378.1, 42444	358.17, 53350.0	dP/dt?
RT Peg	M3e	9.4	215.0, 45599	216.76, 53315.5	
SW Peg	M4e	8.0	396.3, 38750	398.43, 53482.9	
S Per	M3Iab	7.9	822, --	775.33, 53058.8	
S Ser**	M5e	7.0	371.84, 45433	371.69, 53234.1	
AH Ser**	M2	10.0	283.5, 36682	284.83, 53413.8	

*Stars are ordered by the traditional nomenclature: alphabetical by constellation, then by single letter R...Z, then double letters RR...ZZ, then AA...QQ and finally V###; MJD= JD – 2,400,000; GCVS: Gen.Catalog Var.Stars 4th ed., 1985 & <http://www.sai.msu.su/groups/cluster/gcvs/gcvs/>

** Hipparcos “flare stars” included in deLaverny et al. [1998]

Table 1b: C & S type Mira Stars Monitored

Star*	Sp.Type, V [max]	Period, Epoch*	Period, Epoch* GCVS IV	Notes Anova/ Peranso	
W And	S6,1e	6.7	395.93, 43504	406.72, 53221.6	
RR And	S6.5,2e	8.4	328.15, 43390	327.17, 52917.8	
ST And	C4.3e	7.7	328.34, 38976	324.59, 53424.4	
SU And	C6.4N8	8.0	--, --	282.83, 53235.0	dP/dt?
V Aql	C5.4N6	6.6	353, --	524.43, 53608.2	dP/dt?
W Aql	S3.9e	7.3	490.43, 39116	484.53, 53157.9	
UV Aql	C5.4N4	11.1	385.5, 30906	--, --	
S Aur	C4-5N3	8.2	590.1, 42000	554.59, 53169.9	dP/dt?
V Aur	C6.2eN3e	8.5	408.09, 43579	356.18, 53287.1	dP/dt?
TX Aur	C5.4N3	8.5	--, --	163.30, 53370.8	
EL Aur	C5.4N3	11.5	--, --	234.60, 53064.8	
FU Aur	C7.2N0	11.0	--, --	157.04, 53265.2	
R Cam	S2.8e	6.97	270.22, 43978	270.53, 53153.5	
S Cam	C7.3eR8	7.7	327.26, 43360	331.74, 53221.6	
T Cam	S4.7e	7.3	373.20, 43433	370.74, 53160.7	
U Cam	C3.9N5	11.0	--, 43060	--, --	
RU Cam	C0.1K0	8.1	22, --	313.48, --	
ST Cam	C5.4N5	9.2	300:, --	160.30, 53214.9	
UV Cam	C5.3R8	7.5	294., --	--, --	
W Cma	C6.3N	6.35	--, --	295.53, --	
R Cmi	C7.1eJ	7.25	337.78, 41323	335.77, 53114.8	
T Cnc	C3.8R6	7.6	482, --	495.05, 53396.9	
V Cnc	S0e	7.5	272.13, 43485	266.19, 53284.3	
S Cas	S3.4e	7.9	612.43, 43870	636.07, 53059.6	
U Cas	S3.5e	8.0	277.19, 44621	280.90, 52913.8	
W Cas	C7.1e	7.8	405.57, 44209	404.94, 53143.7	
ST Cas	C4.4N3	11.6	--, --	408.53, 53307.0	
V365 Cas	M5S7.2	10.2	136, --	325.73, 52844.8	
S Cep	C7.4eN8	7.4	486.84, 43787	488.08, 52976.0	
V CrB	C6.2eN2	6.9	357.63, 43763	351.86, 53449.8	
R Cyg	S2.5eTc	6.1	426.45, 44595	425.24, 53550.6	
U Cyg	C7.2eNp	5.9	463.24, 44558	488.61, 52919.2	dP/dt?
V Cyg	C5.3eNp	7.7	421.27, 44038	403.23, 53248.1	
RS Cyg	C8.2eN0p	6.5	417.39, 38300	419.58, 53254.4	
RV Cyg	C6.4eN5	10.8	263, --	458.72, 53592.6	
RY Cyg	C4.8N	8.5	--, --	307.22, 53233.4	
SV Cyg	C5.5N3	11.7	--, --	415.47, 53164.7	
TT Cyg	C5.4eN3	10.2	118, --	129.03, 53255.9	
YY Cyg	C6.0evN	12.1	388, 298261	384.62, 52941.8	
AW Cyg	C4.5N3	11.0	--, --	557.88, 52875.9	
AX Cyg	C4.5N6	7.85	--, --	461.75, 52845.1	
V460 Cyg	C6.4N1	5.6	180:, --	158.31, 53183.8	
T Dra	C6.2eN0	7.2	421.6, 43957	410.17, 53283.2	
UX Dra	C7.3N0	5.9	168, --	314.27, 53246.2	
R Gem	S2.9eTc	6.0	369.91, 43325	374.13, 53359.8	
T Gem	S1.5e	8.0	287.79, 44710	289.15, 53153.5	
TU Gem	C6.4N3	9.4	230, --	431.03, 53100.2	
NQ Gem	C6.2R9ev	7.4	70:, --	256.72, --	
S Her	M4Se	6.4	307.28, 45054	307.33, 53638.5	
RR Her	C5.7eN0	8.8	239.7, --	233.47, 53126.3	
R Lep	C7.6eN6	5.5	427.01, 42506	456.19, 53009.3	

SZ Lep	C7.3R8	7.4	--, --	--, --
R Lyn	S2.5e	7.2	378.75, 45175	382.52, 53124.2
T Lyr	C6.5R6	7.8	--, --	430.79, 52892.2
U Lyr	C4.5eN0	8.3	451.72, 42492	--, --
HK Lyr	C6.4N4	7.8	--, --	354.11, 53182.0
V614 Mon	C4.5JR5	7.0	60:, --	--, --
V Oph	C5,2N3e	7.3	297.21, 45071	302.58, 52826.6
TW Oph	C5.5N	11.6	185:, --	459.35, --
RT Ori	C6.4Nb	9.7	321, --	--, --
BL Ori	C6.3NbTc	7.9	--, --	316.01, 53036.8
RX Peg	C4.4JN3	9.7	629:, --	495.24, 52987.9
RZ Peg	C9.1eNTc	7.6	438.7, 54248	433.93, 53096.8
HR Peg	S5.1M4	6.1	50:, --	--, --
Y Per	C4.3eR4	8.1	248.6, 45245	255.81, 53083.3
V466 Per	C5.5N5	10.9	--, --	358.8, 53288.8
T Sgr	S4.5e	7.1	394.66, 44897	382.65, 53049.7
ST Sgr	S4.3e	7.2	395.12, 40463	401.07, 53046.6
AQ Sgr	C7.4N3	9.1	199.6, --	--, --
V1942 Sgr	C6.4N2R8	6.7	--, --	209.68, 52879.6
FO Ser	C4.5R6	8.5	--, --	--, --
TT Tau	C4.2N3	10.2	166.5, --	163.30, 53010.9
SS Vir	C6.3eN	6.0	364.14, 45361	361.85, 53231.7
BD Vul	C6-7Ne	9.3	430, 25758	--, --

 *Stars are ordered by the traditional nomenclature: alphabetical by constellation, then by single letter R...Z, then double letters RR...ZZ, then AA...QQ and finally V###; MJD= JD - 2,400,000; GCVS: Gen.Catalog Var.Stars 4th ed., 1985 & <http://www.sai.msu.su/groups/cluster/gcvs/gcvs/>

UNC-Chapel Hill's Gamma-Ray Burst Follow-up Programs

*Dr. Daniel E. Reichart
Department of Physics and Astronomy
University of North Carolina at Chapel Hill
Campus Box 3255
Chapel Hill, NC 27599-3255
reichart@physics.unc.edu*

Abstract

UNC-Chapel Hill is currently building and organizing both small (half-meter-class) robotic telescopes and large human-controlled telescopes to observe GRBs localized by NASA's Swift spacecraft. We summarize our Swift era plans for the new, robotic 6x0.41-meter (1.0-meter effective diameter) PROMPT telescopes at CTIO in Chile, the new 4.1-meter SOAR telescope also at CTIO, the 8.1-meter Gemini telescopes at CTIO and Mauna Kea in Hawaii, the 9.2-meter (effective diameter) SALT telescope at SAAO in South Africa, HST, and our newest effort, the Skynet Robotic Telescope Network, which already spans both South and North America and is growing rapidly. © 2006 Society for Astronomical Sciences.

1. Introduction

Observations of GRBs and GRB environments over the past nine years strongly indicate that the long-duration/soft-spectrum GRBs are the death cries of massive stars and the birth cries of black holes. Redshifts have been measured for about seventy of these GRBs and their implied isotropic-equivalent luminosities show them to be the biggest bangs since the Big Bang itself, beating supernovae by six to nine orders of magnitude. Given the sometimes extreme brightness of their optical/NIR afterglows in the first few seconds to minutes after the burst – in one case the afterglow was bright enough to see with binoculars despite a redshift that placed it three-quarters of the way across the observable universe – and a high expected rate of occurrence at and beyond the highest redshifts that have been measured for any astrophysical object, GRBs are widely expected to be the next great probe of the early universe, allowing astronomers to reach back in time roughly three times closer to the Big Bang than has been achieved to date.

NASA's Swift spacecraft is now making this possible (e.g., Haislip et al. 2006; see below). Swift's impact on the field has been revolutionary: Compared to previous GRB spacecraft, it is localizing GRBs an order of magnitude more often, and doing so an order of magnitude more accurately and an order of magnitude more quickly. In addition to observing GRBs at gamma-ray wavelengths, Swift observes their afterglows at X-ray, UV, and blue optical wavelengths beginning only $\approx 20 - 70$ seconds after each burst.

Arguably, Swift's highest profile mission objective is to use GRBs as probes to study the early uni-

verse in new and powerful ways, as originally fleshed out by Lamb & Reichart (2000) in support of Swift's Phase A study¹. However, there is a problem: although the number of Swift GRBs with redshifts greater than, say, $z = 5$, is expected to be large – ~ 20 per year – careful consideration of ground-based observing constraints (field up, sun down, weather acceptable) reduces this number to ~ 1 per year per site for which an early-time NIR spectrum can be obtained. This assumes near-100% access to both telescope and instrument. Consequently large numbers of efficient observing facilities are required, preferably with ready access to NIR spectroscopy or at least multi-band imaging. Between high- z events, such facilities can be turned on equally important problems in GRB physics, environments, and diversity².

To these ends, UNC-Chapel Hill is currently building and organizing both small (half-meter-class) robotic telescopes and large human-controlled telescopes that will – in many cases uniquely – meet these new challenges and opportunities. In this paper, we summarize our Swift era plans for the new, robotic 6x0.41-meter (1.0-meter effective diameter) PROMPT telescopes at CTIO in Chile, the new 4.1-meter SOAR telescope also at CTIO, the 8.1-meter Gemini telescopes at CTIO and Mauna Kea in Hawaii, the 9.2-meter (effective diameter) SALT telescope at SAAO in South Africa, HST, and our newest effort, the Skynet Robotic Telescope Network, which

¹ See <http://www.physics.unc.edu/~reichart/early.html> for a brief summary.

² See <http://www.physics.unc.edu/~reichart/late.html> for a brief summary.

already spans both South and North America and is growing rapidly.

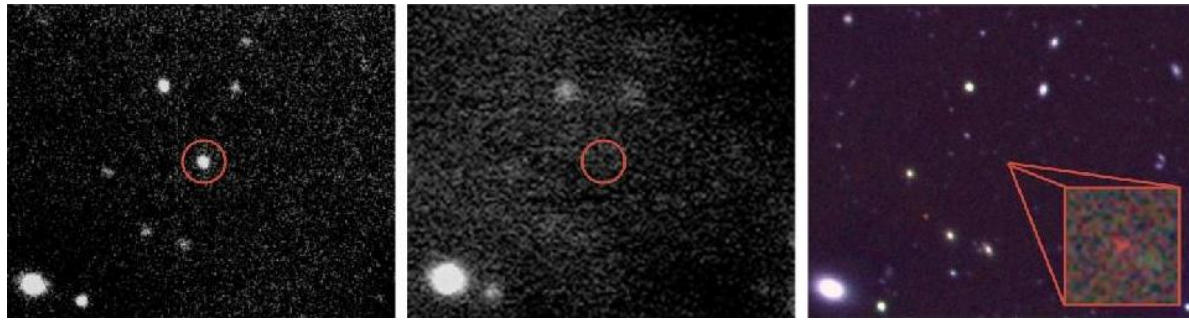


Figure 1. Left panel: NIR discovery image of the bright ($J = 17.36 \pm 0.04$ mag) afterglow of GRB 050904 from 4.1-m SOAR atop Cerro Pachon in Chile. Middle panel: Near-simultaneous non-detection of the afterglow at optical wavelengths, implying $z > 6$, from one of the six PROMPT telescopes atop Cerro Tololo, only 10 km away. Right panel: Color composite image of the very red afterglow 3.2 days after the burst from 8.1-m Gemini South, also atop Cerro Pachon. From Haislip et al. 2006, *Nature*, 440, 181.

Indeed, our multi-telescope, multi-wavelength approach has already met with early success: On September 4th, 2005, UNC-Chapel Hill undergraduate Josh Haislip and I discovered and identified the most distant explosion in the universe yet known, a GRB at $z = 6.3$, using both SOAR and PROMPT (Haislip et al. 2006). For the WMAP cosmology, this corresponds to 12.8 billion years ago, when the universe was only 6% of its current age.

Between the SOAR, Gemini, and SALT telescopes, the robotic PROMPT and Skynet telescopes, and the Follow-Up Network for Gamma-Ray Bursts (FUN GRB), a collaboration of about thirty telescopes that I organized in anticipation of the Swift era, we expect to acquire well sampled light curves and spectra at both early and intermediate times, and spanning both optical and NIR wavelengths, for most rapidly, well localized GRBs, and polarization histories for the brightest GRBs. Public Swift UVOT, XRT, and BAT data will complement these observations at shorter wavelengths and public VLA data (see Kulkarni, Berger & Frail 2002) will complement these observations at longer wavelengths. In addition to early-universe science (e.g., Lamb & Reichart 2000), we expect to make significant headway in the areas of GRB physics, environments, and diversity. Specifically, these results will feed the FUN GRB Collaboration’s UNC-Chapel Hill-based modeling effort, which focuses on GRB physics, environments, and the role of dust/extinction in these environments (e.g., Reichart 2001a,b; Reichart & Price 2002; Moran & Reichart 2005; Nysewander et al. 2005; Haislip et al. 2006; see also Lee et al. 2001; Galama et al. 2003).

2. UNC-Chapel Hill’s Follow-up Programs

Just as BeppoSAX and IPN created a discovery space for ground-based telescopes that could respond on their notification timescales – typically hours to days – the new generation of GRB spacecraft are creating a discovery space for ground-based telescopes that can respond on their notification timescales: seconds to minutes. This relegates much of the new science that will be done in the GRB field to smaller, robotic telescopes and to the most flexible and most efficient of the larger, human-controlled telescopes. UNC-Chapel Hill is currently building and organizing both small (half-meter-class) robotic telescopes and large human-controlled telescopes that will – in many cases uniquely – meet these new challenges and opportunities:

2.1. PROMPT

UNC-Chapel Hill is currently building PROMPT, which stands for Panchromatic Robotic Optical Monitoring and Polarimetry Telescopes, on Cerro Tololo, on the ridge between the GONG and 1.3-m telescopes. PROMPT’s primary objective is rapid and simultaneous multi-wavelength observations of GRB afterglows, some when they are only tens of seconds old. In addition to measuring redshifts by dropout, and early-time SFDs and extinction curves of sufficiently bright afterglows in unprecedented detail, PROMPT is already facilitating quick response observations at 4.1-m SOAR and 8.1-m Gemini South. When not chasing GRBs, PROMPT carries out non-GRB programs, including exoplanet transit searches (e.g., Fischer et al. 2006) and a survey of RR Lyraes in support of NASA’s SIM mission, and serves as a platform for undergraduate and

high school education throughout the state of North Carolina (see §4).



Figure 2 Three of the six PROMPT telescopes at CTIO in Chile.³

When completed in late 2006, PROMPT will consist of six 0.41-m Ritchey-Chrétien telescopes by RC Optical Systems on rapidly slewing ($9^\circ/\text{sec}$) Paramount ME mounts by Software Bisque, each under a clamshell dome by Astro Haven. Five of these telescopes have been outfitted with rapid-readout (<1 sec) Alta U47+ cameras by Apogee, which make use of professional-quality E2V CCDs. The sixth is being outfitted with an LN₂-cooled Micro-Cam by Rockwell Scientific for NIR imaging. Each mirror and camera coating combination has been optimized for a different wavelength range, including a u'-band optimized telescope. Although other filters are available, PROMPT will automatically observe GRB localizations in u'g'r'ri'z'YJH, six of them simultaneously. The R-band telescope will additionally measure polarizations. The polarimeter is being designed and built at UNC-Chapel Hill's Goodman Laboratory for Astronomical Instrumentation.

PROMPT is being built in two phases: Phase I, which was funded by \$130,000 from UNC-Chapel Hill and a \$100,000 gift from alumnus Leonard Goodman, began in September 2004 and is now complete. Phase I consisted of enclosure construction and the assembly of temporary 0.36-m Schmidt-Cassegrain telescopes by Celestron, with the goal of establishing reliable and robust operations, and to test software. Phase II, which is funded by \$912,000 from NSF's MRI and PREST programs, is now underway and consists of upgrading to final optics, the NIR camera, and the polarimeter.

The five optical telescopes are now complete, except for the polarimeter, which will be deployed in

³ See <http://www.physics.unc.edu/~reichart/promptpics.html> for more pictures.

mid-2006. The NIR camera, sporting an improved version of HST's NICMOS3 FPA, has just arrived at UNC-Chapel Hill, but will require considerable integration with PROMPT's control software, called Skynet (see §3), before it can be deployed in late 2006.



Figure 3. PROMPT's NIR Camera

Between HETE-2, Integral, and now Swift, PROMPT is observing GRB localizations on the rapid timescale about once every three months (we observed GRB 050908 within 25 seconds, GRB 051109 within 75 seconds, and 060306 within 25 seconds of spacecraft notification; Kirschbrow et al. 2005; Haislip et al. 2005; Nysewander et al. 2006), and on longer timescales about once every week. Given our best guesstimates about the star-formation rate at high redshifts, we might observe $z > 5$ GRBs on the rapid timescale as often as once per year, and $z > 7$ GRBs on the rapid timescale perhaps once every two to three years. PROMPT's ability to observe afterglows simultaneously in many filters, including NIR filters, and to do so quickly before the afterglow fades away will allow it to “promptly” pick out record breakers (e.g., Haislip et al. 2006).

2. 2. SOAR & Gemini

Record breaker or not, we are using PROMPT photometry and astrometry to inform our quick response programs on 4.1-m SOAR and 8.1-m Gemini South, which are only one mountaintop away and consequently subject to the same observing constraints. UNC-Chapel Hill is a 17% partner in SOAR, which was dedicated in April 2004 and is now well into commissioning and beginning early science. Furthermore, UNC-Chapel Hill has a three-year commitment from the SOAR Board to interrupt on the rapid timescale. Additionally, UNC-Chapel Hill and the FUN GRB Collaboration, in coalition with

the US/UK Gemini GRB Collaboration, were awarded 21 hours of quick response time on Gemini South in Semester 2005B and we expect to be awarded time on both Gemini telescopes in future semesters. All three telescopes are capable of NIR and optical spectroscopy and imaging, as well as able to switch instruments within minutes. Our primary goal is broad spectral coverage for redshift determination, metallicity and re-ionization studies, and spectrophotometry for modeling, unless the afterglow will be too faint by the time that observations can commence, in which case deep, multi-band imaging is the goal. We coordinate PROMPT, SOAR, Gemini, SALT, and FUN GRB Collaboration efforts from UNC-Chapel Hill's new Henry Cox Remote Observing Center.

in South Africa, which was dedicated in November 2005 and is also now well into commissioning and beginning early science. UNC-Chapel Hill has been awarded SALT's Performance Verification Phase GRB program, and we have already used SALT to observe a handful of GRBs. Although SALT's fixed-altitude design is generally not ideal for rapid follow-up observations of GRBs, we intend to use a good fraction of our time for follow-up spectroscopy and deep, multi-band imaging of GRB afterglows that we observe with PROMPT, SOAR, and Gemini South on the rapid timescale, about a half-day earlier. Additionally, UNC-Chapel Hill in collaboration with Tanvir et al. has been awarded 21 orbits on HST in Cycle 15, to study high-redshift afterglows and host galaxies at later times.



Figure 4. The SOAR telescope at CTIO in Chile.

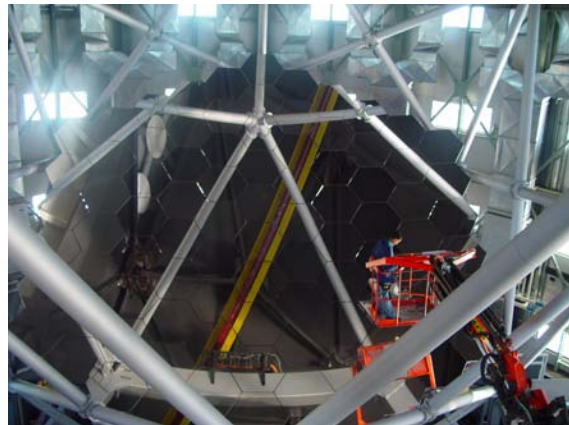


Figure 6. The SALT telescope at SAAO in South Africa.

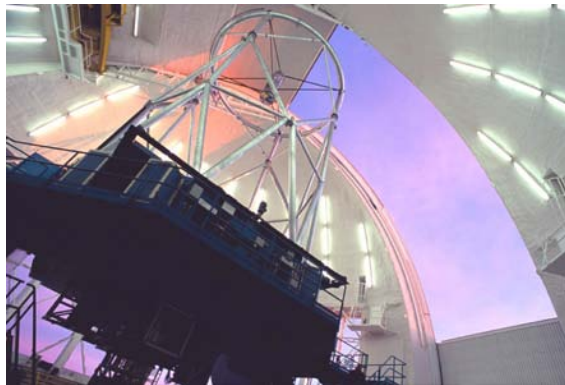


Figure 5. The Gemini South telescope at CTIO in Chile.

2. 3. SALT & HST

UNC-Chapel Hill is a 3% partner in the 9.2-meter (effective diameter) SALT telescope at SAAO



Figure 7. HST.

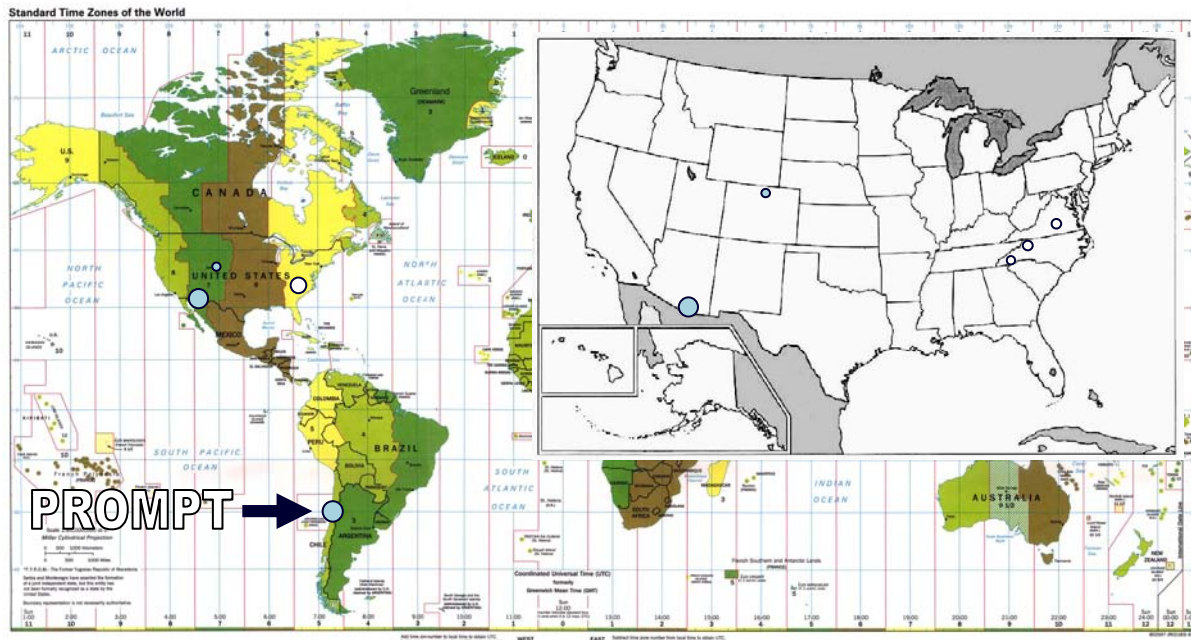


Figure 8. The current state of the Skynet Robotic Telescope Network. Carolina blue circles represent telescopes or clusters of telescopes that have already been integrated into Skynet. White circles represent telescopes or clusters of telescopes that are scheduled for integration this summer.

3. The Skynet Robotic Telescope Network

PROMPT is under the control of “Skynet”, a prioritized queue scheduling system that we are developing at UNC-Chapel Hill. Skynet is written in LabView and runs on a computer at UNC-Chapel Hill’s Morehead Observatory. Skynet interacts with MySQL databases and commands dumb-by-design “Terminator” programs at each telescope, which control the hardware. Images are automatically transferred back to a 1.1 terabyte RAID 5 with tape backup at Morehead Observatory, making use of communication libraries that we wrote for remote use of SOAR. Users can submit jobs and retrieve data from any location via a PHP-enabled web server that interacts with the MySQL databases.⁴ However, GRBs receive top priority and are automatically added to the queue via a socket connection.

Furthermore, we have written Terminator very generally, such that any mount that can be controlled by “TheSky” and any camera that can be controlled by “MaxIm DL”, or mounts and cameras that are ASCOM compliant, can easily be integrated into Skynet. We have already integrated a 32-inch robotic telescope in Arizona and a 14.5-inch robotic telescope in Colorado, and have been contacted by owners of telescopes in California, Illinois, New Mex-

ico, North Carolina, Tennessee, Virginia, and Wyoming. Three more telescopes, two in North Carolina and one in Virginia, are scheduled for integration this summer, and the two North Carolina sites (Dark Sky Observatory and Pisgah Astronomical Research Institute) have additional and larger telescopes (two 16-inches, a 24-inch, and a 32-inch) that will be integrated if this summer’s efforts prove successful.

Skynet then synchronizes GRB observations across telescopes, even if continents apart, which makes interpreting SFDs much easier, especially if the afterglow is not fading as a power law at early times. When not chasing GRBs, which is most of the time, users are able to queue jobs on each other’s telescopes, including PROMPT, at a guest priority level, giving them access to additional facilities and instrumentation, not to mention sky coverage and weather flexibility.

This and the ability to queue schedule one’s own telescope, without requiring students to stay awake night after night, has already generated a great deal of interest, so far all by word of mouth. Given the level of interest, we feel that we will be able to grow the network by about ≈ 1 square meter per year. By the end of the decade, Skynet should have the same total area as a 2 – 3 meter diameter telescope.

⁴ <https://fungrb.physics.unc.edu/skynet/>

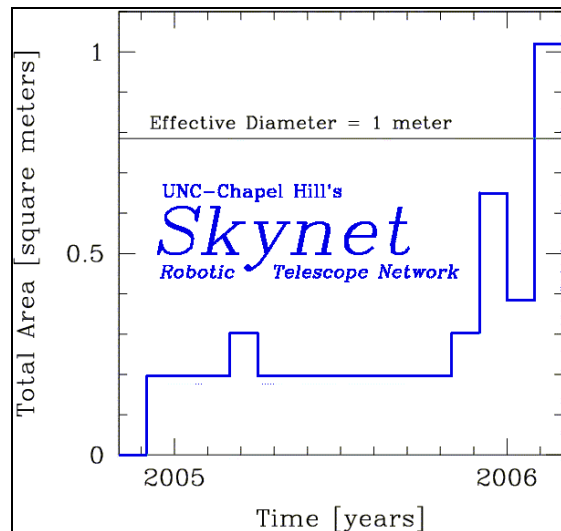


Figure 9. The emergence of Skynet.

4. Education and Public Outreach

When not chasing GRBs, PROMPT is being used by undergraduate and high school students across the state of North Carolina for a wide variety of projects. In addition to UNC-Chapel Hill, PROMPT Collaboration institutions include Appalachian State University, Elon University, Fayetteville State University, Guilford College, Guilford Technical Community College, North Carolina Agricultural and Technical State University, UNC-Asheville, UNC-Charlotte, UNC-Greensboro, UNC-Pembroke, Western Carolina University, and Hampden-Sydney College just across the border in southern Virginia.⁵ Each of these institutions has about 400 hours per year of observing time between the six PROMPT telescopes, giving them guaranteed access to a professional observatory and the southern sky. PROMPT Collaboration access began February 1st, 2006.

Furthermore, since PROMPT is fully robotic, none of these institutions have to raise additional money to send students to Chile to use the telescopes – a very expensive proposition. Instead, students simply submit observing requests to Skynet using the web interface. PROMPT automatically observes each target, usually that night, and then Skynet returns the collected images to the students for analysis.

UNC-Chapel Hill's Morehead Planetarium and Science Center (MPSC) has about 2,300 hours per year of observing time for K-12 education and public outreach. MPSC hopes to bring PROMPT into every high school in the state of North Carolina. Funded by a \$50,000 NASA/STScI IDEAS grant, MPSC is de-

⁵ See http://physics.unc.edu/~reichart/prompt_documents.html for letters of support.

veloping a curriculum for high school science classes that will allow them to submit observing requests to Skynet using the same web interface. This curriculum will also satisfy new statewide graduation requirements.

Finally, funded by an NSF CAREER grant, we have established two programs to bring PROMPT Collaboration students together. The first is the PROMPT Summer Fellowship Program, in which two undergraduates from PROMPT Collaboration institutions other than UNC-Chapel Hill spend 12 weeks with my group in Chapel Hill, where they will chase GRBs with us, help with our commissioning of PROMPT and Skynet, gain experience with large telescopes such as SOAR and possibly SALT, and learn IRAF.⁶ Additionally, this year's PROMPT Fellows will help to complete 16-inch robotic telescopes that their home institutions are building for Skynet (\$3).



Figure 10. NRAO-Green Bank's 40-foot telescope and participants and coordinators of ERIRA 2005.

Between Swift and UNC-Chapel Hill's follow-up programs, PROMPT Collaboration students will directly experience NIR, optical, UV, X-ray and gamma-ray astronomy – but not radio astronomy. Consequently, our second program supports five PROMPT Collaboration undergraduates, including at least one non-UNC-Chapel Hill student, to attend *Educational Research in Radio Astronomy (ERIRA)* at NRAO, Green Bank, a week-long summer program that I established in 1992 and have coordinated each year since.⁷ Other coordinators include Dr. Andrew Stephens (Gemini Observatory) and Mr. Walter Glogowski (Ridgewood High School, Norridge, IL). Fifteen participants are selected from a national pool

⁶ See http://physics.unc.edu/~reichart/prompt_summer_fellowship_program.html for more information.

⁷ See <http://physics.unc.edu/~reichart/erira.html> for more information.

on the basis of enthusiasm first and background in astronomy second. This makes for a diverse and highly motivated group.

The participants spend one week training to operate a 40-foot diameter radio telescope, which they then use to map the invisible universe and carry out small research projects. Observations are carried out day and night, and what little time remains is spent attending a crash course on radio astronomy, research talks, workshops, and tours, in addition to processing the collected data and completing the small research projects. Naturally, the participants find very little time for sleep, but I select only the most enthusiastic applicants who would not have it any other way.

5. Acknowledgements

DER very gratefully acknowledges support from NSF's MRI, CAREER, PREST, and REU programs, NASA's APRA, Swift GI and IDEAS programs, Dudley Observatory's Ernest F. Fullam Award, UNC's Junior Faculty Development Award, and especially Leonard Goodman and Henry Cox.

6. References

- Fischer, D. A., et al. 2006, ApJ, 637, 1094
- Galama, T. J., et al. 2003, ApJ, 587, 135
- Haislip, J., et al. 2005, GCN 4220
- Haislip, J. B., et al. 2006, Nature, 440, 181
- Kirschbrown, J., et al. 2005, GCN 3947
- Kulkarni, S. R., Berger, E., & Frail, D. A. 2002, GCN, 1718
- Lamb, D. Q., & Reichart, D. E. 2000, ApJ, 536, 1
- Lee, B. C., et al. 2001, ApJ, 561, 183
- Moran, J. A., & Reichart, D. E. 2005, ApJ, 632, 438
- Nysewander, M. C., et al. 2005, ApJ, submitted (astro-ph/0505474)
- Nysewander, M., et al. 2006, GCN 4849
- Reichart, D. E. 2001a, ApJ, 553, 235
- Reichart, D. E. 2001b, ApJ, 554, 643
- Reichart, D. E., & Price, P. A. 2002, 565, 17

The International Variable Star Index (VSX)

*Christopher L. Watson
San Diego, CA 9212
skygeex@gmail.com*

*Arne A. Henden
American Association of Variable Star Observers
25 Birch Street
Cambridge, MA 02138
arne@aavso.org*

*Aaron Price
American Association of Variable Star Observers
25 Birch Street
Cambridge, MA 02138
aaronp@aavso.org*

ABSTRACT

The International Variable Star Index (VSX) is a new utility now available at the AAVSO. This program serves two distinct functions: an easy portal to access information about variable stars that is far more extensive than the GCVS; and a method of uploading variable star information. The information access includes all known cross-references, basic parameters such as period and variability type, and finding charts. The upload feature permits information update on known variables (such as a new period) as well as entering new variable stars into the system. This paper will show examples of how to use VSX and describes the vetting guidelines.

1. Introduction

The International Variable Star Index (VSX) is a comprehensive relational database of known and suspected variable stars gathered from a variety of respected published sources and made available through a powerful Web interface. The interface provides tools for visitors to search and view the data, registered users to revise and add to the data, and authorized moderators to vet the data, creating a consistently reliable “living” catalog of the most accurate and up-to-date information available on these objects.

Data on variable stars are constantly changing. New and ongoing surveys are locating new variable stars every day. Corrections to errors in the data are always coming in. However, all of this work to refine what we know about these stars is happening at different times and in different places. The mission of VSX is to bring all of that new information together in a single data repository, make it accessible to the public via a simple web interface, and provide the tools necessary for the controlled and secure revising of the data.

VSX was conceived and created by amateur astronomer Christopher Watson in response to the specific desires of the members of the Chart Team and the Comparison Star Database Working Group of the American Association of Variable Star Observers (AAVSO), as well as the broader perceived need for a globally-accessible central “clearing-house” for all up-to-the-minute information on variable stars, both established and suspected. The VSX web site was designed to be the on-line medium by which variable star data are made available to the public and through which the data are maintained, revised, and commented upon. This database literally comes alive with input from the world of registered contributors.

In order to keep VSX up to date and populated with the latest corrected findings, authorized moderators constantly review and revise the metadata, always citing sources for any new details, and fully documenting the rationales behind any additions or changes. By maintaining a strict version control on all records, the history of the gathered knowledge on each variable star can be traced, validated, and followed up by those who rely on this information to be accurate.

Moderators use a secure login to access on-line tools for working with the database. All modifications or additions submitted are queued in a staging table and peer reviewed. When the submission is cleared, it is promoted to the live database, and all particulars about the change/addition are logged with the revision. The modification is assigned a revision number, which can be referenced at any time to retrieve any version of the data for any particular star. Promoted revisions later determined to be erroneous for any reason, can be rolled back. The data moderators reserve the right at all times to reject a submission for modification or new variable star.

Web-based tools for querying VSX in various ways are available to the public. The public data returned in a query transaction contains all the accumulated data for the most recent revision level for each star in the recordset, including details of all modifications made to the data, and references to support those changes. Previous revisions can also be viewed. The public interface does not include the means for modifying the data in any way, but a form for sending suggestions for modification to the Project Administrator is made available.

2. The Database

The VSX database was initially populated with the entire Combined General Catalog of Variable Stars (GCVS 4.2, 2004 Ed.). This included the main lists from Vol. I-III, the NSV catalog of suspected variable stars and its supplements, all cross-identifications from Vol. IV, and all references and remarks from all volumes.

Differences between the published 2004 Edition of the GCVS and the “living” version available from the Sternberg file servers were then culled and integrated. On top of this base data set were added the published catalogs of red variables from the Northern Sky Variability Survey (NSVS), the detected variables from the 3rd All Sky Automated Survey (ASAS-3), all new variables reported in the various volumes of the Information Bulletin on Variable Stars (IBVS), the Miras and eclipsing binaries found and published from Phase 2 data of the Optical Gravitational Lensing Experiment (OGLE-II), the

bright contact and near-contact binaries extracted from data of the Robotic Optical Transient Search Experiment (ROTSE-I), and the new variable stars discovered from offered images to the MISA0 Project.

All together, this became the Base 1.0 Version of the VSX object table. Internal relations between the object, reference, remark, and cross-identification tables were established programmatically using the various source data. New, unpublished cross-identifications between the various catalogs were generated through custom cone search algorithms, and then verified.

3. The Site

VSX can be accessed from a link on the home page of the Web site for the American Association of Variable Star Observers (AAVSO) at <http://www.aavso.org>. The VSX Web site and database is hosted and maintained by AAVSO staff and volunteers on hardware located at AAVSO headquarters in Cambridge, Massachusetts, USA.

3.1. Home page

The home page (Fig. 1) for VSX presents several top-level links into the application:

1. Search – A link to the Search form where the database may be queried.
2. Submit – Links to the New Star submission forms for adding new variable stars to the database.
3. Register – The Registration form used to create a new login and user profile for VSX.
4. Log In – Used to log in to VSX. Necessary for making any submissions.
5. Account – Access to the currently logged-in user’s profile.
6. About – An overview of VSX, details about its creation, acknowledgments, and references.

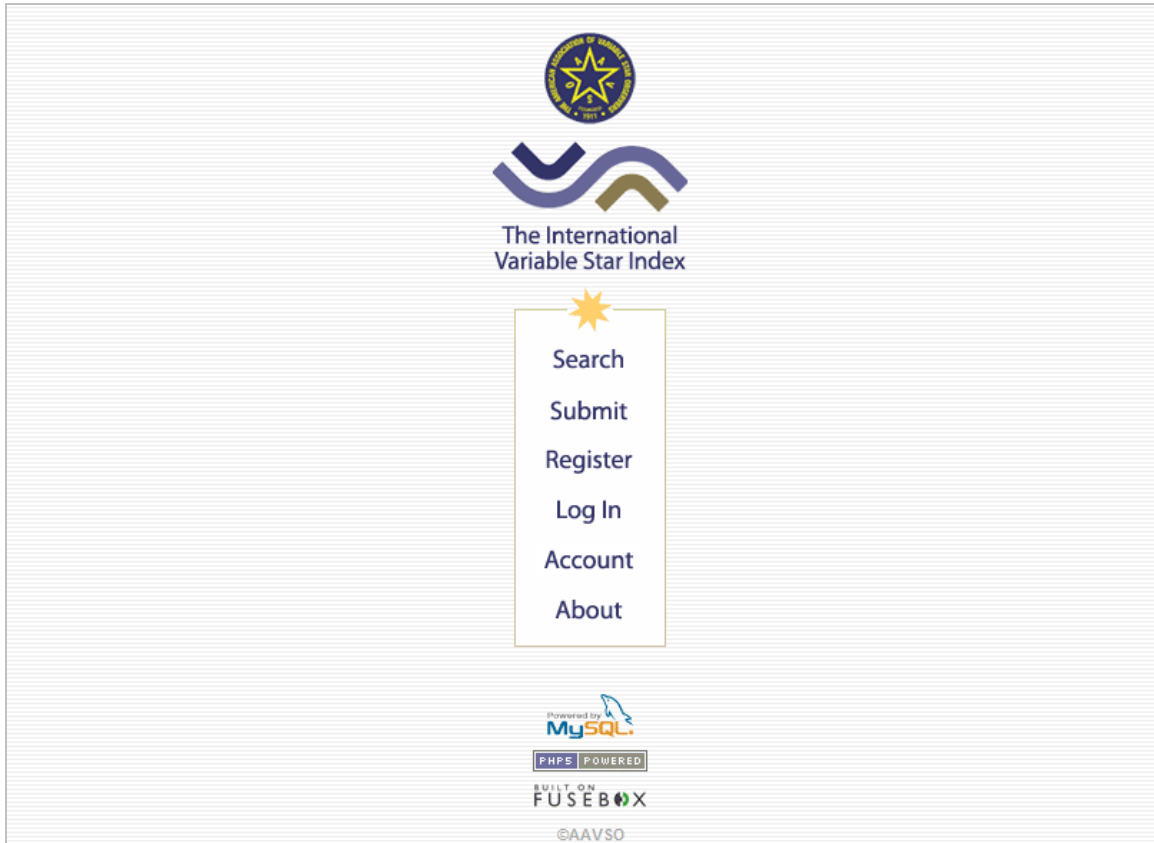


Figure 1. International Variable Star Index Home page

3. 2. Search page

The Search page (Figs. 2, 3 and 4) is the primary Web interface for access to the VSX database. It provides an easy way for the user to search the database by supplying complete or partial information in one or more fields.

Using the More and Less buttons, the Search form can be expanded or collapsed between three different “levels” of field collections. The lowest, most basic search level gives the user the ability to search on just the Name field. The mid-level search adds the ability to perform a cone search using a set of central coordinates and a radius (or a box size). The highest search level adds several more available fields: maximum and minimum magnitude ranges, period range, epoch range, rise time range, nova year range, variable type, and spectral type.

All search levels permit the ordering of the result set by nine different criteria (in ascending or descending order): historical GCVS designation sequence, strict alphabetical, right ascension, declination, maximum magnitude, variable type, spectral type, constellation, and—in the case of cone searches—angular distance from the given central coordinates.

Another option on the search form gives the user the choice to include or exclude from the result set proven variables, suspected variables, and/or known non-variables (objects originally classified erroneously as variable, or found not to exist, or proven constant).

All input to this form is saved in session scope when submitted, and is conveniently recalled when this form is revisited during the same browser session. Help pop-ups are available for each section of this form.



Figure 2. Name Search.

Search VSX
Enter information in any or all of the search fields.

Name
Examples: SS Cyg, V456 Sgr, NSV 1009
%And, NSVS%+%, Z %

Position Sexagesimal Decimal °
Examples: 21 42 42.8 +43 35 10
07:04:04 -03:50:51
34.837 -2.978

Size Radius Box size

Include Variables Suspects Non-variables

Order by Descending

Click **More** for extended search options, **Less** for basic name searches.

Figure 3. Coordinate Search.

Search VSX
Enter information in any or all of the search fields.

Name
Examples: SS Cyg, V456 Sgr, NSV 1009
%And, NSVS%+%, Z %

Position Sexagesimal Decimal °
Examples: 21 42 42.8 +43 35 10
07:04:04 -03:50:51
34.837 -2.978

Size Radius Box size

Max mag. between and

Min mag. between and

Period between and d

Epoch between and JD

Rise dur. between and %

Nova year between and

Var. type
Examples: M, DCEP, EA%

Spec. type
Examples: K, M4e, pec(%)

Include Variables Suspects Non-variables

Order by Descending

Click **Less** to hide extended search options.

Figure 4. Extended Search.

3. 3. Search Results Page

When a search is initiated, and the result set contains more than one matching record, the Search Results page (Fig. 5) displays a concise listing of the results of the database query. This page indicates the total number of objects that matched the selection criteria and presents an abbreviated detailing of those database entries, with basic information such as name, coordinates, variable type, period, and magnitude range. Clicking on any one of the names in this list displays the complete Detail Sheet for that named object. The result set may be re-ordered according to user preference, without having to go back to the Search page.

within 1° of 21 42 42.80 +43 35 10.0 Re-order by

Search Results [16 records]
Click Name to display Detail Sheet for star.

Dist.	Name	Coords (J2000)	Var. type	Period	Mag. range
0.000	<input checked="" type="checkbox"/> SS Cyg	21 42 42.80 +43 35 10.0	UGSS	(49.5)	7.70 - 12.40 V
0.157	<input checked="" type="checkbox"/> NSV 25754	21 43 34.50 +43 36 24.0	VAR:	--	12.30 - 12.50 P
0.323	<input checked="" type="checkbox"/> V1573 Cyg	21 42 28.10 +43 15 58.0	RR	--	17.20 - <17.60 p
0.408	<input checked="" type="checkbox"/> NSVS 2143518+431408	21 43 51.77 +43 14 08.0	L:	344.0	10.77 - 11.19 R1
0.446	<input checked="" type="checkbox"/> V1668 Cyg	21 42 35.30 +44 01 55.0	NA	--	6.00 - 20.00 V
0.555	<input checked="" type="checkbox"/> NSV 13834	21 40 11.10 +43 16 26.0	--	--	5.11 - ? V
0.618	<input checked="" type="checkbox"/> NSVS 2139408+431818	21 39 40.83 +43 18 17.5	M	348.0	10.91 - 12.64 R1
0.618	<input checked="" type="checkbox"/> NSV 25722	21 39 40.70 +43 18 20.0	--	--	13.80 - <14.50 V
0.618	<input checked="" type="checkbox"/> V1250 Cyg	21 39 40.70 +43 18 20.0	SRA	265.0	15.50 - 17.30 p
0.665	<input checked="" type="checkbox"/> UU Cyg	21 39 28.10 +43 16 40.0	CST	--	8.90 - ? p
0.676	<input checked="" type="checkbox"/> NSVS 2146219+434351	21 46 21.92 +43 43 50.9	M	205.0	10.70 - 12.50 R1
0.766	<input checked="" type="checkbox"/> Q Cyg	21 41 43.90 +42 50 29.0	NA	--	3.00 - 15.60 V
0.801	<input checked="" type="checkbox"/> NSVS 2140216+441557	21 40 21.65 +44 15 56.9	L:	233.0	11.01 - 11.92 R1
0.803	<input checked="" type="checkbox"/> V0646 Cyg	21 40 20.90 +44 16 00.0	M	310.4	13.60 - 17.00 p
0.806	<input checked="" type="checkbox"/> NSV 25768	21 47 01.20 +43 47 48.0	LB:	--	11.10 - 11.20 R
0.986	<input checked="" type="checkbox"/> NSV 25729	21 39 54.00 +44 25 55.0	--	--	6.30 - 7.10 V

Figure 5. Search Results Page.

3. 4. Detail Sheet Page

The Detail Sheet page (Fig. 6) presents all available information for a single object and is automatically displayed when a search of the database results in only one matching record, or when a single object is selected from a results list presented on the Search Results page.

The Detail Sheet page is divided into several sections: basic data, link-outs, images, comments and revision history.

The basic data section shows the object name, the AAVSO Unique ID, J2000 and B1950 coordinates, variable type, spectral type, magnitude range, references to the discovery study and finder charts for the object, epoch, outburst year (for N and SN type variables), period, rise duration, and original remarks. This section also includes a button for adding new catalog names as cross-identifications to the target object.

Detail Sheet [ID=10939]

Viability of names from SIMBAD may be set from Preferences.

Name SS Cyg

AUID BBN-938

Other names (+SIMBAD)	1H 2140+433	2E 4511	1RXS J214242.6+433506
1E 2140.7+4321	2E 2140.7+4321	2E 4511	2EUV E J2142+43.6
2RE J2142+433	3A 2140+433		AAVSO 2138+43
ALS 11959	BD+42 4189		BD+42 4189a
CSi+42 4189 1	EM* CDS 1268		EUVE J2142+43.6
GCRV 13641	GEN# +1.00206897		HD 205697
HV 84	INTEGRAL I 121		KPD 2140+4321
LSB+43 24	PLX 5240		RE J2142+433
RE J214241+433511	SBC7 872		SV* HV 84
TYC 3196-723-1	UBV M 50941		UCAC2 46852538
USNO 568	X 21407+433		[BM83]X2140+433
[FS2003] 1134	[KW97] 59-12		

J2000.0 21 42 42.80 +43 35 10.0

B1950.0 21 40 44.50 +43 21 23.0

Var. type UGSS

Spec. type K5V+pec(UG)

Mag. range 7.70 - 12.40 V

Study ref. J.A. Mattei, JRAS Can 74, N5, 317- 320, 1980.

Chart ref. F.Lenouvel, J.Dagullon, JO 39, N1, 9, 1956.

Epoch --

Outburst --

Period (49.5)

Rise dur. --

Remarks SB2 (P = 0.27512995d [08285]). During maxima of brightness there are oscillations of light and X-ray flux with amplitudes about 0.002m V and periods changing between 7.29s and 10.90s [06102, 09032].

Link-outs

Location -- Select -- Go Select a Location for more details.

Images

- SIMBAD
- SIMBAD Clickable Map
- VizieR Coordinate Search
- Aladin Previewer
- Aladin Java Applet
- CDS Bibli (840 references)
- ADS Biblio
- GCVS
- Downes
- AAVSO Charts
- AAVSO Light Curve
- AAVSO Quick Look
- SkyGX

Size 5' x 5' (297 x 298 pixels)

Center 21 42 42.80 +43 35 10.0 (J2000)

Source STScI

Survey POSS2/UKSTU

Red, all sky, 1.0 arcsec/pixel

Negative

Comments

There are currently no additional comments filed for this star.

Revision History

Currently approved revision is checked.

1 Admin, VSX 10/09/05 07:29 AM Initial database population.

Figure 6. Details Sheet Page.

The Link-outs section provides a context-sensitive drop-down menu for selecting and accessing various external Web resources relevant to the target object, including SIMBAD, VizieR, Aladin, CDS and ADS bibliographical indexes, ASAS, NSVS, SDSS, GCVS, Downes, and AAVSO charts, light curves, and Quick Look data.

The Images section can display, upon request, a 5'x5' or 7'.5x7'.5 image centered on the target object, extracted from the Digitized Sky Survey at the Space Telescope Science Institute. Various surveys are available to choose from, including POSS2/UKSTU, DSS1, POSS1, QuickV and HST Phase 2. The im-

ages can be viewed in either negative or positive transformations.

The Comments section provides a preview of comments that have been submitted by VSX users for the target object. Clicking on a comment preview shows the Comment page where the entire comment may be read. New comments may be submitted by clicking the Add Comment button found in this section.

Finally, the Revision History section displays the complete history of revisions submitted for the target object and, for each revision the listing, includes the submitter's name, the date and time of the revision, and a preview of the attached revision comment.

3.5. Revision Submission Page

Submit Revision

Red bar fields are required.

Do not navigate from this page without using the Submit Revision or Cancel button.

Name SS Cyg

Position 21 42 42.80 +43 35 10.0

Var. type UGSS

Spec. type K5V+pec(UG)

Max. mag. 7.7 Amplitude Uncertain

Min. mag. 12.4 Amplitude Uncertain

Passband V (Johnson visual)

Epoch -- JD

Outburst Uncertain

Period 49.5 d Uncertain

Rise dur. % Uncertain

Class Variable

Label

Supporting commentary

NOTE

- Your IP address (127.0.0.1) and user info will be saved with this submission.
- Please make certain all above details are correct before submitting revision.
- Input will be checked for errors and, if any, an opportunity to correct them given.
- All revision submissions must be approved before appearing in the live database.

Cancel Reset Submit Revision

Figure 7. Revision Submission Page.

The submission of revisions to the data for existing objects is accomplished on the Revision Submission page (Fig. 7). This form is accessible from the Detail Sheet for any object. On this page, all the editable fields of the object record are presented in a single form. This interactive form provides visual feedback as to which of the fields have been changed and

also indicates which data are required in any revision submission. A unique custom label and brief commentary supporting the revision must be provided.

Also available from this page is the ability to add new catalog names and cross-identifications to the target object. When an object in the VSX database is in the process of being revised, it is placed in a “locked” state, and cannot be modified by any other user on the system until such time as the lock is released by either the cancellation or completion of the active revision session.

When submitted, revisions are “staged” in a separate table in the database for review purposes. Data moderators then review the revision and assign a status to it. If the status for the revision reaches that of “approved”, the revision is moved to the main object table, and the revised data is then presented as part of any search results, as well as on the Detail Sheet for the object.

Submitters of revisions have the option of receiving system-generated e-mail messages when the status for specific revisions submitted by them has changed.

3.6. Submission Method

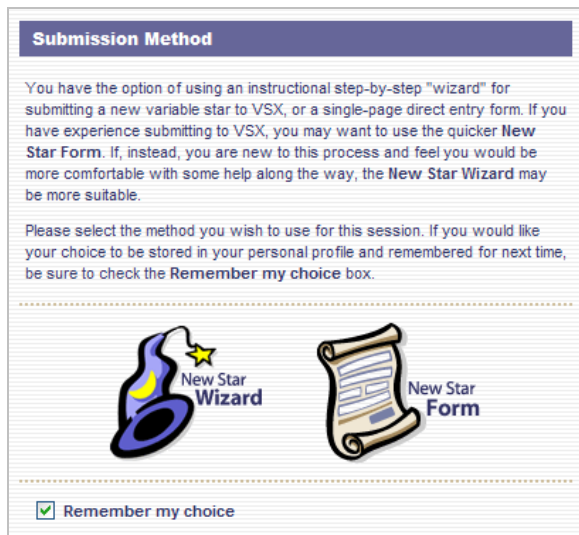


Figure 8. Submission Method Page.

Submitting a newly discovered variable star to VSX is a relatively simple process that can be accomplished in one of two ways: via an expert-level single-page form, or a novice-level multi-page “wizard”. When selecting the Submit function from the VSX main menu, the user must make a choice as to which of these two methods will be employed to complete the submission on the Submission Method page (Fig. 8). The user can elect to make the pre-

ferred method the default choice for a particular login.

3.7. The New Star Form

Figure 9. The New Star Form.

The New Star form (Fig. 9) is a simple single-page form for submitting new variable star discoveries to VSX. It is the quickest and easiest method for adding a new variable star to the database, and is typically used by experienced VSX users who do not require the additional help and directions provided by the Wizard interface (§ 3.8).

When a new variable star is submitted, the data provided is stored in a “staging” table in the database for review purposes. Data moderators review the submission and assign a status to it. If the status for the submission reaches that of “approved”, the submitted data is moved to the main object table, and made available to the Search interface. New variable star submissions to VSX are assigned a provisional IAU-approved designation in the format **VSX JHHMMSS.S+DDMMSS**.

3.8. The New Star Wizard

The New Star Wizard (Figs. 10, 11 and 12) replicates all the input fields from the New Star form (§ 3.7) but presents them in an easy-to-follow multi-page “wizard”-like format. In this manner, the submission of data for a new variable star is accomplished in several steps, each accompanied by helpful directions and complete descriptions of the data required. For those with less experience submitting data to VSX, or those that require some guidance on what to enter into the fields, this method is optimal.



Figure 10. New Star Wizard – Introduction.

The submitter can navigate forward or backward among the pages in the wizard, and all field inputs are remembered, step for step. The last step in the

wizard displays a complete listing of all the input from the previous steps, and provides an interface for directly jumping to specific pages within the wizard to make any necessary modifications prior to submital. Data submitted via the New Star Wizard is dealt with in the same manner by the system as data submitted through the New Star form.

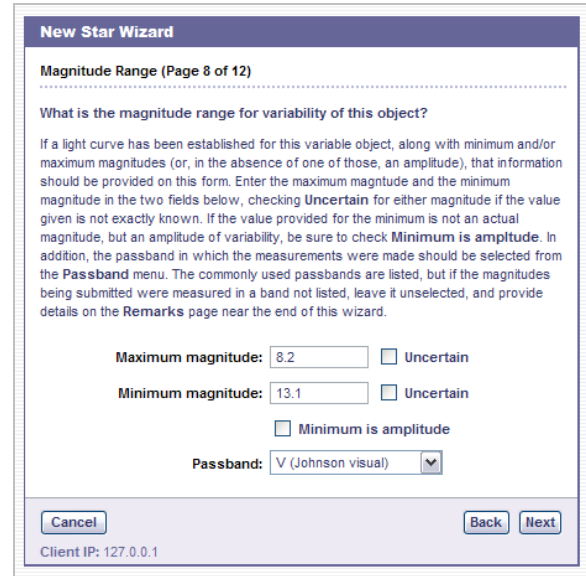


Figure 11. New Star Wizard – Magnitude Range Input.

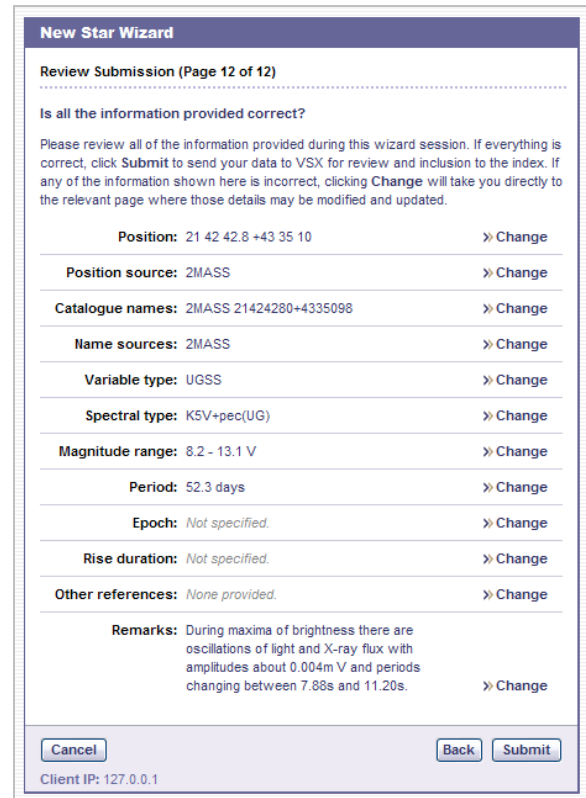


Figure 12. New Star Wizard – Final Review Page.

3. 9. Registration

NOTE Creating a Login with VSX
Use the form below to create a login at VSX. With a valid login, you will be able to submit revisions and comments on variable stars currently in VSX, and make proposals for the addition of new variable stars. Just fill out the form and click the Register button. A confirmation message will be e-mailed to the address provided which contains a registration confirmation link that you will need to click to activate your login.
Thank you for your interest in contributing to VSX.
Clear skies,
VSX Administration

Login Details
Red bar fields are required.

First name
Your given name, including any middle initials.

Last name
Your family or surname.

E-mail
Your primary e-mail address.

Confirm e-mail
Must match e-mail address above exactly.

Country
The country in which you reside.

User name
Name used to log in (6 to 12 characters).

Password
New password to use when logging in.

Confirm password
Must match password above exactly.

Figure 13. Registration Page.

In order to add new variable stars to the VSX database, and to make revisions or add comments to existing variable stars, a user of the VSX system must create a password-protected login via the Registration form (Fig. 13).

The system sends a confirmation e-mail message to the individual applying for a login, and once the user’s identification has been validated through a return link included in the message, the user may immediately log in and submit data. The VSX Web site provides full search capabilities to all visitors, even those without a login, but submission of new or revised data requires that the submitter be logged in to the system. Other features of the Web site are also not available unless one is logged in.

3. 10. Account Access

All details of a VSX user’s profile on the system can be accessed under login and modified from the Account page (Fig. 14). A user profile is created when a user first confirms their registration, and this profile contains information such as mailing address, telephone numbers, affiliations, observer code (if the user contributes observations to the AAVSO), personal or professional Web site address, and other comments. Personal information given to VSX is not shared or sold to any other organization outside of the AAVSO.

NOTE Editing Your Account Info
Use the form below to make any changes you desire to your VSX account details. If your name or e-mail address has changed, or if you wish to change your user name on this system, you will need to register for a new login with VSX. Otherwise, make your changes in this form and click Update.

Profile Details for VSX Admin
Red bar fields are required.

Address 1
Street address for your primary residence.

Address 2
Continuation of address (Apt., Ste., M/S, etc.)

Address 3
Additional address information, if needed.

City
The city for the above street address.

State ZIP
State or province. ZIP or Postal code.

Country
The country for the above street address.

Day Phone
The telephone number at which you may be reached during the day.

Night Phone
The telephone number at which you may be reached in the evening.

Fax
Telephone number for fax communications.

Affiliation
Company or organization with which you are affiliated.

Obs. Code
If you are an AAVSO observer, your observer code.

Web site
If you operate a relevant web site, the URL for it.

Comments
Any additional comments you would care to add.

Figure 14. Account Page.

3. 11. Staged Submissions

All submitted revisions to existing variable stars, new data submitted for variable star discoveries, new cross-identifications, and uploaded supporting documents are “staged” in separate tables within the VSX database and are not immediately made available to the public. Submissions in these categories are reviewed by authorized moderators before being promoted to the publicly-accessible tables. Moderators logging in to the VSX system are presented with notice that there are submissions waiting in the queue to be reviewed. Specialized tools available only to the moderators are then used to review and disposition the submissions. The Staged Submissions page (Fig. 15) lists all submissions needing review. Any sub-

mission can be reviewed individually by clicking on its name or title.

Name	Status	Submitted by	Date/Time	Comment
Z UMi	Revision	Dill, Albert	2006-03-28 20:47 UTC	2005AJ...130:2295Z
VSX J022253.2+463034	New	Munkacsy, Mark	2006-03-17 20:56 UTC	139 comp star on AAVSO AX And (f) chart
HQ Mon	Revision	Bonnardeau, Michel	2006-03-17 19:20 UTC	A cataclysmic variable (not a RV). Reference: G.M. Wahlgren et al (1985) BAAS 17 589. It is already listed in VSX as a UK.
CK Aqr	Revision	Bonnardeau, Michel	2006-03-17 19:05 UTC	Type is EW (and not DSCT as 1st observations suggested). Reference: J.F. Le Borgne, E. Poretti, A. Figer (1989) BV5 3316.
VSX J073237.6-133309	New	Bonnardeau, Michel	2006-03-16 08:42 UTC	Probably an IP
VSX J064034.6-375011	New	Bedient, James	2006-03-16 05:30 UTC	The ASAS-3 database has good coverage of this object.
VSX J161429.8+344526	New	Huziak, Richard	2006-03-15 22:33 UTC	New var discovered by MIZ April 05
VSX J161614.3+344806	New	Huziak, Richard	2006-03-15 21:54 UTC	New variable discovered by MIZ in Agr 05. Star was listed as a comp star for TV Her up to the 599 AAVSO chart. B-V -0.1

Figure 15. Staged Submissions page.

3.12. Review/Addition Review

Revisions submitted for existing variable star records, as well as data submitted for new variable star discoveries, are reviewed in detail on the Revision/Addition review page (Fig. 15). For revisions, this page displays in clear distinction the differences between the most recent revision of the record and the revision being reviewed. The basic data for both revision levels are displayed side by side, with differences clearly color-coded.

For new data on discoveries, only the submitted data is displayed. The status for the revision/addition is then set by the moderator. If marked as Approved, the relevant data is moved to the publicly-accessible tables by the system automatically. No database administration skills are necessary for moderators.

3.13. Submitted File Review

Submitted revisions that are accompanied by the upload of supporting documents (such as light curve plots and/or finding charts) are reviewed on the Submitted File review page (Fig. 17). The content of the uploaded file may be viewed by the moderator, and the basic parameters for the file, as stored in the VSX system, can also be reviewed. As on the Revision/Addition review page, the status for the uploaded file is set by the moderator, and if marked as Approved, the file is made available in the listing of Supporting Documents on the Detail Sheet for the pertinent star.

3.14. Submitted Catalog Name Review

New cross-identifications submitted for any existing object in the VSX database are reviewed by the moderators in much the same way as revisions/additions and uploaded files are reviewed, on the Submitted Catalog Name review page (Fig. 18).

Previous Revision		Revision 1	Current Revision		Revision 2
Fields being revised are shown in green.			Revised fields are shown in red.		
Name	CK Aqr		Name	CK Aqr	
J2000.0	21 01 02.30 -11 04 27.0		J2000.0	21 01 02.30 -11 04 27.0	
B1950.0	20 58 19.20 -11 16 15.0		B1950.0	20 58 19.23 -11 16 14.7	
Var. type	DSCT		Var. type	EW	
Spec. type	--		Spec. type	--	
Mag. range	12.90 - 13.80 p		Mag. range	12.86 - 13.47 V	
Epoch	04 Sep 1961 (JD 2437547.3190)		Epoch	04 Jul 1987 (JD 2446980.9290)	
Nova year	--		Nova year	--	
Period	0.12406245		Period	0.2833	
Rise dur.	45%		Rise dur.	--	
Submitted: Mar 17, 2006 at 19:05:46 UTC by Bonnardeau, Michel					
Comment: [EW (and not DSCT)] Type is EW (and not DSCT as 1st observations suggested). Reference: J.F. Le Borgne, E. Poretti, A. Figer (1989) BV5 3316.					
Select an appropriate status and click Assign Status.					
Cancel			Revision	Assign Status	
			New		
			Revision		
			Reviewed		
			Pending		
			Rejected		
			Approved		
» Copyright » Privacy » Contact » Bugs					
The International Variable Star Index © 2005-2006 The American Association of Variable Star Observers (AAVSO) Version 1.0b1					

Figure 16. Review/Submissions page.

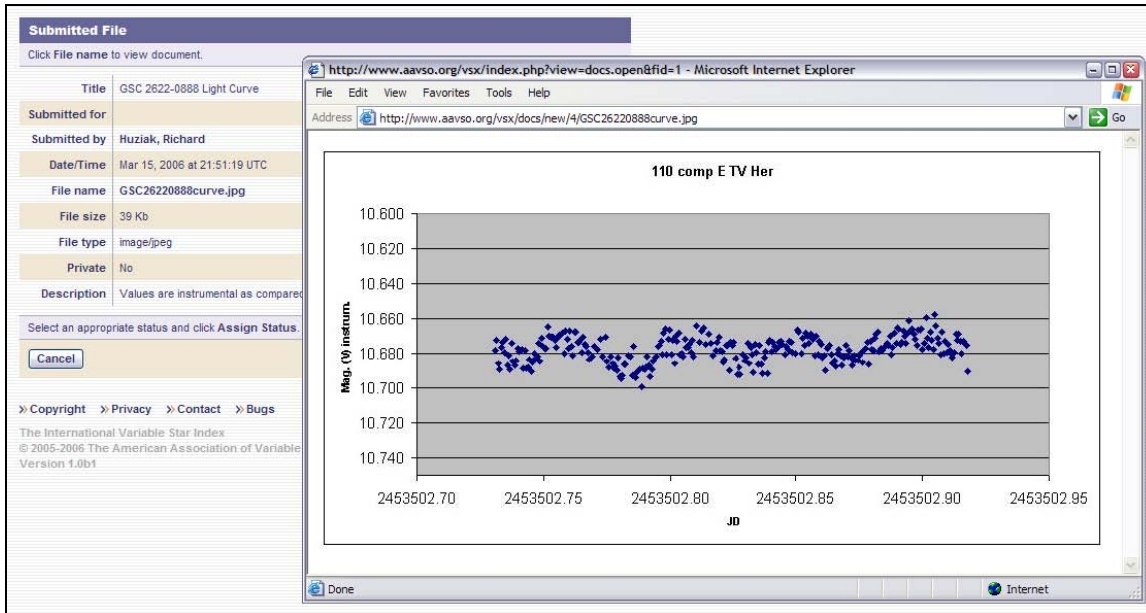


Figure 17. Submitted File Review page.

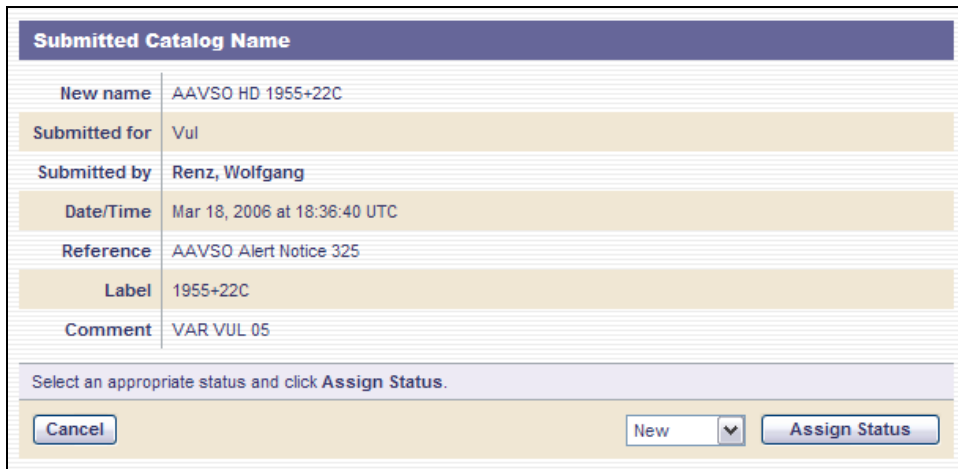


Figure 18. Submitted Catalog Review page.

4. Site Maintenance

The AAVSO owns and maintains the VSX database and Web site, and the day-to-day upkeep of the VSX system falls to AAVSO staff and volunteers. On occasion, newly published variable star catalogs may be imported to the database by the system administrators.

Volunteer data moderators with extensive experience in variable star science and database systems regularly review all user-submitted revisions and

reported discoveries for completeness, accuracy, and suitability before being made available via the Web interface.

A separate Web-based issue tracking system, also maintained by the AAVSO, accepts bug reports and feature suggestions from VSX users. The Web application code is managed through a source and version control system, and is updated as necessary to fix reported bugs, or to improve the system.

CCD Photometry from a Small Observatory in a Large City

Jennie McCormick
 Farm Cove Observatory
 CBA Pakuranga and MicroFUN Farm Cove
 2/24 Rapallo Place
 Pakuranga, Auckland, New Zealand
 farmcoveobs@xtra.co.nz

Abstract

Since 2000, Farm Cove Observatory in Auckland New Zealand has contributed observational data to several international collaborative teams. During this time, the author has supplied 1339 hours of data to the Center for Backyard Astrophysics, directly contributed to the co-discovery of the extra-solar planet, OGLE-2005-BLG-071 and has discovered three new eclipsing binary stars. The observational data from FCO has now been used in a number of peer-reviewed scientific publications. This paper describes the observatory equipment, the software used, and provides details on the observations carried out for the international collaborative teams. The paper demonstrates what can be achieved using a small telescope in a large city. © 2006 Society for Astronomical Sciences.

1. Introduction

Farm Cove Observatory (FCO) is situated in New Zealand's largest city, Auckland, (population ~1.3 million) and is sited close to sea level on the banks of the Waka-aranaga Reserve in the eastern suburb of Pakuranga.

The observatory was constructed in 1999 and has clear unobstructed views of the eastern, northern, and northwestern skies. Unfortunately, the house, neighboring structures, and trees obscure a large area of the southern sky below 40° elevation.

The observatory is privately owned and operated by the author and currently contributes data to several international research collaborations (Figure 1).

Since 2000, the primary research has been time series photometry of Cataclysmic Binary stars for the Center for Backyard Astrophysics (CBA) (Patterson 1997). Professor Joseph Patterson from Columbia University, New York heads the team. Farm Cove Observatory is known within the group as CBA Pakuranga.

In 2004, observations commenced on gravitational microlensing events for the Microlensing Follow-up Network (MicroFUN) (Gould 2006). This group consists of an international collaboration of professional astronomers supported by a small group of amateurs. In 2005, FCO took part in the co-discovery of OGLE-2005-BLG-071, the second extra-solar planet discovered using the gravitational microlensing technique (Udalski 2005). Farm Cove Observatory is known within this group as MicroFUN Farm Cove. Professor Andrew Gould from

Ohio State University (OSU) leads the MicroFUN team.

Since December 2005, FCO has contributed regular magnitude measures on Blazer OJ+287 for the British Astronomical Association (BAA) (Pietila 1998).

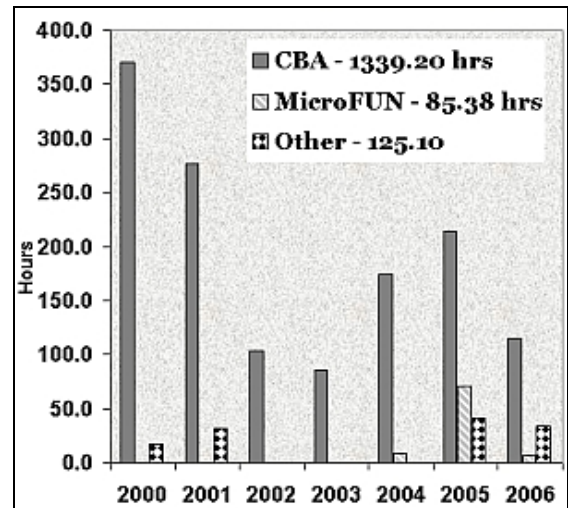


Figure 1. FCO data acquisition since January 2000.

2. Observatory Equipment

FCO operates one of the first Go-To telescopes manufactured by Meade - an LX200 25cm f/10 telescope (Figure 2). A focal reducer is not used with this system. The telescope is mounted on a custom-made wedge and supported by a permanent pier. This particular telescope has proven to be a very reliable re-

search tool and to date, no operational or electronic problems have been encountered.

The recent purchase of a DewZee dew control and light baffle (Resource International, San Jose, CA) for the optical tube has proved successful. A small number of modifications were made to the baffle to allow for extra rigidity and a snug fit over the tube. This product was purchased solely as a light baffle to reduce stray light entering the telescope from neighboring properties. It is also used in conjunction with a Kendrick Dew Remover. (Kendrick Astro Instruments, Toronto.)



Figure 2. Meade LX200 25cm / SBIG ST7e

An SBIG ST7E dual chip CCD camera is on permanent loan from the CBA. The separate auto-guiding chip is an important feature of this camera because it allows for accurate tracking during long exposures on faint MicroFUN targets. The longest exposures used routinely are 300s duration. All data are currently acquired without filters.

The small CCD chip, 765 x 512 pixels, gives a field of view of 9.6 x 6.4 arc-minutes when operating at f/10. The size of the chip does not produce any significant disadvantages to the work carried out at FCO. All comparison and check stars can be found within the field of view making the need for a larger chip unnecessary. The major advantage of the smaller image size is the shorter image download time and smaller FITS files for ease of handling and storage.

The image scale is 0.75as/pixel in 1x1 binned mode (2.25as/pixel with 3x3 binning).

All CBA and magnitude measure photometry is imaged in 3x3 binning mode and matches well the typical seeing Full Width Half Maximum (FWHM) of 2.5-3.5arc-sec (Figure 3). Only in fields of very high stellar density are 1x1-binned images used.

The telescope and computers are networked to the house, making it possible to monitor and control the CCD camera and telescope from a warm and comfortable environment. The dome is rotated by hand; this requires regular repositioning over the course of the night.

3. Data Acquisition and Telescope Control

Several software packages are used for data acquisition, telescope control, and data processing. The ability to pick and choose the best features from each package is essential because no single product is currently available to satisfy all these requirements.

The images are acquired using CCDSOFT V (Software Bisque, Golden CO). This package has a user-friendly interface, allowing for efficient control of both the camera and guide chip. The only disadvantage encountered with this product is an inability to display a large display window giving FWHM values and other important information during focusing.

The Sky Version 5 (Software Bisque, Golden CO) is used for telescope control, image recognition and is an excellent aid for check star identification. This software integrates closely with the Meade LX200 and has proven to be a very stable and reliable program.

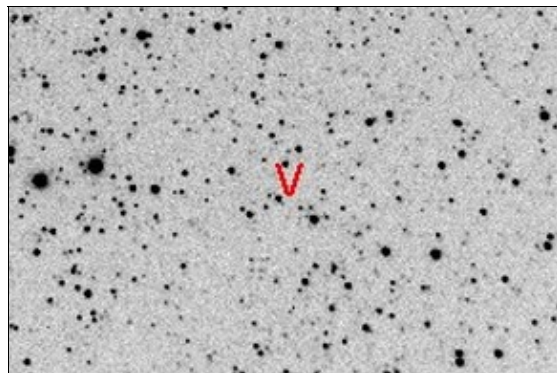


Figure 3. Calibrated 3x3 binned 20s CCD image of WX Cen (north up, east left)

4. Calibration Procedures

All dark and flat field frames are calibrated and stored in libraries as masters. These are typically used

over a period of 60 days. Each master frame consists of approximately 30 median averaged frames and in the case of flat fields, the appropriate master dark frame is subtracted.

Flat fields are produced using a 5mm white plastic sheet, which is fitted securely into place over the light baffle (Figure 4). A red darkroom light is used to illuminate the interior surface of the dome. This has proved to be a quick and effective procedure when time constraints are present and it consistently produces evenly illuminated calibration frames.

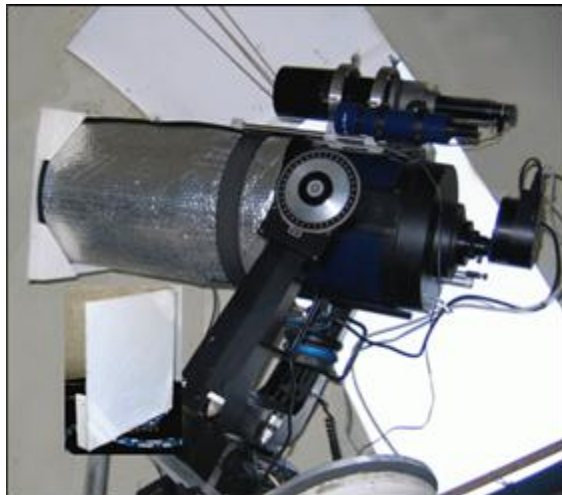


Figure 4. Flat field board fitted to the telescope.

5. Photometric Reductions

Almost all photometry carried out at FCO is done differentially. Given that a full night observing run can produce ~1000 FITS format data frames, a reliable and versatile reduction program is essential. The primary requirement is the ability to automatically calibrate each FITS image frame and then measure the differential magnitude of all stars within the field.

This is accomplished using the freeware Windows software MuniWin/C-MuniPack (Motl). It has been specifically designed for efficient reduction of up to 1000 frames for time series photometry and has a simple, intuitive user interface. All CBA data is processed through this software package.

CCD Soft V5 is used for quick and easy flat field and dark frame calibration on numerous folders of images. It is especially useful when MicroFUN requires calibrated frames immediately for gravitational microlensing events.

MaxIm DL (Diffraction Ltd, Ottawa, Canada) complements both MuniWin and CCDSoft. This package allows for comprehensive image analysis on all frames where necessary, and handles individual accurate photometric reductions when required.

Reduced data are submitted by email in simple text format while calibrated CCD frames are uploaded to a nominated FTP server if necessary.

6. Target Selection

There are benefits to being an independent observer. Perhaps the two most important of these are the freedom to pick and choose observational projects of interest and the ability to re-assign all telescope time at short notice. With this in mind, it is possible to observe two or even three targets over the course of a night. Naturally, this depends on what observations are required and the rise and set times of each object.

The CBA communicates monthly observation target lists for both northern and southern hemisphere observers. In the case of FCO, the small aperture size of the telescope often dictates which target will be observed. For many of the CBA targets, short exposure times are preferred as the stars commonly exhibit phenomena on time scales of a few hours and in many cases, a few minutes.

Short exposure times are required to adequately sample high frequency signals in data (e.g rotation rate of a white dwarf), but unless the star is bright, this reduces the signal-to-noise ratio (SNR). In most cases achieving both an acceptable SNR and an adequate sampling frequency requires a compromise. In practice at FCO, if the white light magnitude lies in the range 13-15 then exposure times of 15-30s still gives a useful SNR. Any fainter than this and longer exposures become essential.

Moreover, if the expected amplitude of the signal is large, then accepting a lower SNR (and hence allowing a faster sampling frequency) may be a better option.

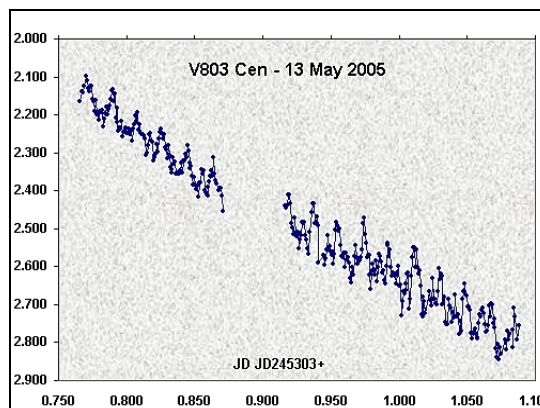


Figure 5. Example of V803 Cen (Patterson 2000) light curve from FCO showing a strong periodic signal.

MicroFUN gravitational microlensing targets are seasonal due to the visibility of the galactic bulge. All

observations are made in this region of sky because of its high stellar density, increasing the probability of detecting gravitational microlensing events. Accessibility of the galactic bulge in early autumn (March), allows for limited observations from 3.00am local time. During the winter months (April through August) the bulge passes almost overhead in Auckland and is accessible throughout most of the night.

Due to the limited size of the telescope, only high magnification events are observable at FCO. However, these are the times when the sensitivity to detecting planets is at its greatest. Typically, targets as faint as magnitude 18 in white light are observable. At these faint magnitudes, exposures of 300s are used together with the autoguider. This guarantees accurate tracking will be continually maintained throughout the observations.

Working in the galactic bulge can cause problems due to the crowded fields. However, this is offset by the numerous stars available for auto-guiding, allowing long exposures.

In very crowded fields aperture photometry is impractical. Instead, the calibrated images are uploaded by FTP and processed through the OSU photometry pipeline, which uses DOPHOT (Schechter 1999).

Magnitude measures and other observations can be made at any time during a CBA or MicroFUN observing run. The observations carried out on Blazer OJ+287 (Pietila 1998) for the BAA consist of approximately twenty 60s integrations. These are calibrated and then averaged to obtain a single accurate magnitude measurement. Such a short interruption during primary observations has, thus far, caused no major inconvenience to the primary observing programmes.

Three new eclipsing binary stars were discovered while observing CBA targets in 2005 and 2006. (McCormick 2005) Each of the discoveries were found in a CBA target field, a task made possible by MuniWin and its ability to extract differential photometry for all stars in a CCD image (Figure 6).

7. Conclusions

Despite the disadvantages of an urban location and a small telescope, Farm Cove Observatory has been able to contribute observations to several astronomical research collaborations. These have proven to be successful partnerships as many of the observations obtained are used and published in peer-reviewed journals.

The flexibility to change observing programs at short notice is a key factor to the successes obtained

as demonstrated by the co-discovery of extra-solar planets using gravitational microlensing techniques.

CCD photometry presents constant challenges and offers a wide variety of observational opportunities. It is a particularly stimulating field to work in, providing both a high level of personal satisfaction as well as the opportunity to make a useful contribution to the science of astronomy.

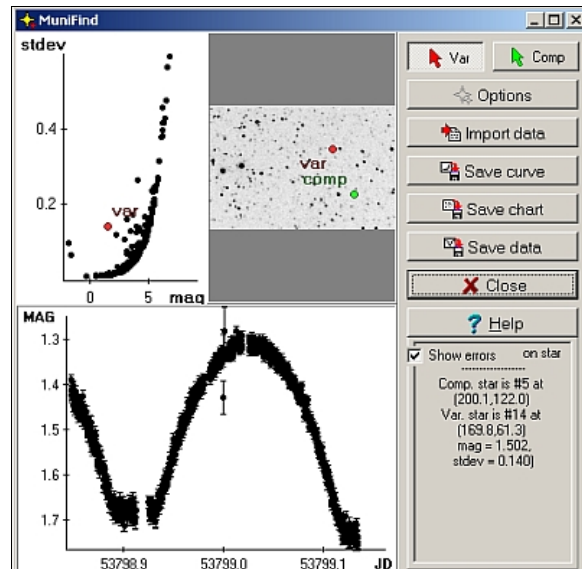


Figure 6. MuniWin extractive photometry (Find Variable) window.

8. Acknowledgements

Professor Joseph Patterson, Center for Backyard Astrophysics at Columbia University, for the permanent loan of the SBIG ST7e CCD camera and his many kind words of encouragement and support.

Professor Andrew Gould and the MicroFUN team at Ohio State University for their support and guidance throughout the gravitational microlensing seasons.

Fred Velthuis, Dr Grant Christie and Tim Natusch for their technical support and advice with the operation of Farm Cove Observatory.

9. References

Gould, A., Udalski, A., An, D., Bennett, D.P., Zhou, A.Y., Dong, S., Rattenbury, N.J., Gaudi, B.S., Yock, P.C.M., Bond, I.A., Christie, G.W., Horne, K., Anderson, J., Stanek, K.Z., DePoy, D.L., Han, C., McCormick, J., et al. Microlens OGLE-2005-BLG-169Lb Implies Cool Neptune-Like Planets are Common, *ApJ*, to appear (2006)

McCormick, J., Christie, G.W. New Eclipsing Binary Star USNO-A2.0 0675-31638784, IBVS 5700, No 54 (2005)

Motl, D. C-MUNIPACK package of software utilities for reducing astronomy CCD images. <http://integral.sci.muni.cz/cmunicipack/index.html>

Patterson, J., Kemp, J., Skillman, D., Harvey, D., Vanmunster, T., Jensen, L., Fried, R., McGee, P., Walker, W.S.G., Retter, A. Cataclysmic Variables with the CBA, AAS (1997)

Patterson, J., Walker, W.S.G., Kemp, J., O'Donoghue, D., Bos, M. and Stubbings, R. V803 Centauri, A Helium-Rich Dwarf Nova. PASP 112, 625 (2000)

Pietila, H. Possibilities and Predictions of the OJ 287 Binary Black Hole Model, ApJ 508, 669 (1998)

Schechter, P.L., Mateo, M., Saha, A. DOPHOT, a CCD photometry program, description and tests. PASP 105, 693 (1999)

Udalski, A., Jaroszynski, M., Paczynski, B., Kubiak, M., Szymanski, M.K., Soszynski, I., Pietrzynski, G., Ulaczyk, K., Szewczyk, O., Wyrzykowski, L., Christie, G.W., DePoy, D.L., Dong, S., Gal-Yam, A., Gaudi, B.S., Gould, A., Han, C., Lepine, S., McCormick, J., Park, B.G., Pogge, R.W. et al. A Jovian-mass Planet in Microlensing Event OGLE-2005-BLG-071, ApJ 628, L109 (2005)

Faint CV Monitoring at CBA Pretoria

L. A. G. Berto Monard

Bronberg Observatory / CBA Pretoria

PO Box 11426, Tiegervoort 0056, South Africa

lagmonar@csir.co.za / bmonard@mweb.co.za (home)

Abstract

The regular monitoring of faint cataclysmic variables (CV) is one of five observing programs that are run at CBA Pretoria. It started off in 2002 with about 120 CVs and related objects in the program. The intention was to observe those targets as often as possible with unfiltered CCD. There were continuous additions of more CVs by digging deeper in the CV atlas, new finds, and reclassified stars while some were taken off the list. At the end of 2004 the number of CVs in the observing program exceeded 200. With only one telescope and one observer and so many other things to observe, the actual number of snapshot CV observations have been much less than hoped. Despite this, the program has shown to be very successful. Publications have been referring to reported findings from this program while even more publications resulted from observing campaigns (time resolved photometry) dedicated to CVs that were found in outburst by observations at CBA Pretoria. In most cases they were the first real-time outburst detection of that CV. The present paper will not deal with those published or alerted finds but will show observing results of other CVs from the list just to give an indication of the broader meaningfulness of such a program. A selection of fifteen light curves obtained after three years of monitoring will be shown and discussed. The choice of the 15 stars was based on their possible interest and the fact that they have been positively observed on most occasions, since they were mostly brighter than magnitude 18 CR (unfiltered with red zero-point).

1. Introduction

CBA Pretoria is housed at the Bronberg Observatory, 40 km East of Pretoria Centre at coordinates $25^{\circ} 54' 32''$ S, $28^{\circ} 26' 18''$ E and an altitude of 1590m.

The site is located on top of the Bronberg ridge, which stretches from Pretoria to just east of the observatory.

The observatory was built in 2001 to initially provide shelter and an observing platform for visual observations with a 32cm Newtonian telescope and with the aim of later housing a SCT with CCD camera for dedicated participation in the CBA network. The first real observing success came on 16 Sep 2001 with the visual discovery of supernova SN 2001el in NGC 1448.

Beginning in 2002, the observatory was equipped with a 30cm Meade LX200 classic (Schmidt-Cassegrain GOTO) telescope with CCD camera SBIG-ST7. Combined with a focal reducer (3.3x) it gives an effective f/3.7. A filter wheel with BVRI filters was added in Dec 2004.

The observing instrumentation was pier mounted and polar aligned for easy access and immediate observing.

2. Observing Programs at CBA Pretoria

Unless mentioned differently observations are done with unfiltered CCD.

2.1. Time series photometry

The program started at the beginning 2002 as part of the CBA network to study the behaviour of CVs from observations taken over periods of weeks at different time zones. Observations were also done in collaboration with VSNET campaigns and simultaneously with satellite observations as organized by AAVSO, VSNET, or individual astronomers. Regularly, exploration targets are measured, usually one year old novae, newly found bright CVs, exoplanets for eventual transits, a minor planet, and even a comet that happened to pose on the images of the observed CV.

2.2. SN Searching

The present search program consists of about 1500 galaxies, of which 100 are primary and 600 are secondary targets. This classification is based on the

expected SN production of the listed galaxies and the frequency of observations is planned accordingly.

2. 3. Faint CV Monitoring

This program started off with 170 targets in early 2002 and extended to over 220 targets in 2005. It is further being optimized for maximum value. The idea was to observe those CVs as often as possible.

The plan for the future is to prioritize, to settle for a smaller number of listed CVs, and to observe those more often.

2. 4. TOO

Observations to follow up on transients – XT, GRB, novae, etc. – and unusual objects when alerts are made via the Internet. Bright objects are usually observed filtered in V and R_c . Astrometry is sometimes applied on the images to improve the reported coarse coordinates or in case of nova confirmations. GRB observations are reported to AAVSO-HEN.

2. 5. Southern Symbiotic Stars

Started at the end 2004, this project aims to monitor monthly all known and suspected Z And systems in the Southern Hemisphere in the V band. About 200 targets are presently listed. Not much is known about most of those symbiotic stars. In addition to light curves, some interesting developments (eclipsing systems, Mira pulsations of the secondary, symbiotic novae) will be observed in the years to come.

3. Faint CV Monitoring Program

The purpose is to produce long term light curves of the program stars by regular monitoring of their brightness in terms of unfiltered CCD magnitudes (CR) relative to reference stars with a constant brightness and calibrated/derived R_c magnitude. Of specific interest are the evolution between low and high activity states of magnetic CVs (polars and intermediate polars), the occurrence of outbursts in dwarf novae and novalikes, fading episodes of VY Scl type CVs, and activity of Xray binaries.

Long term lightcurves will assist the astrophysicists with type characterization of lesser known or 'uncertain' CVs. In cases of an uncertain identification of the suspect CV, the stored images taken over a long period will eventually allow pinpointing the actual CV on the basis of brightness variations or outbursts.

The targets selected for this program originate from the CV atlas, X transient catalogs, and alerts. Only stars south of Declination +10 were considered.

The mixture of CV types on the observing list has been varied. Beginning in 2006, the list comprised 211 targets.

- 44 Non-typed CVs
- 49 Known and suspected dwarf novae (ug)
- 10 Known and suspected DQ Her stars (IP, dq)
- 49 Known and suspected polars (am)
- 7 LMXB and XN
- 6 Novalikes (ux, nl, vy, sw sex, non-types)
- 4 Known and suspected AM CVn types (ibwd)
- 10 Known and suspected recurrent novae (nr)
- 9 Young novae (often monitored to see if modulation revealing time series are possible after more than one year after the explosion)
- 25 Known and suspected old novae for recurrence or other brightenings (non-cv sometimes)

Note that some CVs are documented with more than one possible classification. Therefore, in this case, the sum of parts is larger than the total.

In March 2006, the number of program CVs was reduced to 163. CVs scrapped from the list were mainly of type ug with outburst magnitudes brighter than 15 and young novae that became too faint.

4. Observations

4. 1. Procedure

Observing is done manually via a PC and the telescope control keypad. Images are taken using CCDOPS 5 and are stored in the FITS format. AIP4WIN is used for image calibration (dark and flat) and data processing (image stacking and differential photometry). Usually 2 to 5 images are taken per target depending on the expected brightness. After the calibration, images of acceptable quality are stacked for improved S/N and increased limiting magnitude. In this way, most CVs are monitored at the 18 to 19th magnitude level. Still, a fair amount of such observations remain negative most of the time.

4. 2. Photometric Accuracy

Although the observations are regularly reported and will possibly be kept in databases, the magni-

tudes cannot be considered very accurate. In the observing reports, it is stated that the derived CR magnitudes result from differential photometry to non-red comparison stars with R magnitudes. Those magnitudes are taken directly or derived from published photometric data or, lacking any thing better, UCAC2 magnitudes of constant comparison stars that are selected on the basis of non-red colour and reliability of the data.

In the latter case, R magnitudes of selected reference stars for the sequence are derived by the empirical formula:

$$R = O - 0.3 (J-K)$$

$$V = O + 0.7 (J-K)$$

O being the tabled UCAC2 magnitudes and J and K being published NIR magnitudes. The assumption is made that $J-K = V-R$, which is approximately valid. The advantage of differential (aperture) photometry is that without loss of accuracy (but gain in precision!) comparison stars can be selected that are about two magnitudes brighter than the measured star. In addition, this allows for an improved accuracy since validation can be sought by comparing the derived V values to those of ASAS3 data, which typically shows agreement to about 0.1V. The reference sequence is further improved by regularly checking the magnitude differentials between the major comparison stars on the acquired field images. This has been applied to a large extent to the V sequences of star fields for the symbiotic stars monitoring program.

Estimated uncertainties (errors) for observations in the CV program are typically 0.2-0.5 mag in accuracy and 0.1-0.3 mag in precision, much of this depending on the source of reference for the photometry and the faintness of the measured star.

In view of the program objectives, the precision is particularly important since it allows monitoring the small night-to-night variations in the magnitudes of the observed CVs. Since most of the brighter observed CVs have known orbital modulation amplitudes, actual changes in activity of the CV can be noticed from the data. In some cases, the cycle modulation amplitude of bright CVs (magnitude 17 or less) has been derived from time series photometry at CBA Pretoria.

Note: The drawbacks of unfiltered observing of CVs must be well understood in that the red/IR excess sometimes determines the measured brightness. This mostly concerns CVs that are strongly reddened or where the red light from the secondary is dominant during quiescence. This red/IR light is readily picked up by the NIR tail of the Si photosites, showing the

CV much brighter than it would from behind a V filter.

Even in those cases, the increased activity of the system manifested by means of an increased brightness at shorter wavelengths might still be picked up in unfiltered mode and certainly in the case of outbursts.

4.3. Observing Frequency

Observations are done as often as time, weather, and other observing priorities allow. Special efforts are made to follow up on interesting episodes or unusual behaviour of some of the program stars. Occasional flare-ups of stars like UZ can be picked up by dense monitoring. The past years have shown that due to other observing priorities, most program CVs have been under observed.

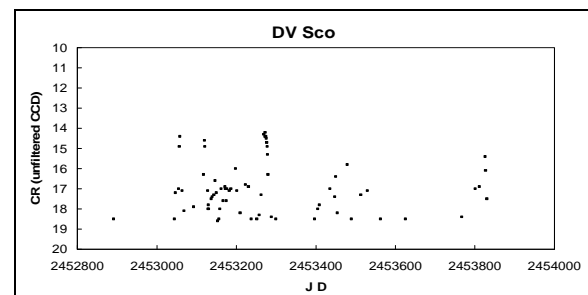
4.4. Past Successes

Most of the discoveries made by this observing program can be found in alerts, publications and timestudies. Timestudies of lesser known CVs that were observed to be in outburst at were also made at CBA Pretoria. Examples are: 2QZ J021927-3045, BZ Cir, DV Sco, V663 Ara and CTCV J0549-4921.

5. Discussion of Results After Three Years

Light curves of 15 faint CVs made over about three years are presented. They are tabled in alphabetical order in the table below with data from the CV atlas (Downes, Feb 2006). Findings are discussed and comments are given on the individual CVs. Quoted magnitudes refer to unfiltered magnitudes with red zero-point (CR) unless stated differently.

5.1. DV Sco

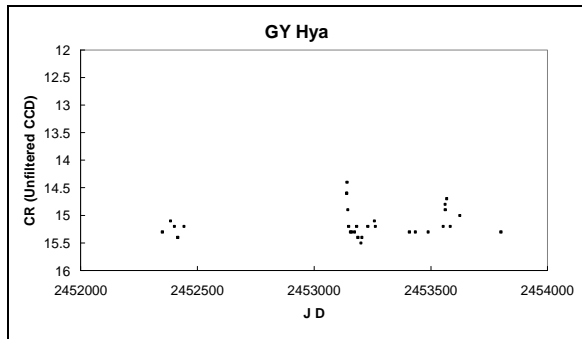


This star has regular outbursts around magnitude 14 and a quiescent magnitude below 18.

Name	Alternate Name	RA	DE	Type	Magnitude range	Period (d)
DV Sco	HV 4225	16:50:27.93	-28:07:58.6	ugsu	13.8 B - <18.4 B	-
GY Hya	S 6576	14:30:30.47	-25:52:38.0	ug	14 p - 16 p	0.347237
QS Tel	RE 1938-461	19:38:35.80	-46:12:56.6	am	15.2 V - 17.4 V	0.097187
UW Pic	RX J0531-4624	05:31:35.59	-46:24:05.9	am	16.4 V - 17.2 V	0.09264
V662 CrA	Plaut 3-1235	18:35:30.53	-36:56:44.7	ug	15.7 p - <19.6 p	-
V834 Cen	1E 1405-451	14:09:07.30	-45:17:16.2	am	14.2 v - 17 v	0.070498
V895 Cen	EUVE J1429-38	14:29:27.22	-38:04:09.5	am	16.5 v - 17.5 V	0.198553
V1025 Cen	RX 1238-38	12:38:16.38	-38:42:46.0	dq	16.1 V -	-
V1043 Cen	RX J1313-3259	13:13:17.14	-32:59:12.2	am	16 V -	0.174592
V2839 Sgr	Plaut 3-281	18:16:19.29	-31:42:09.8	UG:	15.3 p - 17.2 p	-
V3608 Sgr	Plaut 3-1233	18:35:24.55	-35:32:04.5	UG	15.6 p - 18.7 p	-
V3774 Sgr	Plaut 3-1453	18:41:41.18	-32:54:33.9	ug	14.7 p - 17.7 r	-
VW Tuc	HV 6327	00:20:19.11	-73:52:08.1	UG:	15.4 p - <16.5 p	-
VX Ret	EC 04030-5801	04:04:05.70	-57:53:26.6	ug	14.7 B - 18.1 B	-
WX Pyx	1E 0830.9-2238	08:33:05.74	-22:48:32.2	am:/dq	16.2 V - 17.7 V	0.2307

Short runs of time series photometry at CBA Pretoria during a long outburst in September 2004 showed the distinct shape of superhumps. There is a need for further dense monitoring to better establish the outburst frequency and to conduct longer time series photometry during a future superoutburst.

5. 2. GY Hya



The mean magnitude in quiescence is around 15.2. The long term light curve shows outbursts or active states around magnitude 14.3.

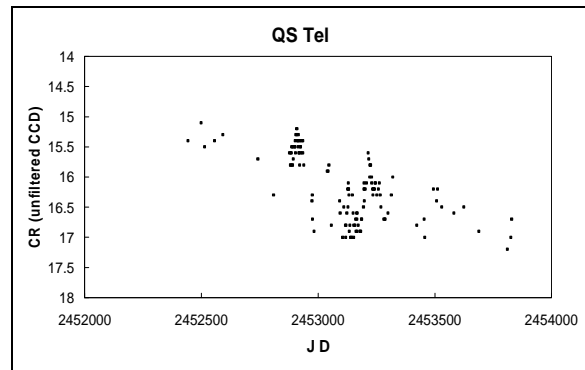
Time series photometry of long duration at CBA Pretoria during a spotted outburst in May 2004 showed the eclipsing nature of the system and gave a good indication of the orbital period. In comparison to time series photometry made during quiescence, the orbital light curve shows deeper eclipses during outburst, which hinted at the WD region as the eclipsed region. However, the mean unfiltered magnitude over the cycle didn't change much (< 1 magnitude) from quiescence to outburst.

Follow up time series at later epochs did improve the accuracy of the orbital period down to the resolution given in the CV atlas and which is in close agreement with the spectroscopically determined period by Peters, C.S. (2005).

Multicolour time series light curves might show even deeper eclipses at the shorter wavelength bands.

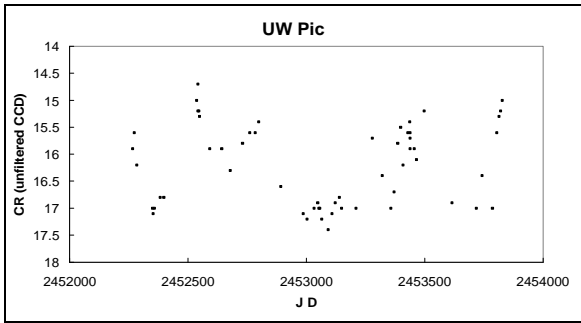
The main characteristics of this long period CV seem to be well established and its continuous monitoring was stopped in favour of other targets.

5. 3. QS Tel



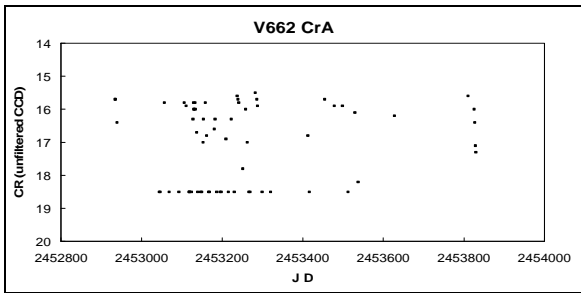
This star has been in the active phase at the start of observations in 2002. The mean magnitude was around 15.5. The active phase seems to have ended during Aug 2003. Arguably a transition state occurred for nearly two years. The low state has continued up to date. Further monitoring is planned.

5. 4. UW Pic



This is a polar alternating steadily between high and low states. Time series unfiltered photometry was done during the active phase. More observations are needed to derive a cycle of states.

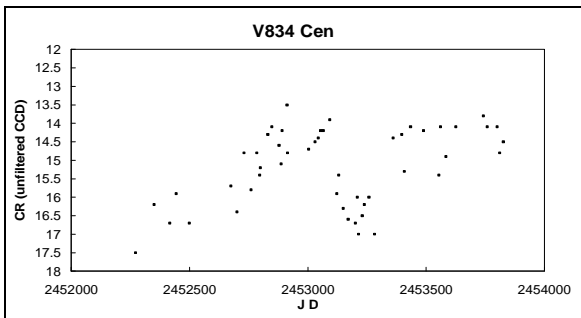
5. 5. V662 CrA



Despite its large outburst amplitude, this CV has lots of them. They are mostly of short duration while the long outbursts last a couple of weeks. On two occasions (6 May and 23 Aug 2004) time series photometry was done about midway through such long outbursts. No humps appeared in the light curve. This is possibly this is an ugss type.

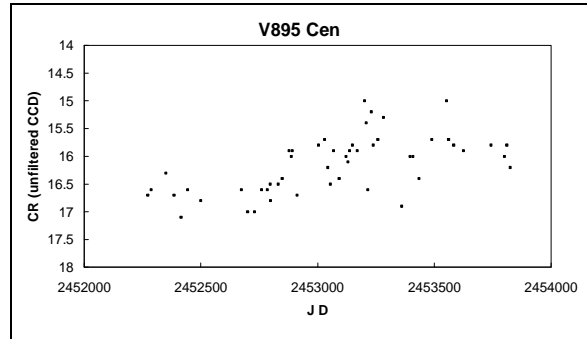
The frequency of short and long outbursts will be further researched by continuous dense monitoring.

5. 6. V834 Cen



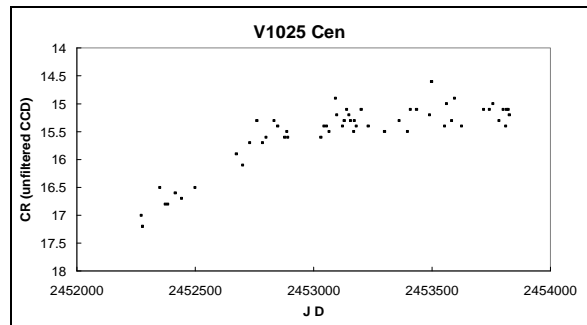
The difference between low and high states is about 2.5 magnitudes (16.5-14.0). There is a hint of a cycle period around 800 days.

5. 7. V895 Cen



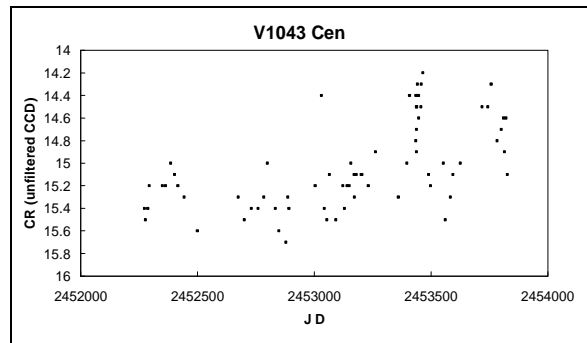
The mean magnitude has increased from 16.7 to 15.7 over the period 2003 to 2006. Is this part of a periodic cycle?

5. 8. V1025 Cen



The star has reached the high state since the beginning of 2003 and remained there until now.

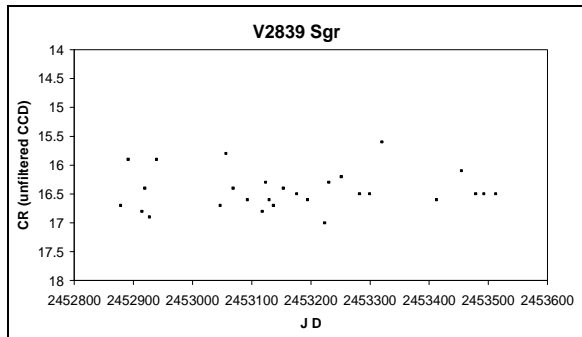
5. 9. V1043 Cen



Observations reported by Thomas et al. in their 2000 paper showed this star to be close to 16.0V. The mean brightness has increased considerably since then and this trend continues. Two outburst stages were recorded in 2005-2006, with magnitudes around 14.4. It is difficult to predict how this polar will further evolve in the years to come. One way to find out

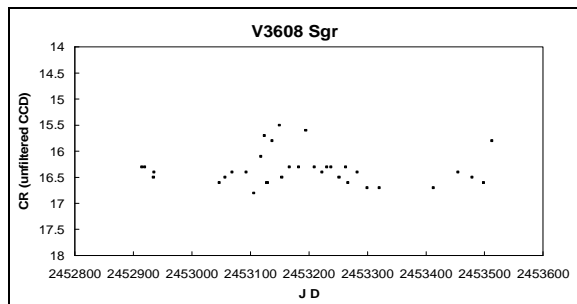
is a more dense coverage at CBA Pretoria. Sporadic filtered photometry might be considered.

5. 10. V2839 Sgr



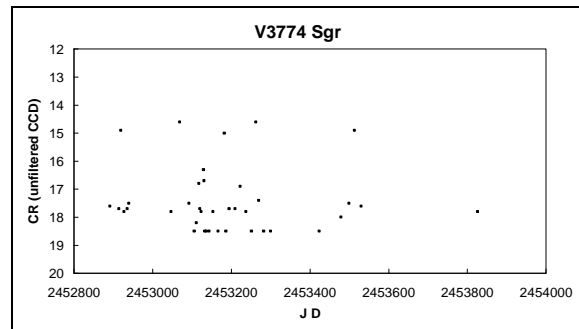
Initially the ID of this suspect CV was uncertain, indicated by a circled area on a field image in the CV atlas. Observations over one year pinpointed the suspect on the basis of variability. In order to probe the orbital period and eventual type of the suspect CV, time series photometry was conducted in 2004. It established the R Rab nature of this variable with a period close to 1d or, more likely, 0.5d. No further observations were done.

5. 11. V3608 Sgr



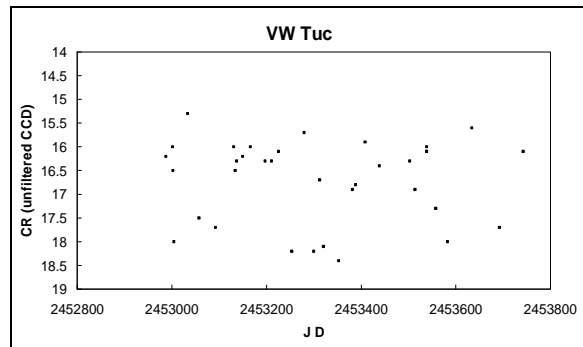
This is similar to V2839 Sgr, i.e., another R Rab star with a similar light curve and period.

5. 12. V3774 Sgr



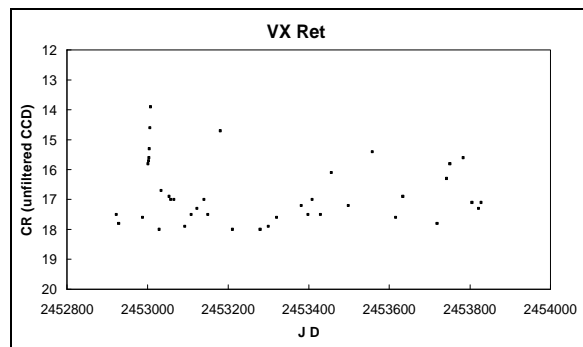
This star has shown outbursts at regular intervals. Short time series photometry during outbursts did not reveal any clear modulation. More data are needed.

5. 13. VW Tuc



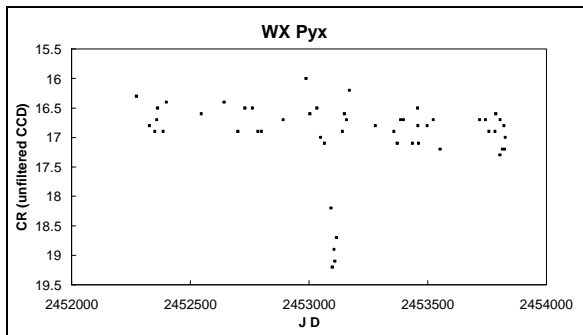
VW Tuc has usually been observed around magnitude 16.2 but with fadings beyond mag 18. This star has an uncertain ‘UG:’ classification. There is a need for more dense coverage, including filtered observations and time series photometry, to see if there is a pattern,. This could be an interesting star.

5. 14. VX Ret



A long outburst was detected in Jan 2004. Short time series did not reveal any obvious modulations. More dense coverage is planned.

5.15. WX Pyx



WX Pyx has been showing a small gradual fading since observations started in Feb 2002. The scattering of nightly data points largely reflects the brightness amplitude during the orbital light curve, which is around 1 magnitude. In April 2004 WX Pyx showed a deep fade of more than two magnitudes during a period of two weeks. Is this a recurring phenomenon? This looks interesting and this polar will be more densely monitored.

6. Conclusions

The first three years of the faint CV monitoring program observing can be considered successful, having made the following achievements:

1. Outburst detection and characterization of suspected or unknown dwarf novae
2. Identification of suspected variables
3. Characterization of non-CVs
4. Evolution of activity states of magnetic CVs. It is clear that much longer monitoring is required to probe for the existence of cycles
5. Shortcomings observed are related to insufficient density of the monitoring.

With regard to specific types of targets, it is difficult and even speculative to report any findings. However, it is clear that in the case of polars, changes in activity states differ considerably from target to target.

The discussed observing period is much too short to show the long-term behaviour of each of those CVs. The changes in activity states and their frequency of occurrence and repeatability of magnitudes need considerably more data.

7. Future of the CV Monitoring Program at CBA Pretoria

There will be a continuous review of the observing list. More dense monitoring of a select few stars along with periodic monitoring for most other listed CVs is the present strategy.

The faint CV monitoring program must be seen as complementing the organized observing programs by associations such as the AAVSO, BAA, RASNZ, and others. It differs in that the target selection is not based on the availability of historical data but rather on recent findings. Organized observing programs of those associations are still catering mainly for visual observers, while those same targets are also presented to CCD observers with the aim of providing more accurate filtered photometry.

The initiative to monitor faint CVs and transient sources often at the limit of an unfiltered CCD camera/small scope combination without much accuracy and without third party validation of the results is not really in line with the mandate of most of those organisations.

Therefore, monitoring faint CVs must be considered a “niche field” for amateurs with an interest in exploring the CV zoo.

8. Acknowledgments

Thanks and appreciation go to many of the world wide observing colleagues and professional astronomers. The following persons I would like to name:

Prof. Joe Patterson (Columbia University, New York) for his continuous advice and leadership of CBA and for his assistance with the acquisition of the observing instrumentation of CBA Pretoria.

Prof. Brian Warner (University of Cape Town, now retired) for discussions on CVs and high speed photometry.

Prof. Boris Gansicke for regular useful inputs specifically on magnetic CVs.

Dr Taichi Kato and other members of the VSNET team for their enthusiastic drive and inept knowledge in prompting to monitor outbursting CVs and other transients

Dr Arne Henden (now AAVSO Director) and Brian Skiff (Flagstaff) for their efforts to provide accurate photometric references

B Dickson (De Beers, South Africa) for his valued assistance with the maintainance of the observing instrumentation at CBA Pretoria.

Brigitte, my wife and companion for over thirty years, for her patience and always support.

No grants or financial subsidies were received for any of the observing programs at CBA Pretoria.

9. References:

CV atlas now archived at
<http://archive.stsci.edu/prepds/cvcat/index.html>

CBA site at
<http://cba.phys.columbia.edu/>

AAVSO at
<http://www.aavso.org/>

VSNET (semi-dormant) at
<http://vsnet.kusastro.kyoto-u.ac.jp/vsnet/index.html>

VIZIER at
<http://vizier.u-strasbg.fr/viz-bin/VizieR>

Digitized Sky Survey at
http://archive.stsci.edu/cgi-bin/dss_form

Meade at
<http://www.meade.com/>

SBIG at
<http://www.sbig.com/>

AIP4WIN at
<http://www.willbell.com/aip4win/AIP.htm>

Gerke J. R et al.: Polars Changing State: Multiwavelength Long Term Photometry and Spectroscopy of

QS Tel, V834 Cen, and BL Hyi, / taken from *astro-ph/ Mar 2006*

Hellier, Coel S.A.: Cataclysmic variable stars. How and why they vary / Springer Berlin, 2001

Monard, B., Bronberg Observatory (CBA Pretoria) annual report for 2003.
Mon. Notes Astron. Soc. South Africa, 63, 89-91 (2004).

Monard, B., Bronberg Observatory (CBA Pretoria). Annual report for 2004.
Mon. Notes Astron. Soc. South Africa, 64, 70-76 (2005).

Peters, Christopher S.; Thorstensen, John R., Spectroscopy of Four Cataclysmic Variables with Periods above 7 Hours. *The Publications of the Astronomical Society of the Pacific*, Volume 117, Issue 838, pp. 1386-1393 (2005).

Thomas H. C. et al., RX J1313.2-3259, a long-period Polar discovered with ROSAT. *Astronomy and Astrophysics*, v.353, p.646-654 (2000).

Warner, B. 1995: *Cataclysmic Variable Stars: A Review of Observational Properties and Physical Structures* (Cambridge Univ. Press)

Cleaning up the GCVS Eclipsing Binary Listings: Strategies and Tools to Maximize Success

Tom Krajci

CBA New Mexico (formerly CBA Tashkent, Uzbekistan)

PO Box 1351

Cloudcroft, NM 88317

tom_krajci@tularosa.net

Abstract

While some may expend their efforts on surveys and discovery of new variable stars, many 'known' variable stars are poorly studied and little more than a one-line entry in a catalog, such as the General Catalog of Variable Stars (GCVS). In fact you will find many periodic variable stars in the GCVS that lack a period, epoch, or both. This is an area where the interested amateur can make scientific contributions. With background research and the right tools and strategies, observing time can be very productive when studying these 'little known' variable stars. © 2006 Society for Astronomical Sciences.

1. Introduction

The beginning photometrist must always face these questions: What stars should I observe? Will I see results in one or two nights? Do I need special filters? This paper proposes an observing project that has as its target list a subset of the GCVS eclipsing binary listings. With proper star selection and background research, the amateur is practically guaranteed to capture an eclipse on the first night or two. This project requires no special filters, which makes it ideally suited to the beginner and is an excellent topic for a high school science fair project.

2. The General Catalog of Variable Stars (GCVS) and Your Initial Target List

The General Catalog of Variable Stars (GCVS) is the starting point from which to generate a list of target stars that lack ephemeris data. Geert Hoogev-
een has also done an excellent job of compiling a variable star catalog from other sources to supplement the GCVS listing. Importing these listings into a spreadsheet makes it easy to sort and filter them by right ascension, variable type, min and max magnitude, epoch, period, and so forth. As a beginner you may want to select only brighter, higher amplitude variables of these types: E, EA, EB, EW. The easiest is type EW because this family has such short periods. As you gain more experience and confidence you can take on more challenging stars.

3. Performing Background Research on Your Target Stars – Weeding out low Probability Candidates

The initial target list you've culled from the GCVS needs to be filtered by comparing it against data from other sources. This is important in order to select only those targets for which you can create a reasonably accurate ephemeris. With this ephemeris, you can predict when eclipses are likely to occur and maximize the productivity of your observing time. Without a good ephemeris, you can do no better than choose a random observing schedule, which can be very unproductive and unrewarding.

There are several sources of data you can research: online publications, archived publications (not accessible through the Internet), online photometric surveys, and online survey images.

Online publications include the Information Bulletin on Variable Stars (IBVS), the AAVSO Published Times of Minimum Database, Eclipsing Binaries Minima Database, Atlas of O-C Diagrams of Eclipsing Binary Stars, and many others. See the references at the end of this paper for a listing of online publications and variable star observing organizations. If all else fails there is the NASA ADS Astronomy Query Form, but don't forget to look up alternate names of your star in SIMBAD.

These various publications and organizations are largely a source of eclipse timings that help determine an accurate ephemeris.

Archived publications are not available on the Internet. This means you must travel to nearby observatory, university, or city libraries that have archives

available for research. This availability is different for each person, but if the trip is not too long, it may provide valuable eclipse timing information from old epochs that help improve the accuracy of predictions for the current epoch. One other option is to collaborate with a friend that has easier access to archived publications. Such collaborations can be very rewarding.

Online surveys include the Northern Sky Variability Survey (NSVS), The All Sky Automated Survey (ASAS), Hipparcos data (text and graphic form), and The Amateur Sky Survey (TASS) MarkIV Engineering Run Database. Note that with Hipparcos data you need to search by Hipparcos catalog number. You can determine if a given star has a Hipparcos catalog number by cross-referencing in the GCVS, or using SIMBAD. Generally stars must be 10th magnitude or brighter to have a Hipparcos catalog number.

If you're lucky, you'll find that your 'unknown' GCVS target star has a Hipparcos catalog number and the Hipparcos team has been able to determine an unambiguous period and epoch. This information may be good enough for you to predict future eclipses and easily capture one. However, it may turn out that the Hipparcos team has not determined the period with enough precision, or that their period is an aliasing artifact. In both cases you will need data from other sources, if available, or additional observations on your part.

You'll soon learn that each online survey has different sky coverage and magnitude limits. Hipparcos covered the entire sky but only to about magnitude 10. NSVS covered the northern sky down to about magnitude 14. TASS currently covers the northern sky. ASAS currently covers the southern sky. Each online survey also has different data to provide. Hipparcos time data is already in heliocentric day format, but others are not and heliocentric time corrections must be applied for later analysis and period searches.

It's important to examine a survey image of each target star to determine two things. First, are the GCVS coordinates accurate? Second, is the star field crowded? This can be a factor in what online photometric data you can get and what quality it will be. The online photometric surveys (not Hipparcos) used wide field imaging systems with pixel sizes that made it difficult to resolve stars closer than about 1 arcminute. A quick look at a survey image will tell you if such a problem exists for your target star. If there is a close neighbor star, it means the photometric data may be a blend of the two stars. This means that photometric precision may suffer – you'll see more scatter in the measurements – and that any amplitude in the variable star will be smaller than the true value.

At this point you've collected all available data on your target stars. You may find that some stars have little additional data beyond the entry in the GCVS. These stars can be dropped off the list as low probability of success candidates. Some stars will have a small amount of data – perhaps one or two publications with a few eclipse timings – and maybe one online photometric survey that provides data. These stars can be considered medium probability of success candidates. Some stars will have a robust data set from online publications, archived publications, and more than one photometric survey. These stars can be considered high probability of success candidates. Let's continue to work with these high probability stars.

4. Making Sense of all Your Background Research.

You now have a collection of old eclipse timings and fairly recent photometric data for your high probability stars, and you need to analyze them to see if they provide a meaningful epoch and period.

First, did any published source provide a period? If yes, you can plot all eclipse timings on an O-C (observed minus calculated) chart. (We'll see an example of this later.) At a glance this will tell you if the period is reasonably accurate or not.

If no period is provided, you'll have to search for candidate periods. One tool for this is TomCat software, written by Bob Nelson. This software will analyze a list of eclipse timings over a range of periods and provide a graphic plot of how likely a given period is the correct solution. Keep in mind that if you only have a small number of eclipse timings it may be difficult or impossible to determine the correct period unambiguously. We'll assume that we've either had a reasonably accurate period provided, or that we've determined it with TomCat and a healthy number of eclipse timings.

Now we can analyze online photometric data and compare its results to older eclipse timings. Initially the photometric data looks like a random jumble because the time sampling is random and often at large time intervals. Periodic behavior is not evident.

If we have a reasonably accurate period from old eclipse timings, we can phase plot this data using this period. Don't forget to make the applicable heliocentric time corrections to this data, except for Hipparcos. Even a simple spreadsheet can be used to accomplish both tasks. If the period is unknown we'll have to search for likely candidates. Bob Nelson's software Period Search is well suited to this task. You can search ranges of periods and examine a graphic output that shows the likelihood that any pe-

riod has a strong periodic component. As you analyze candidate periods closely, you can call up a phase plot to see if you get a reasonable looking light curve that displays either a primary eclipse or both a primary and secondary eclipse.

As you analyze online photometric data for candidate periods, you may be surprised to see phase plots that have three or more eclipse events. Is this a rare triple eclipsing system? No, it's an aliasing artifact. With a small amount of sparsely sampled photometric data there may be more than one candidate period that looks good to period analysis software. This is where human judgment comes in when looking at phase plots. In some cases, especially with very short period systems that have essentially identical primary and secondary eclipses, it may be very difficult to judge the best candidate period. Often one long observing run can help answer this question for short period systems.

Now that you've determined the most likely period from online photometric data, it's important to also derive an eclipse timing from the data. A spreadsheet can be used to extract this, and I'll gladly email copies of what I've developed for this purpose.

In the final stage of analysis you compare all data sources. Do old eclipse timings indicate a certain period? Do they agree with the most likely period and phase plot from online photometric data? Does the eclipse timing from online photometric data show a significant change in the O-C plot? Will you have to use a slightly different period to make predictions for the current epoch?

If all your data sources support one another and point to an unambiguous period and epoch, you know that you've selected a star with a high probability of success. Generate a list of predictions for the current observing season so that you can make a schedule. You'll find that some periods may appear to be relatively short, but the opportunities they offer to catch an eclipse may come only a few times a season. If you are working on a number of target stars, it's helpful to assign a high priority to those that have few observing opportunities each season.

5. WW Lyncis – One Example

One star in the GCVS with no listed period or ephemeris is WW Lyn, which is fairly bright at around 12th magnitude. The GCVS references one article (Kinman 1982), and a quick look at that article appeared to indicate the case was closed – period, epoch, and light curve were all there. This paper labels the star as RR-VI-37. See page 322 for a finder chart. To be thorough I decide to compare those results with online photometric data.

This star was too faint for Hipparcos and too far north for ASAS. A quick query of NSVS data and a phase plot showed a disparity. The light curve did not appear to support that paper's period.

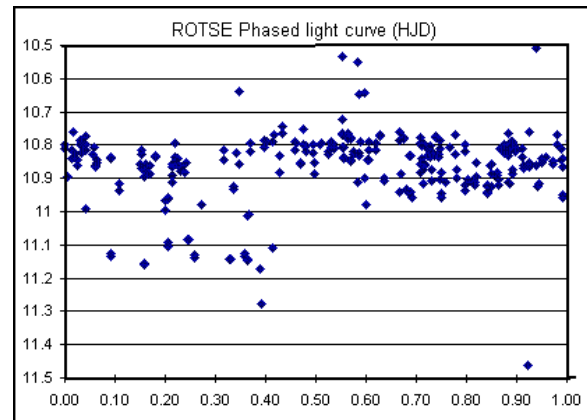


Figure 1. WW Lyn phase plot for a period of 1.208 days.

Converting the NSVS data to HJD and analyzing it in Period Search, there were several aliased candidate periods. However the phase plot at a period near 5.812 days looked the most promising.

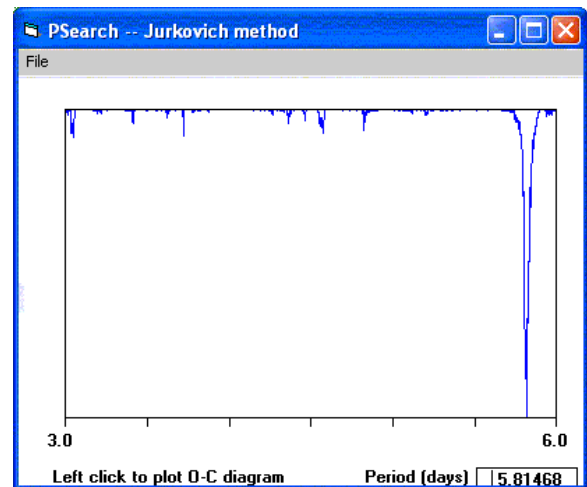


Figure 2. WW Lyn output from Period Search showing likely period near 5.81 days.

Using that period, an epoch from the middle of all NSVS data was extracted. (Note: Kinman's period of 1.208 days is an alias of 5.812.)

The next step was to compare the eclipse timings from Kinman's paper in an O-C plot, using the period and epoch from NSVS data. Another disparity showed up. Kinman's timings largely plotted on a straight, horizontal line, but at a considerable offset from the NSVS data.

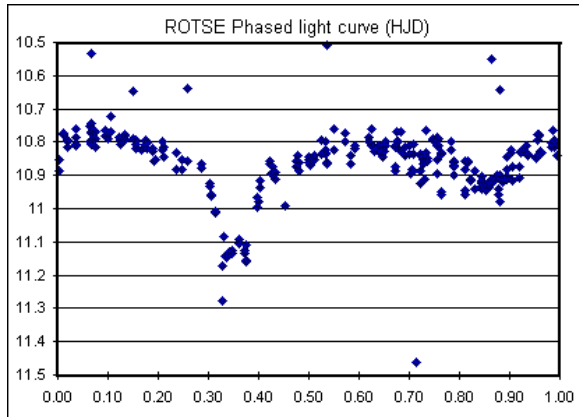


Figure 3. WW Lyn phase plot for a period of 5.812 days.

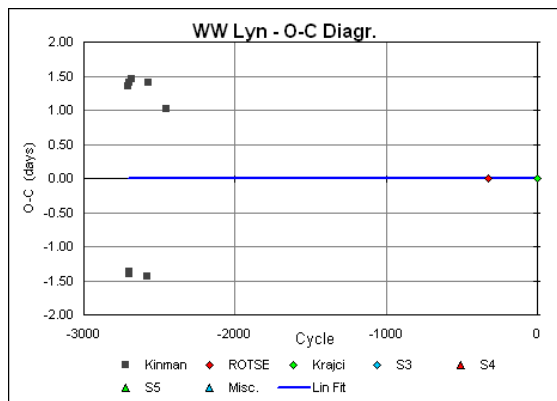


Figure 4. O-C plot using Kinman's timings (no phase correction applied).

A little head scratching showed that Kinman's timings were all offset by $\frac{1}{4}$ of the NSVS period. Because Kinman's period was an alias of the NSVS period, and his timings were off by a simple fraction of the period, I applied this correction to Kinman's timings. (Sometimes aliased signals have an associated phase shift.) With O-C plots lining up well I felt reasonably confident that I could predict and capture an eclipse of this star.

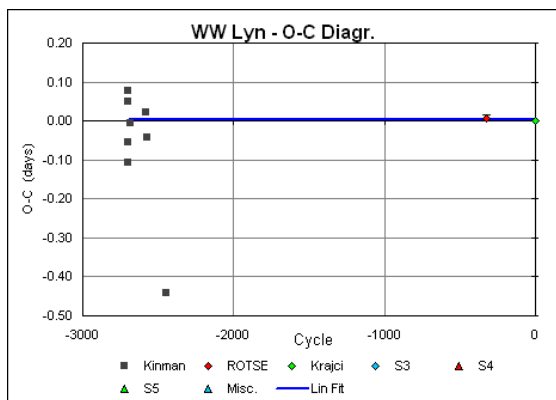


Figure 5. O-C plot using Kinman's timings (phase correction applied).

A period of 5.812 days meant that I had a good observing window only about once a month. Eventually weather cooperated and I was in fact able to capture an eclipse of this star, as predicted with this period.

The moral to the story is there can be errors in published values. Cross-checking between multiple sources is an essential part in finding and eliminating these errors.

6. Some Additional Comments

The process I've outlined above appears linear, but it may become iterative, especially when you are researching stars with sparser data sets that initially appear conflicting. This paper can serve as a starting point for the beginning photometrist, and experience will guide you in how to better select target stars.

Serendipity is its own reward. Discoveries of new variable stars will happen as you work more target stars. If you photometrically data mine all stars in your field, or just use several comparison stars and eventually find that one of your comp's is not constant, eventually you'll make a discovery.

Sometimes your target star is not an eclipsing binary, but an RR Lyr instead. This will be apparent when the descending leg to minimum light has a shallower slope than the ascending leg coming out of minimum light.

Or your target star may be an eclipsing binary, but the period appears to be changing and, perhaps, in unusual ways. This may be a star worthy of longer-term study.

In your first attempts you may not want to choose stars for which epoch and period are unknown. You may want to choose stars for which the period is known (perhaps to low precision) but that have not been observed for several or more years. A good source of such stars is the Rolling Hills Observatory Eclipsing Binary Ephemeris Generator <http://www.rollinghillsobs.org/perl/calcEBephem.pl>. It provides eclipsing binary predictions for a user-defined geographic location. It also lists how many orbital cycles since the epoch of last observation recorded in the database. There are many GCVS stars with periods and epochs that have not been observed in years or decades.

7. Conclusion

Many known variable stars are in need of greater study. Many are lacking even basic data in the GCVS. Dedicated observations by interested amateurs and students can make substantial contributions to improving our knowledge of variable stars. Back-

ground research of all available data identifies stars that can be easily solved with only one or two night's new data.

Along the way you can make unexpected and surprising discoveries, establish professional and amateur collaborations across the globe, and find inspiration in exploring and solving some of the mysteries of the heavens.

8. Acknowledgements

I'd like to thank the AAVSO Eclipsing Binary work group for their mentoring and support. <http://www.aavso.org/observing/programs/eclipser/>

9. References

Kholopov, P.N., Samus, N.N., Frolov, M.S., Goranskij, V.P., Gorynya, N.A., Kireeva, N.N., Kukarkina, N.P., Kurochkin, N.E., Medvedeva, G.I., Perova, N.B., and Shugarov, S.Yu. 1985-88. General Catalogue of Variable Stars, 4th edition, Volumes I-III, (Moscow, Nauka Publishing House) <ftp://ftp.sai.msu.su/pub/groups/cluster/gcvs/gcvs/iii>

Hoogeveen, Geert, Catalogue of variable stars <http://www.xs4all.nl/~gertho/Catalogue.htm>

Northern Sky Variability Survey (NSVS, aka ROTSE) <http://skydot.lanl.gov/nsvs/nsvs.php>

The All Sky Automated Survey (ASAS) <http://archive.princeton.edu/~asas/>

Hipparcos data (text) http://www.rssd.esa.int/hipparcos_scripts/HIPcatalogueSearch.pl?hipepId=1

Hipparcos data (graphic) <http://www.rssd.esa.int/Hipparcos/apps/PlotCurve.html>

TASS (The Amateur Sky Survey) MarkIV Engineering Run Database <http://sallman.tass-survey.org/servlet/markiv/template/DataDownload.vm;jsessionid=2AA08D14B42E894700FA2A8B7D4632FC>

ECLIPSING BINARIES OBSERVING PLAN (Sebastian Otero) http://ar.geocities.com/varsao/EA_observations.htm
http://ar.geocities.com/varsao/eclipsing_binaries_observing_plan.htm

INFORMATION BULLETIN on VARIABLE STARS <http://www.konkoly.hu/IBVS/IBVS.html>

AAVSO Published Times of Minimum Database <http://www.aavso.org/observing/programs/eclipser/ebtom.shtml>

Bob Nelson's O - C Files, http://www.aavso.org/observing/programs/eb/omc/nelson_omc.shtml

Eclipsing Binaries Minima Database <http://www.oa.uj.edu.pl/ktt/>

Atlas of O-C Diagrams of Eclipsing Binary Stars <http://www.as.ap.krakow.pl/o-c/index.php3>

Smithsonian/NASA ADS Astronomy Query Form http://adsabs.harvard.edu/abstract_service.html

Bundesdeutsche Arbeitsgemeinschaft für Veränderliche Sterne e.V. (BAV) http://www.bav-astro.de/index_e.html

Mitteilungen über Veränderliche Sterne (MVS) <http://www.stw.tu-ilmeneau.de/science/pub/MVS/content.html>

Swiss Astronomical Society Bulletins (BBSAG) <http://www.astronomie.info/calsky/>

Association Française des Observateurs d'Étoiles Variables (AFOEV) <http://cdsweb.u-strasbg.fr/afoev/>

British Astronomical Association Variable Star Section (BAAVSS) <http://www.britastro.org/vss/>

SIMBAD <http://simbad.u-strasbg.fr/sim-fid.pl>

Rolling Hills Observatory Eclipsing Binary Ephemeris Generator <http://www.rollinghillsobs.org/perl/calcEBephem.pl>

Kinman, T. D.; Mahaffey, C. T.; Wirtanen, C. A. An RR Lyrae survey with the Lick astrograph. V - A survey of three fields at intermediate latitudes towards the galactic anticenter. http://adsabs.harvard.edu/cgi-bin/nph-bib_query?bibcode=1982AJ.....87..314K&db_key=AST&data_type=HTML&format=&high=4152f330d822360

The Detection of the WZ Sge-type Nature of the Dwarf Novae ASAS 023322-1047.0 and ASAS 102522-1542.4 by the Center for Backyard Astrophysics

Tonny Vanmunster

CBA Belgium

Walhostraat 1A, B-3401 Landen, BELGIUM

Tonny.vanmunster@cbabelgium.com

Tom Krajci

CBA New Mexico

PO Box 1351 Cloudcroft, New Mexico 88317, USA

tom_krajci@tularosa.net

Berto Monard

CBA Pretoria

PO Box 11426, Tiegerpoort 0056, SOUTH AFRICA

bmonard@mweb.co.za

Lewis M. Cook

CBA Concord

1730 Helix Ct., Concord, CA, USA

Lew.cook@gmail.com

Pierre de Ponthière

CBA Lesve

15 rue Pré Mathy, B-5170 Lesve (Profondeville), BELGIUM

pierredeponthiere@gmail.com

David Boyd

British Astronomical Association - Variable Star Section

5 Silver Lane, West Challow, Wantage, OX12 9TX, UK

drsboyd@dsl.pipex.com

Tim R. Crawford

AAVSO

Arch Cape Observatory, 79916 W. Beach Road, Arch Cape, OR 97102, USA

tcarchcape@yahoo.com

Michael J. Armstrong

AAVSO

2638 East Indianola Ave, Phoenix, AZ 85016, USA

marmst1@cox.net

Diego Rodriguez

M1 Group

San Pablo N°5, Los Negrals (Alpedrete), 28430 Madrid, SPAIN

drodrig@jet.es

Abstract

We present the results of a detailed analysis of 13,116 time series CCD photometry observations of the cataclysmic variable stars ASAS 023322-1047.0 and ASAS 102522-1542.4, collected during

175.1 hours over 23 nights in early 2006 by 9 observers. We report also the detection of outburst orbital humps and common superhumps, establishing the variables as genuine new members of the rare class of WZ Sge-type dwarf novae. Our observations furthermore provide an excellent basis to illustrate how the pro-am partnership of the Center for Backyard Astrophysics is implemented in practice. © 2006 Society for Astronomical Sciences.

1. Introduction

On every clear night, there are an amazing number of CCD photometry projects waiting for exploration by dedicated and skilled amateur astronomers. They range from asteroid research to variable star observing and exoplanet studies. Many of those projects are vastly rewarding and have been inspired by professional astronomers seeking the active assistance from amateurs. Reversibly, some projects originate from a circle of highly motivated amateurs, and attract – through their scientific relevance – the attention of professional astronomers. In either case, the result often is a flourishing pro-am collaboration.

Our paper focuses on one such type of pro-am projects: CCD photometry of cataclysmic variables, and the related pro-am network called the Center for Backyard Astrophysics (CBA). The CBA is a multi-longitudinal network dedicated to studies of periodic phenomena in cataclysmic variable stars (Skillman (1993), mostly with CCD cameras mounted on small backyard telescopes. An example observatory is presented in Figure 1.

Early 2006, the ASAS3V instrument of the ASAS All Sky Automated Survey (Pojmanski (2002) discovered two new bright variable stars that were given the designations ASAS 023322-1047.0 and ASAS 102522-1542.4. Both objects became the subject of an intensive, worldwide CCD observing campaign, headed by the CBA.

2. Detection of ASAS 023322-1047.0

ASAS 023322-1047.0 was detected by the ASAS3V instrument (telephoto lens 180/2.8, diameter 65mm on CCD with Johnson V filter) on 2006, Jan 20.12 UT [$JD +3756.3$] at $V = 12.08$ (Pilecki (2006). No object brighter than $V = 14$ was visible on an ASAS3V image of Jan 18.08 UT [$JD +3754.3$].

Precise astrometry of the new object was done using CCD images by D. Rodriguez (2006), Spain, and yielded a position of $RA = 02h33m21.41s$ and $Decl = -10^{\circ}47'04.09''$ (J2000.0). A star at mag $B = 18.18$ is visible at this location in the USNO-B1.0 catalog. The large amplitude of about six magnitudes,

combined with a location far from the galactic plane, already presented a first indication of the dwarf nova nature of the variable star.

Immediately following the outburst discovery, an international observing campaign was initiated by the CBA. The objective was to monitor the new object photometrically as intensively as possible, and to study periodic phenomena at different stages of the outburst cycle. The CBA is extremely well suited for this kind of research, given the range of terrestrial longitudes at which the network operates, allowing to reach very sensitive limits for the detection of periodic signals and to resolve ambiguities easily in daily cycle count.



Figure 1. CBA Belgium Observatory, one of the nodes of the CBA network, is remotely operated by Tonny Vanmunster. It features two CCD-equipped 0.35-m telescopes on computerized mounts

Observations collected by the CBA consist of differential photometry with respect to a nearby comparison star, mostly in unfiltered light. We measure photometric periods by splicing long light curves of

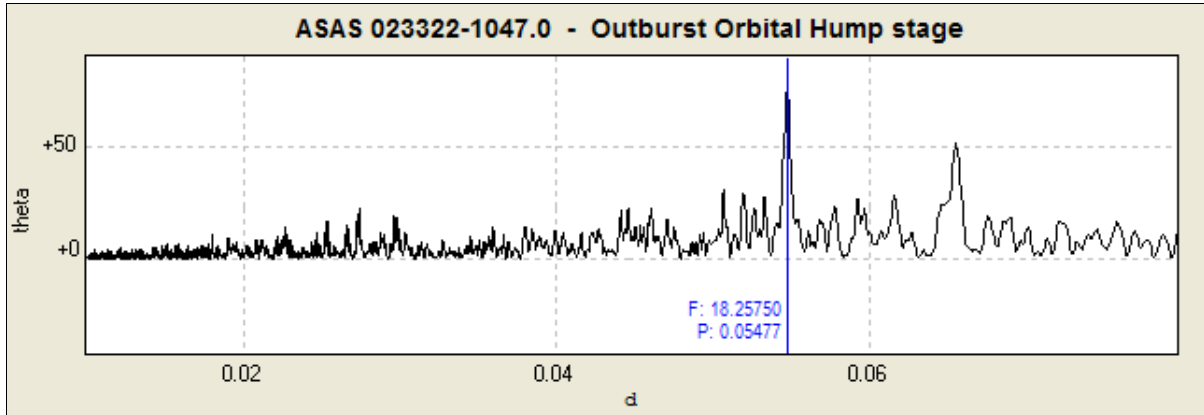


Figure 2. ANOVA Period Window of ASAS 023322-1047.0, displaying the outburst orbital hump period at 0.05477d.

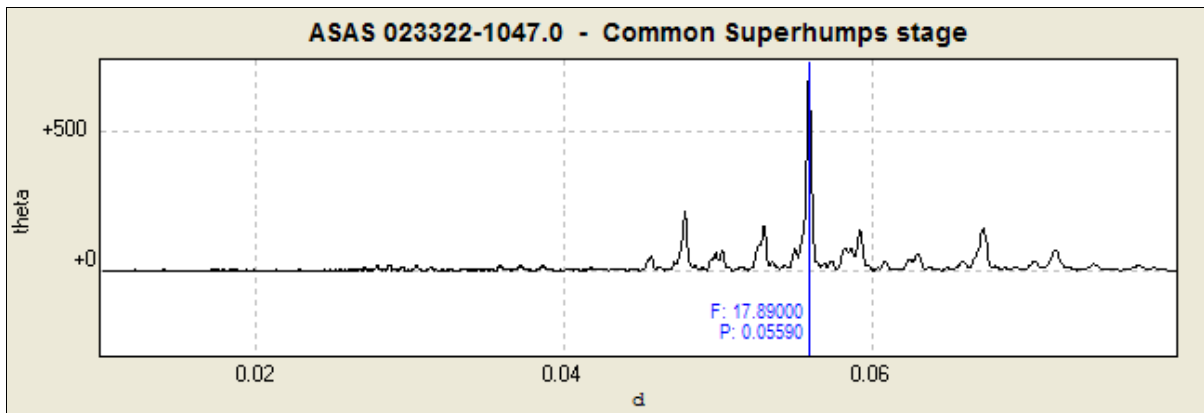


Figure 3. ANOVA Period Window of ASAS 023322-1047.0, displaying the common superhump period at 0.05590d.

differential magnitudes, and by calculating their power spectra or some other statistic (e.g., an Analysis of Variance) to evaluate the quality of a period fit.

There are numerous fine details to this enterprise, For example, before merging data we usually subtract the mean and (linear) trend from each night's time series since it greatly reduces the low-frequency noise arising from erratic night-to-night variability. We also tend to verify that a periodic signal displays no color dependence, so the data can be merged with no great loss of integrity. This is quite important, because we always merge time series data from disparate sources. Since unfiltered light suffers from differential extinction (the blue CV is fainter at large air mass than the redder comparison star), we often discard observations obtained at large air mass.

3. The Outburst Orbital Hump Stage of ASAS 023322-1047.0

On Jan 23, 2006, T. Vanmunster (2006a) announced the detection of *outburst orbital humps*,

sometimes also called *early superhumps*, in the light curve of ASAS 023322-1047.0 based on unfiltered time series CCD photometry obtained at CBA Belgium Observatory using a 0.35-m f/6.3 telescope and ST-7XME CCD camera. Outburst orbital humps have a typical double-peaked waveform (Figure 5) and were first identified in the 1978 outburst of WZ Sge. They mostly appear within one day of the outburst, maintaining an essentially constant double-humped waveform, and then are replaced by a common superhump, which develops in a normal manner. Outburst orbital humps are still of an uncertain nature (Patterson (2002) but are now considered a standard signature of WZ Sge-type dwarf novae. Our observations thus established ASAS 023322-1047.0 as a genuine new member of the rare class of WZ Sge-type dwarf novae.

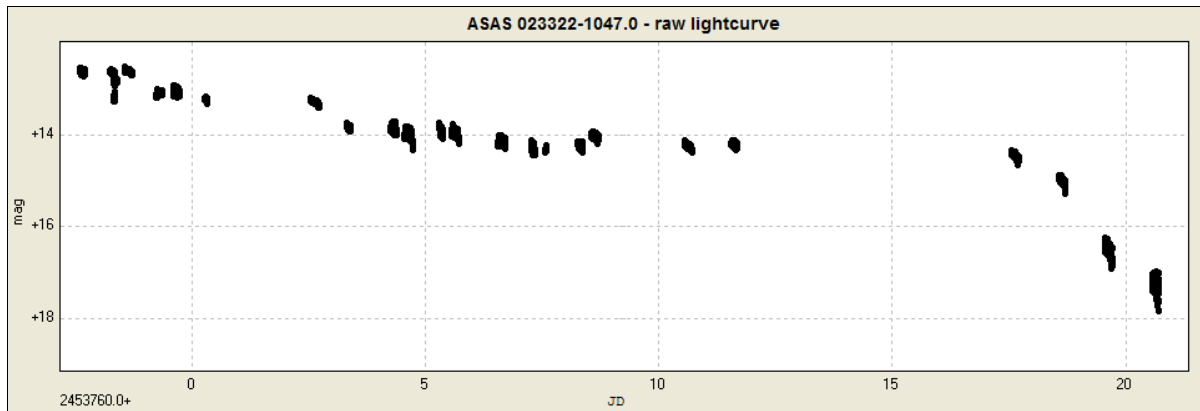


Figure 4. Raw lightcurve of ASAS 023322-1047.0, depicting the entire outburst interval, and combining 4971 CCD observations collected by the authors.

This class of dwarf novae is a subclass of the SU UMa-type dwarf novae and is particularly interesting since WZ Sge-type variables have very rare and long-lived eruptions (Bailey (1979) and show few or no normal outbursts. The latter phenomenon can not be fully explained yet with today’s mass transfer models of dwarf novae, turning WZ Sge-type cataclysmic variables into very interesting research targets.

The dwarf nova nature of ASAS 023322-1047.0 was furthermore independently detected through spectroscopic observations by C. Aguilera, using the SMARTS 1.5-m telescope at Cerro Tololo Interamerican Observatory on behalf of Howard E. Bond and F. Walter of the Space Telescope Science Institute (Bond (2006a)). A spectrum taken on 2006, Jan 22.12 UT, covering 3550-5300 angstroms (\AA), showed broad, shallow absorption lines of the hydrogen Balmer series and He I 4471 \AA , which is typical of a dwarf nova at maximum light.

Further CCD time series observations were collected by CBA and AAVSO photometrists Tom Krzjci, David Boyd, Berto Monard, Michael Armstrong, Tim Crawford, and Diego Rodriguez. In all, we accumulated 2222 CCD observations over 28.2 hours covering a time span of 5.8 days [from JD +3757.6 till JD +3763.4], i.e. the entire initial outburst stage of ASAS 023322-1047.0 (Table 1).

A detailed period analysis using the ANOVA method (Schwarzenberg-Czerny (1996) of the software package *Peranso* (<http://www.peranso.com>), reveals an outburst orbital hump period $P_{\text{orb}} = 0.05477 \pm 0.00010$ d (Figure 2). This is one of the shortest orbital periods of WZ Sge-type dwarf novae presently known. A phase diagram of the dominant signal clearly reveals the double-peaked outburst orbital hump waveform, with average amplitude just below 0.05 mag. (Figure 5). We subtracted the dominant signals and studied the residual time series but did not find significant weaker periodic signals.

Our findings for this stage of the outburst were confirmed shortly afterwards by H. Maehara (2006a) based on observations by VSOLJ (Variable Star Observers League of Japan) members K. Nakajima, S. Kiyota and H. Maehara.

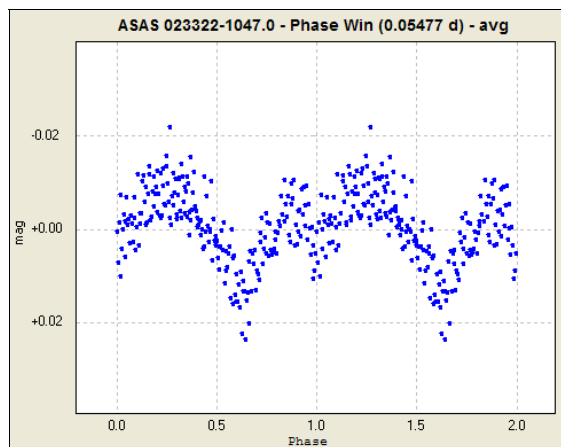


Figure 5. Phase diagram of ASAS 023322-1047.0, obtained by folding all observations from the outburst orbital hump stage over a period of 0.05477d, and displaying the average value for each bin of 10 observations.

4. The Common Superhump Stage of ASAS 023322-1047.0

Following the detection of outburst orbital humps in ASAS 023322-1047.0, the object entered its main outburst stage on Jan 28th [JD +3764] (Figure 4), trading in outburst orbital humps for *common superhumps*: the periodic wave increased very rapidly in amplitude and became single peaked (Figure 6). Common superhumps are a feature of all SU UMa-type dwarf novae in superoutburst and result from the light coming from the rim of the precessing elliptical accretion disc (Hellier (2001)).

Common superhumps with an amplitude of 0.2 mag were first announced by H. Maehara (2006b) based on CCD observations obtained on Jan 28.4 UT [$JD +3763.9$]. CCD observations by T. Vanmunster (2006b) half a day earlier, on Jan 27.9 UT [$JD +3763.4$], were still showing outburst orbital humps with an amplitude of 0.05 mag. The transition from the outburst orbital hump stage to the common superhump stage therefore must have been fast and quite spectacular.

A total of 2012 time series CCD observations were collected over 34.2 hours by CBA members during the common superhump stage of the outburst, covering a time span of 7.4 days between Jan 28.7 UT and Feb 5.2 UT [from $JD +3764.2$ till $JD +3771.7$]. Using the ANOVA method of *Peranso*, we find a common superhump period $P_{sh} = 0.05590 \pm 0.00005d$ (Figure 3), and an average amplitude of 0.16 mag (Figure 6). The P_{sh} value is one of the shortest superhump periods found in WZ Sge-type dwarf novae. The superhump period excess value $P_e = (P_{sh} - P_{orb}) / P_{orb}$ of ASAS 023322-1047.0 equals 2.1%, a value that is in line with expectations for dwarf novae with an orbital period of 1.3 hours (Hellier (2001)).

5. Rapid Fading Stage of ASAS 023322-1047.0

Around Feb 11th [$JD +3778$], ASAS 023322-1047.0 entered its rapid fading stage, when the magnitude of the system dropped by an average of 0.99 mag per day. CBA member Tom Krajci monitored this outburst stage with 737 unfiltered CCD observations obtained during 14.0 hours, covering a time span on 3.1 days between Feb 11.1 UT and Feb 14.2 UT [from $JD +3777.6$ till $JD +3780.7$].

A detailed analysis of the light curve at this stage of the outburst shows weak humps that are roughly anti-phased (shifted in phase by $\sim 180^\circ$) with the common superhumps (i.e. hump maxima occur where minima would be expected). These are called *late superhumps*. The transition from common superhumps to late superhumps in dwarf novae is currently not yet understood (Hellier (2001)).

Finally, it should be noted that no rebrightenings have been reported for ASAS 023322-1047.0 (see also Figure 4).

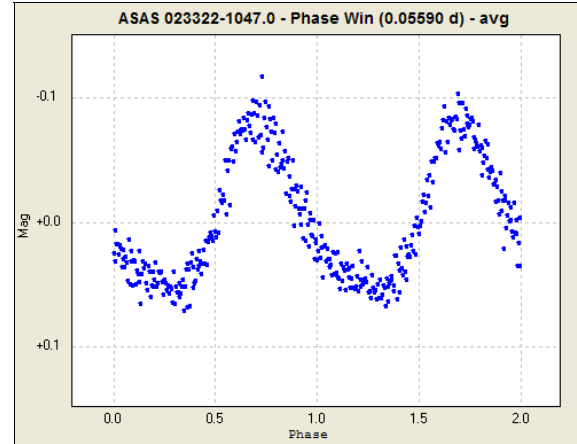


Figure 6. Phase diagram of ASAS 023322-1047.0, obtained by folding all observations from the common superhump stage over a period of 0.05590d, and displaying the average value for each bin of 10 observations.

6. The Detection of ASAS 102522-1542.4

The outburst of ASAS 023322-1047.0 was still in full development when yet another ASAS discovery was announced by Grzegorz Pojmanski (2006), Warsaw University Astronomical Observatory, based on observations of 2006, Jan 26.25 UT [$JD +3761.8$]. The ASAS3V instrument this time found an object of $V = 12.219$, that was not visible on images of Jan 23.26 UT [$JD +3758.8$], down to a limiting magnitude of $V = 14$. The new variable star, designated ASAS 102522-1542.4, is located at RA = 10h25m22.24s and Decl = $-15^\circ 42' 22.030''$ (J2000.0). Also this time, there was an USNO-1B star close to this position, at mag B = 19.32, denoting a large-amplitude outbursting object.

Again, an international observing campaign was set up by a few CBA members in conjunction with the already ongoing CBA campaigns initiated by our mentor, Prof. Dr. Joe Patterson.

The dwarf nova nature of ASAS 102522-1542.4 was revealed through spectroscopic observations obtained by A. Pasten on behalf of F. Walter and Howard E. Bond of the Space Telescope Science Institute (Bond (2006b)), on 2006, Jan 29.18 UT, using the SMARTS 1.5-m telescope at Cerro Tololo Interamerican Observatory. His spectrogram, covering 3500-5300 Å, showed broad, shallow absorption lines of the Balmer series and He I 4471 Å, typical for a dwarf nova at maximum light.

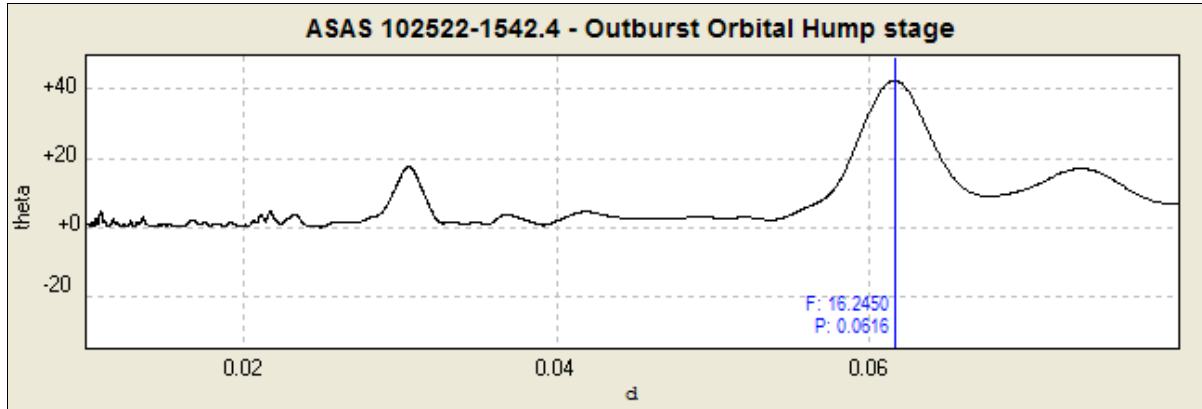


Figure 7. ANOVA Period Window of ASAS 102522-1542.4, displaying the outburst orbital hump period at 0.0616 d.

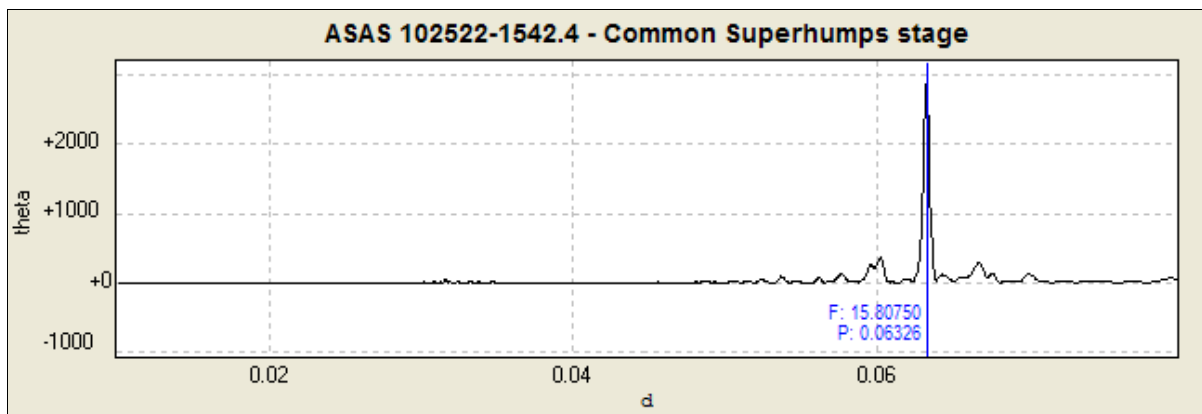


Figure 8. ANOVA Period Window of ASAS 102522-1542.4, displaying the common superhump period at 0.06326 d.

7. The Outburst Orbital Hump Stage of ASAS 102522-1542.4

The initial outburst stage of ASAS 102522-1542.4 was very well covered by CBA time series observations from Tom Krajci, Lew Cook, and Tonny Vanmunster (Table 2). A total of 1236 observations was used in our analysis, revealing double-peaked outburst orbital humps with an amplitude of 0.03 mag (Figure 9). The duration of this stage may have been fairly short: the discovery by ASAS3V was made on Jan 26.2 UT, and outburst orbital humps lasted till Jan 28.5 UT. An analysis of this part of the light curve, using the ANOVA method of *Peranso*, yields an outburst orbital hump period $P_{\text{orb}} = 0.0616 \pm 0.0018$ d (Figure 7).

Clearly, the detection of outburst orbital humps in ASAS 102522-1542.4 (Vanmunster (2006c), and the accurate determination of their characteristics, would never have been possible on the basis of data accumulated by just one observer. For example, the double-hump structure has a second (minimal) peak amplitude of less than 0.01 mag, and this second peak

becomes visible only by combining the time series observations of the three above mentioned CBA stations. The unfavorable location of the variable in the evening sky furthermore mandated observations by geographically dispersed observatories to resolve the cycle count problem.

Our findings for this stage of the outburst are well in line with conclusions derived by H. Maehara (Maehara (2006c), based on observations by VSOLJ members K. Nakajima, S. Kiyota, and H. Maehara obtained on Jan 27th and 28th.

8. The Common Superhump Stage of ASAS 102522-1542.4

Time series CCD observations, obtained by T. Vanmunster at CBA Belgium Observatory shortly after Jan 29.2 UT [$JD + 3764.3$], showed the appearance of single-peaked common superhumps with an amplitude just below 0.1 mag (Vanmunster (2006d). These observations, combined with the detection of outburst orbital humps, clearly established ASAS 102522-1542.3 as a new member of the WZ Sge-type

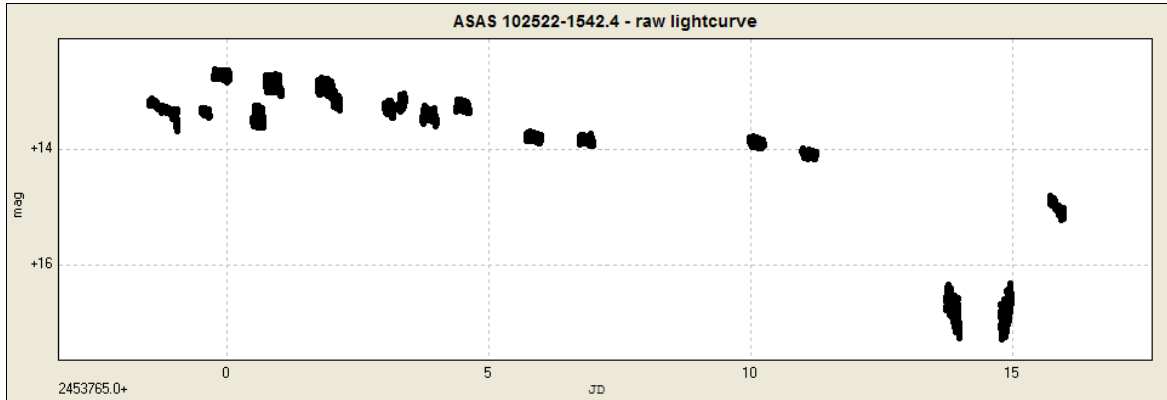


Figure 11. Raw lightcurve of ASAS 102522-1542.4, depicting the entire outburst interval, combining 8145 CCD observations collected by the authors.

dwarf novae, a conclusion that furthermore was confirmed by the appearance of echo outbursts (see section 9).

A total of 5973 CCD observations was collected between Jan 29.2 UT and Feb 4.5 UT [from JD +3764.3 till JD +3771.7], by CBA members Tom Krajci, Pierre de Ponthiere, Lew Cook, Berto Monard, and Tonny Vanmunster. An ANOVA-based period analysis using *Peranso* reveals a common superhump period $P_{sh} = 0.06326 \pm 0.00007$ d (Figures 8, 10). Common superhumps grew from an amplitude of less than 0.1 mag on Jan 29.0 UT to over 0.25 mag by Jan 30.5 UT.

Based on the above outburst orbital hump and common superhump period, we find a superhump period excess value $P_{\epsilon} = 2.8\%$, a value that is very well in line with expectations for a system with an orbital period of about 1.5 hours (Hellier (2001).

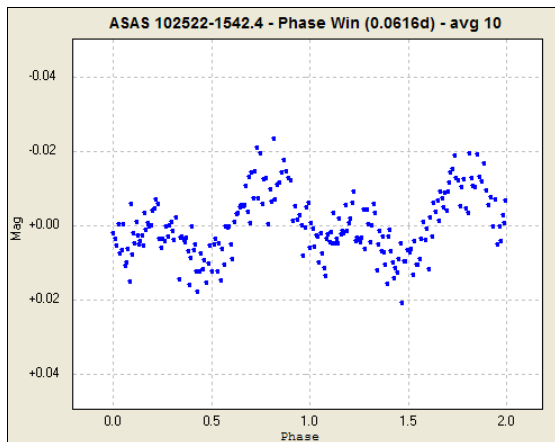


Figure 9. Phase diagram of ASAS 102522-1542.4, obtained by folding all observations from the outburst orbital hump stage over a period of 0.0616d, and displaying the average value for each bin of 10 observations.

9. The Echo Outburst Stage of ASAS 102522-1542.4

ASAS 102522-1542.4 entered a rapid decline phase shortly after Feb 10.0 UT [JD +3776.5] (Figure 11). CBA member Tom Krajci obtained unfiltered time series CCD observations on Feb 12.2 UT [JD +3778.7], when ASAS 102522-1542.4 had an average magnitude of 16.7, and showed common superhumps (not late superhumps) with an amplitude of 0.4 mag superimposed over a declining trend of approx. 1.9 mag/day. Later that day, H. Maehara reported the object at mag 17.5 (Maehara (2006d).

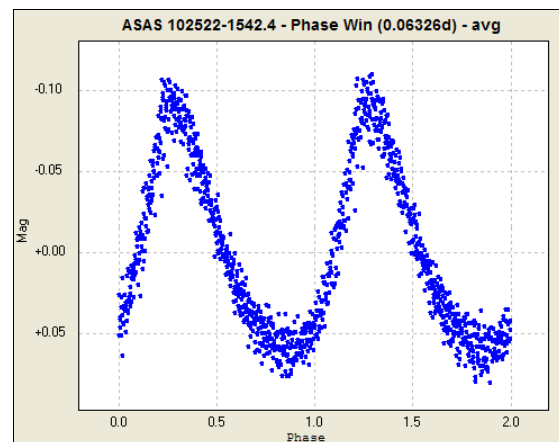


Figure 10. Phase diagram of ASAS 102522-1542.4, obtained by folding all observations from the common superhump stage over a period of 0.06326d, and displaying the average value for each bin of 10 observations

One night later, between Feb 13.26 UT [JD +3779.77] and Feb 13.46 UT [JD +3779.97], a re-brightening or *echo outburst* was observed in

Time series ID	Observer	Equip.	Start HJD	End HJD	Duration (d)	Total Obs
Outburst Orbital Hump stage						
ObsSet #7	Michael Armstrong	(6)	2453757.6011	2453757.6961	0.10	79
ObsSet #6	Berto Monard	(4)	2453758.2518	2453758.3408	0.09	249
ObsSet #10	Diego Rodriguez Perez	(5)	2453758.3180	2453758.3570	0.04	34
ObsSet #4	David Boyd	(8)	2453758.3181	2453758.3921	0.07	97
ObsSet #3	Tom Krajci	(2)	2453758.5492	2453758.7220	0.17	453
ObsSet #1	Tonny Vanmunster	(1)	2453759.2236	2453759.2582	0.03	42
ObsSet #2	Tonny Vanmunster	(1)	2453759.2584	2453759.3748	0.12	140
ObsSet #5	Tom Krajci	(2)	2453759.5921	2453759.7342	0.14	385
ObsSet #9	Tim Crawford	(7)	2453759.5985	2453759.6939	0.10	96
ObsSet #8	David Boyd	(10)	2453760.2803	2453760.3362	0.06	72
ObsSet #11	Tom Krajci	(2)	2453762.5476	2453762.7214	0.17	473
ObsSet #12	Tonny Vanmunster	(1)	2453763.3068	2453763.3926	0.09	102
Common Superhumps stage						
ObsSet #1	Tonny Vanmunster	(1)	2453764.2551	2453764.3879	0.13	150
ObsSet #2	Tom Krajci	(2)	2453764.5520	2453764.7253	0.17	340
ObsSet #4	Tonny Vanmunster	(1)	2453765.2937	2453765.3831	0.09	109
ObsSet #3	Tom Krajci	(2)	2453765.5505	2453765.7200	0.17	353
ObsSet #5	Tom Krajci	(2)	2453766.5550	2453766.7165	0.16	207
ObsSet #6	Tonny Vanmunster	(1)	2453767.2583	2453767.3559	0.10	110
ObsSet #8	Tom Krajci	(2)	2453767.5515	2453767.5988	0.05	58
ObsSet #7	Tonny Vanmunster	(1)	2453768.2652	2453768.3694	0.10	130
ObsSet #9	Tom Krajci	(2)	2453768.5523	2453768.7109	0.16	198
ObsSet #10	Tom Krajci	(2)	2453770.5532	2453770.7069	0.15	200
ObsSet #11	Tom Krajci	(2)	2453771.5526	2453771.6878	0.14	157
Decline stage						
ObsSet #1	Tom Krajci	(2)	2453777.5579	2453777.7008	0.14	185
ObsSet #2	Tom Krajci	(2)	2453778.5569	2453778.7115	0.15	200
ObsSet #3	Tom Krajci	(2)	2453779.5592	2453779.7061	0.15	185
ObsSet #4	Tom Krajci	(2)	2453780.5635	2453780.7011	0.14	167

Table 1. Log of observations for ASAS 023322-1047.0. **Equipment legend** : (1) 0.35-m f/6.3 telescope, ST-7XME unfiltered; (2) 0.28-m f/10 telescope, ST-7 unfiltered; (3) 0.20-m f/10 telescope, ST-7XMEI unfiltered; (4) 0.32-m f/3.7 telescope, ST-7XME unfiltered; (5) 0.20-m f/8.5 telescope, ST-9E unfiltered; (6) 0.25-m f/6.6 telescope, ST-7XME V filter; (7) 0.30-m telescope, ST-9 V filter; (8) 0.35-m f/5.3 telescope, SXV-H9 V filter; (9) 0.44-m telescope, TI TC-245 unfiltered; (10) 0.35-m f/5.3 telescope, SXV-H9 unfiltered.

Krajci's observations, when ASAS 102522-1542.4 rose by a rate of approx. 2 mag / day (average magnitude 16.8) and still showing common superhumps with an amplitude of 0.4 mag. A period analysis for both nights using the ANOVA method of *Peranso*, yields a common superhump period $P_{sh} = 0.06305 \pm 0.00014d$. This value is 1.4% shorter than the common superhump period derived during the main stage of the outburst. Such a reduction in P_{sh} during an outburst is not uncommon. The explanation for it is probably the gradual emptying of the accretion disc, which causes its radius to shrink (Hellier (2001)).

The appearance of small eruptions, called *echo outbursts*, during the return to quiescence is a phenomenon that has been observed in only a few WZ Sge-type cataclysmic variables so far. The best-studied cases are EG Cnc (Patterson (1998) and WZ Sge (Patterson (2002)). Echo outbursts are of uncertain origin but somewhat resemble the normal outbursts of dwarf novae. Several ideas have been pro-

posed to explain echoes. The most common explanation (Osaki et al. (1997, 2001) is that after the main superoutburst, enough matter resides in the outer torus of the accretion disk to drive subsequent thermal instabilities. However, the emptying torus and the declining viscosity become quickly insufficient to power further outbursts.

The variable continued to rebrighten to approx. mag 15 on Feb 14.2 UT [$JD + 3780.7$], as is apparent from the last set of observations in Figure 11. A more detailed view of that segment of the light curve indicates that humps are completely absent now, and the only thing left is a linear decline at a rate of approx. 1.1 mag / day.

10. Conclusion

The discovery of two new dwarf novae within less than one week in early 2006, and the subsequent detection of their WZ Sge-type nature, is probably unique in the history of cataclysmic variable star

Time series ID	Observer	Equip.	Start HJD	End HJD	Duration (d)	Total Obs
Outburst Orbital Hump stage						
ObsSet #2	Tonny Vanmunster	(1)	2453763.5110	2453763.6801	0.17	204
ObsSet #1	Tom Krajci	(2)	2453763.7517	2453764.0502	0.30	718
ObsSet #3	Lew Cook	(9)	2453763.9385	2453764.0543	0.12	314
Common Superhumps stage						
ObsSet #3	Tonny Vanmunster	(1)	2453764.5099	2453764.6635	0.15	178
ObsSet #1	Tom Krajci	(2)	2453764.7373	2453765.0405	0.30	700
ObsSet #5	Pierre de Ponthiere	(3)	2453765.4908	2453765.6422	0.15	359
ObsSet #4	Tonny Vanmunster	(1)	2453765.5096	2453765.6974	0.19	224
ObsSet #2	Tom Krajci	(2)	2453765.7339	2453766.0336	0.30	759
ObsSet #9	Tom Krajci	(2)	2453766.7303	2453767.0308	0.30	706
ObsSet #7	Lew Cook	(9)	2453767.0436	2453767.1597	0.12	289
ObsSet #6	Lew Cook	(9)	2453768.0107	2453768.1612	0.15	492
ObsSet #10	Berto Monard	(4)	2453768.2717	2453768.3969	0.13	330
ObsSet #8	Tom Krajci	(2)	2453768.7275	2453768.9971	0.27	604
ObsSet #11	Berto Monard	(4)	2453769.3732	2453769.6267	0.25	717
ObsSet #13	Tom Krajci	(2)	2453770.7187	2453770.9920	0.27	351
ObsSet #12	Tom Krajci	(2)	2453771.7267	2453771.9831	0.26	308
Decline stage						
ObsSet #1	Tom Krajci	(2)	2453778.7281	2453778.9724	0.24	315
ObsSet #2	Tom Krajci	(2)	2453779.7689	2453779.9677	0.20	257
ObsSet #3	Tom Krajci	(2)	2453780.7142	2453780.9648	0.25	320

Table 2. Log of observations for ASAS102522-1542.4. Equipment legend : see Table 1.

observing. More important, however, was the intensive monitoring of the two objects throughout their outburst cycle, revealing an interesting mix of features observed in other WZ Sge-type variables, and features that are still rare (e.g., echo outbursts).

The results that we obtained for ASAS 023322-1047.0 and ASAS 102522-1542.4 are a nice illustration of the fact that the CBA, despite its informal structure, is capable of consistently delivering high quality output. What's more, that data is often obtained by amateurs who are endowed with the same curiosity about cataclysmic variables shown by the best of professional scientists. Since its start in the 1970s, the CBA has been highly respected by the astronomical community. It now is the world's most powerful machine for finding periods in cataclysmic variable stars. Evidently, it's a tremendous experience to be part of the CBA and to actively contribute to scientific CCD photometry projects.

11. References

- Bailey, J.A. 1979, MNRAS, 189, 41p.
- Bond, H.E., (2006a), vsnet-campaign 1639, Jan 22, 2006
- Bond, H.E., (2006b), vsnet-alert 8830, Jan 30, 2006
- Hellier, C., (2001), Cataclysmic Variable Stars : how and why they vary, Springer-Praxis
- Maehara, H., (2006a), vsnet-alert 8815, Jan 26, 2006
- Maehara, H., (2006b), vsnet-alert 8825, Jan 28, 2006
- Maehara, H., (2006c), vsnet-alert 8843, Feb 6, 2006
- Maehara, H., (2006d), vsnet-alert 8865, Feb 13, 2006
- Osaki, Y., Shimizu, S., Tsugawa, M., 1997, PASJ, 49, L19
- Osaki, Y., Meyer, F., Meyer-Hofmeister, E., 2001, A&A, 370, 488
- Patterson, J., et al., (1998), Superhumps in Cataclysmic Binaries. XV. EG Cancri, King of Echo Outbursts, PASP, 110, 1290
- Patterson, J., et al., (2002), The 2001 Superoutburst of WZ Sagittae, PASP, 114, 721
- Pilecki, B., (2006), AAVSO Alert Notice #333, Jan 21, 2006
- Pojmanski, G., (2002), Acta Astronomica, 52,397
- Pojmanski, G., (2006), AAVSO Alert Notice #334, Jan 28, 2006

Rodriguez, D., (2006), Coordinates and photometry for ASAS 023322-1047.0, CVnet-outburst, Jan 21, 2006

Schwarzenberg-Czerny, A., (1996), ApJ, 460, L107-110

Skillman, D.R., Patterson, J., (1993), ApJ, 417, 298. For general CBA information, see also : <http://cba.phys.columbia.edu>

Vanmunster, T., (2006a), ASAS 023322-1047.0: weak possibly periodic signal, CVnet-outburst, Jan 23, 2006

Vanmunster, T., (2006b), ASAS 023322-1047.0: superhumps finally emerged, CVnet-outburst, Jan 29, 2006

Vanmunster, T., (2006c), ASAS 102522-1542.4: are these early superhumps, CVnet-outburst, Jan 29, 2006

Vanmunster, T., (2006d), ASAS 102522-1542.4 is a new UGSU-type dwarf nova, CVnet-outburst, Jan 29, 2006.

A Compact, Off-the-Shelf, Low-Cost Dual Channel Photometer

Thomas C. Smith
Dark Ridge Observatory
5456 Bolsa Road, Atascadero, CA 93422
tcsmith@tcsn.net

Russell M. Genet
Orion Observatory
4995 Santa Margarita Lake Road, Santa Margarita, CA 93453
russmgenet@aol.com

Christine L. Heather
Physics Department
California Polytechnic State University, San Luis Obispo, CA 93407
cheather@calpoly.edu

Abstract

Photometric observations of short-period variable stars are time constrained because each basic observational sequence must be completed before the variable significantly changes its magnitude or color. A choice must be made. Should the scarce time within a sequence be devoted to making several observations in the same color band that, when combined, will significantly improve photometric precision over that of a single observation? Or, should the single observations be spread sequentially across color bands to provide both magnitude and color, thus enhancing astrophysical interpretations? A third alternative has occasionally been employed for many years, which is one of making a sequence of simultaneous observations in two or more color bands by using a dichroic beam splitter to partition the light into separate color bands with a separate detector being devoted to each band. The two-channel CCD photometer we describe can be operated in the Johnson-Cousins V and I_c bands simultaneously (or alternatively in B and R_c). The compact photometer, which can be assembled from off-the-shelf, low-cost components, uses a dichroic beam splitter (for V and I_c), a Meade flip mirror system, and two SBIG CCD cameras. Our preliminary results suggest that this doubling of observations has been made without any sacrifice in photometric precision. © 2006 Society for Astronomical Sciences.

1. Overcoming the Limits of Time Constrained Photometry

It has been amply demonstrated that multi-color photometry with sub-millimagnitude precision can be achieved with small-aperture telescopes equipped with sequential filters if the observed stars are non-variable or are slowly varying. One beats down the photon and scintillation noise inherent in small-telescope observations via extended observations in each color band.

Photometric observations of short-period variable stars however, are time constrained because each basic observational sequence must be completed before the variable significantly changes its magnitude or color. Should the scarce within-sequence time be

devoted to making several observations in the same color band which, when combined, will significantly improve photometric precision over that of a single observation? Or, should the single observations be made sequentially in two or more different color bands to bolster astrophysical significance? Rather than choosing between these alternatives, one can use dichroic beam splitters to partition incoming photons into two or more different wavelength bands that can be observed simultaneously.

Besides observing two or more colors without reducing the number of observations in a color band, another distinct advantage of simultaneous color observations over sequential observations is that the derived color differences (such as V-I_c) are more precise when taken simultaneously. That's because, for highest accuracy, atmospheric changes should affect

color bands similarly and thus subtract out when one takes the color difference. This may not be the case with sequential observations. Fully realizing this benefit, however, requires true simultaneity, i.e. the integrations must begin together and be of the same length.

Over the years, a number of multi-channel photometers have gathered useful data. These include the two-channel photomultiplier system by Geyer and Hoffmann (1975), the Bonn University Simultaneous Camera (BUSCA) described by Reif et al (1998), the University of Tokyo's 15-channel system (Doi et al 1998), and the four-channel high-speed CCD ULTRACAM photometer (Dhillon and Marsh 2001).

Despite their successful use over the years, simultaneous multi-channel CCD photometers remain rare for three good reasons. First, the costs of multiple CCD cameras (one for each channel), the dichroic filters, and the housing are significantly greater than the cost of a single CCD camera equipped with a sequential filter wheel. Second, multiple CCD cameras and dichroic filters obviously take up more space than a single camera/filter-wheel combination. This can be a serious problem with smaller telescopes, such as the compact Schmidt-Cassegrain fork-mounted go-to systems. Finally, one could not purchase – off-the-shelf – compact, low-cost multi-channel systems. This has been a serious impediment to their wide spread use.

The Johnson-Cousins system has been widely used for decades, and employs low-cost, sturdy glass filters. Because the Johnson-Cousins bands significantly overlap each other, a dual-channel system that employs a dichroic beamsplitter to separate the incoming light into two color bands cannot employ adjacent bands. Traditionally, magnitudes have been primarily reported in V, while color differences have been variously reported as B-V, V-R_c, V-I_c, etc. Although there is considerable merit in observing in three or even more color bands, many of the benefits of multi-color observations can be obtained by observing in just two bands, providing both a magnitude and a color difference (a significant improvement over providing a magnitude alone). For precise, time constrained photometry of fast-changing variable stars, a simultaneous two-color photometer may be a good compromise between the number of color bands and cost and space. As CCD cameras are most sensitive in V, R_c, and I_c, V magnitudes combined with a V-I_c color may, for a dual-channel photometer, provide the widest wavelength baseline consistent with good detector quantum efficiency.

2. An Off-the-Shelf Low-Cost Dual-Channel Photometer

Our system utilizes an off-the-shelf, \$50 Edmund Industrial Optics 50x50mm dichroic beam splitter with a crossover at about 660 nm, which, as luck would have it, happens to be near middle of the R_c band. Most, but not quite all, of the V long-wavelength tail is to one side and the entire I_c short-wavelength tail is to the other. This makes the splitter well suited, albeit not perfect, for a V and I_c two-channel system. For about \$500, Custom Scientific, in Phoenix, Arizona, can provide 50x50mm dichroic beam splitters at any specified wavelength, such as 700nm, which would be slightly preferable although more expensive. We were initially concerned that the advertised surface quality of the Edmund beam splitter (2 wavelengths) might be inadequate, but image degradation did not turn out to be significant.

The optical-mechanical interface for our test two-channel system needed to: (1) firmly attach to our compact Schmidt-Cass telescope; (2) hold our dichroic beam splitter at 45 degrees (with fine adjustments in both axis so the centers of the two cameras' fields-of-view could be made to coincide); and (3) firmly support our two SBIG cameras (along with any focal reducers inserted in the optical path). The low-cost, off-the-shelf Meade Model 647 Flip-Mirror System (2") admirably performed all three functions. We simply replaced the mirror that came with the system with the Edmund dichroic beam splitter. The fine adjustments on the Meade system were invaluable.

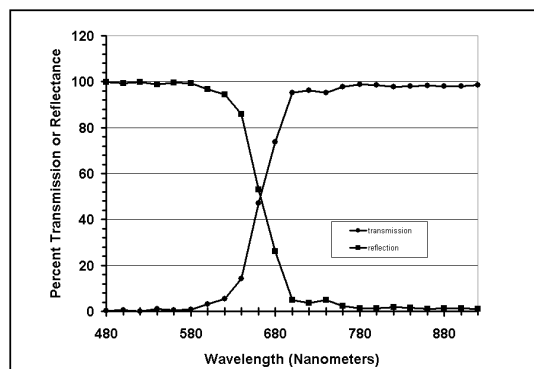


Figure 1. Transmission and reflectance curves for the low-cost Edmund Industrial dichroic beam splitter. These curves are based on data supplied by the manufacturer. One of us (Heather) performed independent spectrophotometer tests of this filter.

To evaluate our dual-channel concept, we temporarily used the Dark Ridge Observatory's SBIG ST7XE CCD camera, and the Orion Observatory's ST8XE CCD camera. We incorporated both cameras in our test dual-channel system on Dark Ridge's 14-

inch Meade LX-200GPS telescope. We purchased an additional CCD camera for each observatory so we can have a dual-channel system operating at each location. Since these “second” cameras need neither autoguiding or motorized filter wheels, we used the newly available, low cost, smaller-sized ST402 CCD cameras, with CCD chips chosen to match our current cameras.

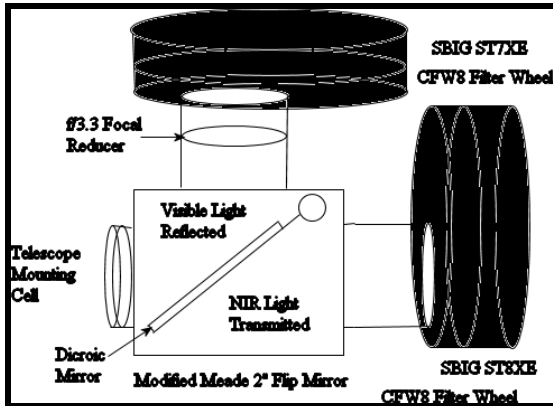


Figure 2. Our initial test configuration used an SBIG ST7 camera (V filter) with an f/6.3 focal reducer and an SBIG ST8 camera (I_c filter) without any focal reduction. Both were attached to a Meade Flip Mirror System (mirror replaced with an Edmund Industrial dichroic beamsplitter) which, in turn, was attached to the Dark Ridge Observatory’s 14-inch f/10 Meade LX200GPS Schmidt-Cass telescope. Our two operational configurations will be similar except one of the cameras has been replaced, in each case, with the lower cost, smaller SBIG ST402 camera (without an autoguiding chip or filter wheel).



Figure 3. This is an overview of the two-channel test-photometer. The Meade 14-inch LX-200GPS telescope is on the far left. Coupled directly to it is the Meade 2” flip mirror system. The f/6.3 focal reducer and SBIG ST7XE camera and filter wheel are shown in the upper middle, while the SBIG ST8XE camera and filter wheel are shown on the right.



Figure 4. This shows the Edmund Industrial dichroic filter which replaced the mirror in the Meade flip mirror system (with the system’s side cover removed).

To control our CCD cameras, we used two instances, in separate memory spaces, of Software Bisque’s CCD camera control software, *CCD Soft*. We did not experience any difficulties controlling two cameras, one with an autoguiding chip.

3. Initial Results

Prior to the initial operation of our two-channel photometer, we had been observing the short-period W UMa-type binary V1191 Cyg. All our observations were made in R_c. We continued our observations of V1191 Cyg with our test dual-channel system, making nearly, although not exactly, simultaneous observations in V and I_c. We have not yet addressed questions of synchronization. Shown below is a recent one-channel R_c light curve and, taken some two weeks later, simultaneous V and I_c light curves obtained with our test dual-channel system.

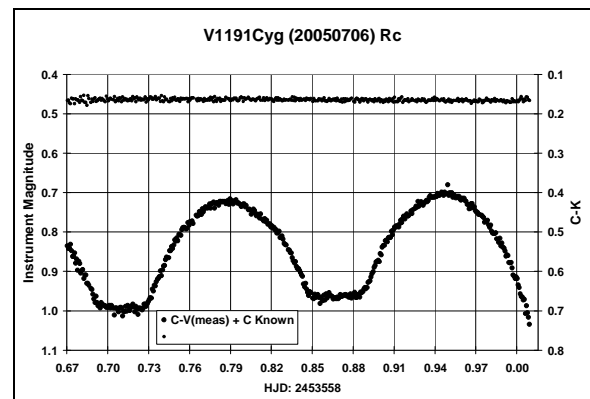


Figure 5. Observations of V1191 Cyg with a single-channel photometer in R_c (bottom curve) made at the Dark Ridge Observatory using an SBIG ST7XE camera with 90-second integrations. The precision of the observations, as suggested by the one-sigma standard deviation of the comparison-check observations (top curve) over the entire night was 3.7 millimagnitudes.

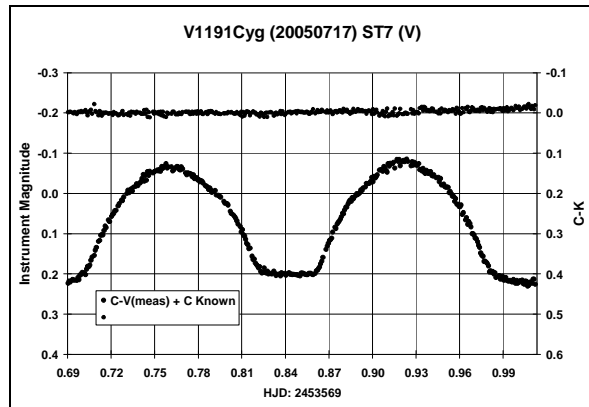


Figure 6. V-band observations from the two-channel photometer of 1191 Cyg. Integrations were 60 seconds (as opposed to 90 seconds for the observations shown in Figure 5). The overall standard deviation for the night (top curve) was 5.7 millimagnitudes.

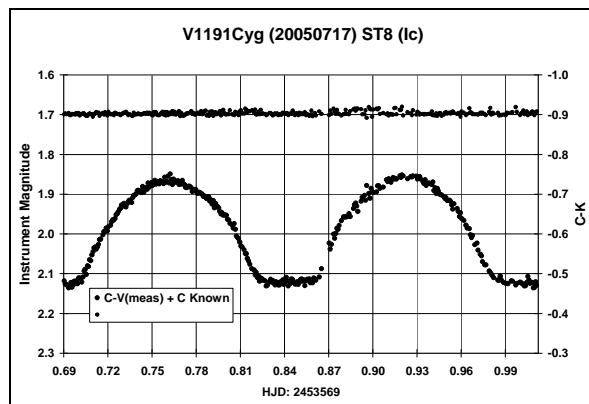


Figure 7. I_c -band observations from the two-channel photometer of 1191 Cyg. Integrations were 60 seconds. The overall standard deviation for the night (top curve comparison - check) was 4.6 millimagnitudes.

4. Conclusions

Photometric observations of fast-changing variable stars, such as the W UMa eclipsing binaries we observe, are time constrained. One way of overcoming such time constraints is to make simultaneous photometric observations in two color bands using a dichroic beam splitter to partition the light. We devised and evaluated a two-channel photometer assembled from low-cost off-the-shelf components. We concluded that our two-channel system worked as well as our somewhat similar one-channel system while providing twice the data.

5. Acknowledgements

We are pleased to acknowledge helpful suggestions by Arne Henden, Kenneth Kissell, John Percy, and Dirk Terrell.

6. References

Geyer, E.H., and M. Hoffmann. 1975. "A Double Beam Photoelectric Photometer for Astronomical Applications." *Astron. Astrophys.* **38**, 359-362.

Reif, K., K. Bagschik, G. Klink, R. Kohley, H. Poschmann, K.S. de Boer, P. Mueller, U. Mebold, J. Schmoll, and U. Heber. 1998. "BUSCA: Simultaneous Imaging in Four Optical Bands." *Astronomische Gesellschaft Meeting Abstracts*, Heidelberg.

Doi, M., H Furusawa, N. Fumiaki, S. Okamura, M. Sekiguchi, K Shimasaku, and N. Takeyama. 1998. "UT 15-Color Dichroic-Mirror Camera and Future Prospects." *Proc. SPIE*, **3355**, 646-657.

Dhillon, V., and T. Marsh. 2001. "ULTRACAM—Studying Astrophysics on the Fastest Timescales." *New Astronomy Reviews*, **45**, 91-95

Extrasolar Planets and the Race to Uncover the First Habitable Terrestrial Planet

Aaron Wolf
kheldar@ucolick.org

Gregory Laughlin
ucolick observatory
1156 high street
santa cruz, ca 95064-1077
laughlin@ucolick.org

Abstract

Over the last decade, advances in technology and scientific technique have allowed scientists to discover more than 150 planets outside of our solar system. By using a number of different techniques, including radial velocity measurement, transit observation, astrometry, and spectroscopic observation, we have pushed the limits of our understanding of planets and how they form throughout our galaxy. With each year, we edge ever closer to the ultimate goal of discovering a terrestrial planet in the habitable zone, and perhaps even an undeniable detection of life outside of our solar system. This paper focuses on the possibility of locating the first terrestrial habitable planet by searching for transits around the lowest mass M stars. While these small and photometrically active objects provide many challenges for photometric study, they are perfectly well suited to the capabilities of the amateur community. The goal is now to find the first habitable terrestrial from the ground. © 2006 Society for Astronomical Sciences.

1. Introduction

In 1916, in circular #30 of South Africa's Union Observatory, Robert T. A. Innes reported the discovery of a faint red star in Centaurus. This otherwise unremarkable star, more than 100 times too faint to be seen with the naked eye, attracted his attention because it was rapidly moving with respect to other stars in the same part of the sky. This large proper motion indicated that the star was almost certainly a close neighbor of the Sun, and in 1917, this suggestion was verified. The distance to the star was measured to be only 4.22 light years, closer to the Sun than any other known star. Its extremely faint appearance, in spite of its close proximity, made it the intrinsically least luminous star known to astronomy at that time. Proxima Centauri, as the star was later named, is now known to be merely the nearest, and most famous, of the roughly 50 billion red dwarfs, or M stars, which inhabit our galaxy.

While M stars are the most abundant stellar type, their low intrinsic luminosities place serious constraints on our ability to study them. Even so, there exist about one hundred M stars that lie close enough to the earth such that their apparent luminosities are brighter than sixteenth magnitude, the current practi-

cal limit for transit observations with a high-end amateur telescope. The question then remains, is it possible that these small faint stars could harbor planets? The remainder of this paper provides relevant background information on M stars and discusses the possibility of finding terrestrial habitable planets around M stars. We argue that not only do we expect that terrestrial planets are common companions to red dwarfs, but also the transit signals of these objects are perfectly suited to the talents of the ground-based amateur astronomy community. We are leading this observational effort, along with other transit and radial velocity related projects, from our extrasolar planets website www.oklo.org. Our investigation shows that the first habitable terrestrial extrasolar planet can be found around an M star, it can be detected from the ground, and it can be done with equipment and techniques accessible to amateurs.

2. Lifespan and Evolution of M stars (Red Dwarfs)

Red dwarfs, or M stars, are by far the most common type of star, and they differ fundamentally from the Sun in several ways. Proxima, for example, has about 11 percent of the Sun's mass, and an aver-

age density several times that of lead (11.4 gm/cc). The Sun's average density, on the other hand, is only 1.4 times that of water (1 gm/cc). Proxima's total luminosity is about a thousand times less than the Sun, yet even this rather modest energy output has a difficult time escaping from Proxima's interior. The center of Proxima is so opaque that radiation cannot efficiently transport all of the energy produced by fusion in the interior to the surface. Proxima must therefore resort to convection, a process in which the turbulent motion of stellar gas physically carries energy away from the center.

The basic process of convection can be observed in a pot of water heated on a stove. Prior to the start of actual boiling, hot water wells up near the center of the pot, divests some of its heat at the surface, and then dives back down. Convection also carries the energy through the outer two percent of the Sun's mass, and the uppermost layer of convective cells are visible as granulation on the solar surface.

An important implication of this is that M stars are highly photometrically active, with their total luminosity fluctuating on a time-scale of, at worst, only a few nights. We will see later that this fact poses an important challenge to photometric monitoring of these objects.

Proxima's whole interior is convective, and hence all the stellar material is continuously and thoroughly mixed. A helium nucleus forged in Proxima's nuclear-burning core can expect to visit the surface regions within a relatively short time. This freedom of movement is in direct contrast to the interior of the Sun, where the core is radiative rather than convective. Helium that forms in the center of the Sun never strays far from its place of origin. The Sun's core thus becomes slowly enriched in helium, while the original composition of the outer regions remains unaffected.

The Sun can't access its entire store of hydrogen, and this will profoundly shorten its productive, hydrogen-burning lifetime. A completely convective low-mass star like Proxima, on the other hand, maintains access to its entire initial reserve of hydrogen fuel. Complete convection, coupled with an underwhelming power output, allows red dwarfs to survive almost unaltered, long after the higher mass stars have turned into white dwarfs, or self destructed in supernova explosions. Two trillion years from now, Proxima Centauri will still be shining, much as it shines today.

The ultimate fate of red dwarfs such as Proxima, was explored using a stellar evolution code in Laughlin, Bodenheimer, and Adams (1997). Figure 1 is adapted from that paper. It indicates that a 0.1 solar mass star will live for about 6 trillion years before exhausting its hydrogen. Instead of becoming red

giants, the lowest mass stars actually become dramatically brighter and bluer before ending their lives as helium white dwarfs.

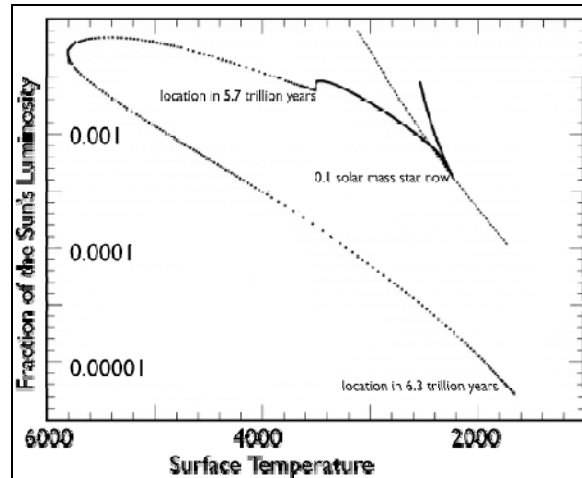


Fig. 1. Evolution of a 0.1 solar mass star in the Hertzsprung Russell Diagram

3. Radial Velocity Observations of M stars

About 130 red dwarfs, nearly all of which are more massive than Proxima, are close enough to the Sun such that their apparent luminosity is bright enough ($V < 11$) to allow radial velocity observations. These red dwarfs have been part of the California-Carnegie Planet Search list for about 8 years. To date, only one M-dwarf system (GJ 876) has been found to harbor Jupiter-mass planets. The occurrence rate of Jupiter-mass planets, therefore, seems to be roughly a factor of ten less for red dwarfs than for stars that are similar in mass to the Sun.

Should we interpret this as a clue that M stars do not tend to form planetary companions? On the contrary, the fact that Jupiter-mass planets seem to be rare in orbit around red dwarf stars seems to be a natural consequence of the core accretion theory of planet formation. In the core-accretion theory, the formation of a giant planet occurs when a large core of solid material (with a mass of roughly ten times the Earth's mass) rapidly accretes gas from the surrounding protostellar disk. The smaller the parent star, the longer it takes for the core to form.

In a protoplanetary disk surrounding a newborn red dwarf star, by the time the cores form, the gas has generally been lost. We predict, then, that Neptune-mass and smaller mass planets will be very common around red dwarfs, whereas Jupiter-mass planets will be quite rare.

It is also interesting to note that the apparent lack of Jupiter-mass planets around M stars seems to sup-

port the hypothesis that core accretion is the dominant mechanism for planet formation. Alan Boss, of the Carnegie Institute of Washington, has recently published a preprint that shows that if the alternate gravitational instability mechanism is the dominant mode of giant planet formation, then Jupiter-mass planets should be just as common around red dwarfs as they are around solar-type stars.

There are now observational indications that suggest that low-mass planets may indeed be common around red dwarfs. The radial velocity surveys have recently reported the detection Neptune-mass companions in short-period orbits around the red dwarfs GL 581 and GL 436. Additionally, a team of observers using the microlensing method, have detected the signature what appears to be a planet with 5.5 Earth Masses orbiting a distant red dwarf.

4. Habitable Planets Around Red Dwarfs

The possibility of discovering the first habitable extrasolar planet is quite exciting, so before discussing whether we expect these objects to exist around M dwarfs, we will provide ample motivation by exploring the properties that they would possess. Thus, let us imagine an Earth-sized world orbiting a star with a tenth of a solar mass. A metal-rich 1/10th solar mass red dwarf has a radius about 1/10th of the Sun's radius, and a surface temperature of about 2750 Kelvin (compared to 5800 Kelvin for the Sun). This radius and temperature gives the red dwarf about 1/2000th of the Sun's energy output.

Therefore, in order for our putative habitable world to receive the same amount of energy that Earth gets from the Sun, it needs to orbit at a distance of 0.022 AU. From Kepler's third law, we see that this corresponds to an orbital period of 3.85 days. An Earth-like planet with a period of 3.85 days will be tidally locked to the red dwarf.

In the absence of any significant perturbing bodies, its orbit will be almost perfectly circular, and its spin period will be the same as the orbital period. Like the Moon with respect to the Earth, the planet will always show one face to the red dwarf: one hemisphere will have an eternal day, the other hemisphere eternal night.

Naively, one might think that such a situation would be disastrous for planetary habitability. The lit side of the planet will bake, and the night side will be inhospitably cold. Worse yet, if the night side grows cold enough for the atmospheric gases to condense, then the resulting cold trap will rapidly render the planet airless and uninhabitable. Interestingly, however, simulations show that this situation will not

occur. A 1997 study by Joshi et al. used a global climate model to investigate how the Earth's climate would respond if the Earth were tidally locked to the Sun. The results were encouraging: the substellar point on the surface was warmer than the Saharan Summer, and the antisolar point on the dark side was colder than the Antarctic Winter, but the atmosphere did not collapse. The oceans and atmosphere effectively transported heat from the dayside to the night, and the tidally locked Earth remained habitable.

5. The Formation of M Dwarf Terrestrial Companions:

The all-important question still remains: Do we expect habitable terrestrial planets to form around 0.1 solar mass stars? A planet with a 3.85 day period orbiting a 0.1 solar mass red dwarf is about 20 times closer to its parent star than Mercury is to the Sun. Is it reasonable to expect to find a planet orbiting this close? As a first piece of evidence, we know for sure that the nearby 0.32 solar mass red dwarf GJ 876 is accompanied by a 7.5 earth mass planet with an orbit of only 1.9379 days (Rivera et al. 2005).

Most important, recent simulations performed by University of California, Santa Cruz graduate student Ryan Montgomery are supporting the existence of habitable terrestrial planets around M dwarfs. Montgomery has performed an extensive set of computer calculations that simulate the last evolutionary stages of planet formation from an initial swarm of planetesimals that make up the protoplanetary disk of a young low-mass red dwarf star. This simulation employs the Wetherill-Chambers method, which has had good success in explaining the latter stages of formation of the terrestrial planets in our own Solar System.

The simulation's underlying physical picture has a star and a disk that are of order one million years old, having already completed the initial stages of planet formation. Grains of solid material have stuck together to build larger and larger objects in the disk. Most of the gas that was originally in the disk has either accreted onto the star, or has been photoevaporated by high-energy photons originating from both the parent star as well as neighboring stars.

Currently, three sets of calculations have been completed, while a large number of additional runs are still computing. In the first set, containing sixty individual simulations, we assume that two Neptune-like giant planet cores have already managed to form beyond the protostellar ice-line.

The ice-line begins where the temperature is lower than 150K, the freezing point of water at zero pressure, and thus planets can grow more quickly due

to the increased availability of solid material. We also assume that the innermost Neptune-mass core has undergone planetary migration, placing it at a distance of ~ 0.2 AU from the central star.

This situation was chosen so as to be in analogy with the known Neptune-mass planets orbiting the red dwarfs GL 436 and GL 581. In a second set of sixty simulations, no giant planet cores were included. In our simulations, the Neptune-mass cores assume a role similar to that which Jupiter and Saturn are believed to have had during the formation phases of the terrestrial planets in our own solar system.

In each of the 120 simulations that comprise the first two sets, we distribute 1000 planetesimals in initially circular orbits in the region between 0.04 AU and 0.12 AU surrounding the eventual stellar habitable zone for the 0.12 solar mass star. Each planetesimal contains 0.003 Earth masses (about a quarter of a lunar mass). The swarm of planetesimals is then allowed to evolve under its own self-gravity, the gravity of the star, and the gravity of the ice-giant cores, if present. Planetesimals that collide with each other are assumed to conserve total angular momentum in their collision, while merging to form larger composite objects. Some planetesimals collide with the ice giants or with the star, or are thrown out of the system.

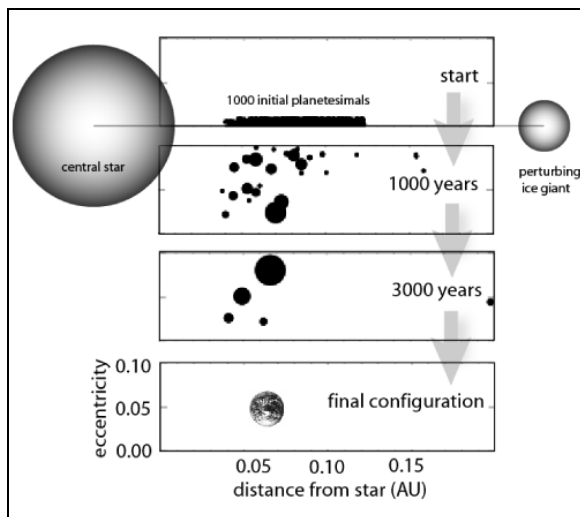


Fig. 2. Schematic diagram showing evolution of swarm of planetesimals to form terrestrial mass planets

In a typical simulation, depicted in Figure 2, the swarm rapidly works itself down over a period of a few thousand years into a system of several terrestrial mass planets. Earth-mass planets in the habitable zone of the star are a very common outcome of both sets of simulations, though they form more readily in the systems with ice-giant cores.

In a third set of thirty simulations, we lowered the masses of the planetesimals to 0.0003 Earth-

masses, decreasing total disk mass by a factor of ten. The results of these simulations were the formation of Mars-sized or smaller bodies in the stellar habitable zone. These results have a simple interpretation.

The final stages of terrestrial planet formation in the protoplanetary disks of red dwarf stars appears to be an efficient process. If one starts with an adequately high effective surface density of solid material in the disk, then one frequently gets Earth-mass planets in the habitable zone. If one starts with a lower surface density, then one gets final sets of terrestrial planets that, on average, have proportionally lower masses.

6. A Case for High Surface Densities

Having demonstrated the importance of initial surface density to the final outcome of the simulations, we expended great effort in determining the appropriate surface density. If one makes reasonable extrapolations from the minimum-mass solar nebula that formed our own solar system, or if one extrapolates from the dust disks which are observed around young stars in the solar neighborhood, then one should adopt a low surface density.

This was the approach taken by Sean Raymond, presented at AbSciCon, 2006. Raymond's results agreed quite well with our low-surface density simulations, namely, Mars-sized or smaller planets in the habitable zones of red dwarfs. Sub-millimeter observations of dust masses in young stellar systems also seem to agree with the low surface densities employed in the "less-successful" simulations.

These observations, however, only measure the amount of mass in dust, and are not directly sensitive to the amount of mass in large, planetesimal-sized bodies. Furthermore, such measurements give the dust mass at large distances, greater than one astronomical unit from the star, and hence do not give information about the mass of solids present in the innermost region of the disk.

According to these arguments, we choose to favor the high surface density scenario based on the "Minimum Mass Nebulae" for the inner regions of GJ 876 (0.32 solar mass) and Jupiter (0.001 solar mass). These are the two objects closest in mass to our hypothetical 0.12 solar mass star whose "terrestrial planet" systems we can measure.

In the case of the Jupiter satellite system, the moon Io has a mass of 8.93×10^{25} grams, an orbital radius of 0.0028 AU, and an orbital period of 1.8 days. This implies a minimum solid surface density of approximately 12,000 grams per square centimeter at the 1.8 day orbital radius in the proto-Jovian nebula necessary to form Io. In the case of GJ 876, planet

“d” has a mass of 4.5×10^{28} grams (7.5 Earth masses), an orbital radius of 0.02 AU, and an orbital period of 1.94 days.

If we make the reasonable assumption that GJ 876 d fed off material reaching out to a radius of 0.075 AU, then this implies a minimum solid surface density of 11,000 grams per square centimeter at the 2.0 day orbital radius in GJ 876’s protoplanetary nebula. The effective surface densities of solid material implied by these two systems are thus remarkably similar, each valued at about 10,000 grams per square centimeter at a 2-day orbital period.

Accordingly, we allow these two real-world bounding cases to guide our choice of appropriate initial surface density, adopting a solid surface density of 11,000 grams per square centimeter at the 2-day orbital radius for our 0.12 solar mass star (0.015 AU).

We apply this constraint using a reasonable $r^{-3/2}$ falloff in surface density as we move away from the star, suggesting a fiducial density of 2000 grams per square centimeter at a habitable-zone radius of 0.045 AU. It is this final value for the surface density that was employed in our first two sets of preferred simulations.

7. Possibilities for Ground-Based Detection

If habitable planets do commonly form in orbit around low mass red dwarfs, as Montgomery’s simulations indicate, our analysis shows that our chances of detecting and characterizing them are surprisingly good. The radius of a 0.1 solar mass star is roughly 10 times smaller than the Sun, and 10 times larger than the Earth. This means that the transit of an Earth-sized planet will block about 1% of the red dwarf’s light.

For the example case of our planet on a 3.85 day orbit, the transit will be relatively brief, lasting about 40 minutes. In principle, a 1% photometric dip is readily detectable, and in fact, amateur astronomers who participate in the transitsearch.org collaboration, which is one of our projects organized from www.oklo.org, routinely achieve detection thresholds of considerably better than 1%.

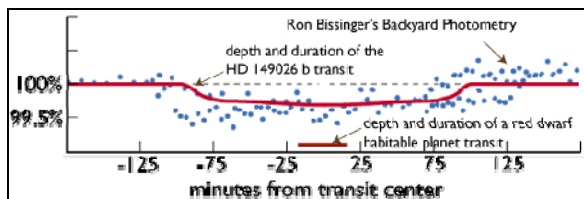


Fig. 3. Comparison of skilled amateur photometry of HD 149026 transit with potential habitable terrestrial planet transiting parent M star.

Figure 3 shows Ron Bissinger’s observation of the transit of HD 149026 b, which has a transit depth of 0.3%, compared to the depth and duration of the transit of an Earth-sized planet. Skilled amateurs such as Bissinger or Tony Vanmunster have backyard techniques that are good enough to detect the passage of even a Mars-sized body in front of an 11th magnitude 0.1 solar mass red dwarf.

Montgomery’s simulations were also used to help determine the feasibility of ground-based detection by skilled amateurs. Once a particular simulation run is completed, we choose a random angle from which the system is to be viewed. We then generate photometry that is typical of what high-end amateur observers such as Ron Bissinger or Tony Vanmunster are capable of regularly achieving (see Figure 3).

Next we “observe” the system by creating a simulated photometric time series over a period of several hours, during the intervals in which a transit might possibly occur. Figure 4 displays just one example of a simulated successful transit detection.

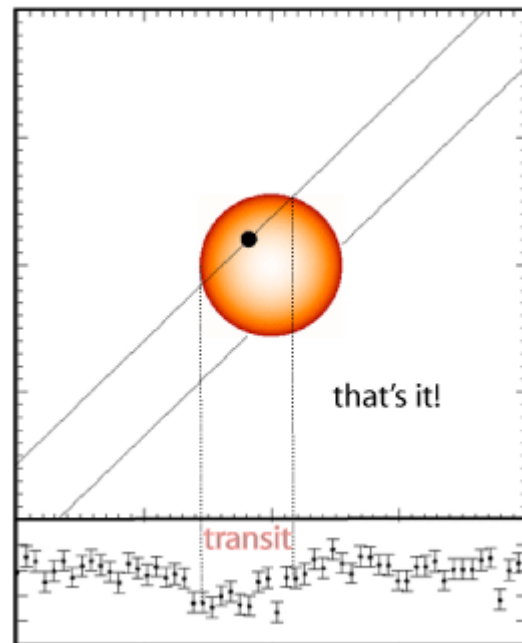


Fig. 4: Synthetic detection of a habitable terrestrial planet transiting an M dwarf with high-end amateur equipment.

It is important to note that the useful technique of “folding” photometric data in order to find periodic intensity dips will likely be of little use in locating the transit of a red dwarf companion. This is because these low mass stars are highly photometrically active, and thus tend not to have night-to-night photometric stability.

It is thus absolutely important that photometric observations are made simultaneously by multiple

observers in order to ensure confidence in a potential detection. Even with these constraints, it is encouraging to note that in total, our simulations imply about a 1.0% a-priori probability that a 0.12 solar mass red dwarf has a detectable, habitable planet.

8. Conclusion

The final question that remains, then, is how many suitable red dwarfs are available on the sky? Even though the lowest-mass M stars are the most common type of star, they are also exceedingly dim. A 3m-class telescope, such as the Shane Reflector on Mt. Hamilton would be required to properly search the magnitude range $V=16-18$ where the lowest-mass red dwarfs begin to be plentiful (and indeed, many 0.1 solar mass stars within 10 parsecs still remain to be discovered). In the meantime, however, we recommend that observers join our efforts, which are being coordinated from www.oklo.org, and immediately consider obtaining high-cadence photometry of the nearby stars presented in Figure 5. Each candidate star has a one percent chance of harboring a detectable transiting, potentially habitable planet. It is now our responsibility to find that lucky system.

	distance (ly)	mass	Vmag	RA	DEC
Proxima	4.2	0.11	11.09	14:30	-62
Barnard's star	6.0	0.17	09.53	17:57	+05
Wolf 359	7.8	0.09	13.44	10:56	+07
Ross 154	9.7	0.17	10.43	18:50	-23
Ross 248	10.3	0.12	12.29	23:41	+44
Ross 128	10.9	0.16	11.13	11:47	+01
DX Cancri	11.8	0.09	14.78	08:30	+27
GJ 1061	12.0	0.11	13.03	03:36	-44
GJ 54.1	12.1	0.13	12.02	01:12	-17
GJ 83.1	14.5	0.14	12.27	02:00	+13

Fig. 5: Selection of nearby M dwarf stars from the RECONS catalog of the 100 nearest stellar systems maintained by Todd Henry and his collaborators at Georgia State University

Detecting Exoplanets by Gravitational Microlensing using a Small Telescope

Grant Christie
Auckland Observatory
PO Box 24-180, Auckland, New Zealand
grant@christie.org.nz

Abstract

Gravitational microlensing is a new technique that allows low-mass exoplanets to be detected at large distances of ~ 7 kpc. This paper briefly outlines the principles of the method and describes the observational techniques. It shows that small telescopes with a CCD camera can make unexpectedly useful observations of these events. © 2006 Society for Astronomical Sciences.

1. Introduction

Auckland Observatory has been active in variable star research since 1969 when a UBV photoelectric photometer was constructed and used on the 0.5m Zeiss Cassegrain telescope. Since 2003 a CCD camera has been used, and this has greatly increased the range of projects that can be undertaken.

The observatory is sited in a large park within Auckland City and suffers from the usual problems of urban light pollution. Moreover, Auckland is a relatively cloudy site suggesting that the most efficient observing strategy is to acquire data at a fast rate while the sky is clear and to give priority to projects that are tolerant of cloud interruptions.

Time series photometry of cataclysmic variable stars (CVs) provides an efficient way to use the available telescope time. Almost any observations, even those interrupted by passing cloud, can still provide a scientifically useful result. These observations are done as part of the CBA network (CBA-Auckland).

Beginning in 2003, we have also been observing gravitational microlensing events. The observational techniques are similar to those used for CVs except that the fields are always very crowded and the time scales of interest are generally longer, allowing longer exposures to be used.

Intrigued by the possibility of contributing to the discovery of an extra-solar planet, Auckland Observatory joined the MicroFUN collaboration based at Ohio State University in 2004.

Up until this time, observations of gravitational microlensing events were done by telescopes larger than 0.6m, although most were 1m or larger.

As most of these events are in the galactic bulge of the Milky Way, Auckland is very well placed geographically (latitude -36.9). Moreover, our time zone (GMT+12) means that we can start observing an event just as the telescopes in Chile have to stop. So while the telescope we use is small (0.35m SCT), our favorable geographic location plus the ability to schedule long hours of coverage at short notice has proved to be surprisingly successful.

This paper will introduce the basic principles of gravitational microlensing, concentrating on its application to exoplanet detection. Then we will describe the equipment, the observing protocol, and the data processing techniques. Two examples of recent planet detections will be presented.

2. Gravitational Microlensing

The gravitational field of every star acts as a lens, deflecting the path of light passing through it. A schematic of the basic geometry is given in Figure 1.

For stellar masses, the field of view of the gravitational lens is tiny (~ 1 mas) so the probability of seeing another star within its field of view is extremely small, typically of order 10^{-6} .

While it is quite impractical to monitor any single lens in the hope of seeing a star pass through it, there are several well-established and efficient surveys specifically designed to detect gravitational microlensing events. This is achieved by surveying regions in the galactic bulge where star densities are very high and measuring the brightness of roughly one hundred million stars each night.

There are two microlensing surveys currently active. One is the Optical Gravitational Lensing Experiment (OGLE) which detects ~ 600 events per year using 1.3m Warsaw Telescope at Las Campanas

Observatory in Chile. The other is Microlensing Observations in Astrophysics (MOA) which presently detects ~50 events per year using a 0.4m telescope at Mt. John Observatory in New Zealand. A new 1.8m telescope dedicated to the MOA survey is about to start operation at Mt. John.

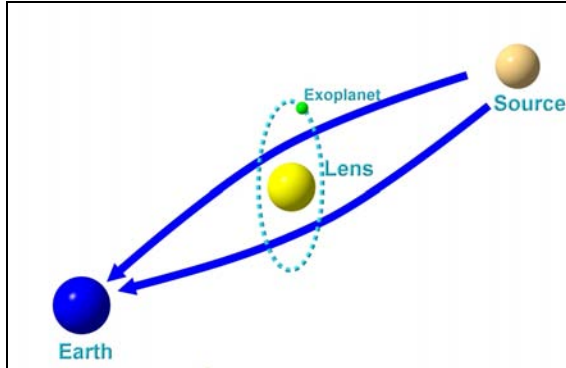


Figure 1. The geometry of a gravitational microlensing event. The gravitational field of the lens both magnifies the image of the source star and brightens it. The presence of an exoplanet causes caustics in the lens.

The source star is usually in the galactic bulge and hence at a distance of 6-8kpc. The lens star can be anywhere in between the observer and the source but is typically around 2-5kpc.

When there is perfect alignment between the source and the lens stars, the image formed by the lens of the source star is a circle, commonly called the Einstein ring. Because the Einstein ring provides a natural scale, most dimensions in microlensing are expressed in units of Einstein radius.

If the gravitational lens is formed by a single isolated star, the mathematical form of the lens magnification, A , is very simple:

$$A(u) = (u^2 + 2) / \{u(u^2 + 4)^{1/2}\} \quad (1)$$

where u is distance of the source star from the center of the lens in units of the Einstein radius. The parameter, u , is commonly called the *impact parameter*. A microlensing event that conforms to this simple relationship is called a point-source point-lens (PSPL) model.

Note that the impact parameter itself is a function of time because the source star is moving through the lens. The lens magnification reaches a maximum when the impact parameter is a minimum; this occurs when the source star is closest to the center of the lens.

Depending on factors such as the relative distances of the lens and the source, it will usually take 50-100 days for the source star to cross the Einstein ring.

Any departure from this classical PSPL behavior is considered to be an anomaly and these can be caused by a variety of effects.

One fairly common anomaly is caused by the source star being a giant with a “large” angular diameter. A solar-type dwarf subtends an angular size of $\sim 0.6\mu\text{as}$ at the galactic center so a giant star may subtend an angular size that is an appreciable fraction of the Einstein radius.

Gravitational microlensing observations can enable the diameter of the source star to be determined to very high accuracy ($\pm 0.05\mu\text{as}$) and in favorable events, it is also possible to measure directly the limb darkening and even the oblateness of the star (Rattenbury et al, 2005).

However, the anomalies in which we are most interested are those caused by planets orbiting the lensing star. When the lens is composed of two gravitating bodies, we get a more complex lens than the simple symmetric form given in Eq. (1).

In the case of a binary lens, caustic lines are formed within the lens which have some extremely useful properties. Caustics are closed contours that correspond to lines of nearly infinite magnification. If a source star passing through the lens crosses a caustic, the apparent brightness of the event increases sharply as the caustic magnifies the size of the source star.

Thus, even though the planet’s mass is much smaller than the lens star, the caustics caused by the planet have a fortuitously large and directly observable effect on the event light curve: they cause a measurable anomaly (Abe et al, 2004).

To detect a planet, we require only that the source star pass over or close to a caustic. Fortunately, the planet caustics are also found close to the lens star and when the source star is close to the lens star (i.e. u is small), the magnification can become very large. At this point, the event can be bright enough to be observed with small telescopes just when it is at maximum likelihood of crossing a caustic.

Thus microlensing events of very high magnification are exquisitely sensitive to the presence of planets. It also means that in order to detect a planet around the star, the event needs only to be intensively observed close to the maximum brightness, which is a relatively brief period of typically 1-5 days. This kind of coverage requires a network of observatories spaced in longitude and preferably at a southern latitude.

The caustics formed by a star/planet pair are a closed contour so that caustic crossings must occur as pairs – one being the entry and the other being the exit crossing. Caustic crossing are short time-scale events and because there is seldom advance warning

when they are to occur, intensive photometric monitoring is required.

For massive planets similar to Jupiter, the mass ratio is $\sim 1.0 \times 10^{-3}$ whereas for Earth-mass planets, the mass ratio is $\sim 3.0 \times 10^{-6}$ (relative to the Sun). In the case of a Jovian mass planet, the probability of a detection reaches 100% over quite a large area surrounding the lens.

Once an event has been detected by a microlensing survey – that is, a *source* star is detected crossing the field of view of the *lensing* star – an alert is issued to follow-up networks which then decide if the event merits close monitoring.

The principal criterion is for the event to have a very high magnification, preferably >100 . Although such cases are rare, they offer a very high probability of detecting a planet if one is present (Rattenbury et al, 2002).

Once the light curve for an event has been obtained, (albeit with inevitable gaps), a search is made for models that can accurately reproduce it. The key parameters sought are:

- the planet-star separation on the sky
- the diameter of the source star
- the angle of the source star trajectory to the planet-star axis and,
- the planet-star mass ratio.

Essentially the process involves trialing very large numbers of possible trajectories of the source star through the lens, iteratively changing the free parameters, while seeking an optimal match to the observational data.

For some events, the model can be determined quickly while in more complex situations it may take months of intensive effort to locate a solution.

So while events of very high magnification (>100) are rare, they are by far the most sensitive to the presence of planets. The aim of MicroFUN is to identify such events and then to activate an intensive observational campaign with the contributing observatories.

It should be noted that many observed microlensing events follow the simple PSPL model and exhibit no anomalies. Nevertheless, even in such cases it is usually possible to show that there are no planets in quite broad exclusion zones around the parent star. This is valuable information that over time will help determine how many stars have planets and how many do not.

3. Equipment

The Nustrini Telescope at Auckland Observatory is a 0.35m Celestron Schmidt-Cassegrain manufactured in 1980. It is operated at f/11 giving a focal length of 3.85m and an image scale of 53.75 arcsec mm⁻¹. The primary mirror is locked in place and focusing is effected by a electric Crayford focuser with digital readout (Jim's Mobile Inc, Lakewood CO).

The telescope is mounted on a Paramount GT1100s mounting (Software Bisque, Golden CO) that is fully controlled by a computer. The absolute RMS pointing error is ~ 45 as and periodic error is <0.5 as peak-to-peak. The software control of the mount is through The Sky V5 (Software Bisque, Golden CO). Exposures of up to 600s are possible giving minimal image elongation without guiding.

The seeing in Auckland is typically in the range 2.3-3.5as with wind speeds <20 km hr⁻¹.

The CCD camera used is an Apogee AP8p (Apogee Instruments Inc., Roseville CA) with a 1kx1k SITE003 thinned, back-illuminated chip. It is thermoelectrically cooled and operates at -20°C during the summer and -25°C otherwise. This detector has high quantum efficiency and quite broad spectral response; the 24 μm pixels have a well depth $\sim 350k\text{e}^-$. The camera is operated in 1x1 binned mode giving an image scale of 1.29as/pixel. The field of view is 22 arc-minutes, but for time series photometry only, a central subframe of 512x512 pixels is used. No filters are currently used although observing with an I-band filter may be advantageous.

The CCD camera is controlled by MaxImDL/CCD (Diffraction Limited, Ottawa, Canada).

4. Image Calibration

The AP8p camera bias level is nominally set at 3030ADU. However, it drifts slowly during the night so regular bias frames are taken to ensure proper dark frame subtraction. Flat fields are taken using either the dusk or dawn twilight sky whenever conditions permit. Typically, 12 full frames are taken at an altitude of 70° facing away from the sun. These are then bias subtracted, dark subtracted, normalized and median combined to produce a master flat.

Bias subtracted dark frames of long exposure time (~ 24 hr of total dark exposure) are scaled to match the exposure time of the science frames.

The science frames are first bias subtracted and then the scaled dark frame is subtracted. Finally, the science frame is divided by the master flat.

5. MicroFUN

The MicroFUN collaboration is based at Ohio State University (Department of Astronomy) and has been in operation since the 2003 season. It is led by Professor Andrew Gould who is largely responsible for selecting the target list and coordinating the observing network.

The alerts issued by the OGLE or MOA surveys are monitored by MicroFUN for events favorable to planet detection. The most favorable (high magnification) events usually provide the least warning because the rise to maximum magnification

might only take a few hours. On the other hand, an otherwise low interest event can suddenly become riveting if the source star crosses a caustic.

Each observatory in the network may be requested to stop a planned observing program and switch to the microlensing event at very short notice. Small observatories can usually do this without problem but for telescopes larger than 1m, this may not be possible because of scheduling issues. Thus, while large telescopes provide high accuracy photometry, they cannot be relied upon to be available at the critical time.

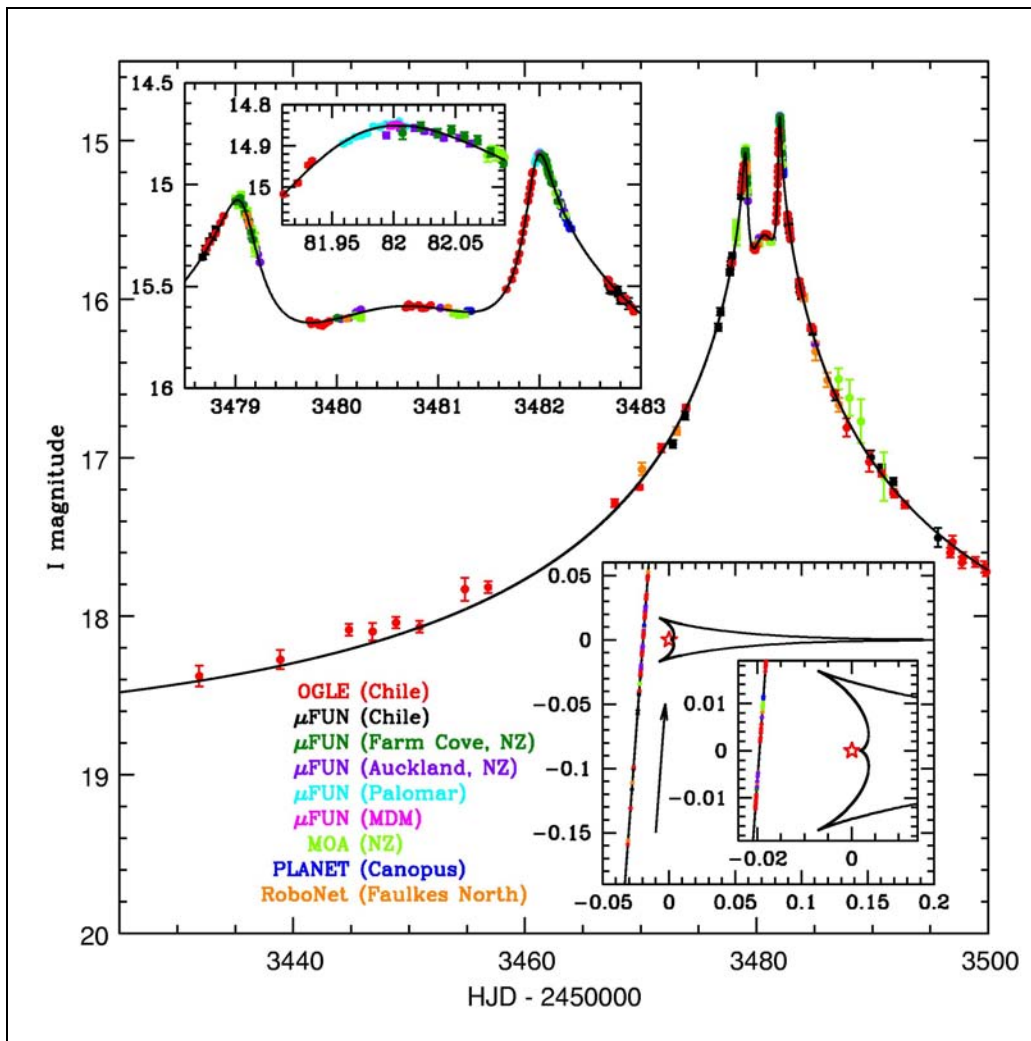


Figure 2. The light curve of OGLE-2005-BLG-071. The upper insert shows the detail at maximum while the lower insert shows the path of the source star through the binary lens. The two peaks in the light curve are caused by the passage of the source star close to, but not actually crossing, the caustic cusps. Units are Einstein ring radius. (Udalski et al, 2005)

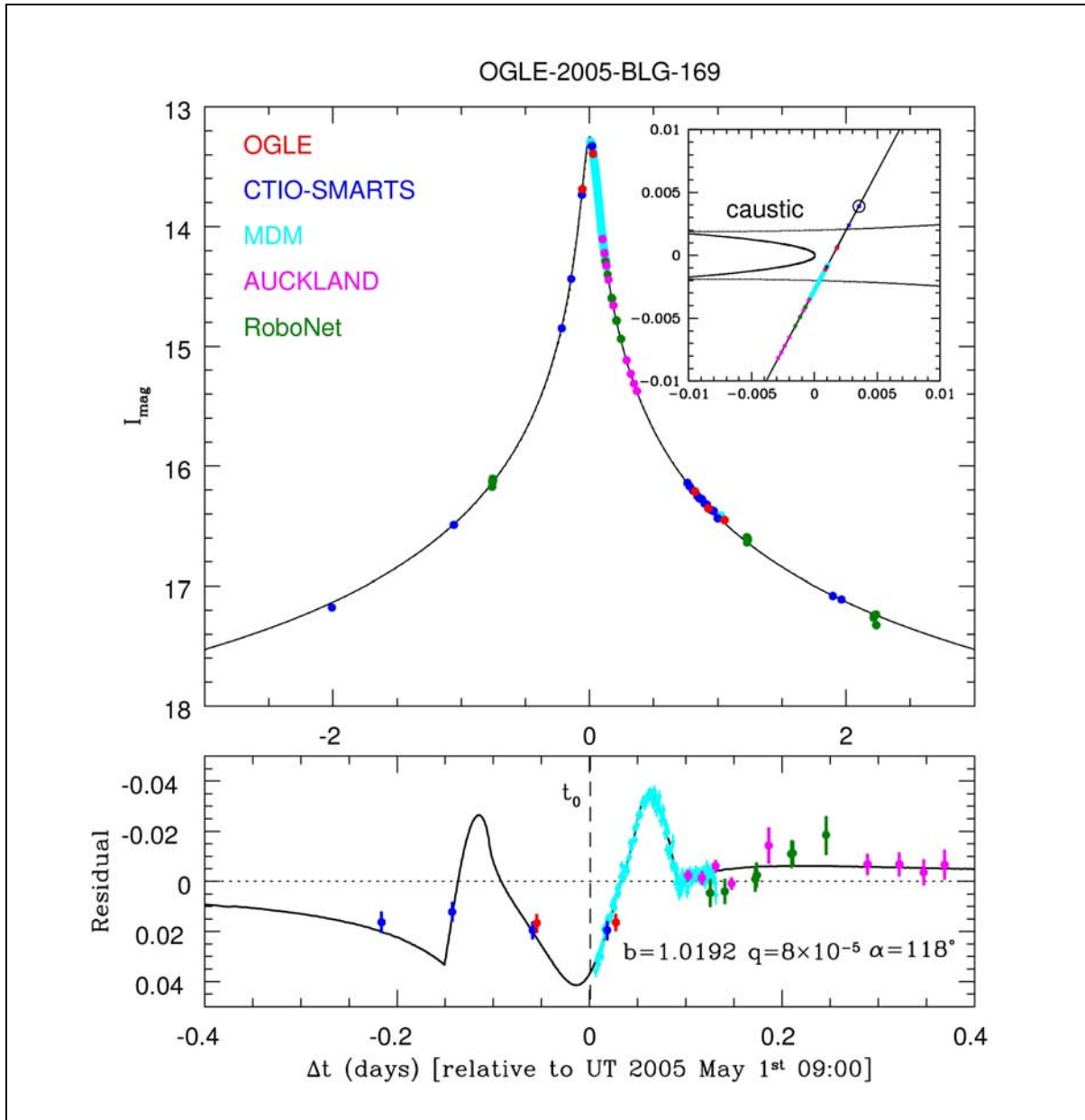


Figure 3. The light curve of OGLE-2005-BLG-169 is shown in the upper plot. The geometry the source star passing through the binary gravitational lens with two caustic crossings is shown in the insert. The lower plot shows the anomalous deviation of the light curve from the simple PSPL model. (Gould et al, 2006).

6. Observing Microlensing Events

During the 2005 microlensing season, Auckland Observatory contributed 248 hours of photometry on 27 events notified by MicroFUN (26 from OGLE, 1 from MOA). Two of these events have now been analyzed in detail, leading to the discovery two exoplanets.

The first one in April 2005 was a planet with a mass of three Jupiters in event OGLE-2005-BLG-071 (Udalski et al, 2005) - the final light curve for the

event is shown in Figure 2. The peak magnification was $A \sim 70$ and the planet caused anomalies which were large (0.75 magnitudes).

The second event occurred about 10 days later and detected a Neptune-mass planet (13 Earths) in event OGLE-2005-BLG-169 (Gould et al, 2006). This was a very high magnification event ($A \sim 800$) and was therefore extremely sensitive to planets. Its final light curve in Figure 3 shows that the amplitude of the anomaly is about 3-4%.

A number of the other events observed in 2005 also displayed clear anomalies but these still await detailed investigation.

The first microlensing observations from Auckland were made in the 2003 at the request of the MOA collaboration. These attempts were only partly successful because it proved difficult to identify the faint target in a crowded field.

This problem was resolved by first improving the telescope pointing using TPoint (Software Bisque, Golden CO) and, second, using the "Image Link" facility available in The Sky, the program used to control the mounting.

The protocol used now is to first slew to the microlens coordinates, which locates the field to ~ 1 arcminute. A short exposure is taken and registered using "Image Link". Essentially, this involves extracting the position of the stars from the CCD image and matching this pattern to the stars in that vicinity listed in the stellar databases available (GSC, UCAC 2 or USNO A2.0). Image Link takes only a few seconds and exactly aligns the CCD image over the chart of the star field which includes the marked position of the microlens.

This positively identifies the microlens on the CCD frame and confirms the telescope pointing to ~ 1 arcsec. The telescope is re-positioned to center on the microlens and then the imaging sequence is started. Exposure times in the range 120-600s can be used without autoguiding.

Once the first full length exposure is downloaded, the field is positively identified by inspection using the annotated image provided by the survey team (OGLE or MOA). In crowded fields this procedure can be very difficult because the survey image has been taken with a much bigger telescope under much better seeing conditions. However, the fact that we already know that the microlens is located at the center of our image is a significant advantage.

Using this procedure, it now only takes a few minutes to start an observing run on any microlens after receiving an alert.

The image field of view need not be large because the fields are always crowded and there is no shortage of reference stars. We image using a 512x512 pixel subframe located at the center of the field (and thus on the optical axis); this corresponds to 11x11 arc-minutes. After calibration, the images are usually cropped to 200x200 pixels to reduce the FTP upload time.

Once an imaging sequence is started, the only interruptions, apart from the weather, are to take sets of bias frames, as discussed above, or to improve the focus.

The image scale must be chosen to ensure the star images are fully sampled. The full-width half-maximum (FWHM) of a bright stellar image should be in the range of 2-3 pixels. All reduction codes used in crowded fields require the fitting of a point spread function (PSF) to each stellar image and this cannot be done accurately if the image has been under sampled. An example of a typical microlensing field is given in Figure 4.

The primary disadvantage from *over* sampling the image (i.e. FWHM > 3 pixels) is that there will be more shot noise in the stellar image than is necessary. Nevertheless, this creates fewer problems than are encountered with under sampled images.

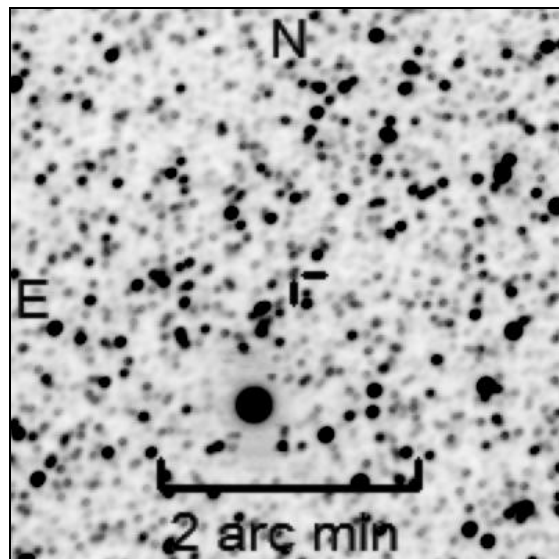


Figure 4. The CCD image of event OGLE-2005-BLG-071 (10x120s) from Auckland Observatory.

It is important to ensure the focus is as good as possible. Often the microlens will be blended with the images of nearby stars so the possibility of accurately disentangling the light from overlapping star images is improved if the FWHM is small (but not significantly < 2 pixels).

In most microlensing events, the objective should be to maximize the total exposure time. If the microlens is bright, in which case there are likely to be caustic crossings with little advance warning, continuous imaging guarantees no critical event will be missed. If the microlens is faint, then even with a small telescope, binned observations over a period of hours can still provide an accurate magnitude estimate that contributes to the coverage of the event. Successful results have even been obtained by binning 6 hours of exposure time to yield a single observation.

7. Image Reduction

The crowded fields of microlensing events preclude the use of aperture photometry techniques. Aperture photometry is only used at the telescope while an event is in progress to provide quick updates to other members of the follow-up network.

On completion of an observing run the Auckland images are calibrated as described above and usually cropped to 200x200 pixels. They are transmitted by FTP to OSU where they are processed through the DoPhot reduction code (Schechter, 1999). This provisional PSF photometry is then posted on the MicroFUN website and used to monitor the progress of the event.

Because of the wide differences between the various MicroFUN telescopes, detectors and filters used (or not used), this initial data set is not internally consistent. Some observatories process their own images using other reduction codes and only submit the reduced magnitudes.

If the event proceeds to the modeling phase, all the photometry has to be reduced to a common system. The first step is to process all images of the event through the same image reduction pipeline to remove possible systematics due to different algorithms.

The most accurate photometric reduction codes currently available use differential image subtraction (DIA) (see Alard & Lupton, 1998; Alard, 1999; Wozniak, 2000; Bond, 2001). This is the method used by the microlensing survey teams and it has been found to be close to optimal in terms of information extraction. For recent microlensing events, processing all photometry through the OGLE DIA pipeline has significantly improved the accuracy; this is especially true for images obtained with small telescopes when the microlens is faint.

8. Conclusion

Gravitational microlensing is developing as a powerful technique for detecting extra-solar planets. It has already achieved some notable successes with three planet discoveries so far coming from observations in the 2005 season and more are likely.

It has been found that small telescopes providing intensive coverage of high magnification events is a surprisingly effective strategy, even when operated from an urban location. The key is their ability to re-allocate all telescope time at short notice to follow an interesting event while it is near maximum brightness.

The observation of gravitational microlensing events is both technically challenging and extremely

rewarding. No two events are the same so the observer has no idea what to expect. Caustic crossing events, which can only be described as photometrically spectacular, can occur at any time and often with little or no prior warning.

Most important, planet discoveries excite the public and attract media attention to astronomy – both important considerations for a public observatory like Auckland

9. Acknowledgements

A travel grant provided by the MicroFUN collaboration is gratefully acknowledged, as is the support of the Auckland Observatory and Planetarium Trust Board.

I am indebted to Phil Yock (MOA) for first suggesting I should observe gravitational microlensing events.

The support and encouragement of Andrew Gould and Richard Pogge (MicroFUN) is greatly appreciated and I thank Andrzej Udalski and the OGLE team for their steady stream of interesting events.

Finally, I thank Jennie McCormick for sharing the excitement throughout.

10. References

- Abe, F., Bennett, D. P., Bond, I. A., Eguchi, S., Furuta, Y., Hearnshaw, J. B., Kamiya, K., Kilmartin, P. M., Kurata, Y., Masuda, K., Matsubara, Y., Muraki, Y., Noda, S., Okajima, K., Rakich, A., Rattenbury, N. J., Sako, T., Sekiguchi, T., Sullivan, D. J., Sumi, T., Tristram, P. J., Yanagisawa, T., Yock, P. C. M., Gal-Yam, A., Lipkin, Y., Maoz, D., Ofek, E. O., Udalski, A., Szweczyk, O., Zebun, K., Soszynski, I., Szymanski, M. K., Kubiak, M., Pietrzynski, G., Wyrzykowski, L., Search for Low-Mass Exoplanets by Gravitational Microlensing at High Magnification, *Science*, 305, 1264 (2004).
- Alard, C. and Lupton, R.H. A method for optimal image subtraction, *ApJ* 503, 325 (1998)
- Alard, C. Analysis of the OGLE microlensing candidates using the image subtraction method, *A&A* 343, 10 (1999)
- Bond, I., Difference Imaging Analysis of the MOA Image Data Base, in *Microlensing 2000: A New Era of Microlensing Astrophysics*, ASP Conference Proceedings, Vol. 239. p.33, Edited by J. W. Menzies and Penny D. Sackett. San Francisco: Astronomical Society of the Pacific, 2001.

Gould, A., Udalski, A., An, D., Bennett, D.P., Zhou, A.Y., Dong, S., Rattenbury, N.J., Gaudi, B.S., Yock, P.C.M., Bond, I.A., Christie, G.W., Horne, K., Anderson, J., Stanek, K.Z., DePoy, D.L., Han, C., McCormick, J., et al. Microlens OGLE-2005-BLG-169Lb Implies Cool Neptune-Like Planets are Common, *ApJ*, submitted (2006)

Rattenbury, N. J., Bond, I. A., Skuljan, J., Yock, P. C. M., Planetary microlensing at high magnification, *MNRAS* 335, 159 (2002)

Rattenbury, N. J., Abe, F., Bennett, D. P., Bond, I. A., Calitz, J. J., Claret, A., Cook, K. H., Furuta, Y., Gal-Yam, A., Glicenstein, J.-F., Hearnshaw, J. B., Hauschildt, P. H., Kilmartin, P. M., Kurata, Y., Masuda, K., Maoz, D., Matsubara, Y., Meintjes, P. J., Moniez, M., Muraki, Y., Noda, S., Ofek, E. O., Okajima, K., Philpott, L., Rhie, S. H., Sako, T., Sullivan, D. J., Sumi, T., Terndrup, D. M., Tristram,

P. J., Wood, J., Yanagisawa, T., Yock, P. C. M., Determination of stellar shape in microlensing event MOA 2002-BLG-33, *A&A* 439, 645 (2005)

Schechter, P.L., Mateo, M., Saha, A. DOPHOT, a CCD photometry program, description and tests. *PASP* 105, 693 (1999)

Udalski, A., Jaroszynski, M., Paczynski, B., Kubiak, M., Szymanski, M.K., Soszynski, I., Pietrzynski, G., Ulaczyk, K., Szewczyk, O., Wyrzykowski, L., Christie, G.W., DePoy, D.L., Dong, S., Gal-Yam, A., Gaudi, B.S., Gould, A., Han, C., Lepine, S., McCormick, J., Park, B.G., Pogge, R.W. et al. A Jovian-mass Planet in Microlensing Event OGLE-2005-BLG-071, *ApJ* 628, L109 (2005).

Wozniak, P. R., Difference Image Analysis of the OGLE-II Bulge Data. I. The Method, *Acta Astronomica*, 50, 421 (2000).

Single Channel UBV Photometry of Long Period Eclipsing Binary VV Cephei

Jeffrey L. Hopkins
Hopkins Phoenix Observatory
7812 West Clayton Drive
Phoenix, Arizona 85033-2439 USA
phxjeff@hposoft.com

Philip D. Bennett
Department of Astronomy and Physics
Saint Mary's University
Halifax, NS B3H 3C3 Canada
pbennett@ap.stmarys.ca
and
Eureka Scientific, Inc.
2452 Delmer Street, Suite 100,
Oakland, CA 94602-3017 USA

Abstract

With a period of 20.3 years, VV Cephei is the second longest known eclipsing binary system. The last eclipse was in 1997-98. The observation of long period eclipsing binaries requires a special kind of dedication. Few of these systems are followed in detail between eclipses. These stars are bright, and so obtaining telescope time for extended periods at professional observatories is nearly impossible. Therefore, amateur photometrists with modest backyard observatories and time to devote can make an important contribution by monitoring these stars. To this end, the Hopkins Phoenix Observatory started a dedicated effort in the summer of 2005 to obtain UBV data for VV Cep around the predicted time of secondary eclipse, which has never been observed for this system. This paper will summarize the current observing program and present the data.

1. Introduction

During August 2005 the Hopkins Phoenix Observatory was contacted by Philip Bennett and asked to include the long period eclipsing binary star system VV Cephei in its UBV observing program. In addition to monitoring the system for light variations at different wavelengths, there was hope that the elusive secondary eclipse estimated for the fall/winter of 2005 could be observed.

VV Cephei (M2~Iab +B0-2V, $V_{\max} = 4.91$) is the second longest known eclipsing binary, having a period of 20.34 years and an eclipse lasting 490 days. The longest period eclipsing binary system is Epsilon Aurigae with a period of 27.1 years. A secondary eclipse for VV Cephei was predicted in 2005 based on the orbit of Wright (1977) [1]. The Hopkins Phoenix Observatory monitored this system from August 2005 to February 2006.

This star system is interesting from several points. With a diameter 1,000 times that of the Sun,

the primary super giant star is amongst the largest known stars. Primary eclipse occurs when the B star goes behind the M star and produces a drop in the shorter wavelength radiation. Secondary eclipse occurs when the much smaller B star passes in front of the M star and should result in a slight decrease in the longer wavelength radiation.

The two stars of the system are in quite different evolutionary stages. The primary star is an evolved super-giant M star, while the secondary is a hot B star still on the main sequence. Both stars appear to be intrinsically variable.

The primary displays intrinsic photometric variability typical of M supergiant, while the hot secondary shows large changes in continuum flux in the ultraviolet. The hot star has an associated accretion region, which may account for the ultraviolet variability. Because of the difference in color between the primary and secondary stars, its variability can be seen and separated using filtered photometry.

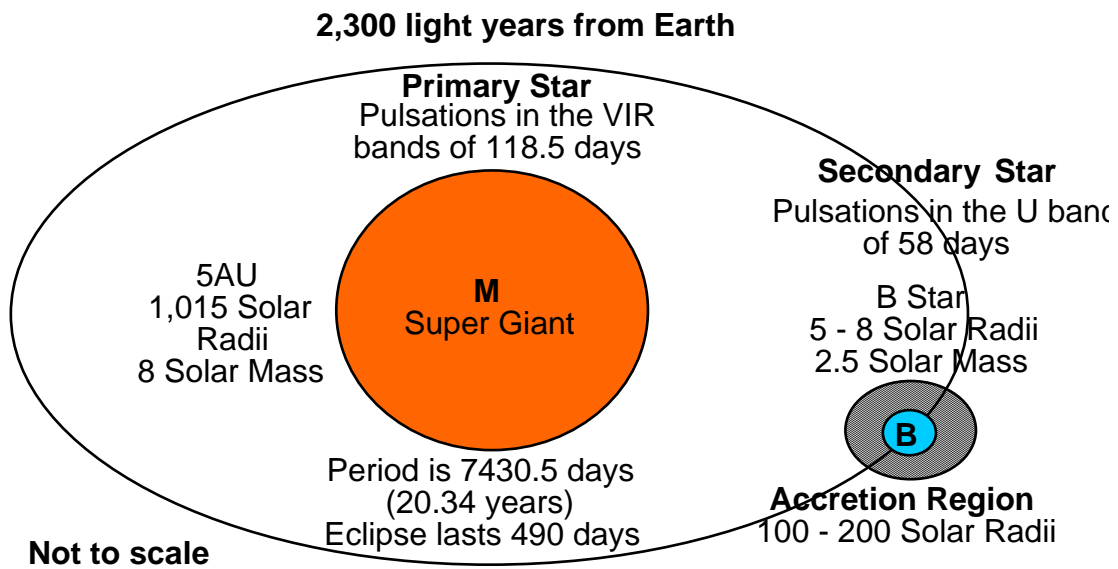


Figure 1. VV Cephei Star System Schematic

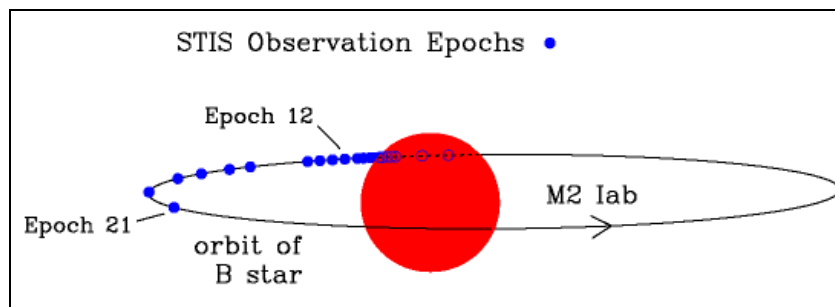


Figure 2a. VV Cephei Star System, SITS Observations

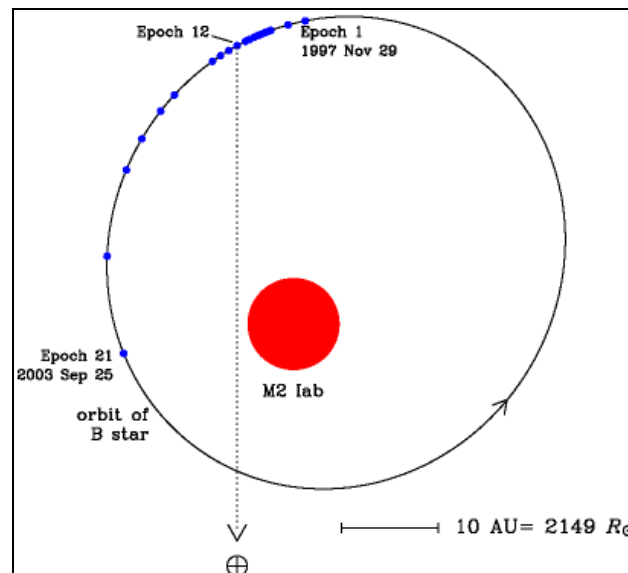


Figure 2b. VV Cephei Star System - Orbital Plane, SITS Observations

Figures 2a and 2b show the orbit of VV Cephei to scale from the Wright (1977) [1] positions of the B star at different epochs as derived from observations with the Hubble Space Telescope's Space telescope Imaging Spectrograph (HST/STIS) by Bennett and Bauer [5].

2. Hopkins Phoenix Observatory Photometry

2.1. Equipment

UBV band photometry uses an HPO photon counting photometer with a 1P21 photomultiplier tube with standard filters and 8" Celestron C-8 telescope (see Figure 2). The C-8 has been adapted to a Meade LX-90 fork mount. The photometric system has been calibrated using standard stars.

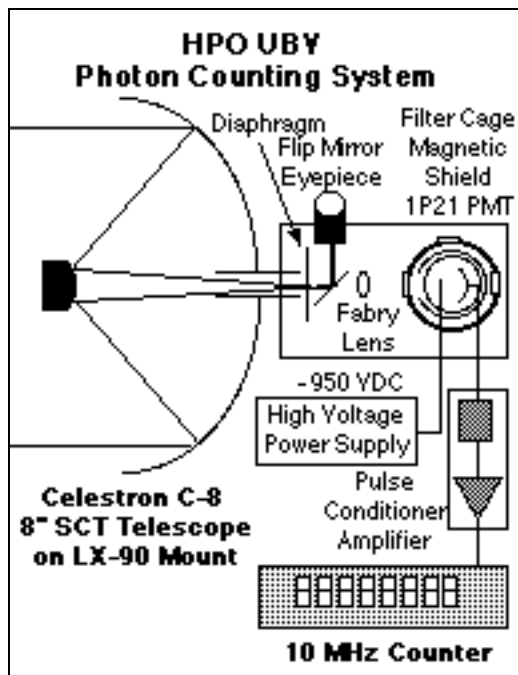


Figure 2 HPO UBV System Block Diagram

3. Hopkins Phoenix Observatory Observations

The Hopkins Phoenix Observatory (latitude 33.48 degrees North, longitude 112.22 degrees West. Altitude 1,097 feet ASL) has been obtaining UBV data of VV Cephei starting late summer of 2005.

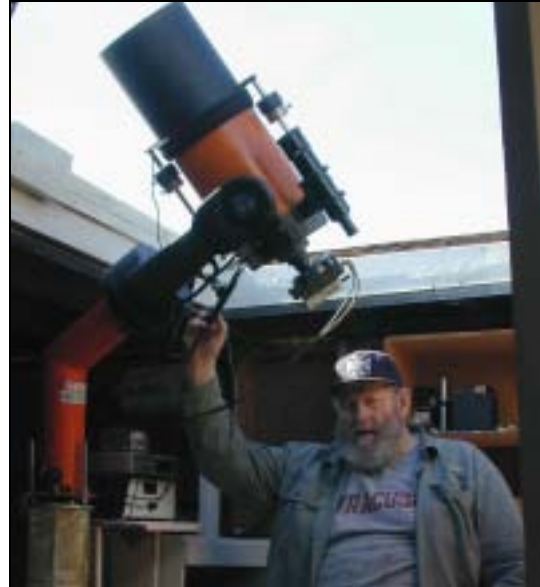


Figure 3. Hopkins Observatory UBV Equipment

Typical observations of a star consisted of 3-10 second readings of each star (star + sky) in each band followed by 1-10 second reading of the sky in each band. Observations were made using differential photometry with the sequence of comparison, program, comparison, program, comparison, program, comparison and check star as the last star measured.

Initial data reduction adjusts for dead time for the photon counting data and adjusts for counts per second. The three star observations for each band are averaged and sky readings subtracted. The air mass of the observation is also calculated. The air mass for the middle observation was used as the air mass for the final data point.

Data were then transferred into another program to calculate magnitudes and adjust for extinction and color coefficients. Three differential values were then calculated referenced to the comparison star. The results were then normalized to the comparison star's published value. The three readings were averaged and a standard deviation determined as an indication of the data spread. Typical UBV data have standard deviations of better than 0.01 magnitudes and often approach 0.001 magnitudes.

Observing season for VV Cephei at the latitude of the Hopkins Phoenix Observatory begins in the spring and runs through January. However, because of the extreme weather in the summer in Phoenix, Arizona, observations are limited due both to seasonal storm activity and observatory temperatures that can exceed 100 degrees F at midnight.

4. Data

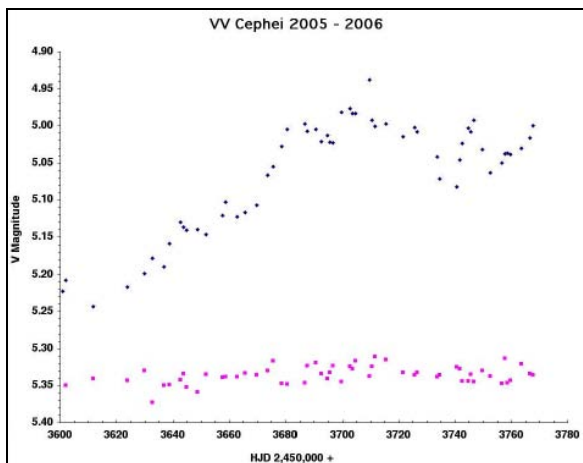
The comparison star used was 20 Cephei (HR8426) using the assumed magnitudes of U=8.46, B=6.68, and V=5.27.

The check star used was 19 Cephei (HR8428). Observational data for August 2005 through January 2006 are shown in the table below.

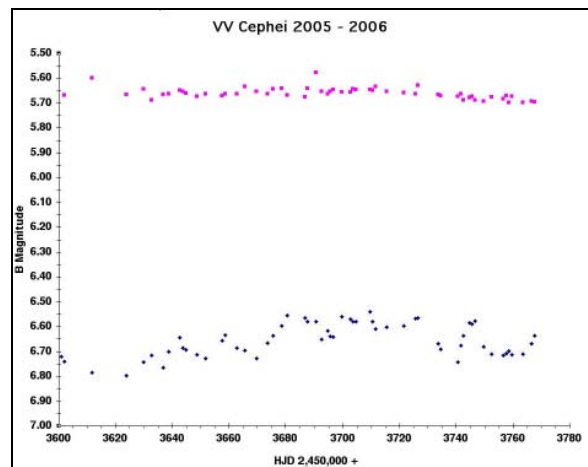
HJD	X	V	#	SD	B	#	SD	U	#	SD
January 2006										
2453767.59	1.8497	5.000	3	.006	6.637	3	.0077	7.088	3	.007
2453766.59	1.8021	5.016	3	.003	6.669	3	.0133	7.170	3	.030
2453763.59	1.7433	5.030	3	.004	6.712	3	.0182	7.222	3	.002
2453759.58	1.6629	5.039	3	.001	6.714	3	.0105	7.228	3	.013
2453758.58	1.6463	5.037	3	.005	6.698	3	.0041	7.181	3	.012
2453757.60	1.7032	5.038	3	.013	6.708	3	.0180	7.216	3	.013
2453756.58	1.5834	5.050	3	.009	6.717	3	.0037	7.191	3	.006
2453752.59	1.5882	5.063	3	.040	6.711	3	.0338	7.110	3	.050
2453749.57	1.4464	5.032	3	.004	6.681	3	.0429	7.107	3	.077
2453746.57	1.4219	4.992	3	.011	6.578	3	.0096	7.027	3	.001
2453745.58	1.4303	5.008	3	.009	6.589	3	.0061	7.025	3	.012
2453744.60	1.5121	5.003	3	.012	6.585	3	.0072	6.990	3	.020
2453742.59	1.4336	5.024	3	.003	6.637	3	.0033	7.016	3	.038
2453741.61	1.5435	5.046	3	.007	6.676	3	.0100	7.099	3	.005
2453740.56	1.3324	5.082	3	.007	6.742	3	.0140	7.161	3	.010
December 2005										
2453734.57	1.3074	5.072	3	.029	6.692	3	.0060	7.089	3	.009
2453733.56	1.2774	5.042	3	.013	6.670	3	.0108	7.023	3	.006
2453726.56	1.2276	5.008	3	.004	6.566	3	.0128	6.847	3	.049
2453725.60	1.3324	5.002	3	.018	6.568	3	.0116	6.905	3	.020
2453721.58	1.2551	5.015	3	.005	6.598	3	.0073	6.992	3	.005
2453715.55	1.1826	4.997	3	.004	6.602	3	.0035	6.976	3	.004
2453711.56	1.1742	5.001	3	.003	6.610	3	.0029	6.974	3	.006
2453710.56	1.1730	4.992	3	.007	6.579	3	.0187	6.957	3	.017
2453709.56	1.1708	4.938	3	.027	6.541	3	.0143	6.913	3	.015
November 2005										
2453704.56	1.1611	4.983	3	.002	6.579	3	.0076	6.934	3	.007
2453703.56	1.1615	4.983	3	.003	6.580	3	.0047	6.941	3	.004
2453702.62	1.2259	4.977	3	.002	6.570	3	.0023	6.937	3	.001
2453699.59	1.1759	4.982	3	.004	6.561	3	.0019	6.952	3	.011
2453696.56	1.1559	5.023	3	.016	6.641	3	.0208	7.052	3	.050
2453695.61	1.1807	5.022	3	.003	6.639	3	.0077	7.008	3	.008
2453694.62	1.1950	5.013	3	.003	6.618	3	.0055	6.968	3	.014
2453692.55	1.1567	5.021	3	.007	6.652	3	.0071	7.011	3	.007
2453690.59	1.1611	5.005	3	.002	6.579	3	.0204	6.873	3	.023
2453687.59	1.1573	5.007	3	.010	6.579	3	.0082	6.859	3	.008
2453686.63	1.1804	4.997	3	.008	6.564	3	.0057	6.839	3	.004
2453680.61	1.1572	5.005	3	.002	6.556	3	.0021	6.819	3	.005
2453678.64	1.1673	5.028	3	.004	6.597	3	.0079	6.873	3	.007

HJD	X	V	#	SD	B	#	SD	U	#	SD
October 2005										
2453675.66	1.1763	5.055	3	.008	6.636	3	.0061	6.966	3	.012
2453673.67	1.1878	5.067	3	.006	6.666	3	.0029	7.018	3	.012
2453669.67	1.1772	5.107	3	.006	6.727	3	.0070	7.070	3	.008
2453665.72	1.2303	5.117	3	.008	6.695	3	.0198	7.023	3	.009
2453662.71	1.2007	5.123	3	.004	6.686	3	.0103	6.940	3	.019
2453658.73	1.2049	5.103	3	.001	6.635	3	.0062	6.956	3	.019
2453657.71	1.1826	5.121	3	.008	6.656	3	.0085	6.947	3	.006
2453651.72	1.1780	5.147	3	.001	6.729	3	.0092	7.034	3	.008
2453648.74	1.1876	5.140	3	.011	6.714	3	.0104	6.963	3	.010
September 2005										
2453644.74	1.1797	5.141	3	.006	6.694	3	.0113	6.942	3	.005
2453643.76	1.1903	5.137	3	.005	6.686	3	.0069	6.917	3	.018
2453642.76	1.1964	5.130	3	.002	6.643	3	.0043	6.869	3	.003
2453638.78	1.2094	5.158	3	.006	6.701	3	.0023	6.946	3	.003
2453636.76	1.1780	5.190	3	.002	6.765	3	.0025	7.042	3	.006
2453632.77	1.1762	5.178	3	.003	6.717	3	.0129	6.960	3	.010
2453629.80	1.2010	5.199	3	.005	6.743	3	.0074	6.925	3	.008
2453623.78	1.1638	5.217	3	.008	6.798	3	.0481	7.122	3	.012
August 2005										
2453611.80	1.1590	5.243	3	.008	6.785	3	.0172	7.110	3	.005
2453601.93	1.3019	5.208	3	.012	6.741	3	.0043	6.922	3	.026
2453600.94		5.223	1		6.720	1		6.976	1	

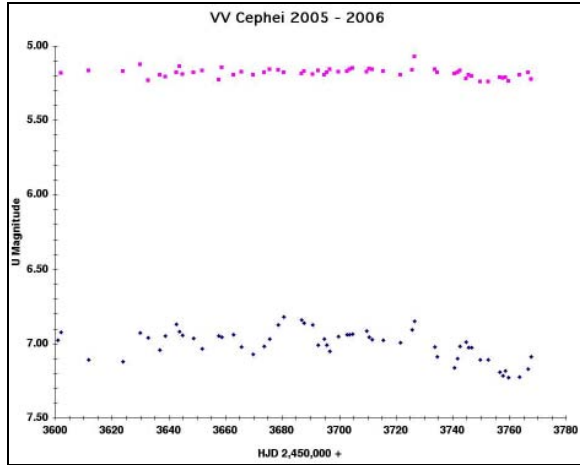
5. Light curves (2005- 2006)



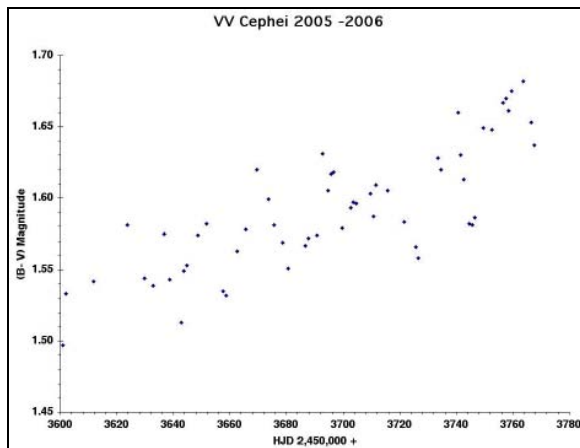
V Magnitudes of VV Cephei (upper plot) and Check Star 19 Cephei (lower plot)



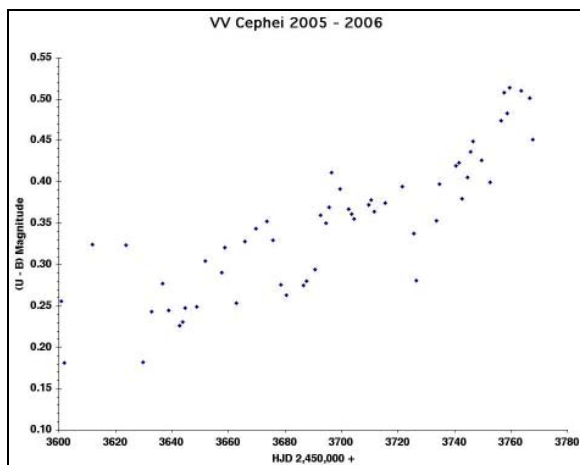
B Magnitudes of VV Cephei (lower plot) and Check Star 19 Cephei (upper plot)



U Magnitudes of VV Cephei (lower plot) and Check Star 19 Cephei (upper plot)



(B - V) Magnitudes of VV Cephei



(U - B) Magnitudes of VV Cephei

6. Conclusions

UBV observations show variations in each band. V data shows an increasing trend of close to 0.3 magnitudes (5.24 to 4.94) and smaller variations of up to 0.1 magnitude (5.08 – 4.99). B variations of around 0.24 magnitudes (6.80 to 6.56) can be seen with a peak near JD 2,453,710. U variations of 0.41 magnitude (7.23 to 6.82) can be seen with a minimum around JD 3,453,760. B-V shows an increase value of 0.18 (1.50 to 1.68) during the observing season. U-B shows a similar increasing value of 0.33 (0.18 to 0.51).

No definite information about a secondary eclipse can be gleaned from the data.

More observations are planned for the next observing season. It may take several seasons to provide sufficient data to determine the precise periods of the variations.

7. References

- [1] K.O. Wright, The system of VV Cephei derived from analysis of the H- alpha line, J. Royal Astr. Soc. Canada, 71, 152-193 (1977).
- [2] G. P. McCook, E. F. Guinan, 118 Day Optical Variations in VV Cep, IBVS Number 1385, 8 February 1978.
- [3] L. Baldinelli, S. Ghedini, S. Marmi, Semiregular 58 Day Variations in VV Cep, IBVS Number 1675, 24 September 1979.
- [4] L. Leedjarv, D. Graczyk, M. Mikolajewski and A. Puss, The 1997/1998 eclipse of VV Cephei was late, 19 July 1999, Astron. Astrophys. 349, 511-514 (1999).
- [5] P.D. Bennett (University of Colorado), W.H. Bauer (Wellesley College), Six Years of HST/STIS Observations of Eclipsing Binary VV Cephei, AAS 204th Meeting June 2004, Poster Paper.

Collaborative Research Opportunities with the Global Network of Astronomical Telescopes (GNAT): Variable Star Research

E.R. Craine

*Global Network of Astronomical Telescopes, Inc./Western Research Company, Inc.
3275 W. Ina Road, Suite 215, Tucson, AZ 85741
ercraine@wrc-inc.com*

R.A. Tucker

*Goodricke-Pigott Observatory Global Network of Astronomical Telescopes, Inc.
Tucson, AZ 85746
gpobs@mindspring.com*

A.L. Kraus

*Department of Astronomy, California Institute of Technology
Pasadena, CA 91125
alk@astro.caltech.edu*

R.B. Culver

*Colorado State University and GNAT
Fort Collins, CO 80523
gnat@lamar.colostate.edu*

M.S. Giampapa

*National Solar Observatory
Tucson, AZ 85726-6732
giampapa@noao.edu*

Abstract

The Global Network of Astronomical Telescopes (GNAT) is modeling its observing system on a network of scan-mode telescopes following the designs of the Moving Object and Transient Event Search System (MOTESS), implemented at Goodricke-Pigott Observatory in Tucson, Arizona. GNAT has developed a comprehensive data pipeline for extracting photometric measurements of all of the stars observed in each of the discrete declination bands observed with the scan-mode system. This enormous volume of observations is leading to an aggressive program of discovery of objects that are in many cases of great interest in terms of follow-up observations. GNAT is reaching out to both the professional and amateur astronomy communities to identify potential collaborators who are interested in participating in a wide variety of follow-up research programs. © 2006 Society for Astronomical Sciences.

1. Introduction

The Global Network of Astronomical Telescopes (GNAT) is modeling its system on a network of scan-mode telescopes following the designs of the Moving Object and Transient Event Search System (MOTESS), implemented at Goodricke-Pigott Observatory in Tucson, Arizona.

The MOTESS system consists of an array of three conventional Newtonian reflectors with 35-centimeter aperture, f/5 primaries of low-expansion Astrosital material and 8 centimeter minor axis secondaries of fused quartz. A temperature-compensating optical support structure using the differential expansion of steel and aluminum rods eliminates the need for focus changes. Since the telescopes are intended to be directed toward a fixed azimuth and elevation for years at a time, there is no problem

with structural flexure due to changing orientation and a relatively lightweight structure has been implemented. In spite of diurnal and seasonal variations in temperature, star image size typically ranges from 2.03 to 2.30 pixels FWHM or 5.75 to 6.5 arcseconds.

The thermoelectrically-cooled CCD cameras, utilizing 1024x1024 SITe TK1024 devices, are operated in continuous time-delay integration mode, often also referred to as 'scan mode'. Imaging begins in evening twilight and continues until morning. The data acquisition program stores the images as 1024x1024 FITS files for convenience. This combination of aperture, f/5 focal ratio, and CCD leads to an effective integration time at the celestial equator of 193 seconds. These CCDs have 24-micron pixels and, in combination with the telescope system, produce an image scale of 2.83 arcseconds per pixel. The resulting field of view is 48.3 arcminutes. Processing of unfiltered images from good nights typically indicates zero-point magnitudes of about 21 or slightly fainter. Sky background on a dark night is about 12,000 ADUs and produces a shot noise contribution of about 110 ADUs rms. A three-sigma stellar detection corresponds therefore to about R magnitude 20.4, assuming a solar-type star.

Scanning at or near the celestial equator permits recording just over 12 square degrees of sky per hour. In normal operation, the three telescopes are aimed at the same declination but spread in Right Ascension at intervals of 15 to 60 minutes to produce a data stream of image triplets separated in time that reveal moving and time-varying objects. At this time, the instruments are centered on +12°18m declination and are producing images for the MG3 survey band. The separation between the three instruments is about 19.75 minutes in Right Ascension.

GNAT has implemented a comprehensive data pipeline for extracting photometric measurements of all of the stars observed in each of the discrete declination bands observed with the scan-mode system. For the first declination band (designated the MG1 Survey), 48 arcminutes wide and centered at +03°18m, this has resulted in 2.5-year photometric light curves for 2.07 million stars with $-3 < R-B < 5$ and $R < 19$ mag. The MG2 band is at declination +02°05m.

From these stars we have created a new catalog of variable stars (the MG1 Variable Star Catalog) numbering 26,042 of which 5,271 are periodic at the 99% confidence level [Kraus et al. 2006]. Only 59 of these stars were previously known to be variable and appeared as entries in the General Catalog of Variable Stars (GCVS).

GNAT is presently completing construction of six more telescopes, and is nearing completion of data reduction of a second 2-year scan mode strip (in

concert with MOTESS). We anticipate producing a second catalog of newly discovered variable stars early in 2007, which is expected to be somewhat larger than the MG1 catalog. Two more declination scan observing programs are currently underway.

The yield of usable data is expected to be on the order of 1.3 terabytes per year. Based on our experience with the MG1 survey, we can expect the discovery of a large number of interesting objects that may even represent new classes of stellar variability. GNAT is therefore seeking the active participation of the astronomical community, amateur and professional alike, in the exploration of this unique and accessible database.

We outline here resources that are presently available, describe some of the specific projects that are underway or await additional collaborators, and describe how interested parties can participate in the program.

2. GNAT Organizational Structure

GNAT is a privately supported, membership based organization which is formally constituted as a not-for-profit 501(c)(3) corporation. It is administered by a Board of Directors and a slate of officers who serve one-year terms. Operationally, GNAT activities are administered through a series of working groups, each managed by a Working Group Chairman. The current working groups and acting Chairs are tabulated in Table 1.

Table 1. GNAT Working Groups

- | | |
|----|--|
| 1. | Methods in Instrumentation (R.A. Tucker) |
| 2. | Solar System Observations (R.A. Tucker) |
| 3. | Stellar Photometry (E.R. Craine) |
| 4. | Standards (D.L. Crawford) |
| 5. | Data Pipelines (A.L. Kraus) |
| 6. | Terrestrial Atmosphere (D.L. Crawford) |
| 7. | Education/Public Outreach (R.B. Culver) |
| 8. | Resource Development (E.R. Craine) |

The current GNAT protocol is to manage imagery and associated observational data through the working groups. Each has a set of projects underway, and a list of additional projects that are contemplated for future activities. Participation in working group projects is available to all interested members of GNAT.

Periodically, GNAT data will be released from control of the working groups and transferred into the public domain. These data releases will generally coincide with the addition of new data sets to the "members only" data pool. In this way, individuals

and institutions that become GNAT members will have preferred and proprietary access to the data for a period of time before the data become public. The time frames for protecting the data are determined by the GNAT Board of Directors in consultation with the GNAT membership. Proprietary periods are planned to ensure that GNAT members can complete their primary research interests with the data before public release.

GNAT membership can be obtained at different levels according to the needs of the member. Base individual membership enables participation in collaborative projects within a single working group; multiple working group participation is also available with a modest fee paid for each additional working group selected. Organizational memberships are available as outright endowments, or, for participating research organizations accommodation can be made for various levels of participation, including establishment of observing programs or dedication of new telescopes in the network. Details of the membership structure and associated privileges can be found at the GNAT website: www.eGNAT.org.

3. The Stellar Photometry Working Group

By way of example of how potential collaborators could work with GNAT, we describe current activities of the Stellar Photometry Working Group (SPWG).

The SPWG is in the early stages of developing its research programs. Its efforts resulted in the creation of the MG1 Variable Star Catalog, which was intended as a test bed for the first experimental GNAT data reduction pipeline using the MG1 survey observations described in the introduction. These observations, consisting of deep, unfiltered images, were originally intended for astrometric detection of asteroids and were deep, unfiltered images.

Nonetheless, the MG1 Variable Star Catalog has yielded the discovery of just under 26,000 previously unknown variable stars. Two additional surveys using MOTESS instrumentation are underway, and we anticipate adding six GNAT telescopes to the observing program, which will begin observations in the 2006-2007 time frame. Thus, we can reasonably expect to produce data for on order 100,000 new variable stars during the next two years.

The MG1 Variable Star Catalog consists of a file that is a Statistical Summary for each entry and a second file that contains all of the reduced photometry for each star. Included in the data for each entry in the Statistical Summary file are the following: MG1 serial number, epoch 2000.0 right ascension and dec-

lination, number of observations; median, mean, standard deviation, skew and kurtosis of the observations; several variability test statistics based on a Welch-Stetson [1993] analysis, and a periodogram analysis.

With nearly a quarter billion photometric reductions to date, and a projected rapid increase in this data rate, there is clearly a wealth of data for interesting research projects. These projects fall into two broad categories: 1) those which can be undertaken in their entirety with the extant survey data, and 2) those that require additional follow-up observations. We suggest here a few which are either underway or contemplated.

3.1. Recovery of Known Variables

This task has been completed for the MG1 survey, but will need to be repeated for each additional variable star catalog we produce. The goal is to determine which previously known variable stars are recovered in the GNAT photometric data and how the GNAT data compare with the published data. This provides several useful results. It allows determination of limitations that may exist in the data pipeline for the GNAT data, and can provide guides for improvement; it also serves as a check of the published data, and in some cases, enhances the published results. We note in the statistics in the Introduction that known variables comprise fewer than one half of one percent of all of the variables we detect. This project requires no additional observations, but does need extensive literature review and careful matching of published data with GNAT data.

3.2. Supernovae Discovery

The GNAT survey bands intersect a wide range of galactic latitudes, and typically result in the nightly imaging of some tens of thousands of galaxies. These time series observations are ripe grounds for supernova searches. In the prototype MG2 survey three known supernovae have been imaged; one, SN2005ch, was captured several days prior to maximum (see Figure 1) and pre-discovery photometry was reported by Tucker [2005]. Statistical analyses suggest that some 50-100 additional supernovae should reside, presently undiscovered, in the MG1 and MG2 survey data. Many should have accessible pre-outburst light curves. This project requires no further observation, but is a computationally intensive program, which would be well suited to a collaborator with good computer skills and access to suitable computing power (a great student project!).

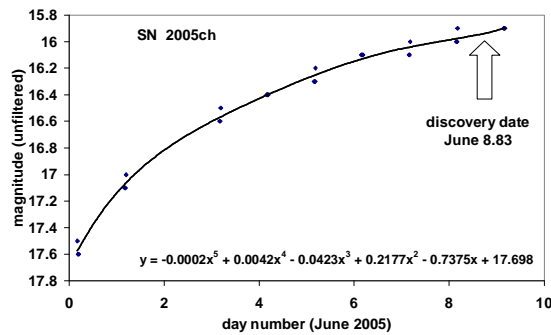


Figure 1. The lightcurve of SN 2005ch obtained from the MG2 observing survey.

3.3. Confirmation of Suspected Variables

Each of the scan mode survey bands potentially includes observations of a number of stars from the Suspected Variable Star List of the GCVS. By cross correlating those positions with the GNAT variable star catalogs, it is sometimes possible to confirm the nature of the variability of the suspected variables. This project requires no further observation and can be done with very modest computing power. It is an activity that should be repeated for each of the GNAT variable star catalogs as the new ones become available.

3.4. Evaluation of Specific Types of Variables

There are small populations of specific types of variables for which rare or interesting light curve data exist in the GNAT variable star catalogs, or in the larger pool of photometric reductions. These include objects such as QSOs and brown dwarfs. The challenge in this project is to establish reliable object identifications and to extract the light curves from the cataloged data. This type of project is of interest because it may provide optical variability data for objects for which such observations have never been made, or have been made infrequently or for short periods of time. Alternatively, the project may be useful in filling gaps in light curves of more frequently observed objects. This project can be done without requirement for further observation or sophisticated computing power.

3.5. Catalog Correlations

A useful and potentially very interesting project involves the cross correlation of entries in the emerging GNAT variable star catalogs with catalog entries in other astronomical surveys of various types. This is another valuable project that would require no fur-

ther observation but would be both time and computationally intensive.

3.6. Serendipitous Discovery of Unusual Stars

Simply by plotting and examining series of light curves in the variable star catalog data, it is possible to find stars with non-periodic but highly irregular variability characteristics. Some of these are quite interesting objects for speculation and certainly beg follow-up observation. This can take the form of additional photometry or spectroscopy. It is a rather tedious process to identify these stars, but the list is slowly growing and collaborators with suitable observing resources are encouraged to participate in this project.

3.7. Short Period Variables

A very large number of stars in the variable star catalog data are of short periods and are highly aliased in the scan mode data (effectively 1-3 observations per night, but separated in time by only about a half hour), resulting in an inability to establish periods without further observation. These stars lend themselves well to follow-up by collaborating observers who can spend a week or two observing a modest number of stars several times per night.

3.8. Eclipsing Systems

Similarly, the variable star catalog data identify a large number of eclipsing systems that need further observation to capture satisfactory detail in the eclipse and to define secondary eclipses and periods.

3.9. Variable stars in Open Clusters

A small number of open clusters are typically imaged in each of the scan mode strips. In most of these cases we have found modest numbers of newly discovered, probably short period, variables in the direction of the clusters. These stars should be examined statistically for likelihood of cluster membership, and they are candidates for follow-up photometric observation to establish periodicity.

3.10. Other Projects

There are numerous other projects using the GNAT photometric data that one can contemplate. Many involve issues of methods of rough classification of the variable stars, statistical analyses of distributions, characterization of selection effects or myriad types of follow-up observations.

4. Comments on Other Working Groups

Although we emphasize the work of the Stellar Photometry Working Group it must be stressed that all of the GNAT working Groups welcome participation of new member collaborators. In this section we list just one or two of the many projects underway in each group.

1. Methods in Instrumentation: 1) CCD camera system construction following MOTESS designs, and 2) assistance in detailed documentation of the scan mode systems.
2. Solar System Observations: 1) discovery programs for asteroids will urgently need additional collaborators as the new GNAT telescopes come on line.
3. Stellar Photometry: has been the focus of this paper and has numerous projects to offer collaborators.
4. Standards: 1) an interesting near term project involves cataloging of constant stars along the celestial equator.
5. Data Pipelines: 1) data reduction from the new GNAT telescopes.
6. Terrestrial Atmosphere: night sky brightness variations as measured in GNAT images.
7. Education and Public Outreach: a major project is underway to collect ideas for, and implement, astronomical educational activities over the broadest possible range of interested students.
8. Resource Development: GNAT needs volunteers to assist with ideas and time for raising funds with anything from philanthropic donations to research grants.

5. How to Participate

GNAT is a dynamically evolving organization that is still trying to determine the most satisfactory means for involving collaborators while simultaneously protecting the interests of all of its participants. Descriptions of this protocol will be periodically updated on the GNAT website (Section 2 above). At present, potential collaborators should contact the appropriate GNAT Working Group chair(s) to explore which projects are available for participation; or, alternatively, to propose an independent research effort. In the latter case, the collaborator may become the Principal Scientist on the project, but will typically take the lead for a small team in the working group who will, at a minimum, assist in access to the data.

Collaborators who desire access to GNAT privately held data will be required to join the organization and agree to be bound by terms that have been established by mutual consent to protect the interests in data of all of the GNAT members. New collaborators will typically work in concert with a small team within the appropriate working group. Collaborators can be professional astronomers, amateur astronomers or students, but all will be bound by the same written rules of conduct and ethics.

6. Conclusion

The MOTESS GNAT prototype photometric survey is yielding extraordinary numbers of newly discovered variable stars that provide fertile opportunities for collaborative research. These opportunities will rapidly expand as additional GNAT operated telescopes come on line. GNAT research projects can be done either as observational follow up projects, or they can be conducted with data that are already available and require no further observation. Interested parties are strongly encouraged to consider joining GNAT and to contact GNAT Working Groups of interest to explore specific research partnerships.

7. Acknowledgements

The GNAT data pipeline work has been undertaken in stages to date primarily by ALK who was supported by the NSO Research Experiences for Undergraduates (REU) Program (2002) which is funded by the National Science Foundation, and for a second summer (2003) by support from Walker and Associates. Additional support for this project has been provided by the National Solar Observatory, the National Optical Astronomy Observatories, Goodricke-Pigott Observatory and Western Research Company, Inc., all of Tucson, AZ. We are also grateful for the support of GNAT members, both individual and institutional.

8. References

- Kraus, A.L., Craine, E.R., Giampapa, M.S., Scharlach, W.W.G., and Tucker, R.A. The First MOTESS-GNAT Variable Star Survey. Submitted for publication (2006).
- Tucker, R.A. Supernova 2005ch. IAU Circular No. 8540, Central Bureau for Astronomical Telegrams, INTERNATIONAL ASTRONOMICAL UNION, June 10 (2005).

Welch, D.A. & Stetson, P.B. Robust Variable Star Detection Techniques Suitable for Automated Searches: New Results for NGC 1866. *A.J.*, 105, 1813-1821 (1993).

Recent Asteroid Lightcurve Studies at the Palmer Divide Observatory

Brian D. Warner
Palmer Divide Observatory
17995 Bakers Farm Rd.
Colorado Springs, CO 80908
brian@MinorPlanetObserver.com

Abstract

Finding the period and amplitude of asteroid lightcurves has been the main objective at the Palmer Divide Observatory since 1999. Since that time, more than 230 lightcurves have been measured, the majority of them having been produced in the last three years. In the last two years, special consideration has been given to the Hungaria group as well as potential binary asteroids. The latter effort has been in cooperation with the Binary Asteroids Survey conducted by Petr Pravec of Ondrejov Observatory. This report details recent results and their implications in terms of solar system evolution. ©2006 Society for Astronomical Sciences.

1. Introduction

The reasons for determining asteroid lightcurve parameters have been covered in several places, for one in my book, “A Practical Guide to Lightcurve Photometry and Analysis” (Warner 2006). In brief, the periods derived from the lightcurves can be correlated against size, family or group, location within the solar system, taxonomic class, or a combination of these and other attributes. The can lead to the development of theories regarding the evolution of the asteroid system or their structure and density. The latter are important when attempting to determine the extent of the threat of certain asteroids should they collide with Earth.

When several lightcurves are obtained over a sufficient range of *viewing aspects*, the shape and orientation of the spin axis of the asteroid can be determined. With the large surveys coming on line, the work of shape and spin axis modeling can proceed at even greater rates, assuming that data is supported by lightcurves, which are more and more obtained by amateurs.

Spin axis orientation becomes important in determining if certain asteroids might have a common origin and to what degree the *YORP effect* (Yarkovsky-O’Keefe-Radzievskii-Paddack) has on rotation rates and spin axis orientation (see Vokrouhlický 2003). This in turn can lead to further developments in theories concerning asteroid evolution and dynamics.

All of the above and much more can be determined in no small part by simply finding the period

and amplitude of a lightcurve. It is relatively easy work for an amateur equipped with a telescope, CCD camera, and software for measuring images and finding the lightcurve parameters.

2. The Palmer Divide Observatory

The Palmer Divide Observatory has been in operation at its current location since 1999, which is about 25 miles north of Colorado Springs, CO, and 8 miles east of Monument, CO. The elevation is 2300 meters. The observatory consists of two building housing three telescopes (Figure 1).



Figure 1. The Palmer Divide Observatory. The left-hand building houses the 0.5m R-C telescope while the right-hand one houses two 0.35m SCT telescopes.

The main building contains a 0.5m Ritchey-Chretien telescope built by ScopeCraft in Kanab, UT

(Figure 2). The camera is a Finger Lakes Instrumentation IMG camera with Kodak 1001E chip (1Kx1Kx24 μ m). The field of view is approximately 22x22 arcminutes. The camera includes an FLI filter wheel with BVRC filters.



Figure 2. The 0.5m Ritchey-Chretien.

The second building contains two 0.35m Meade LX-200GPS telescopes (Figure 3). One telescope is equipped with the same FLI-1001E camera as the 0.5m telescope while the second telescope has an SBIG ST-9E camera with Kodak 206E chip (512x512x20 μ m). The second 0.35m scope also uses a f/5 focal reducer to increase the field of view and provide a better pixel scale match.



Figure 3. The two 0.35m LX-200GPS telescopes.

All three telescopes have a pixel scale of about 2.5 arcseconds per pixel, which suits the average seeing at PDO. Most imaging is done unguided with exposures ranging from 60 to 240 seconds. The longer exposures do suffer from some trailing, especially on the 0.5m. However, it is not severe enough to hamper accurate photometry. A guide scope and independent guider are being fitted on the 0.5m to allow for even long exposures when working fainter targets, be they closer but smaller or larger and more distant.

3. General Program Description

The general program involves selecting targets, taking the images, measuring the images, and then analyzing the resulting data.

3.1. Searching for Targets

The general approach to a night's work involves several considerations. All of these combined result in an initial set of three to five asteroids to be worked.

3.1.1 Altitude and Magnitude

A first-pass search using a search utility in MPO Canopus finds all asteroids at least 30° above the eastern horizon at the planned start of observations. The search is further confined to those asteroids within reach of the instruments available. One or more of the telescopes may already be committed to certain targets and so the magnitude range may be set to accommodate only those that can be set on new targets.

3.1.2 Hungarias

A separate and stand-alone search utility finds all those Hungarias that are brighter than a given magnitude and have a solar elongation greater than 90° (sometimes 120°). The search includes the RA and Declination of each asteroid and so it can be easily determined which Hungarias, if any, can be considered.

3.1.3 Binary Asteroid Candidates

Whether found as part of the Hungaria or regular target searches or by members of the Binary Asteroids group run by Petr Pravec, priority is given to these known candidates over all others, save the Hungarias.

3.1.4 Proximity

If possible, more than one asteroid is assigned to each of the 0.35m telescopes. As long as the distance between two targets is not great, the slew time and accuracy is sufficient to maintain a good sampling of both curves and not lose the target because of an inaccurate slew. Periodic Auto-Synchronization is performed with the controlling MPO Connections scripts to assure the scope remains close to target and in focus throughout the run.

3.1.5 Multiple Target Blocks

On occasion, usually long winter nights, even a pair of asteroids will set long before the onset of twilight. In this case, a script may be set up to move the telescope to work yet another asteroid (or pair) for a few hours. On some nights, up to eight asteroids have been worked for at least a few hours.

The problem with working these additional asteroids is that they are often a month or two from opposition and so they take some time to be where they can be worked for longer periods. During this time, long gaps can occur due to weather or the moon, making it difficult to tie multiple nights together. For some reason, the probability that these additional asteroids will have long periods seems to be high. Given that long period asteroids need to be followed for prolonged stretches of time and that large gaps in coverage makes period analysis even more difficult, it would seem that Murphy is working overtime when it comes to selecting these additional targets.

3.1.6 Visual Double Stars

In response to the all-too common bad luck of picking targets for a second set on a given night, I have recently taken to observing visual double stars via CCD. There are more than 100,000 doubles in the Washington Double Star Catalog (Mason 2006), many of which have not been measured in years. It's a simple matter to use the search routine in MPO Connections to find a list of 50 or so doubles and create a script to image them in both V and R at least four times. Double stars also make an excellent diversion during full moon when the moon is obscuring all worthwhile asteroids. Of course, there are many bright asteroids needing follow up work for shape and spin axis work as well.

3.2. A Typical Night

Setup begins about sunset when the roofs of the buildings are rolled off and telescopes and the computers in the observatories turned on. All operations are run from in my house, located about 25 meters from the observatories. I use RAdmin (“virtual desktop”) software to control the observatory telescopes remotely (<http://www.famatech.com/>). Figure 3 shows a schematic of the networking layout. This system has proved to be very efficient and has meant not being out on cold winter nights more than necessary.

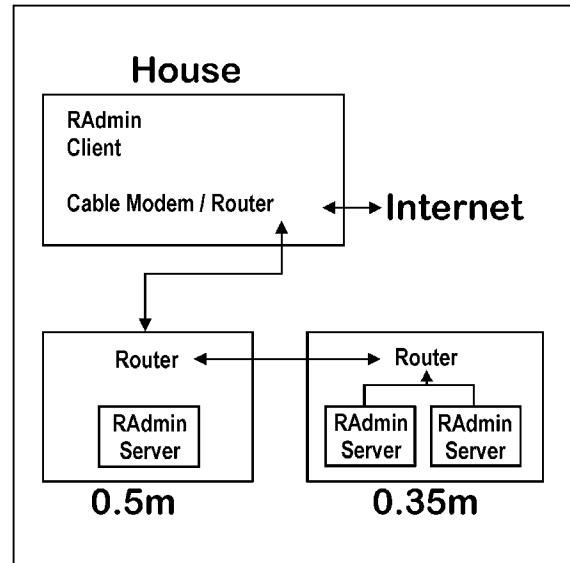


Figure 4. Network layout at PDO

Once inside, I run the search routines described in the previous section and determine which asteroids or other targets are to be observed. Scripts for MPO Connections are written on each controlling computer (via RAdmin). If the same targets are being worked as the previous run, the existing script is updated to save the files to a different directory and reset the time for morning twilight. If a new script is required, I usually just modify an existing one and so save some time by not having to create a new one from scratch.

3.2.1 Initial Scope Positioning

After the scripts are loaded, I send the scopes to a bright star near the meridian. All three scopes start from a known home position and so a slew to that initial star almost always puts that star within the field of the CCD camera. The true position of the scope is found by comparing the image against a chart centered on the star's position and the scope's pointing is updated, if necessary.

After this initial sync, the scopes are each sent either directly to their first target field or, if the field is not quite high enough, to a bright star relatively near the asteroid field. An autofocus routine is run just prior to the start of actual observing.

3.2.2 The Observing Run

The scripts are started 30 minutes before the end of astronomical twilight or when the field is at least 25-30° high. While working below 30° is not generally recommended, the extra 10-30 minutes of observing time can be important.

Figure 4 shows a typical script for two targets in MPO Connections. This script obtained about 150 images of each asteroid during the night. The position of the scope was periodically updated and the focus reset, all without any human intervention. At the end of the night, when 4091 Lowe reached 30° in the west or Nautical Twilight began, whichever came first, the camera cooling was turned off and the tele-

scope sent to its home position. Most of this was done while I was sleeping. All that was required in the morning was to upload the images to the analysis computer, remotely shutdown the observatory computers, and close the roofs. If I could just figure out a way to put garage door openers on those roofs, I wouldn't have to go outside at all – except to use the binoculars or 5" refractor!

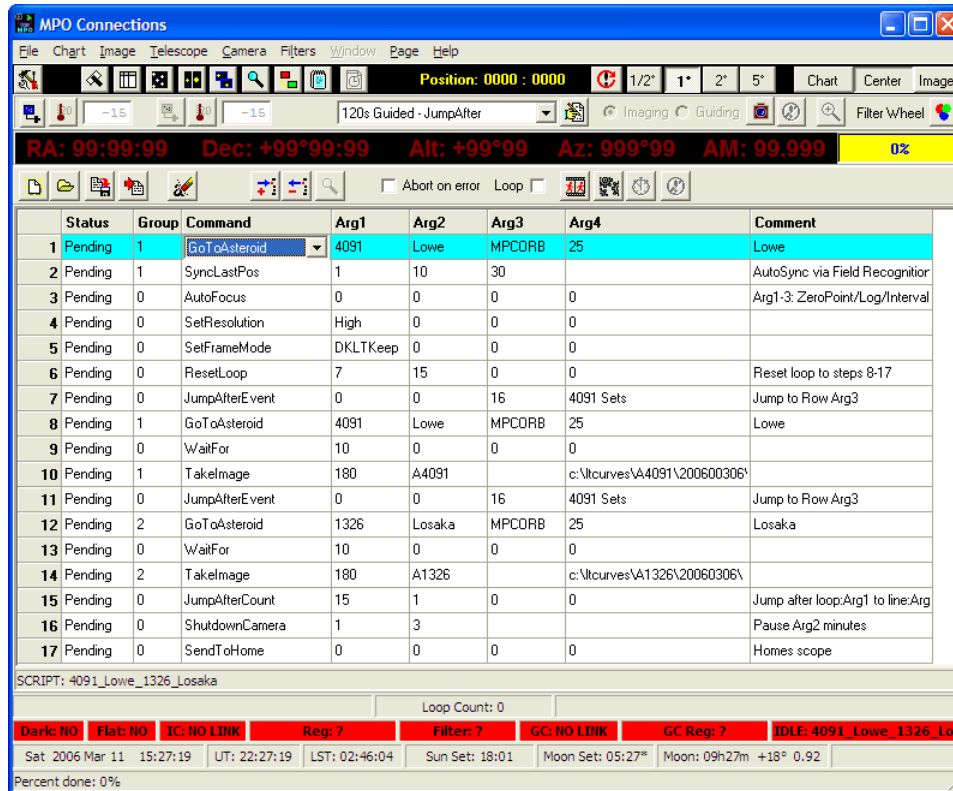


Figure 4. The screen shot above shows a typical MPO Connections script that is used to work two asteroids continuously through the night and then shutdown the camera and telescope at the end of the run.

3.3. Standardizing Observations

In the sample script above, no provision is made for filtered observations. Typically, most of the light-curve work has been conducted using a clear filter and, more recently, no filter – which provides a 0.3m gain over the clear filter. For shorter period asteroids, filtered observations are not required since it's possible to catch enough of a cycle in a single night and so matching runs from several nights is fairly straightforward.

However, this practice needs to change. First, it's much harder to match sessions for an asteroid if the period is long and/or the sessions are spread out over several weeks and even months. Second, baseline lightcurves to be used by Mikko Kaasalainen and others in combination with data from large surveys must be calibrated to a standard system. Last, but not necessarily finally, merging data sets used in the bi-

nary asteroids program run by Petr Pravec is much simpler and introduces fewer random variables if all data are on a standard system.

A recent article in the *Minor Planet Bulletin* by Richard Binzel (2005) and outlined in greater detail in my book (Warner 2006) makes reducing to approximate standard magnitudes relatively quick and easy. With only a little refinement, using two filters for a limited number of observations, even more accurate results can be obtained.

3.4. Data Reduction and Period Analysis

Once the images are uploaded to the analysis computer, the one in the house that controls the observatory computers, the images are measured in MPO Canopus. This program uses aperture photometry to determine the raw instrumental magnitudes of the target and up to five comparison stars. The differ-

ential value between the target and average of the comparisons is used for period analysis.

The period analysis uses the Fourier analysis algorithm developed by Alan Harris (1989). This is the “industry standard” for asteroid lightcurve work, though it works quite well on other types of objects as well, e.g., eclipsing variable stars.

If more than one night’s data is involved, the average magnitude of the comparisons for the first night is taken as the zero point and all the other session zero points are adjusted to make their data match the curve for the first night. Unless the magnitudes are reduced to a standard system, even an internal one, these shifts are purely arbitrary. However, if the data for each night cover a significant portion of the cycle, the error is usually $<0.01m$.

Figure 5 shows a typical lightcurve obtained at PDO where the data from each session met the requirements for a straightforward matching. Here, the curve has at least double coverage over almost 75% of the cycle, providing a very “solid” solution.

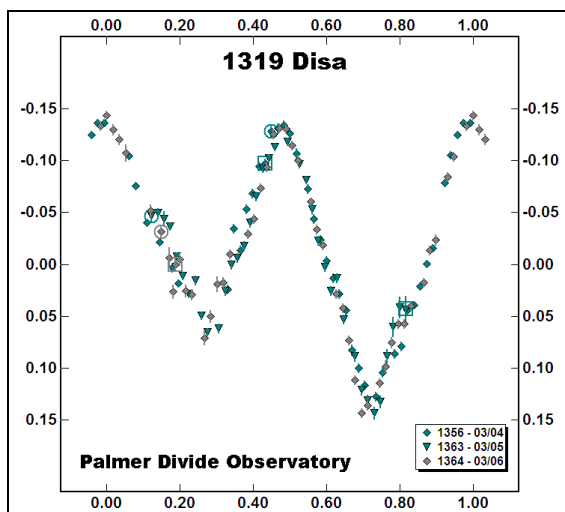


Figure 5. The lightcurve of 1319 Disa obtained at the PDO in March 2006. The synodic period of the curve is $7.080 \pm 0.003h$. The amplitude of the curve is $0.26 \pm 0.02mag$.

Figure 6 shows a slightly different situation, one where each session did not cover a significant portion of the curve. In this case, a reasonable solution was possible because the data covered large segments of the assumed cycle and a minimum and two maxima were captured. While the period of 42.16h is likely correct, it is not as certain as the one for 1319 Disa.

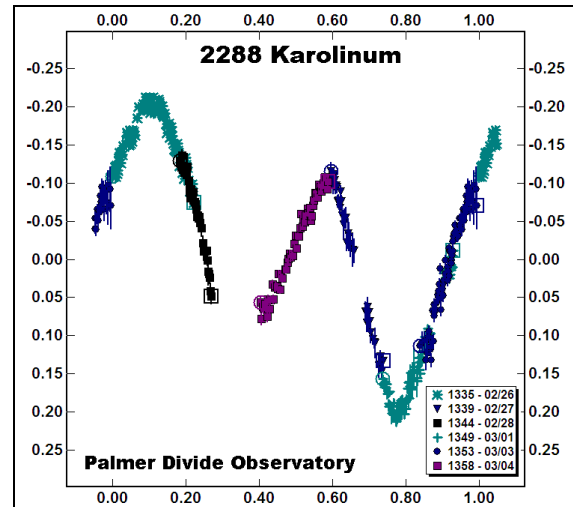


Figure 6. The lightcurve of 2288 Karolinum. The synodic period was reported to be $42.16 \pm 0.04h$. Catching the minimum and maximums was critical to finding a solution.

3.4.1 Avoiding Aliases

The most important thing to keep in mind when doing period analysis is “never trust a computer.” No matter how well written the analysis routine, it can be fooled into finding the wrong solution when the data groups are spaced just right with respect to the period. These incorrect periods are known as aliases and they are a bane to those doing lightcurve work regardless of the type of object.

Periods found with sparse sampling spaced days apart should be considered highly suspect. The best way to eliminate the problem of aliases is to get two good nights back-to-back, meaning as long of runs as darkness allows. It’s not always possible but – if nothing else – minimize the time between sessions and be aware of alternate solutions. My book provides more details and examples of this issue.

As to when you can call it quits even though you don’t have complete coverage of a curve, there’s not a simple answer. It might be said to be when you have enough data such that no other solution makes sense, which makes it a pure judgement call. Given that period analysis has often called a mix of science, experience, and black magic, there may be no definitive answer.

4. Results

4.1. Combined Asteroid Lightcurves

The number of asteroid lightcurves has risen dramatically in the last few years, as can be see in Figure 7.

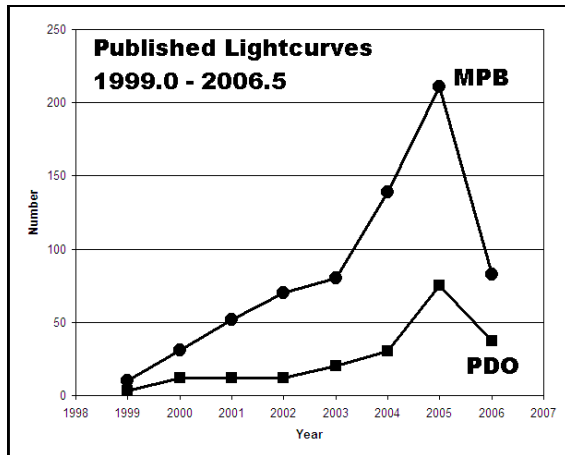


Figure 7. Total lightcurves published in the *Minor Planet Bulletin* between 1990 and mid-2006. MPB is the total number published each year. PDO is the number curves submitted by the Palmer Divide Observatory, with some of those being in collaboration with other observatories.

From only 10 lightcurves published in the *Minor Planet Bulletin* in 1999, the number rose to 211 curves in 2005. With half of 2006 on record, there may be a slight decrease but it still looks to exceed 150 since the 2006 statistics do not include the 40 PDO lightcurves submitted or awaiting write-up at the time of this writing.

This paints only part of the picture, the one dominated by formally published amateur contributions. The lightcurve list maintained by Harris (2006) gives data on approximately 2100 asteroids with about 1650 of those having reliable periods listed. Included in that list are data from professionals and – among others – the group of observers under the direction of Raoul Behrend. This group, of which many are amateurs, has produced a very large number of curves. However, most of the results remain unpublished save on the Behrend web site (2006).

4.2. Hungaria Asteroids

The Hungarias are high albedo objects that have semi-major axes just outside that of Mars (~1.8-2.0 AU), high inclination, but relatively small eccentricity. Because of the higher albedos (0.3-0.4) shown by about half the group and their proximity to Earth, the Hungarias are among the smallest main belt asteroids that can be covered regularly by amateur sized equipment.

The Hungarias are important because they provide a sampling of non-planet crossing bodies about the same size as NEAs, which do have planet-crossing orbits. Since some theories regarding NEA rotation and binary development rely on planetary influences, a comparison of the Hungaria and NEA populations can demonstrate the validity or refute the

validity of these theories. If the two groups have similar spin axis properties and binary population densities, then other factors besides those of planetary influence must be considered.

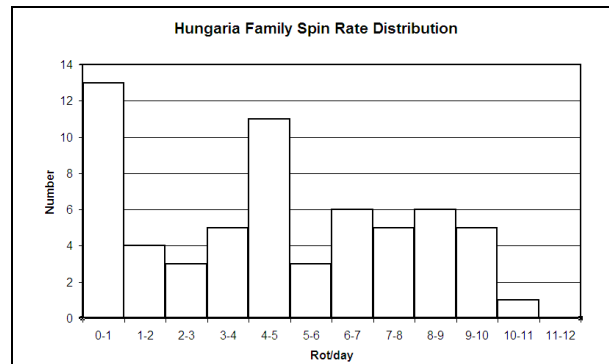


Figure 8. Hungaria Spin Rate Distribution. The X-axis is in rotations per day, or Period(h)/ 24.0.

Figure 8 shows the spin rate distribution of the 62 Hungaria asteroids included in the Harris list (PDO contributed data for 44, or 71%, of those.). A quick look shows that two groups dominate, those with rotation periods >18h and those with periods between 4.8 and 6.0 hours. This distribution is similar to the NEA population (Harris and Pravec 2006), which indicate strong similarities in the forces that control spin axis rates for the two populations and so they are mostly independent of planetary forces.

There is one difference of note, however. The small number of very fast rotators would seem to indicate that the “spin barrier” does not exist in the Hungarias. The spin barrier dictates when an asteroid must be monolithic in order to survive its fast rotation. Slower rotating asteroids are likely “rubble piles”, or loose conglomerations of material held together as much by, if not more than, gravity and not physical structure.

The often-heard refrain of “More Data!” applies very much to the study of the Hungarias. The sample has grown significantly in the last two years but a much larger number of lightcurves from this group is needed before speculation regarding similarities and differences with NEAs and Main Belt asteroids can be turned into solid theory or fact.

4.3. Binary Asteroids

Asteroids with satellites were once only speculation with a few tantalizing bits of evidence from occultation observations and sparse lightcurves. As of March 4, 2006, there were 89 asteroids with at least one satellite with a distribution among groups given by Johnston (2006) as:

- 26 Near-Earth asteroids
 - 5 Mars crossing asteroids
- 34 main-belt asteroids (one w/ two satellites)
 - 1 Jupiter Trojan asteroid
- 23 Trans-Neptunian objects (one w/ two satellites).

From 2004 October to 2006 February, the Palmer Divide Observatory made the initial discovery of six binary asteroids (in chronological order):

- 9069 Hovland
- 5405 Johnson
- 76818 2000 RG79
- 3309 Brorefeld
- 5477 1989 UH2
- 34706 2001 OP83

Confirmation and final determination of these discoveries would not have been possible without the contributions of the Binary Asteroids Group under the direction of Petr Pravec, Ondrejov Observatory (Pravec 2005).

The BinAst group has been responsible for the discovery of several other binaries in the past two years – mostly within the NEA and Hungaria populations, leading to a paper by Pravec that included more than 50 co-authors, many of them amateurs (Pravec 2006). The work requires higher precision, 0.02m or less in most cases, and often following the same target for days if not a week or more. However, the scientific rewards are enormous. More observers are needed, especially those in South America, Europe, and AsiaPac.

5. Diversions

During the course of observing asteroids, which means sitting on the same field all night, it's not uncommon to pick a comparison star that is variable. The variable star search routine in MPO Canopus (see Stephens and Koff) is also used to examine stars in the field for previously unknown or unclassified variables.

Admittedly, no emphasis is placed on finding or following up variable stars. Those that have been found tend to be >14m and so unless it is an eclipsing variable with total eclipses, a definitive model using Binary Maker 3 (Bradstreet) is not possible. However, this is a worthy pursuit that yields even more data from the same amount of observing time. Those who can and want to put some variety in their work should devote a little time to this field.

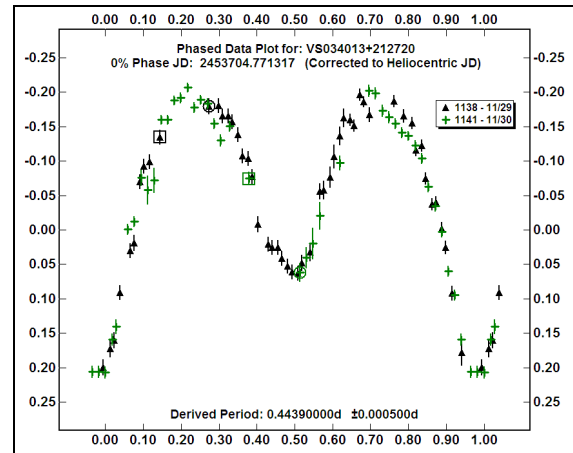


Figure 9. The lightcurve of a variable star “discovered” at PDO. There was no follow up since that took time away from the primary work on asteroids.

A diversion that does not require as much time at the telescope, usually only two to four hours a month, is visual double stars. Work on these at the PDO started in early January 2006, with the result being more than 300 observations submitted to the Webb Society’s Double Star Section Circulars for publication. Bob Argyle has written an excellent book on the subject (Argyle 2004) that serves as a good jumping point. This is an excellent “full moon” project when our own natural satellite obscures the asteroids.

6. Acknowledgements

My thanks to Alan W. Harris of the Space Science Institute and Petr Pravec of the Astronomical Institute, Ondrejov Observatory, Czech Republic, for their continued guidance.

7. References

- Argyle, Bob, ed. *Observing and Measuring Visual Double Stars*, 2004, Springer. ISBN 1-85233-558-0.
- Behrend 2006
- Binzel, R.P., *A Simplified Method for Standard Star Calibration*. 2005, *Minor Planet Bulletin* 32, 93-95.
- Bradstreet, David, *Binary Maker 3 software*, Contact Software, www.binarymaker.com.
- Harris, A.W., Young, J.W., Bowell, E., Martin, L.J., Millis, R.L., Poutanen, M., Scaltriti, F., Zappala, V., Schober, H.J., Debehogne, H., and Zeigler, K.W., (1989). “Photoelectric Observations of Asteroids 3, 24, 60, 261, and 863.” *Icarus* 77, 171-186.

Harris, A.W., Lightcurve Parameters. 2006, CALL site, www.MinorPlanetObserver.com/astlc/default.htm

Harris, A.W., Pravec, P., 2006, private communications.

Johnston, William R., Asteroids with Satellites web site, 2006, <http://www.johnstonsarchive.net/astro/asteroidmoons.html>

Mason, B., Wycoff, G.L., Hartkopf, W.I., Washington Double Star Catalog. 2006, <http://ad.usno.navy.mil/wds/wds.html>

Pravec, P., Photometric Survey for Asynchronous Binary Asteroids. 2005, Proceedings of the 24th Annual Conference of the Society for Astronomical Sciences, B.D. Warner et al, ed., 61-62.

Pravec, P. and 56 co-authors, Photometric Survey of Binary Near-Earth Asteroids. 2006, *Icarus* 181, 63-93.

Stephens, R.D., Koff, R.A., Discovery of Variable Stars as a Byproduct of Asteroid Lightcurve Studies. 2003, Proceedings of the 22nd Annual Conference of the Society for Astronomical Sciences, S. W. Teare and D.A. Keyon, ed., 45-54.

Warner, Brian D., A Practical Guide to Lightcurve Photometry and Analysis, 2006, Springer. ISBN 0-387-29365-5.

Vokrouhlický, D., D. Nesvorný, and W. F. Bottke (2003) The vector alignments of asteroid spins by thermal torques. *Nature* **425**, 147-151.

Follow-up Data for Large Photometric Surveys

Mikko Kaasalainen

*Department of Mathematics and Statistics
PO Box 68, FI-00014 University of Helsinki, Finland
Mikko.Kaasalainen@helsinki.fi
www.rni.helsinki.fi/~mjk*

Abstract

Contrary to what one might think, amateur photometry will become increasingly important and considerably more time-efficient in the era of extensive astronomical surveys. Appended to a sparsely sampled data sequence, even one ‘traditional’ dense lightcurve of an asteroid will boost the reliability of the resulting physical model significantly. Amateur observers have the chance to obtain thousands of well-defined spin and shape models of asteroids in the near future as the data from surveys such as Pan-STARRS and LSST start flowing in. This is a unique opportunity to map the asteroid population: no other observing mode can reach such a vast number of targets. ©2006 Society for Astronomical Sciences.

1. Introduction

Photometric data from amateur astronomers have played a well-recognized and increasingly important role in planetary studies for several years now. This meeting is a prime manifestation of the fact. The program collaboration has perhaps three main components. In historical order these are:

1. Period analysis for more than 1000 asteroids, including the detection of many binary systems.
2. Full physical (spin, shape and scattering) modelling from combined datasets, also with data other than photometric (including, e.g., radar, stellar occultations, thermal infrared, and adaptive optics).
3. A vast quantity of physical models using accurately calibrated photometry from large surveys (Pan-STARRS, LSST, etc.) as the main database.

Item I has resulted in statistically important catalogues by Harris, Pravec, and others. Despite the inevitable observational selection effects, we are beginning to have some idea of the period distribution of asteroids. Item II has produced the first reasonably large (more than 100 objects) catalogue giving us some idea what asteroids are really like: how their spin axes are distributed in space, what kinds of shapes and irregularities they exhibit, what are their actual (spin/shape corrected) solar phase curves like, what can we say about their surface properties, etc. We now have several ‘ground truths’ from space missions, laboratory studies, etc. (Kaasalainen et al. 2001, Kaasalainen 2005, Marchis et al. 2006) from

which we know that photometric modelling gives a good global portrait of the target. Similarly, we know that combining thermal infrared observations with these models yields, e.g., accurate estimates of surface regolith properties (Mueller et al. 2005). The models can even be used for getting a colour map of the surface using data at different wavelengths and thus gain some insight on mineral distributions (Nathues et al. 2005). The spin properties can reveal evolutionary surprises (Slivan et al. 2003), in particular in connection with the YORP effect from thermal radiation (Vokrouhlicky et al. 2004 and references therein).

While the level of detail from ground-based observations cannot reach that of in situ space missions, the latter are going to remain few in number. Photometry alone has the chance to give us a well representative and statistically significant coverage of the physical properties of the whole asteroid population and its subpopulations. In this context item III, the topic I will discuss here, will actually blow up the bank.

2. Large surveys and Sparse Photometry: a New Era in Astronomy

Observational astronomy is going through a change of paradigm. Rather than picking an individual target and sitting on it, we first scan the skies and record everything. Such surveys will give us the first proper global celestial map, with a vast number of targets for which we have preliminary characteristics available. From this catalogue (from hundreds of thousands of asteroids to a billion stars) we can then pick targets for closer individual scrutiny. This

change is not unlike the advent of aerial photography in geographic studies a century ago: the globe was soon mapped without having to send explorers all over the place. Only now the scale of the mapping is entirely different, starting from solar system objects and reaching through the Galaxy and beyond. Ground-based and satellite surveys such as Pan-STARRS, Gaia, and LSST will completely change our way of viewing the universe. Also, since we record just about everything we can, the selection effects and biases are not nearly as strong as with pre-determined target lists.

So everything is going to change, and asteroid science not the least. Originally the asteroid survey mode was intended for astrometry, especially with the determination of the orbits of near-Earth objects in mind, and this mode of operation has already been in use for some time (LINEAR and LONEOS). The new surveys, with Pan-STARRS in the forefront, will make use of the rapid developments in optical and data processing equipment not only to produce much larger quantities of data much faster, reaching considerably fainter targets – they will also obtain more accurate details. A particular feature of this is the possibility to have calibrated sparse photometric sequences over several years. Sparse means that the data points are typically separated by hours, days or even weeks. Typical Pan-STARRS sequences (or cadences, as the parlance goes) range from 50 to 500 or more points per 10 years per asteroid for tens of thousands of objects (Durech et al. 2006). Gaia will produce somewhat more sparsely distributed points over five years for a few times smaller target group (Kaasalainen 2004). In both cases, the calibration accuracy is expected to be better than 0.01 mag.

It is at first sight almost counterintuitive that sparse sequences are sufficient for asteroid modelling as shown in Kaasalainen (2004) and Durech et al. (2006). After all, the sampling interval is for most targets much longer than the sidereal period, so ordinary time series methods such as Fourier or power spectrum analysis (used for determining the periods of traditional lightcurves) are completely useless. The reason for the sufficiency is that the underlying well-defined mathematical model is highly constraining: only a certain type of an object can create a given sparse sequence as long as there are enough points at various observing geometries. In fact, sparse sequences are handled just like the ordinary lightcurve inversion problem: the mathematical model takes care of ‘filling the gaps’. Now we just have to scan a wide range of potential periods as the rotation period is not apparent in the data before the actual modelling.

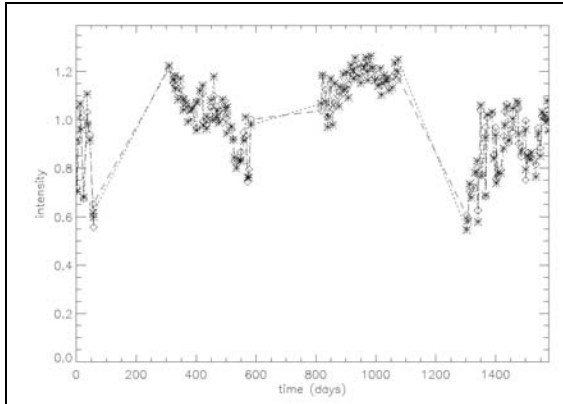


Figure 1. A typical sequence from a groundbased survey (asterisks and dotted line) with the model fit (diamonds and dashed line).

A typical requirement is some 100 well-distributed data points over five years for main-belters, while for NEAs even less is sufficient (Kaasalainen 2004). The calibration accuracy should be at least around 0.05 mag, so the new surveys can indeed meet the requirements. The surveys can make use of data at smaller solar elongations than those typical for ordinary lightcurves since only one point is needed at a time; thus the geometry coverage is wider (i.e., the observational gaps between apparitions are narrower). This is why the observation geometry range of ground-based surveys is not really very much smaller than that of satellite-based ones. For example, Pan-STARRS can reach solar elongations slightly less than 60 degrees, while Gaia’s minimum is at about 45 degrees. Fig. 1 shows a typical photometric sequence of a main-belt asteroid from a simulated ground-based survey, together with the model fit. The connecting lines are added just for viewing convenience – of course, the brightness does not change linearly between the points. Fig. 2 shows the correct result of the trial period scan.

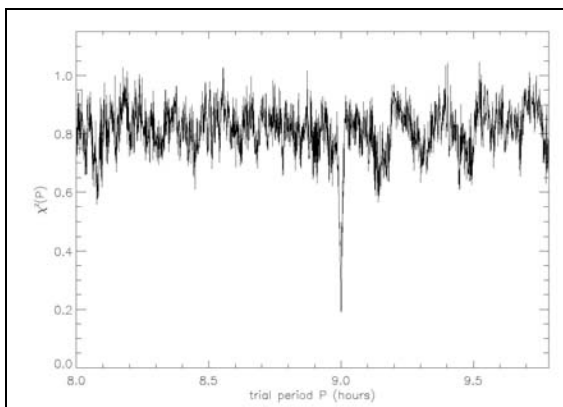


Figure 2. Chi-square as a function of the trial period has a global minimum at the correct value even though the period is not apparent in the data.

Despite the rather strong calibration noise of 0.04 mag, the model from this sequence has a pole direction only a few degrees away from the correct one, and the shape model well represents the rough global features of the object.

3. Amateur Contributions

Of course one cannot expect to get too much out of a handful of data points, especially if a number of these are noisier than expected (there are bound to be several outliers no matter what the engineers say). The models from sparse photometry are rough and in many cases (mildly) nonunique. This is where follow-up observations and thus amateur contributions come in.

Even just one additional dense lightcurve would be of great help in at least the following cases:

1. *There is more than one possible period fitting the sparse data.* This happens if the number of sparse data points is subcritical. The number is a complicated function of survey strategy and technical choices and can thus vary a lot. (This may also happen with faint targets for which data are noisy, but then the magnitude range is usually out of the reach of amateur observers.) Several targets will be in this class. Also, since the number of objects is so large, each target will only be given some standard computer time for analysis. Most of this time is spent in period scanning, and some targets will run out of the allocated pipeline time for period search as there will be both very fast and very slow rotators. Such targets will thus be flagged with ‘period not found’ and saved for later analysis. Additional lightcurves will help to determine what the actual period region is.
2. *Even if the period is known, there may be more than one independent pole solution.* This, again, happens with slightly too small sparse datasets. Here one should note that for objects moving close to the plane of the ecliptic there are always two dependent poles with roughly the same ecliptic latitudes and longitudes some 180 degrees apart. This ambiguity cannot be solved by photometric means, regardless of the method.
3. *There are sparse data points that just cannot be fitted.* This usually means that the target is a binary (mutual events affect some data) or a tumbler (or otherwise somehow strange and thus interesting), or the points are just outliers. A dense lightcurve can help in clearing the matter. We expect several targets to be flagged for follow-up observations in this manner.

4. *Quality and reliability check.* Even if everything seems to be fine with the sparse data analysis and we get a full model, we must do random checks to make sure that essentially the same model pops out from the combined sparse and dense datasets. If the models are different, we have overlooked something.
5. *More detail needed.* If the object seems to be strangely shaped, we need more data points to get additional details.

4. How to Contribute

The exact way of contributing to the above cases depends on the survey in question. The earliest upcoming survey is going to be Pan-STARRS (MOPS, moving object processing system), so I take it as an example. Our (viz. the authors of Durech et al. 2006 as well as other MOPS team members) first task after first light (expected early 2007) is to check the performance of the photometric equipment and systems (cases 3 and 4 above). During the first couple of years there will not be enough data for proper modelling, but we can check that the sequences from previously modelled targets are consistent (i.e., are fitted well with the existing model). This will give the first idea of the typical calibration noise level as well as of the size and frequency of outliers. From the second year on we can start to combine the sequences with separate lightcurves and thus have the first pipeline test with a large number of targets as one or more lightcurves and at least rough period estimates are available for over 1000 asteroids. This will further reveal the actual noise and outlier properties (as well as eventually produce the first preliminary models of new targets). Thus amateur data will be used very early in the survey.

After the first three or four years we should expect to begin to have sufficient data for full modelling, so there will be a steady flow of flags for the cases mentioned above. The analysis procedure (pipeline) will be trained to flag such targets automatically. We plan to have a website for the flagged targets for which follow-up observations are needed. This list will grow long, so there will be plenty of targets to choose from. All this should be automated, of course, as maintaining such a website manually will soon become impossible.

5. Discussion

Combining dense lightcurves with sparse photometric data offers a unique opportunity to obtain a large set of reliable asteroid models, thus mapping the physical properties of asteroids en masse for the

first time. Amateur observers are an invaluable data source because the number of follow-up targets is large. This approach makes photometry very time-efficient: a single lightcurve can remove ambiguities and greatly reduce the error limits of the solution. When the data sequences from surveys become publicly available on the Internet, the lightcurve observer can immediately perform the modelling using the analysis procedures that will soon be released as open software. Thus a lucky observer can, after only a few hours' observations, actually see for the first time what a 'new' asteroid looks like on the computer screen. The ultimate goal and reward is, of course, the big picture, census and history record of the whole asteroid population.

6. References

Durech, J., Grav, T., Jedicke, R., Kaasalainen, M., Denneau, L., Asteroid models from Pan-STARRS photometry (2006). *Earth, Moon, and Planets*, in press.

Kaasalainen, M., Torppa, J., Muinonen K., Optimization method for asteroid lightcurve inversion. II. The complete inverse problem (2001). *Icarus* 153, 37.

Kaasalainen, M., Physical models of large number of asteroids from calibrated photometry sparse in time (2004). *Astron. Astrophys.* 422, L39.

Kaasalainen, S., Kaasalainen, M., Piironen, J., Ground reference for space remote sensing: Laboratory photometry of an asteroid model (2005). *Astron. Astrophys.* 440, 1177.

Marchis, F., Kaasalainen, M., Hom, E., Berthier, J., Enriquez, J., Hestroffer, D., Shape, size and multiplicity of main-belt asteroids. I. Keck adaptive optics survey (2006). *Icarus*, in press.

Monitoring Changes in Eclipsing Binary Orbits

Lee F. Snyder
Kings Canyon Observatory
257 Coventry Drive
Carson City, NV 89703
snyder@physics.unr.edu

John Lapham
Paradise View Observatory
3722 Paradise View
Carson City, NV 89703
j.lapham@sbcglobal.net

Abstract

Times of light minimum were determined from observations of seven eclipsing binaries, EP AND, WZ AND, AH TAU, HP AUR, ZZ AUR, GO CYG and UV LEO. Based on these new times of minimum and those collected from the literature, changes in the orbital period of the systems were found and are presented. The literature contains hundreds of papers, which include proposed explanations for these period changes. Most involve apsidal motion, motion around another star (third body), mass transfer between stars, mass loss, magnetic cycles, and braking and angular momentum loss. When identifying an orbital period change in these systems and one of these common mechanism appears to be a feasible or satisfactory hypothesis, we applied the explanation to the occurring orbital changes where system parameters were available. ©2006 Society for Astronomical Sciences.

1. Introduction

Times of light minimum have been acquired on seven eclipsing binaries. Three are EA-type, one is EW-type, one is detached, and two have been classified near contact or EB-type. See the systems listed in Table 1. Four of the systems have been neglected binaries either because they have been recently discovered or overlooked. Enough times of minima on these systems were found in the literature such that, when combined with the times acquired in this paper, we have determined orbital period changes. See Table 2 for all the reference sources for times of light minima and Table 4 lists the times of light minimum obtained this paper. Times of light minima using photographic, photoelectric and CCDs observations were used at numerical value and not weighted. With these changes we can provide estimates of mass transfer and angular momentum loss (AML), which are predicted by theoretical work. We computed O-C curves with the acquired times of light minimum as these diagrams best reveal period changes. The O-C differences for each system have been calculated according to an earlier ephemeris minimum found in the previous written works on each system. The O-C values are computed in days and presented graphi-

cally against epoch or orbit numbers. A least squares polynomial is used to describe the period change or changes resulting in a parabola. The equation for this parabola curve is then added to the earlier ephemeris minimum to obtain a quadratic ephemeris and all errors noted are standard errors for the least-squares fit. The residuals from the quadratic equation were then plotted in a second O-C diagram and a polynomial fit of the fifth order applied.

2. Observations

At the Paradise View Observatory a Meade 14" LX200GPS used an STL-1301E SBIG camera at 2007mm (79") focal length, giving an effective field of view of 1.49 arcsec/pixel (Figure 1). At the Kings Canyon Observatory, an ST-9XE SBIG camera attached to a 12" Meade LX200 classic with a 1920mm (75.6") focal length gave an effective pixel field of view of 2.18 arcsec/pixel (Figure 2).

All times of light minimum were obtained in the VR color system approximating the standard Johnson photometric system. Reduction, charting and computations of the data were accomplished using the software programs listed in Table 3. 72 times of minima were acquired and are listed in Table 4.



Figure 1. Paradise View Observatory



Figure 2. Kings Canyon Observatory

System	Type	Spectral Type	Mag V / R	AML sec year ⁻¹ Observed
EP AND	EW	-/-	11.9/11.3	+1.4 ⁻¹²
WZ AND	Near Contact	F5/G2	11.6/-	+0.019
AH TAU	Semi-Detached	G5/-	11.8/10.76	+0.002
HP AUR	Near Contact	G2V/G8V	11.3/10.22	-0.016
ZZ AUR	Semi-Detached	A7/	11.4/11.1	-0.006
GO CYG	Semi-Detached	AOV/	8.67/8.65	+0.009
UV LEO	Detached	F8/	10.06/9.59	+0.003

Table 1. List of Eclipsing Binary Systems studied. AML = Angular Momentum Loss

(EBMD) Eclipsing Binaries Minima Database	http://www.oa.uj.edu.pl/ktt/
Bob Nelson's O – C files	http://binaries.boulder.swri.edu/binaries
Simbad	http://simbad.u-strasbg.fr/
AAVSO Web	http://www.aavso.org/
Up-To-Date Linear Elements of Eclipsing Binaries	www.as.ap.krakow.pl/ephem/

Table 2. List of Databases used.

Binary Maker 3	Light Curve Synthesis Program
Software Bisque – CCDSoft5	Image Processing and CCD Camera Control Software
Software Bisque - TheSky6	Planetarium Program
Microsoft – Excel	Spreadsheet Software
MPO Software - Canopus & PhotoRed	Data Processing
MPO Software – Connections	Telescope and Camera Control Program
PERANSO	Period Analysis Software
PSI-Plot	Technical Plotting and Data Processing

Table 3. List of software programs used for observations and data reduction.

OBJECT	HJD +2,400,000	Sd ^-3	FIL	TYPE	OBJECT	HJD +2,400,000	Sd ^-3	FIL	TYPE
EP AND	53686.891459	2.63	V	II	WZ AND	53691.907000	4.21	V	II
EP AND	53686.892174	5.85	R	II	WZ AND	53694.691000	6.43	V	II
EP AND	53687.699875	2.81	V	II	WZ AND	53694.691231	7.57	R	II
EP AND	53687.702979	3.91	R	II	HP AUR	53771.817123	3.02	V	I
EP AND	53688.712826	5.29	R	I	HP AUR	53771.816250	1.56	R	I
EP AND	53688.713270	0.423	V	II	HP AUR	53774.662767	2.43	V	I
EP AND	53688.910711	6.72	V	I	HP AUR	53774.661715	3.94	R	I
EP AND	53688.916564	9.87	R	I	ZZ AUR	53779.66503	2.21	V	I
EP AND	53689.720745	2.58	R	II	ZZ AUR	53779.66522	1.63	V	I
EP AND	53689.924354	3.07	V	II	ZZ AUR	53779.66728	2.29	R	I
EP AND	53689.926210	5.67	R	I	GO CYG	53610.838511	1.84	R	I
EP AND	53690.730717	3.74	V	II	GO CYG	53615.856026	3.38	V	I
EP AND	53690.732234	5.32	R	I	GO CYG	53615.856028	4.62	R	I
EP AND	53690.934733	2.74	V	II	GO CYG	53615.861034	1	V	I
EP AND	53690.935283	5.32	R	II	GO CYG	53615.862008	0.98	R	I
EP AND	53691.740136	5.11	R	I	GO CYG	53615.865305	3.64	V	I
EP AND	53691.740367	3.64	V	I	GO CYG	53633.813420	5.27	V	I
EP AND	53692.750290	5.27	V	I	GO CYG	53633.812944	5.11	R	I
EP AND	53692.752596	8.28	R	I	GO CYG	53674.718971	3.91	R	I
EP AND	53694.770288	7.45	R	I	GO CYG	53674.720455	2.79	V	I
EP AND	53694.770604	7.44	R	I	UV LEO	53776.821289	1.82	V	II
EP AND	53694.771004	6.23	V	I	UV LEO	53776.824667	2.81	R	II
EP AND	53694.773560	1.44	V	I	UV LEO	53779.822497	3.64	V	II
WZ AND	53687.730698	2.93	V	I	UV LEO	53779.822860	2.57	R	II
WZ AND	53687.734200	4	R	II	AH TAU	53689.806815	8.14	R	II
WZ AND	53688.772500	46.5	V	II	AH TAU	53689.806920	1.02	R	II
WZ AND	53688.776217	4.38	R	II	AH TAU	53688.807730	1.84	V	II
WZ AND	53689.821571	11.65	R	I	AH TAU	53688.807385	3.38	R	II
WZ AND	53689.823000	14.9	V	II	AH TAU	53689.807335	5.87	V	II
WZ AND	53690.861157	4.8	V	I	AH TAU	53689.807245	5.26	V	II
WZ AND	53690.863880	8.35	R	I	AH TAU	53689.970529	4.6	V	I
WZ AND	53691.903600	7.59	R	II	AH TAU	53689.972385	0.98	R	I
AH TAU	53692.799690	0.01	R	II	AH TAU	53694.795025	3.33	R	II
AH TAU	53692.800870	5.48	V	II	AH TAU	53694.795445	1.84	V	II
AH TAU	53692.966240	1.48	V	I	AH TAU	53694.961573	2.95	R	I
AH TAU	53692.966876	2.09	R	I	AH TAU	53694.962003	1.88	V	I

Table 4. Target Stars with Times of Minima. Type I = primary minimum. Type II = secondary minimum.

3. Case Studies

3.1. EP AND

This system was discovered in 1972 but has been neglected. Only 13 reference papers were listed on Simbad since 1986. The binary is a contact system.

We had only found 38 times of light minimum before we acquired the 23 times for this paper as shown in Figure 3. The O–C diagram is produced from the data set with the linear ephemeris, Eq. 1.

$$\text{HJD} = 2442638 + 0^{\text{d}}.40411057 E \quad (1)$$

With only 53 data points plotted it showed a discontinuously changing period with step variations but at a constant rate. We were fortunate to locate the Bob Nelson database and were able to acquire a total of 304 times of light minimum. We plotted all the O–C points, applied a parabolic least squares to the residuals to obtain the quadratic Eq. 2.

$$\begin{aligned} \text{HJD} &= 2442638.5109 \pm 0.00066 \\ &+ 0^{\text{d}}.40411057 E \pm 1.6^{-7} \\ &+ 9.00901496^{-21} E^2 \pm 5.85^{-12} \end{aligned} \quad (2)$$

A second O–C diagram, (Figure 4), was plotted using equation 2 and a sinusoidal curve in the O–C residuals is evident. This shows a secular period change. Where a sinusoidal curve appears, a third

body orbiting around the binary system can produce it. These periodic variations in the minima timing are caused by the light travel-time difference.

With the quadratic term it is possible to estimate the theoretical amount of angular momentum loss in the system from the equation given by Bradstreet (2000):

$$\begin{aligned} dP/dt &= 2 * (+9.00901496^{-21}) \text{ Quad. Term} \\ &* (1/.40411057) \text{ Period} \\ &* (86400) * (365.25) \text{ sec/day day/year} \\ &= +1.407^{-12} \text{ seconds year}^{-1} \end{aligned} \quad (3)$$

The AMG, Angular Momentum Gain (dP/dt) observed = +1.407-12 seconds/year.

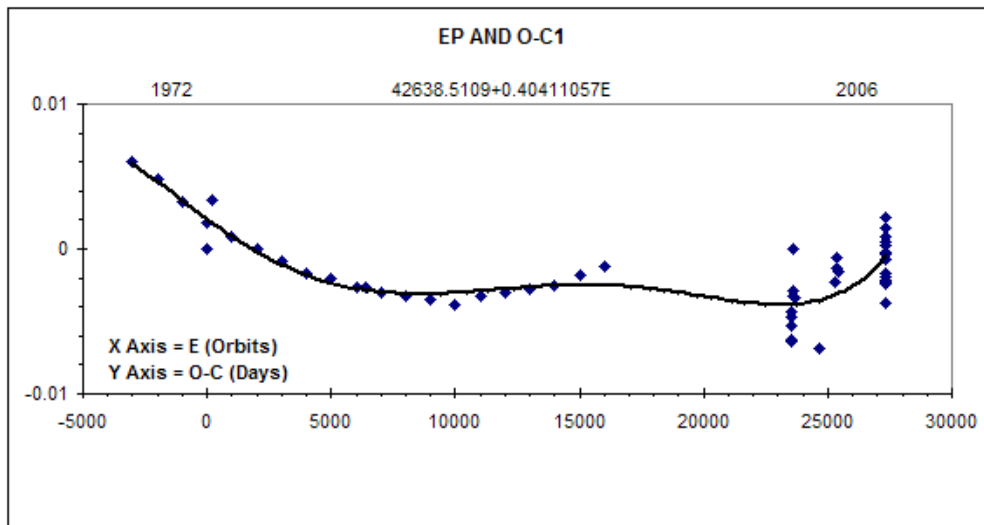


Figure 3.

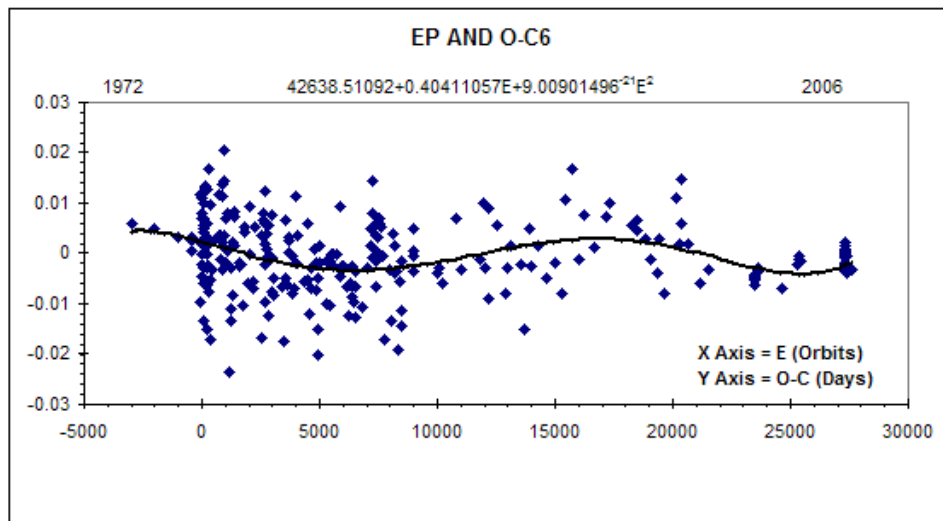


Figure 4.

3. 2. WZ AND

This is a near contact system with both stars convective, F5+G2. From the literature, 199 times of light minimum were gathered and 19 were obtained, this paper. The O-C chart, Figure 5, containing 218 points was computed from the linear ephemeris:

$$\text{HJD} = 2445963.8078 + 0^{\text{d}}.069565936 E \quad (4)$$

As explained in the introduction, a current ephemeris containing a quadratic term was computed:

$$\begin{aligned} \text{HJD} &= 2445963.80785 \pm 0.0006 \\ &+ 0.^{\text{d}}695658345 E \pm 1.94^{-7} \\ &+ 2.129257^{-10} E^2 \pm 2.31^{-11} \end{aligned} \quad (5)$$

The polynomial fitted residual from Eq. 5 is shown in Figure 6. The continual steady increase in the orbital period is shown and the minima this paper confirm the period is still increasing. The AMG, Angular Momentum Gain, Eq. 3, (dP/dt) observed = +0.019 seconds/year. The period and AMG has been continuous for the last 35 years.

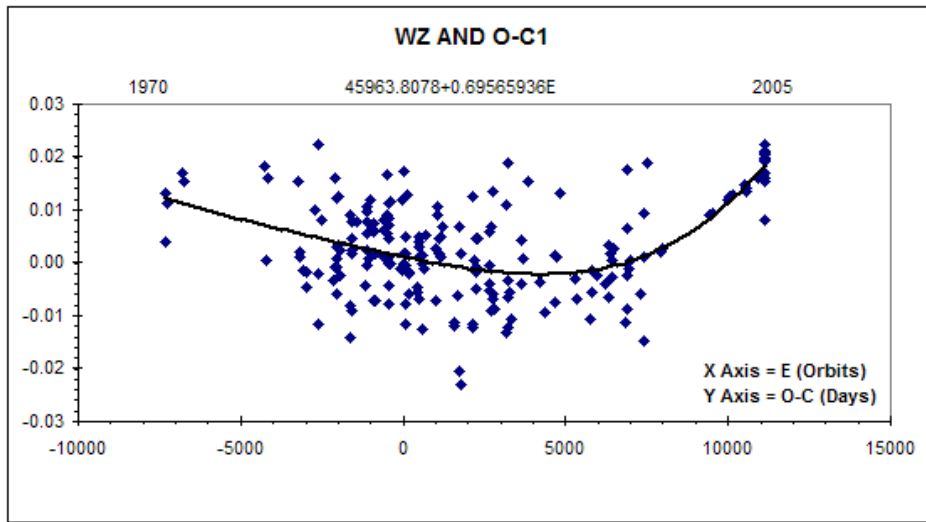


Figure 5.

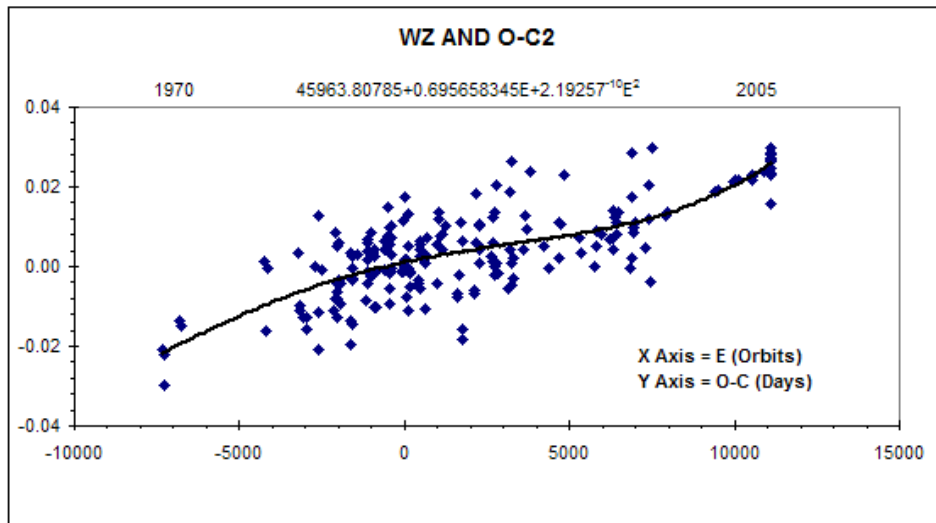


Figure 6.

3.3. AH TAU

A semi-detached system with the primary star a G5. The secondary spectral type is unknown. A total of 126 times of light minima were used in Figure 7 and 8, 16 acquired by this paper. Both diagrams show a recent abrupt increase in the period of the orbit around 2001 and are confirmed by this paper using the linear ephemeris:

$$\text{HJD} = 2447000.2689 + 0.^d33267164 \text{ E} \quad (6)$$

When a quadratic term

$$\begin{aligned} \text{HJD} &= 2447000.26777 \pm 0.0006 \\ &+ 0.^d332671802 \text{ E} \pm 5.97^{-7} \\ &+ 1.09848^{-11} \text{ E}^2 \pm 4.42^{-12} \end{aligned} \quad (7)$$

was applied a sinusoidal trend was evident, Figure 8. The feasibility of a third body around the system is possible. The AMG observed using Eq. 3, $(dP/dt) = +0.002$ seconds/year.

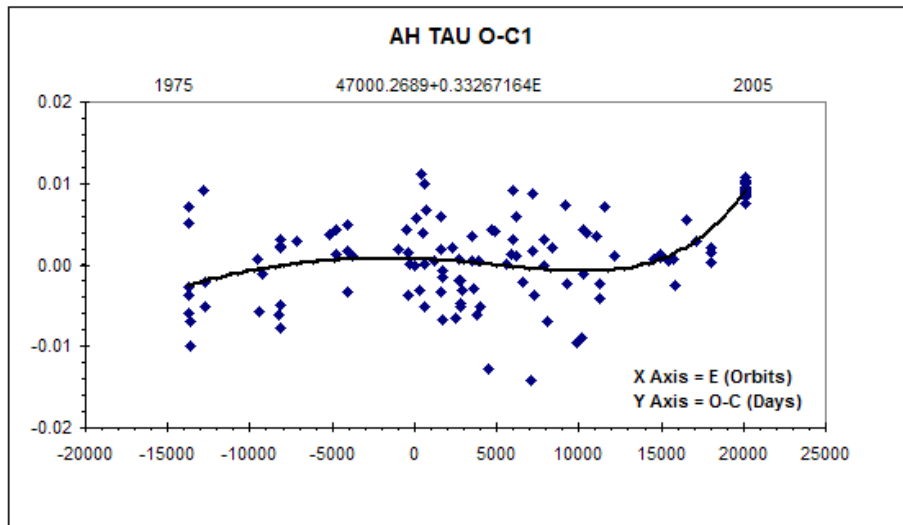


Figure 7.

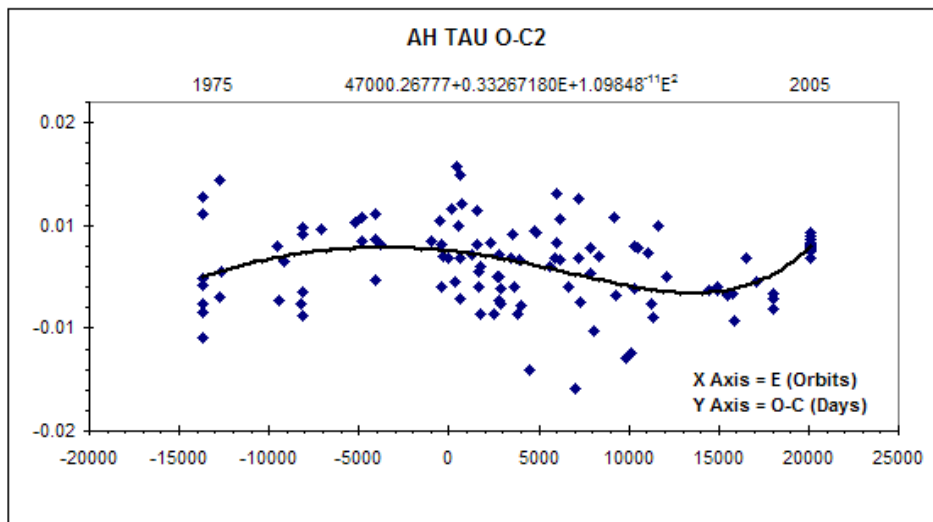


Figure 8.

3. 4. HP AUR

This is a near contact system with two late-type stars, G2V + G8V. A total of 70 times of light minima O-C are plotted, 4 from this paper, covering 30 years. Eq. 8 linear ephemeris was used to compute the O-C points, Figure 9.

This system had some orbit changes prior to 2001 but since that time the diagrams using Eq. 8 and 9 display slight changes, if any at all, Figure 10.

$$\begin{aligned} \text{HJD} &= 2446008.91495 \pm 0.001 \\ &+ 1.^d422821051 \text{ E} \pm 7.04^{-7} \\ &- 3.57509682^{-10} \text{ E}^2 \pm 1.29^{-10} \end{aligned} \quad (9)$$

The scatter of the points prior to 2001 is due to the type of observations used. Visual and photographic observations prior and CCD type after. The AML observed using Equation 3, $(dP/dt) = -0.016$ seconds/year.

$$\text{HJD} = 2446008.9135 + 1.^d42281854 \text{ E} \quad (8)$$

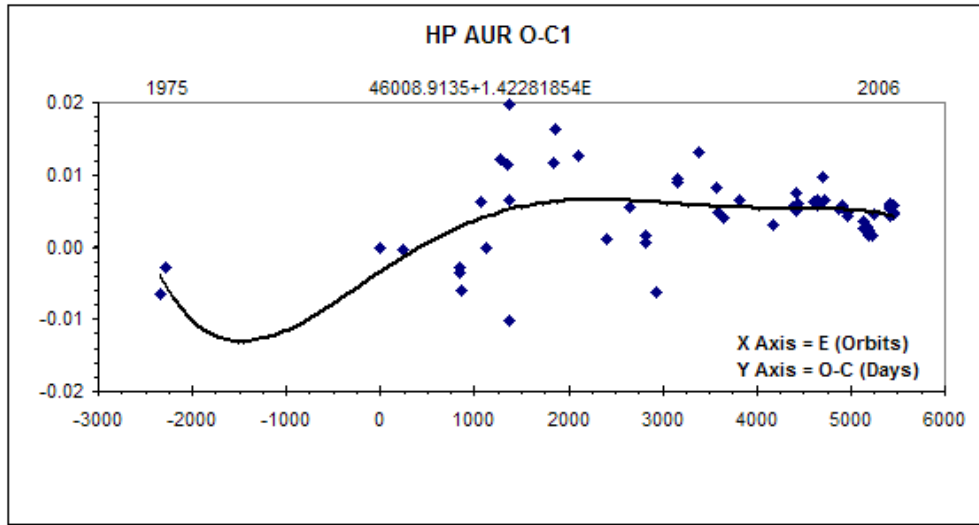


Figure 9.

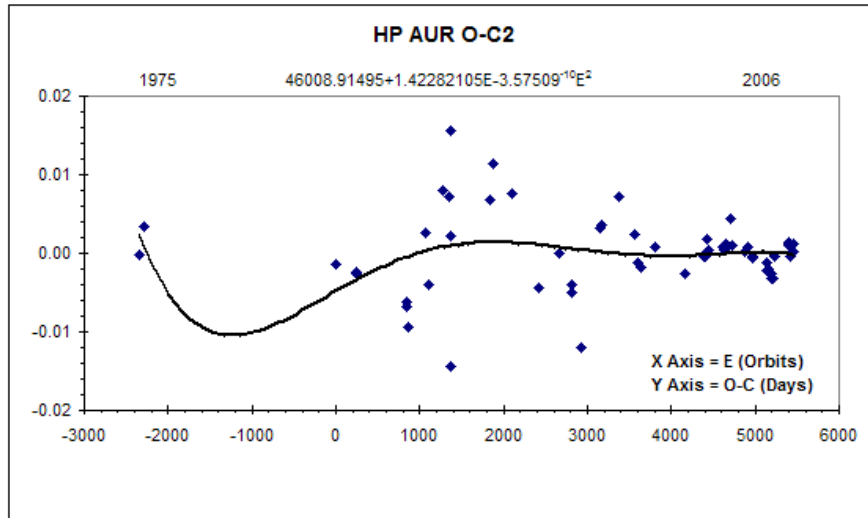


Figure 10.

3.5. ZZ AUR

A semi-detached system with the primary a type A hot star. The spectral type of the secondary is unknown. A least-squares fit using the linear ephemeris (10) is plotted in Figure 11.

$$\text{HJD} = 244962.2221 + 0.^d601217202 E \quad (10)$$

was plotted using Equation 10 a sinusoidal trend is apparent. This shallow sine curve with small amplitude would indicate Keplerian motion caused by a third object.

$$\begin{aligned} \text{HJD} &= 2444962.22827 \pm 0.0007 \\ &+ 0.^d601217202 E \pm 2.65^{-7} \\ &- 6.10504338^{-11} E^2 \pm 2.026^{-11} \end{aligned} \quad (11)$$

Figure 11 displays a steady increase in the orbital period but when a second O–C diagram, Figure 12,

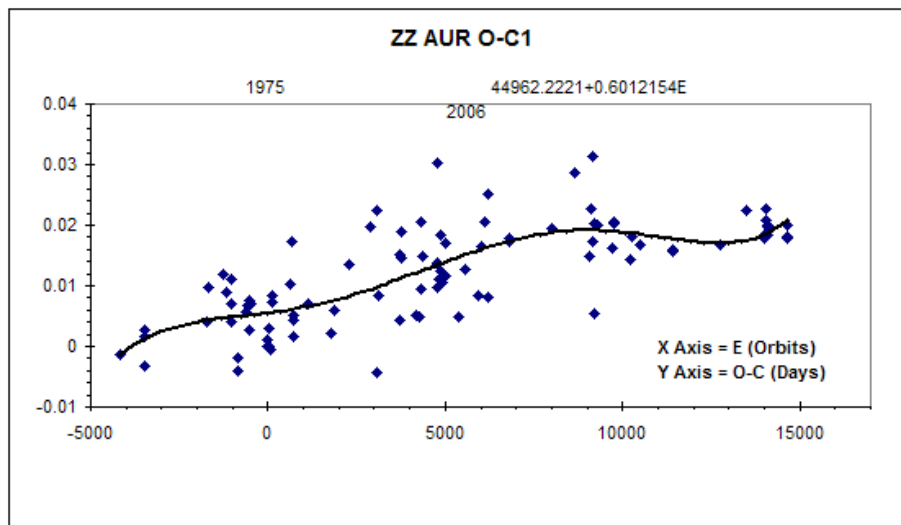


Figure 11.

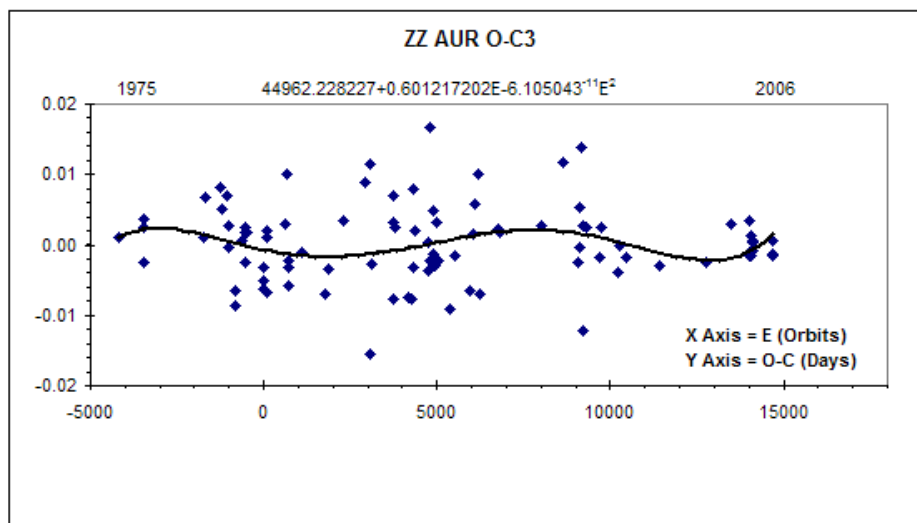


Figure 12.

3.6. OO CYG

With 144 times of light minima used, 21 of them are this paper. The span of time covers 74 years from 1931. This system is semi-detached, the primary being a hot type A0V which has made it difficult to determine the spectral type of the secondary. The linear ephemeris

$$\text{HJD} = 2433930.40561 + 0.^d71776382 E \quad (12)$$

was used to compute the O-C chart, Figure 13. The O-C diagram, figure 14 was plotted using the quadratic Eq. 13

$$\begin{aligned} \text{HJD} &= 2433930.407925 \pm 0.0009 \\ &+ 0.^d717763632 E \pm 1.21^{-7} \\ &+ 9.961248^{-11} E^2 \pm 4.94^{-12} \end{aligned} \quad (13)$$

which shows the true trend of the changes of the orbital period. This period was decreasing since 1931 until an abrupt increase in 1972. This increase continued until 1995 when an abrupt decrease occurred. A paper, Jones (1994a), showed a previously unreported sine curve trend in the residuals. Since that time, October 1993, 52 more times of light minima have been obtained and instead of a smooth sine curve, the wave displays the abrupt decrease that is continuing today. Using the quadratic term the AMG, Eq. 3, $(dP/dt)_{\text{observed}} = +0.009$ seconds/year.

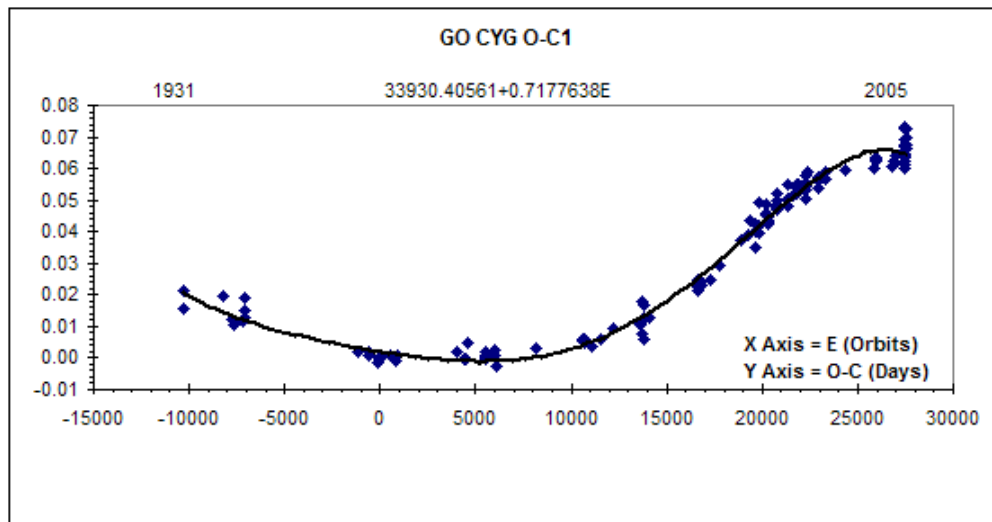


Figure 13.

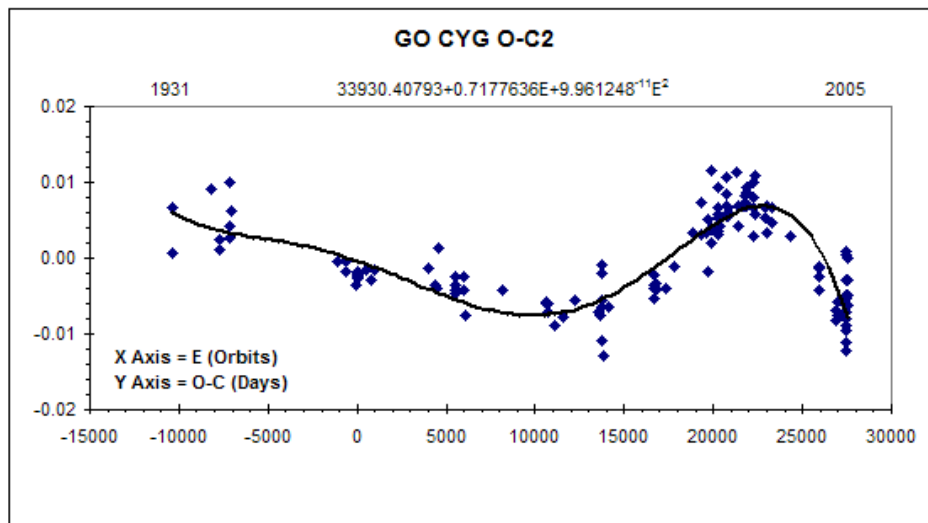


Figure 14.

3.7. UV LEO

This is a short-period detached eclipsing binary with two late-type convective stars, G0 + G2, Popper (1997). We were able to locate 220 published times of light minima and added 4 times with this paper. The linear ephemeris (Eq. 14) was used to compute the O-C chart in Figure 15.

$$\text{HJD} = 2438440.72525 + 0.^d600085011 E \quad (14)$$

The computed quadratic ephemeris (Eq. 15)

$$\begin{aligned} \text{HJD} &= 2438440.726259 \pm 0.0002 \\ &+ 0.^d600085128 E \pm 2.41^{-8} \\ &+ 2.73603731^{-11} E^2 \pm 1.46^{-12} \end{aligned} \quad (15)$$

was applied to the O-C numbers and the residuals plotted in Figure 16. The linear and quadratic plot both show a steady increase in the orbital period since 1939. Using the quadratic term the AMG, Equation 3, (dP/dt) observed = +0.003 seconds/year.

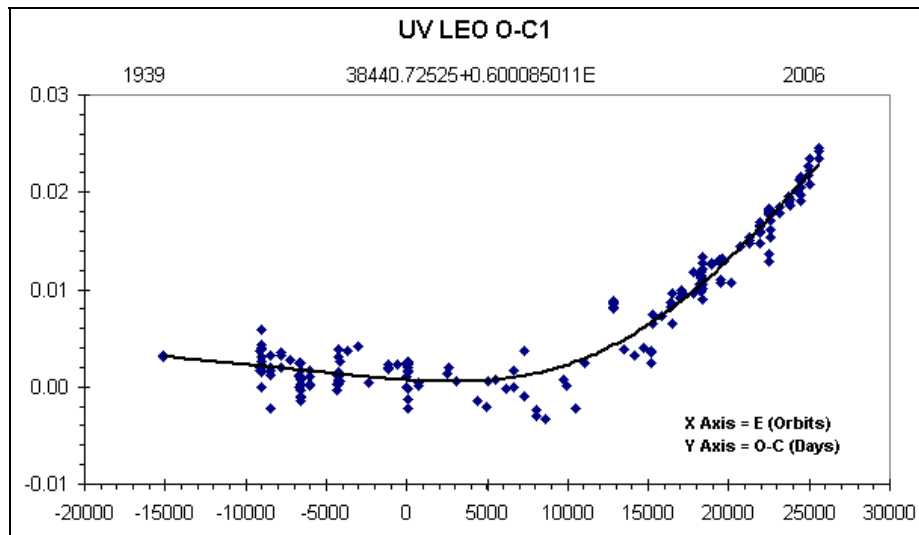


Figure 15.

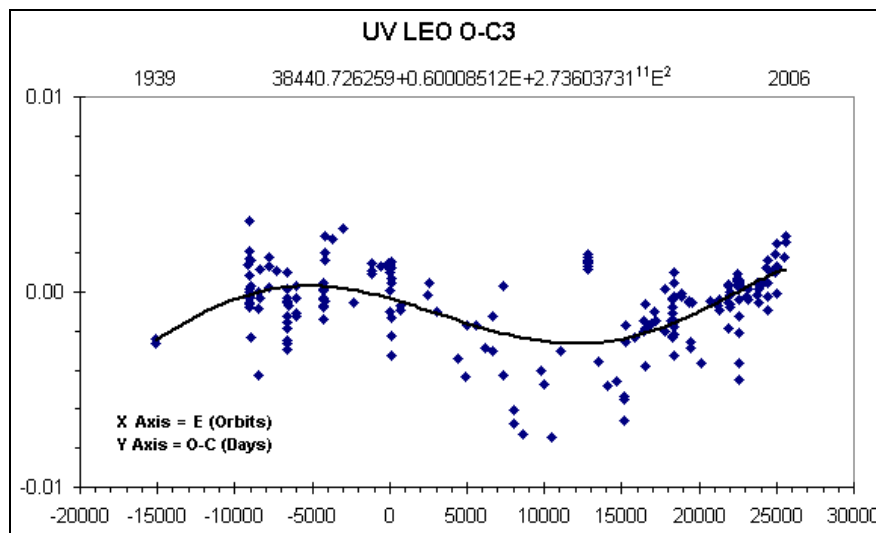


Figure 16.

4. Conclusion / Discussion

We have displayed the fundamental properties of the orbits of seven eclipsing binaries using observed times of light minima and compared them with the computed times, O-C. Despite some gaps in the observed times, the O-C charts have clearly exposed the main features of changes in the orbital periods. No attempt was made to analyze the light curves of the systems or try to determine if apsidal motion is present. A number of proposed mechanisms are in the literature to explain the period changes involving angular-momentum transfer, magnetic coupling, mass transfer and third body effect on the system.

An inferred light-travel time effect demonstrated by a smooth sinusoidal trend in the O-C diagrams is evident in four systems, EP AND, AH TAU, ZZ AUR and UV LEO, Figures 4, 8, 12, and 16 respectively. Of note, three of the systems are close contact or semi-close binaries and one, UV LEO, is detached. The orbital period changes caused by the light-travel time effect must be secular and appear to be independent of the modulated period variations exposed in sections of the fitted polynomial in the O-C diagrams, the so-called step variations.

In the three-body theory for period changes, to compute the mass of the third body, M_3 , and the size of the orbit about the system's barycentre, a , the total mass of the binary, M_b , needs to be known. For AH TAU, $M_b = 1.61 M_\odot$, Yang (2002). We could not find such data for EP AND and ZZ AUR. Using the O-C diagram in Figure 8 and using the timing difference between extremes of the O-C curve and the peak amplitude of the sinusoid, Van Buren (1986), we determined a radius of 0.61 ± 0.03 AU for the motion of the binary around the barycenter. The sine curve has a period of 25.1 ± 1.29 years and this puts $M_3 = 1.59 \pm 0.02 M_\odot$. The 0.61 AU represents the distance between the far and near side of the binary orbit about the system's barycentre. These numbers can be considered plausible and the third-body orbit could cause the orbital period changes.

We did not compute the orbit of a triple system for UV LEO since the sine curve in Figure 16 is asymmetrical. Snyder (1998) reported a more pronounced and symmetrical sinusoid, with the binary's motion about the barycentre of the triple of 0.32 AU and a period of 40.1 years.

We found that the short-term variations are easy to detect because of their short time scale in contrast to long-term changes, which are difficult to expose because of their small amplitude.

We are hoping to research detached systems like UV LEO displaying a light-travel time sine curve which would be free of the other effects inherent with contact and near-contact systems. We computed the Angular Momentum Loss/Gain observed for the seven systems, Table 1, since it required the quadratic term we had already computed to construct the O-C charts.

We would like to present a warning: It was Dugan who said, "Period changes frequently occur after publication of a careful study."

5. References

- Bradstreet, D.H. Private Communications, 2006
- Jones R.A., Snyder L.F., Frey G., et al, "Sinusoidal Variations In the Period of the Eclipsing Binary GO Cygni", 1994, IAPPP Com. No. 54, 34
- Popper D.M., 1997, "Orbits of Detached Main-sequence Eclipsing Binaries of Types Late F to K", AJ, 114, 1195
- Snyder, L.F., "Period Change in UV Leonis", 1998, IBVS No. 4624
- Van Buren, D., "Comment on the Three-Body Theory for Period Changes in RS CVn Systems", AJ, 92, 136.
- Yang, Y., et al, "Period behavior of the W Ursae Majoris contact binary AH Tauri", (2002) A&A 390m 555

Analysis of GSC 2475-1587 and GSC 841-277: Two Eclipsing Binary Stars Found During Asteroid Lightcurve Observations

*Robert D. Stephens
Santana Observatory
11355 Mount Johnson Court
Rancho Cucamonga, CA 91737
RStephens@foxandstephens.com*

*Brian D. Warner
Palmer Divide Observatory
17995 Bakers Farm Rd.
Colorado Springs, CO 80908
brian@MinorPlanetObserver.com*

Abstract

When observing asteroids we select from two to five comparison stars for differential photometry, taking the average value of the comparisons for the single value to be subtracted from the value for the asteroid. As a check, the raw data of each comparison star are plotted as is the difference between any single comparison and the average of the remaining stars in the set. On more than one occasion, we have found that at least one of the comparisons was variable. In two instances, we took time away from our asteroid lightcurve work to determine the period of the two binaries and attempted to model the system using David Bradstreet's Binary Maker 3. Unfortunately, neither binary showed a total eclipse. Therefore, our results are not conclusive and present only one of many possibilities. ©2006 Society for Astronomical Sciences.

1. Introduction

In this age of massive amounts of data being available on the Internet, the process of "data mining" is becoming more popular among professionals and amateurs interested in doing research. Often data collected for one reason can be viewed with different parameters and goals and so reveal even more important scientific results.

On a much less grand scale, our work of finding the parameters of asteroid lightcurves produces anywhere from 50 to 250 images each night of the same field. Since an asteroid moves, the telescope position is usually adjusted from time to time during the night to keep the asteroid near center. This means that some stars drop off one edge while others come into view.

We used differential photometry for our work, meaning that we measure from two to five comparison stars and subtract the average value from that of the asteroid to derive a value used for period analysis. Often, these stars are selected if they are relatively close to the asteroid, isolated from other stars, positioned so that they stay in the field during the

entire run, and somewhat similar in brightness to the asteroid.

Eventually the odds work such that one or more of the comparison stars turns out to be variable. This is not allowed in differential photometry since the average of the comparisons is not constant (discounting extinction effects). In this case, the comparison is eliminated for final period analysis of the asteroid. On occasion, we will go back to the variable and get additional images on subsequent nights in order to determine the period of the curve and its shape. If there is something that makes the curve interesting, as was the case for the two variables covered here, we'll do multi-color photometry to determine additional information about the star and then attempt to model it using Binary Maker 3 (Bradstreet 2006).

2. The Observatories

Santana Observatory is located at Stephens' home in Rancho Cucamonga, CA. The telescope is a Meade 0.3m RCX using an SBIG STL-1001E CCD camera (Figure 1). Despite being deep within

the Los Angeles metropolitan area and its massive light pollution dome, photometry with 0.02m precision can be done on objects down to 14.5 when conditions are good, using a Clear filter and up to 60-second exposures.



Figure 1. Santana Observatory 0.3m Meade RCX.

The Palmer Divide Observatory (PDO) has three telescope/camera setups. One is a 0.5m Ritchey-Chretien with Finger Lakes IMG-1001E camera (Figure 2). The other two telescopes are each a 0.35m LX-200GPS. One uses an FLI IMG-1001E while the other uses an SBIG ST-9E. The latter scope also uses an OPTEC NextGen reducer ($f/5$) to give a field of view similar to the other telescopes. The 0.5m can work down to 17.0 with 0.02m precision with a Clear filter. The 0.35m scopes can often work to 15.5 or a little better when using three to four minute exposures.

All imaging is done unguided, though the 0.5m at PDO is being equipped with an external guider and camera to allow exposures up to 5 minutes with even higher signal-to-noise because of less trailing.



Figure 2. The 0.5m telescope at PDO.

3. Acquiring Data

The work at Santana and Palmer Divide Observatories generally starts with selecting potential targets using the list of lightcurve parameters maintained by Harris and Warner (Harris 2006) against those asteroids well placed at the time observations are planned. Asteroids with no or poorly known lightcurve parameters are given priority, with extra consideration given to targets being surveyed by the Binary Asteroids program under the direction of Petr Pravec (2005) and, at PDO, of the Hungaria asteroids. Once the targets are selected, an automation script is written for MPO Connections. The scripts take images of the asteroid throughout the night, pausing from 15-90 seconds between images.

Periodically, a new GoTo command is issued to force the telescope to recenter the asteroid and, in some cases, refocus the camera. At the end of the night, the camera is shutdown and the telescope is returned to a park position.

At PDO, images are stored on the camera-control computer and then transferred to another computer for processing and measurement. At Santana, the images are stored on a network drive.

4. Measuring Images

Before the images are measured, dark frames and flat fields are applied. Without a proper flat field, the differential photometry can be affected as the comparisons move through the field as the telescope is repositioned to keep the asteroid near center.

Not only can data vary from image to image, a trend can be introduced in the data such that a raw plot of a curve shows a gradual decrease or increase of average magnitude. In one instance when a bad flat was used at PDO, the average magnitude of the curve decreased by nearly 0.07m over a few hours. When trying to match data from night to night or

with other observers, this can introduce all sorts of errors in the analysis.

Final measurements are made using MPO Canopus (Warner 2006a). In this program up to five comparison stars can be used to derive an average value, which is then subtracted from the value for the asteroid to derive a differential magnitude. The data are stored for period analysis, again in Canopus, using the Fourier analysis algorithm developed by Harris (1989).

4. 1. Checking for Variable Comparisons

Once all the images are measured but before period analysis begins, we use a feature in Canopus that plots the raw data of each comparison star. Also available is a plot for each comparison that finds the average instrumental magnitude of the remaining comparisons and then subtracts that from the instrumental magnitude of the given comparison. This provides a strong visual check that one of the comparisons is not variable. Sometimes it is.

Figure 3 shows one of those times when a selected comparison was variable. In this case, it was one of the stars initially selected when 286 Adorea was being worked at Santana Observatory on February 23, 2006.

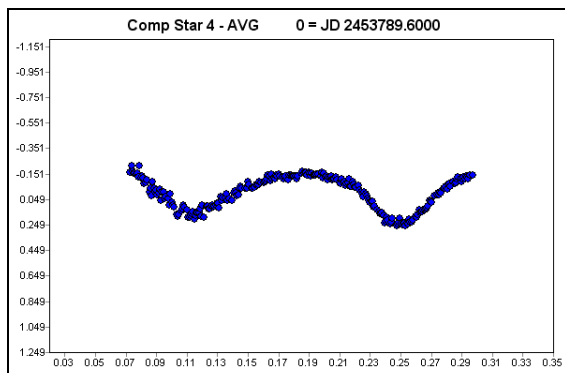


Figure 3. A plot of Comparison 4 minus the average of the other comparisons versus time. If all comparison stars were constant, the plot would be a flat line.

It's important that a plot such as those above (or one generated in a spread sheet using the comparison star data) be used to check for variability. Simple inspection of the target's lightcurve may tell the full story.

For example, look at Figure 4, which is a plot of the raw differential data for 286 Adorea on February 27, 2006 where only constant comparison stars were used. On the other hand, Figure 5 is from the same raw data for the asteroid with exception being that the set of comparisons included one star,

comparison 4, that varied by 0.51mag over a period of 6.59hrs.

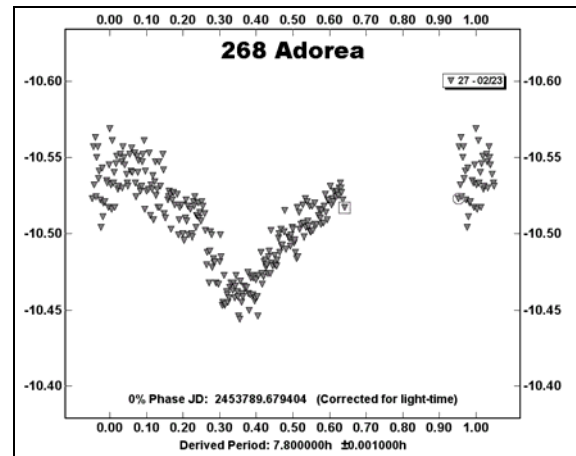


Figure 4. The lightcurve of 268 Adorea using only constant comparison stars.

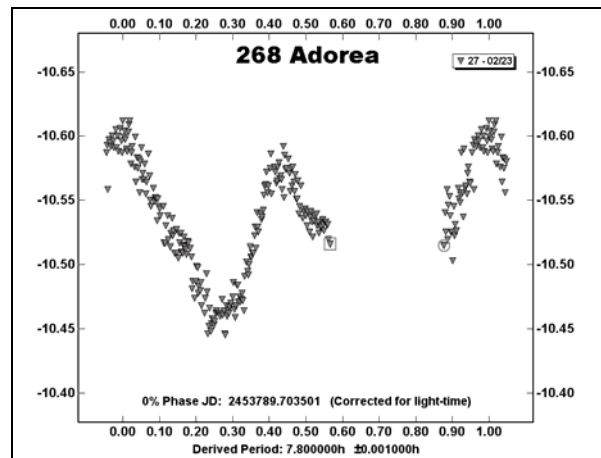


Figure 5. The lightcurve of 268 Adorea using a set of comparison stars where one varies by 0.51mag over 6.59 hours.

4. 2. Reducing to Standard Magnitudes

The initial observations are usually made using the Clear filter. This allows a higher signal to noise (SNR), which – in turn – gives a higher precision to the data. For critical analysis of asteroid lightcurves, a precision of 0.01-0.02mag is usually required, meaning a SNR of about 50-100.

For proper modeling of a binary star, it's necessary to have a good initial estimate of the combined temperature of the system. This means getting images in two or more standard filters. It might be possible to get an approximate temperature using the multi-color photometry from some large surveys. However, they do not use the standard Johnson-Cousins filters. Conversion formulas to the J-C system are available but it's better to determine the

values using the right filters. If nothing else, it's good practice for learning how to do photometric reductions.

4.3. Getting Images

If at all possible, it's best to get at least some initial runs in three standard filters, e.g., B, V, and either R or I. The latter is preferred by many because it provides a larger color difference than V-R and has more scientific value. On the other hand, the I filter can be problematic for thinned, back-illuminated chips because of fringing patterns caused by a spectral line in the sky glow.

The B filter can present its own problems because most CCD cameras are not as sensitive in blue as they are in the longer wavelength spectral regions. However, it is still possible – with longer exposures – to get a sufficient SNR to make reliable determinations of the color index and, therefore, the temperature of the star.

The reduction process used in our work follows that outlined in *A Practical Guide to Lightcurve Photometry and Analysis* (Warner 2006b) and implemented in PhotoRed, a utility program to MPO Canopus.

While still following the more traditional approach to photometric reductions, our process has a few variations that make things a little easier and also allow Clear filter observations to be converted to Johnson V magnitudes with a high degree of accuracy ($<0.02m$ if done carefully). The reduction process dictates how images are obtained each night.

The first step is to shoot two reference fields with well know standard magnitudes in order to find the first order extinction terms for the night. One field must be near the zenith, giving an air mass near $X \sim 1.0$, while the other must be about 30° above the horizon, which means an air mass of about $X \sim 2.0$. The same field can be imaged twice, once when low and then when high, but this relies on the extinction being constant, something that is not very common at most amateur sites.

For each field, we shoot 3-4 images in at least V, R, and C. We sometimes also use B (both) or I (Stephens) to get an independent check of the results using a different filter combination. We repeat the sequence for the target field when it is at least 45° and there is no apparent sky degradation. If there are hints of haze or thin clouds, we wait until a good night and shoot the reference and target fields in as short a time as possible.

The latter is particularly important for the target field since the star is variable. Images taken too far apart in time can result in a color index too large or

small, depending on if the star was fading or brightening during the interval.

On some occasions, an alternate approach is used. There, only a single reference field is used as are assumed values for the first order extinction. The reference and target fields are shot when both have the same or nearly the same air mass. Since the correction to exoatmospheric magnitude is nearly identical for both fields in this case, an adjustment to the nightly zero point based on air mass is not required.

This method is recommended only when one can use a reasonably assumed value for first order extinction that is based on past measurements and when conditions are nearly ideal. If there is haze or thin clouds, then it's best to wait until a good night and get reduction images using two reference fields.

4.3.1 From Raw to Standard Magnitudes

The images for both reference fields are measured first, getting the raw instrumental magnitudes for a number of stars for which there are catalog values in two standard colors. The two colors do not have to be the same as the two filters used. For example, part of the reduction process is to determine the standard color index – say B-V – versus the instrumental color index, which can b-v or even v-r.

Warner has conducted several tests using M67 as a target field while two other fields were used to find first order extinction and the nightly transforms. Reductions were made using B-V versus v-r and then V-R versus v-r to determine the standard V magnitude of five stars (“comparisons”). The resulting V-R color indices, calculated from V and R or directly, and the reduced V magnitudes for each star differed by 0.000 to $0.002m$, i.e., the results were virtually identical.

Once both fields are measured, the first order extinction terms are set to 0 or an assumed value. The data from the higher ($X \sim 1.0$) field are used to find two sets of transforms: the standard versus instrumental color index and standard magnitude in one color versus standard color index.

The data from both fields are then used to find the first order extinction (FOE) method using the Modified Hardie Method (see Warner 2006b). That method requires that color corrections be included, which is why the transforms were found first. The process also finds the corrected nightly zero points based on the new FOE values.

The images for the target field are then measured and the standard color index are found for the comparisons and target. The next step finds the standard magnitudes in one or more colors for the comparisons only. The standard color indices and

magnitudes are used in a differential formula (Miles 1998) to find the reduced standard magnitudes for the target.

4.3.2 Example: GSC 2475-1587

The complete details of the reductions for both stars will not be given. However, it may help to show some of the results obtained for one of the two stars in this study on two different nights and then compare “bottom-line” results for several nights. The critical points where that the color indices and standard magnitudes of the comparisons were similar both nights and that the reduced standard magnitudes of the target for each night could be overlapped without having to adjust the zero points of the data.

Table 1 shows the results from two nights. The reference field used to find the nightly transforms was DW CNC, for which Arne Henden generated standard BVR magnitudes for a number of stars. The first order extinction was assumed and so the target field and that of DW CNC were imaged when

both had nearly the same air mass (see the alternate method described towards the end of 4. 3).

The data for Jan. 29 were found using both B-V versus v-r and then V-R versus v-r. This allowed finding B-V and V-R for the comparisons and target and then to compare the approximate temperatures based on each color index.

The C to V columns show the derived V standard magnitude based on Clear filter observations. The $\Delta C-V$ column shows the difference in the derived V magnitude on the two nights, the largest error being just $<0.03\text{mag}$.

The B-V columns show the derived color indices for the comparisons and target on each night while the $\Delta B-V$ column gives the difference between the values. Based on tables found in Allen’s “Astrophysical Quantities,” (2004) the $\Delta B-V$ values correspond to temperature difference of $< 100\text{ K}$.

Parallel to that comparison is that using the values in the ΔK column, which show the difference in degrees Kelvin based on the derived B-V and V-R color indices. Except for Comparison 1, the differences in temperature are negligible given the star is about 6200 K.

	Jan 29 (B-V versus v-r)				Jan 30 (B-V versus b-v)			
	C to V	B-V	V-R	ΔK	C to V	B-V	$\Delta C-V$	$\Delta B-V$
Comp1	12.920	0.651	0.381	-1200	12.904	0.699	0.016	-0.048
Comp2	14.149	0.510	0.308	50	14.150	0.535	-0.001	-0.025
Comp3	14.070	0.498	0.302	100	14.042	0.482	0.028	0.016
Comp4	13.986	0.491	0.299	100	13.979	0.434	0.007	0.057
Comp5	14.351	0.781	0.447	100	14.325	0.799	0.026	0.018
Target		0.452	0.279	50		0.444		0.008

Table 1. Comparison of reduction results from two nights. See the text for an explanation of the data.

In Figure 6, the Clear to V reductions are plotted in absolute (reduced) standard V magnitudes. In order to get the data to match, the zero point for the data for each session was adjusted according to the values in Table 2.

Date	ZP Adj. (mags)
Jan. 27	+0.000
Jan. 28	+0.147
Jan. 29	-0.002
Jan. 30	-0.003

Table 2. Adjustments in session zero points.

Except for Jan. 28, the average reduced standard magnitude for the target was virtually identical. The transforms from the reference field on Jan. 28 resulted in very high standard deviations in the color indices and reduced standard magnitudes for the comparisons, probably due to passing thin

clouds while images were taken in one or both standard filters.

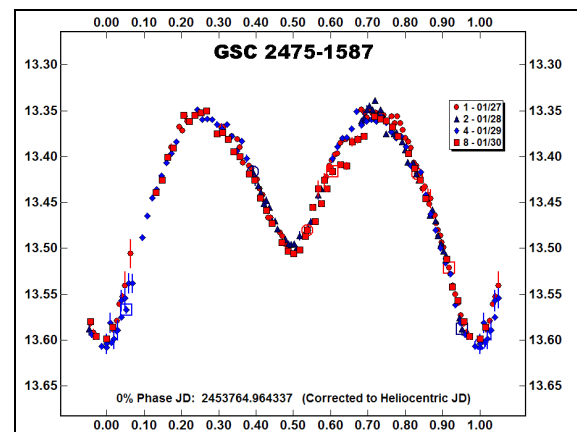


Figure 6. Phased plot of C to V standard magnitudes.

5. Binary Maker Modeling

Binary Maker 3 requires a set of normalized phase/flux pairs to do its modeling of the binary system. MPO Canopus provides this type of data, automatically changing the magnitudes to flux and normalizing to unity at phase 0.25. The user can override the default conversion in the event that a data point with excessive error near phase 0.25 causes adverse effects.

Modeling requires setting a number of parameters that define the mass ratio of the two stars, the temperature of each, effects due to limb darkening, and so on. This can be daunting for those learning the process but, fortunately, the Binary Maker software has an extensive on-line help that gets the user started down the right path.

Another way to get approximate parameters is to refer to a catalog of lightcurves that includes the modeling parameters that were used to solve the system. *Binary Stars: A Pictorial Atlas* by Terrell et al (1992) is an invaluable resource for this purpose. Another is the Catalog and Atlas of Eclipsing Binaries (CALEB), which is available on-line at <http://caleb.eastern.edu>, which includes a wealth of data on dozens of binary system.

5.1. Modeling Limitations

It is not possible to determine the full parameters of a system unless there is a lightcurve and radial velocity information available. A lightcurve alone can establish ratios of certain values but it cannot find absolute values such as the semi-major axis of the system. A radial velocity curve can establish the ratio of the masses. Once those are known, then knowing the period of the system, the semi-major axis can be found. However, the radial velocity curve data cannot be converted without knowing the orbital inclination, which can be given by the lightcurve.

If there are total eclipses indicated in the light, this can be used to put a limit on the inclination and, therefore, the solution for the semi-major axis. Neither of the stars studied here presented total eclipses.

5.2. GSC 2475-1587

This star was found by Warner when working 2856 Roser on 2006 January 27 when it used for a comparison. It is located at J2000 RA: 07h 56m 10s, DEC: +35° 09' 36". The 2MASS catalog gives magnitudes of J=12.595, H=12.369, and K=12.356. The star was not in the All Sky Automated Survey catalog (ASAS 2006) or in the General Catalog of

Variable Stars (GCVS 2006). It was found in the Northern Sky Variability catalog (NSV 2006) where it was reported to be V=13.288 with a scatter of 0.08 ± 0.035 mag with 212 good data points.

Our photometric findings for the variable and comparison stars are listed in Tables 3 and 4.

GSC 2475-1587 Summary	
V (avg)	13.47 ± 0.02 mag
B-V	0.45 ± 0.01 mag
V-Rc	0.28 ± 0.01 mag
V-Ic	0.54 ± 0.02 mag
Period:	0.38919 ± 0.00007 d
Amplitude: (BVR)	0.25 ± 0.01 mag

Table 3. Photometric Summary for GSC 2475-1587.

Comp	V	B-V	V-R	V-I
1	12.925 ± 0.017	0.649 ± 0.022	0.379 ± 0.011	0.754 ± 0.014
2	14.160 ± 0.022	0.507 ± 0.023	0.307 ± 0.012	0.618 ± 0.031
3	14.083 ± 0.030	0.496 ± 0.056	0.301 ± 0.031	0.566 ± 0.030
4	13.987 ± 0.015	0.489 ± 0.061	0.297 ± 0.031	0.518 ± 0.036
5	14.368 ± 0.030	0.778 ± 0.037	0.445 ± 0.019	0.850 ± 0.043

Table 4. Comparison star data for GSC 2475-1587

Since there were not total eclipses, absolute revalues could not be found for the semi-major axis and the masses of the two stars. Based on a correspondence with Dirk Terrell (private communications), the assumption was made that this was a “rare broken contact” binary where one of the stars had receded within its Roche limit while the other star was just filling its Roche lobe. This narrowed the possibilities for the starting parameters.

A number of solutions produced similar matches of the theoretical curve generated by the model and the normalized data generated by MPO Canopus. One of the solutions is shown in Figure 7 with the corresponding model shown in Figure 8. A partial list of the Binary Maker parameters that generated the curve and model is shown in Table 5.

We found that introducing a hot spot on one or both stars and adjusting the temperatures accordingly would reduce the small discrepancies between 0.75-1.00 and near 0.50. Another possibility was to make the orbit very slightly eccentric, $e \sim 0.002$. However, given the proximity of the two stars, that does not seem to be a likely solution (Terrell, private communications).

Assuming a mass ratio of 1.4, it was found that all the solutions favored an inclination of about 55° and that the temperatures of the two stars were about 4500 K and 6500 K. The latter temperature was assumed based on the B-V, V-R, and V-I values we measured. The cooler temperature was adjusted to make the two minimums of the theoretical curve match the actual data.

GSC 2475-1587	Star 1	Star 2
Mass ratio	1.400	
Omega	4.375826	4.375826
Fillout	0.0	0.0
Mean radius	0.408404	0.349737
Temp	4800	6000
Luminosity	0.3068	0.6932
Inclination	53.5	
Spot: Star 1.		
Colat: 90°, Long: 210°, radius: 20%, Temp: 0.60		

Table 5. Binary Maker parameters for GSC 2475-1587.

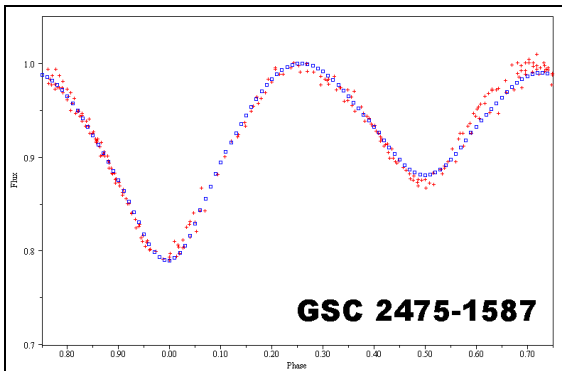


Figure 7. The actual data for GSC 2475-1587 are the round (red) data points. The theoretical curve generated by Binary Maker are the square (blue) data points.

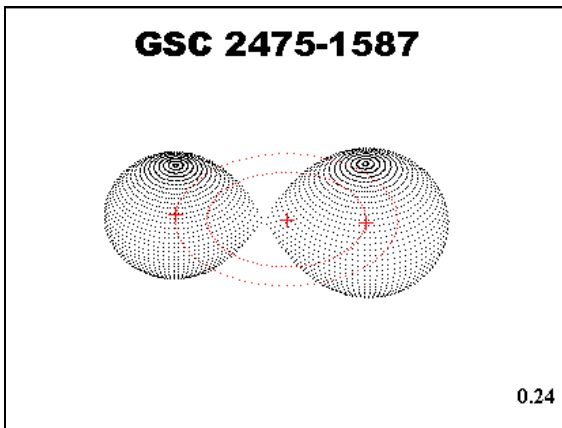


Figure 8. Binary Maker model for GSC 2475-1587.

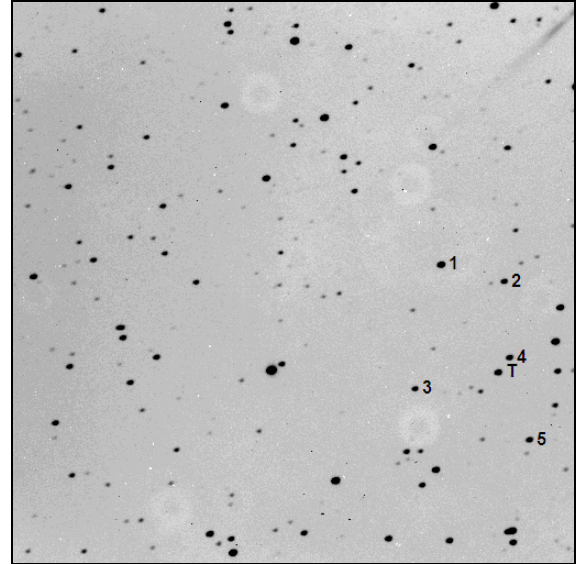


Figure 9. Finder chart for GSC 2475-1587. The comparison stars are marked with numbers. The star is marked by 'T'.

5.3. GSC 841-277

This star was discovered by Stephens on 2006 Feb. 23 UT during his run on 268 Adorea. He started measuring images a few hours into the run and used the comp star plots in Canopus to check on variability. He later measured the images again, selected a different set of comparisons, to get a curve in Clear for the star. Warner then followed the star for the following two nights (Feb 24 and 25 UT) using only V and R filters.

The star is located at J2000 RA: 10h 24m 11.75s, +12° 12' 53.6". The 2MASS catalog gives magnitudes of J=12.062, H=11.611, and K=11.487. The star was not in the All Sky Automated Survey catalog (ASAS 2006) or in the General Catalog of Variable Stars (GCVS 2006). It was found in the Northern Sky Variability catalog (NSV 2006) where it was reported to be V=13.556 with a scatter of 0.138±0.046mag with 99 good data points.

GSC 841-277 Summary	
V (avg)	13.78 ± 0.02
V-Rc	0.490 ± 0.006
Period:	0.274924 ± 0.000055d
	6.5982 ± 0.0013hr
Amplitude: (BVR)	0.51 ± 0.01mag

Table 6. Photometric Summary for GSC 841-277.

Figure 10 shows the V filter observations phased to a period of 0.274924±0.000055d. After reducing the raw data to standard magnitudes, the

V data from Feb. 25 overlapped that from Feb. 24 exactly – no zero point adjustment was required.

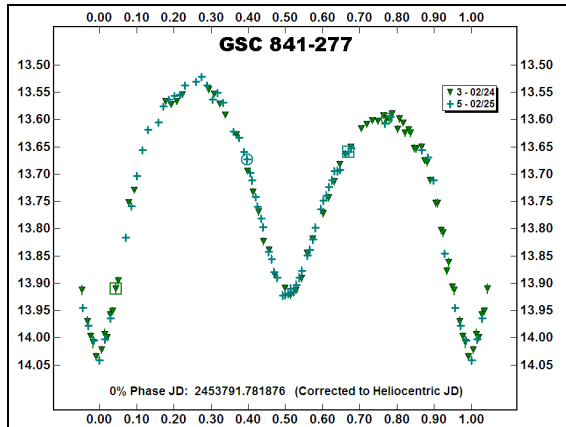


Figure 10. Phased curve of V observations for GSC 841-277. The period was found to be $0.274924 \pm 0.000055d$. The amplitude of the curve is $0.51 \pm 0.02mag$.

Comp Star	V	V-R
1	11.350 ± 0.032	0.238 ± 0.004
2	14.152 ± 0.042	0.665 ± 0.009
3	13.601 ± 0.020	0.364 ± 0.005
4	13.807 ± 0.001	0.479 ± 0.002
5	14.414 ± 0.017	0.375 ± 0.012

Table 7. GSC 841-277 comparison star data.

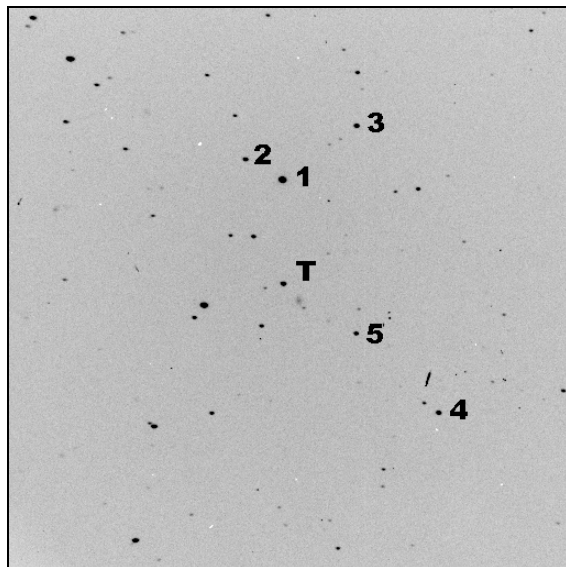


Figure 11. Finder chart for GSC 841-277. The comparison stars are marked with numbers. The star is marked by 'T'.

Figure 11 shows a finder chart for GSC 841-277. Figures 12 and 13 show the Binary Maker lightcurve and models respectively. Once again, it

was necessary to add a spot on one of the stars, this time being a large dark spot on star 2. Table 8 give a summary of the Binary Maker parameters.

GSC 841-277	Star 1	Star 2
Mass ratio	0.800	
Omega	3.371930	3.371930
Fillout	0.100	0.100
Mean radius	0.405711	0.366263
Temp	5000	4700
Luminosity	0.6426	0.3574
Inclination	68.5	
Spot: Star 2.		
Colat: 90° , Long: 270° , radius: 25%, Temp: 0.55		

Table 8. Binary Maker parameters for GSC 841-277.

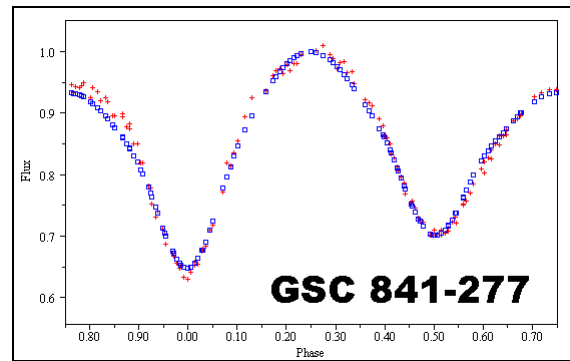


Figure 11. The actual data for GSC 2475-1587 are the round (red) data points. The theoretical curve generated by Binary Maker are the square (blue) data points.

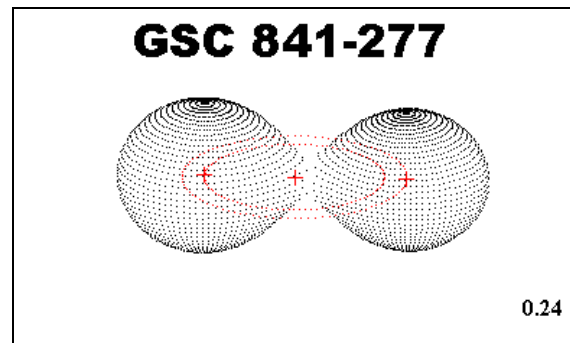


Figure 12. Binary Maker model for GSC 841-277.

6. Conclusion

The authors have discovered many other variable stars during the course of their asteroid light-curve work. In most cases, especially if the stars do not show a total eclipse, no follow up observations are made because of the time taken away from other observing programs. However, should a star show the promise of being something unusual, time

may be given to do at least a minimal amount of study, i.e., to determine the period and amplitude of the lightcurve and find a color index from direct observations.

The exercise of obtaining the images required for reducing observations to standard magnitudes and going through the reductions proved very beneficial in that it showed that the process can be done with relative ease and produce repeatable results from night to night. As our asteroid work takes us more into areas such binaries, long period and tumblers, and support for shape and spin axis modeling, standardizing observations becomes more important.

7. Acknowledgements

The authors thank Dirk Terrell and David Bradstreet for their invaluable insights into deriving the models for the two stars.

8. References

Allen, C.W., Allen's Astrophysical Quantities, Arthur N. Cox ed. 2000, Springer-Verlag, ISBN 0-387-98746-0.

All Sky Automated Survey. 2006, <http://archive.princeton.edu/~asas/>

Bradstreet, David, Binary Maker 3 software. 2006, www.binarymaker.com.

General Catalog of Variable Stars. 2006, <http://www.sai.msu.su/groups/cluster/gcvs/gcvs/>

Harris, A.W., Young, J.W., Bowell, E., Martin, L.J., Millis, R.L., Poutanen, M., Scaltriti, F., Zapala, V., Schober, H.J., Debehogne, H., and Zeigler, K.W., (1989). "Photoelectric Observations of Asteroids 3, 24, 60, 261, and 863." *Icarus* **77**, 171-186.

Harris, A.W., Lightcurve Parameters. 2006, CALL site, www.MinorPlanetObserver.com/astlc/default.htm.

Northern Sky Variability Survey. 2006, <http://skydot.lanl.gov/nsvs/nsvs.php>

Miles, Richard, UBVRI Photometry using CCD Cameras. 1998, Journal of the British Astronomical Association 108, vol. 2, pp. 65-74.

Pravec, P., Photometric Survey for Asynchronous Binary Asteroids. 2005, Proceedings of the 24th Annual Conference of the Society for Astronomical Sciences, B.D. Warner et al, ed., 61-62.

Terrell, D., Mukherjee, J.D., Wilson, R.E., Binary Stars: A Pictorial Atlas. 1992, Krieger Publishing. ISBN 0-89464-041-0.

Warner, B.D., MPO Software. 2006a. www.MinorPlanetObserver.com

Warner, Brian D., A Practical Guide to Lightcurve Photometry and Analysis, 2006b, Springer. ISBN 0-387-29365-5.

Switching to Infrared!

A New Method for Non-professional Imaging in the mid-IR

Thomas G. Kaye
Spectrashift.com
404 Hillcrest, Prospect Heights, IL 60070
tom@tomkaye.com

Abstract

With the continuing expansion of amateur astronomy, some work has been done in the near infrared where CCD's are still sensitive in the 1 micron range. In order to advance into the mid-infrared out to 12 microns, expensive CCD arrays are required that use exotic sensor materials such as Mercury-Cadmium-Telluride (MCT). With the advent of eBay, used MCT detectors cooled by liquid nitrogen are now obtainable at reasonable cost. They are functionally limited to a single pixel, which would generally make them unsuitable for imaging. Raster scanning of the image field in conjunction with a single pixel sensor to rapidly assemble an infrared image is described as a solution to this problem. The image presented here is believed to be the first mid-IR telescopic image of Mars taken by a non-professional. The use of MCT sensors in conjunction with products such as the AO-7 and advanced scripting will be discussed as further roads for development. © 2006 Society for Astronomical Sciences.

1. Introduction

The visible wavelengths have been the hallmark of amateur astronomy with little thought given to wavelengths outside this region. Infrared is familiar to the general public mainly through police surveillance video where the ghostly white image of the perpetrator is seen running through the woods at night. Professional astronomy is now moving toward "full spectrum" coverage from x-ray to far IR. IR offers a completely new look at the skies and is a largely unexplored area for amateur science. Ordinarily infrared CCD arrays are custom-built affairs that would consume most of a million-dollar budget. The challenge in IR imaging centers on the sensor system itself.

Infrared astronomy is generally understood to require space-based telescopes because of atmospheric absorption. Some amateur work has been done in the near IR out to 1 microns where standard CCD's are still sensitive, and out to 2 microns for photometry [West]. In fact there are atmospheric windows from 2 to 12 microns (fig 1.) that can transmit IR. It is in this range that, to the author's knowledge, no amateur has explored and is the subject of this paper.

2. Detectors

Given the lack of available CCD arrays at reasonable cost, a low budget mid-IR detector becomes the bottleneck. Looking back historically at IR detectors before the CCD array, much work was accomplished by single pixel, Mercury Cadmium Telluride (MCT) detectors. These detectors, mounted in a vacuum chamber and cooled with liquid nitrogen, were these detectors of choice for infrared spectrometers throughout the 1990's. Once cooled, they have a sensitive detection range out beyond 14 microns (fig. 2).

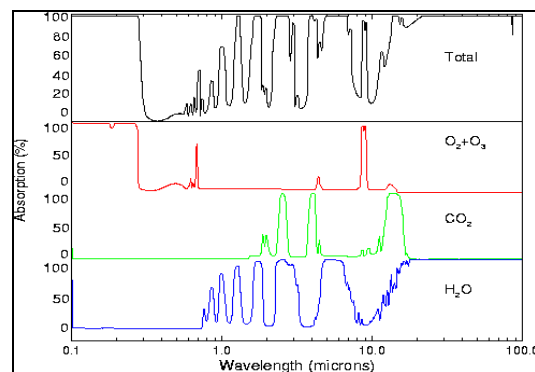


Figure 1. Atmospheric absorption windows. From 2 to 12 microns windows exist in which IR imaging can be accomplished

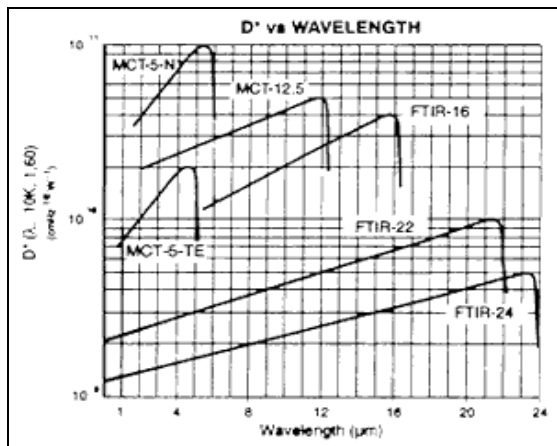


Figure 2. The detection ranges of various MCT detectors. Image courtesy of Infrared Associates Inc.

MCT detectors are typically mounted in a vacuum chamber which, is in effect, a thermos bottle (dewar) to hold liquid nitrogen. The MCT crystal is mounted on a cold finger attached to the inner chamber holding the nitrogen. The vacuum provides insulation and allows a much longer hold time for the cold liquid. A sealed, IR transparent window allows photons into the detector area. A typical IR detector is shown in figure 3.

Liquid nitrogen is usually available at local gas supply houses. Prices range around twenty dollars for 10 liters and is stored in large dewars. The hold time can range from days to weeks depending on the dewar. One liter should easily last a night of observing and the dewar is refilled simply by funneling in more nitrogen.

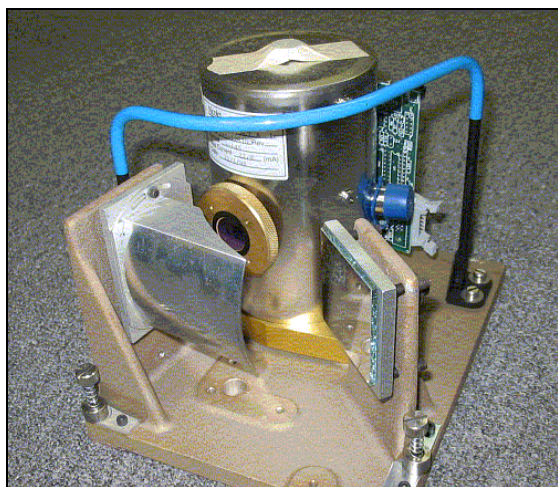


Figure 3. Typical liquid nitrogen cooled IR detector and low noise amplifier.

Noise is a dominant problem in IR systems and low noise amplifiers are required to amplify the weak signal. Thermal noise from the instrument or telescope is also a large component and must be sub-

tracted out. Most schemes from the 1980's involved spinning a propeller style metal blade in front of the detector known as a "chopper" which was at instrument temperature. The instrument would be timed to switch between alternately measuring the spinning chopper blade and the sample, in order to get real time background subtraction.

3. IR Optics

Glass is opaque at mid-IR frequencies. If lenses are required, they must be made from expensive specialized materials such as Zinc Selenide. Fortunately first surface mirrors will reflect IR and have the same focal path as visible light. This does limit any mid-IR investigations to all reflecting telescopes. For single pixel MCT detectors described above, most instruments incorporated a single ZnSe lens to focus the incoming beam on the sensor.

4. IR Imaging Systems

As previously discussed, single pixel detectors have long been a mainstay in IR detection. In the mid 80's video imaging systems were developed that utilized single pixel technology to record 30 frame per second mid-IR video. One of these companies was Inframetrics, which was later bought out by FLIR. Inframetrics produced a series of video systems with a liquid nitrogen MCT detector, one of which is shown in figure 4. The camera employed two high speed flat mirrors, one rotated in the X direction and the other in the Y. The result was a non-lens raster scanned image that could be zoomed in and out by adjusting the degree of scan angle for the mirrors. A typical image is shown in figure 5.



Figure 4. Inframetrics produced this mid-IR imaging system in the 80's. The MCT sensor has a range out to 14 microns and can display video in false color as well as black and white.



Figure 5. Screen shot of image obtained from Inframetrics camera

These systems are now available on eBay for affordable prices. The unit pictured was purchased in working condition for 600 dollars. MCT detectors with low noise amplifiers show up from scavenged equipment and typically sell in the hundred dollar range. With the availability of reasonably priced detectors, the possibility exists that such a detector could be mounted on a small telescope.

5. IR Imaging Test Setup

The current Inframetrics system was tested successfully in stock form on the moon but would not detect Jupiter with the scanning mirror optics alone. The overall sensitivity of the system was largely unknown and would be the single decisive factor in the possibility of building an amateur IR telescope. It was decided to test the system on the largest all reflective telescope in the area.

In October of 2005 the Inframetrics camera was setup at Yerkes in the 0.6-meter (24") Cassegrain dome. Mars was centered in the field and the eyepiece mount was removed from the telescope so prime focus extended a reasonable distance out the back of the telescope. The Inframetrics camera was positioned on its own tripod behind the telescope and adjusted so the focal length of the telescope matched the focal length of the camera's scanning mirror system. The setup is shown in figure 6. While crude, this setup was meant only to determine if the camera was capable of detecting the planet.

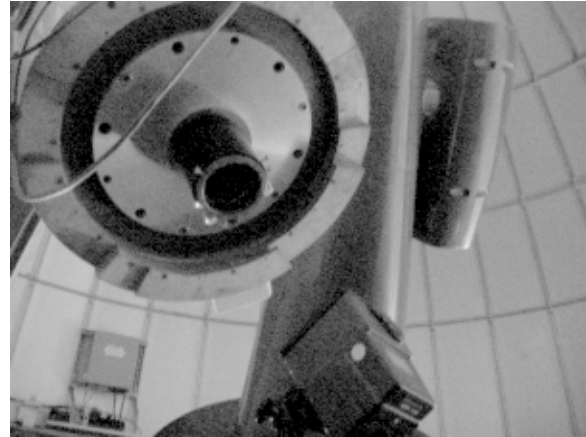


Figure 6. IR camera at prime focus of Yerkes .6 meter (24") telescope.

6. Mars IR Image

What is believed to be the first non-professional, mid-IR, telescopic image of Mars can be seen in figure 7. Since the IR camera had only video output, this was a screen shot of the false colored image. Certainly this image is crude by all standards of astrophotography but the signal to noise is very good at an effective exposure time of 1/30th of a second. This proves conclusively that MCT detectors cooled with liquid nitrogen are capable of detecting planets.

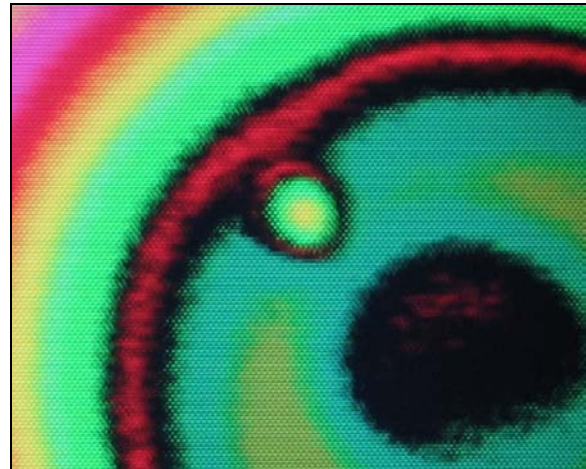


Figure 7. Mars (small circle in center) imaged through the Yerkes cassegrain telescope. Image is a false color screen shot of the monitor.

The size of the Yerkes telescope provided the maximum aperture that would likely be accessible by amateurs. The question remained, what was the minimum aperture required? Inframetrics also produced telescopes with 15cm (6") mirrors as optional attachments to their cameras. One of these optical tubes can be seen in figure 8 directly attached to the IR camera. In essence, this is a typical 15cm (6")

Cassegrain telescope comparable to those available to hundreds of astronomers.



Figure 8. IR camera and telescope attachment.

Figure 9 shows a faint but discernable Mars imaged through 15cm optics. Again it must be remembered that this is at video frame rates and long exposures would be significantly better. This image demonstrates that the full range of typically available telescopes could have IR capability.



Figure 9. Mars image through 15cm (6'') optics at 1/30th of a second exposure time.

7. Design Proposal for Mid-IR Imaging

As demonstrated here, average size telescopes coupled to nitrogen cooled MCT detectors are capable of detecting at least planets and perhaps more with longer exposures. The sensors are inexpensive when purchased used but have the limitation of only

one pixel. The Inframetrics mirror scanning system is a proof of concept but only allows for 30 fps rates. What is needed is a fully software controlled scanning mirror between the telescope and MCT detector.

The AO-7 from SBIG (fig. 10) provides the missing link in this design concept. Originally developed as a guiding improvement device, its uses have been extended for fiber optic spectroscopy [Kaye 2005]. Historically the AO-7 was controlled automatically by routines embedded in the software. The most recent release of Maxim-DL has provided full scripting control of the mirror tilt in both X and Y directions. Used in conjunction with high performance mounts allowing unguided exposures, the AO-7 coupled to an MCT detector should be able to step scan across an image. The exposure times can be adjusted as needed in the software.

Noise subtraction can be accomplished by tilting the mirror to an off target position and recording the ambient background from a dark portion of the sky. This technique known as “nodding” is still in use today [A1]. This noise can be subtracted after every pixel or at the end of a line scan for faster integration. Since pixel information is downloaded one at a time, exposure times can be adjusted on the fly to accommodate large differences in signal to noise such as across the terminator of the Moon.



Figure 10. The AO-7 from SBIG provides fully scriptable control of the tip / tilt mirror. This can be used to step scan an image with a single pixel detector.

8. Conclusions

This proof of concept test demonstrates that mid-IR imaging is on the verge of feasibility for non-professional astronomers. Although the actual imaging device and software are awaiting development,

there are no technical roadblocks to construction. An even simpler system could be devised without an AO-7 using a high performance mount. The target could be drift scanned across an IR target with the detector signal integrated for appropriate pixel widths. Once the target left the detector, the mount would reposition in front of the target and a fraction lower, for the next drift scan.

The ultimate resolution of such a system is yet to be determined but even with the lowest resolution, thermal maps in false color could be combined with visible images to add detail. Planetary targets are a given, however, depending on the systems ultimate sensitivity, many other targets are possibilities including nebula, molecular clouds, cool stars and comets.

Time-based studies are the most opportune areas of study for non-professionals and thermal evolution of targets offer areas ripe for investigation. Thermal changes in comets, planetary storms, moon impacts and other as yet unknown phenomena await to be studied in the IR.

9. Acknowledgements

The author would like to thank Vivan Hoette from Yerkes for access to the telescope, Martin Mika for pictures of the imaging setup and Eric Goldstein for technical assistance.

10. References

West, D. Single channel infrared photometry with a small telescope. <http://www.aavso.org/observing/programs/pep/singlechannel.shtml>

A1. ww2.keck.hawaii.edu/inst/tools/chp/chopping.html

Kaye, T. G. , Schwartz, M. "Implementation of a fully automated fiber spectrograph and first data", (2005) Proceedings of the 24th Society for Astronomical Sciences

Ground Imaging for Solar Sail Orbit Determination: A Proof of Concept

Mark S. Whorton
NASA Marshall Space Flight Center
Huntsville, Alabama 35812
Mark.whorton@nasa.gov

John E. Hoot
Software Systems Consulting
615 S. El Camino Real
San Clemente, California 92672
jhoot@sscorp.com

Mark S. Whorton
NASA Marshall Space Flight Center
Huntsville, Alabama 35812
Mark.whorton@nasa.gov

Abstract

Solar sail propulsion systems enable a wide range of space missions that are not feasible with current propulsion technology. Hardware concepts and analytical methods have matured through ground development to the point that a flight validation mission can now be realized. Astronomical observations may play an important role in the flight validation of solar sail propulsion systems. Astrometric data and visual magnitude estimation has great potential for contributing to orbit determination, thrust performance verification, and optical model validation. This paper presents an overview of ground imaging techniques and proof of concept tests that are applicable to solar sail orbit determination. The concepts described here will demonstrate the benefit of collaboration between astronomical imagers and mission analysts for a flight validation mission. © 2006 Society for Astronomical Sciences.

1. Introduction

With very few exceptions, all spacecraft missions have been designed and conducted according to the principles established by Johannes Kepler in the early seventeenth century. Kepler had the genius to assimilate Tycho Brahe's voluminous observational data into a radical new paradigm. No longer did the Greek notion prevail that the heavenly bodies moved in perfect circles. To make Tycho's data fit, Kepler reasoned that planetary orbits were ellipses with the sun at a focus, which became the first of his three laws of planetary motion. Later, Isaac Newton brought mathematical formalism to Kepler's description of planetary motion. Spacecraft missions today are still designed with Keplerian elements and Newton's laws of motion.

Scientists often devise mission objectives that are difficult to accomplish with current state-of-the-

art technology. Missions such as asteroid surveys, high inclination solar orbits, and comet rendezvous place enormous demands on a typical reaction-mass propulsion system. Other missions demand an entirely new class of non-Keplerian orbits. Exotic missions such as station-keeping at artificial Lagrange points and orbits displaced from the ecliptic require a continual thrusting for the duration of the mission. These important missions cannot be achieved with conventional expendable propellants. Solar sail propulsion systems have the potential to meet these mission demands.

2. Fundamentals of Solar Sailing

Solar sail propulsion utilizes the constant pressure exerted by the sun's radiation to push the sailcraft along its path. Solar photons transfer momentum to an object during a collision, much like billiard

balls colliding on a pool table. A photon's momentum is the product of its mass and velocity, and while the latter is quite large, the vanishingly small mass means the photon momentum is quite small. The combined effect of a large number of photons is required to generate an appreciable momentum transfer, which implies a large sail area. And since acceleration is inversely proportional to mass for a given thrust force, the mass of the sailcraft must be kept to a minimum.

Figure 1 illustrates how the thrust force is utilized for propulsion. Incident rays of sunlight reflect off the solar sail at an angle θ with respect to the sail normal direction. For the model assuming perfect reflectivity, there are two components of force. The first is in the direction of the incident sunlight and the second is in a direction normal to incidence that represents the perfectly reflected photons. When the two components vectors are summed the result is that the two components of force along the sail surface cancel each other and the components normal to the surface add together to produce the thrust force in the direction perpendicular to the sail surface. For a 40 meter x 40 meter square sail at 1 AU from the sun, the solar radiation thrust force is 0.0296 Newtons.

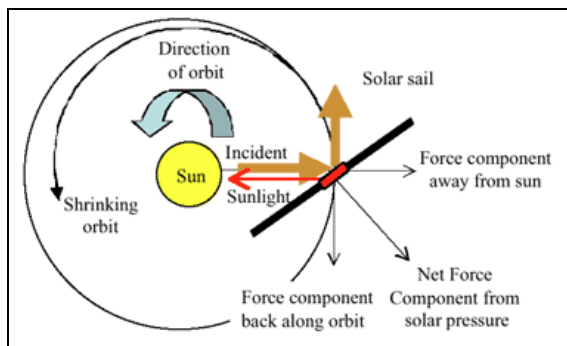


Figure 1. Solar Radiation Thrust Force (NASA/JPL).

Solar radiation pressure can be used to either increase or decrease the orbit energy. If the sail is oriented such that the thrust force is opposite the direction of motion, as in Figure 1 for a heliocentric orbit, the orbit spirals inward. Conversely, if the thrust is in the direction of motion, the sailcraft orbit spirals outward. Orbit inclination changes result when a component of the thrust force is oriented perpendicular to the orbit plane.

Various configurations have been proposed for solar sail vehicles. One of the earliest concepts was a Halley's Comet rendezvous mission using a heliogyro (middle of Figure 2). Heliogyros have reflecting surfaces formed by long blades rotating about a central axis and pitch controlled like a helicopter to provide attitude control. Another approach that is currently in development is a square sail comprised of

four triangular sail quadrants. These systems are typically three-axis stabilized, as opposed to spinning, with attitude control torques provided either by articulating tip vanes or varying the center of pressure/center of mass offset. Spinning disk sails have also been proposed.

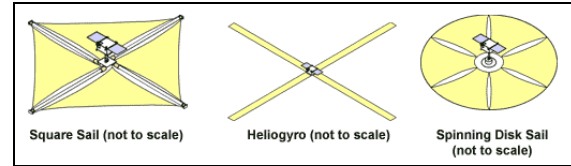


Figure 2. Solar Sail Design Concepts (NASA/JPL).

3. Solar Sail Flight Validation

For the past several years NASA has been investing in several aspects of solar sail propulsion technology. Teams have conducted research on analytical methods for modeling the shape and motion of the sail and support structures under solar radiation pressure loading. Others have developed prototype solar sail hardware systems including the sail membranes, structural supports, deployment mechanisms, and control actuation systems. This work has been converging toward a ground test of the prototype 20 meter square solar sail systems and the correlation of test data with analytical tools. Verifying the design processes and analytical tools on a scale system is a step in the process of validating the technology in a larger scale flight experiment. The first generation of science missions call for 80 meter square sails, so the intermediate goal for a flight validation mission in earth orbit is likely to be a 40 meter square sail.

A fundamental question is how one would go about verifying the performance of a solar sail as a propulsion system. The resultant thrust produced by a solar sail is a function of many variables that are difficult to measure on the ground or predict from analysis. The parameters can be loosely grouped into two categories: one associated with the thrust vector direction (i.e. pointing orientation of the sail) and the other associated with the thrust vector magnitude (i.e. reflectivity of the sail). Factors such as sail shape, both global and local, support structure deformations, disturbance torques such as atmospheric drag and gravity gradient, and the spacecraft attitude control system all influence the direction of the thrust vector. Likewise many factors such as membrane topology (wrinkles, billow, etc), specular and diffuse reflectivity, absorptivity, emissivity, and sail temperature affect the magnitude of the resultant thrust.

Two approaches can be used to estimate thrust performance – indirect methods and direct methods. Indirect methods utilize ground tracking station data and Global Positioning System (GPS) measurements

for orbit determination from which the thrust profile that results in the measured trajectory is estimated. Orbit determination is the process whereby the spacecraft position and velocity is obtained, and in some cases also estimates errors in the analytical model of the spacecraft and measurement systems. Another approach would be to utilize acceleration measurements to directly measure the thrust performance. Enabling both approaches requires a navigation system architecture comprised of direct inertial measurements aided by GPS and ground station tracking data.

Several issues complicate the orbit determination and thrust estimation problem. Environmental forces, torques, and instrument biases all contribute to errors in direct thrust measurement. GPS measurement accuracy is a function of the orbit (altitude primarily) and hence may be useful for only certain times. Ground tracking data is a function of the availability, cost, and location of the tracking station. Hence a range of measurement data types combined with a judicious choice of orbit and attitude profiles is necessary to potentially isolate and eliminate error sources, model the sailcraft properties that affect the thrust vector, and accurately estimate the thrust performance.

4. Pro-Am Collaboration

One additional data source that can potentially be of significant utility for thrust estimation is ground astronomical observations. Two types of ground observations are particularly beneficial: astrometric data and visual magnitude data.

Astrometric data is typically used to estimate the six constant Keplerian elements of satellite, comet, and asteroid orbits. In the case of solar sails, the Keplerian elements are functions of time. Hence the aggregation of astrometric data will be beneficial to reconstruct the trajectory and estimate the thrust vector time history. Likewise visual magnitude data will be useful to correlate spacecraft optical properties as a function of vehicle attitude. It bears repeating that these properties directly affect the sail's performance as a propulsion system and are quite difficult to accurately predict or test on the ground. This astronomical data has the potential to directly impact the quality of the thrust estimation and model validation and hence may significantly contribute to the success of a solar sail flight validation mission.

The orbit chosen for flight validation is a compromise between affordable launch access and acceptable environmental constraints. One orbit under consideration is a 1500km circular near-polar orbit. This orbit is high enough to effectively eliminate atmospheric drag, minimize gravity gradient distur-

bance torques, and guarantee no eclipses. Another alternative is a highly elliptical orbit with longer dwell times at apogee during which the effect of solar thrust can be maximized.

Astronomical imaging for mission analysis in either the circular or elliptical orbits will be a challenging endeavor. For the circular orbit, the angular velocity in the orbit plane is 2.98 degrees/sec and the angular size of the sail is 55 arcseconds. Figures 3 and 4 show the angular rate and size of the sail, respectively, as a function of apogee height in representative elliptical orbits. This is a much smaller angular rate than the circular orbit, but nonetheless this rate may pose a challenge for accurate tracking.

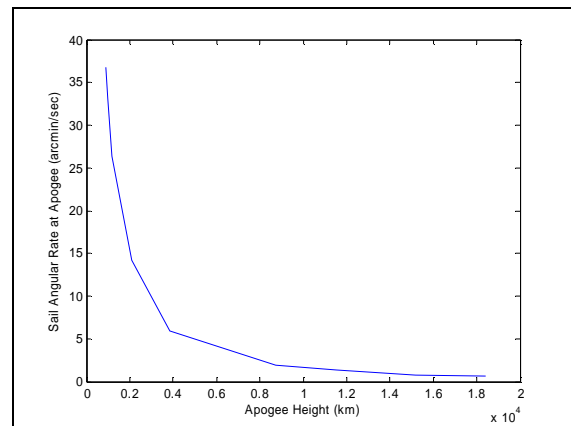


Figure 3. Sail Angular Velocity at Apogee Passage

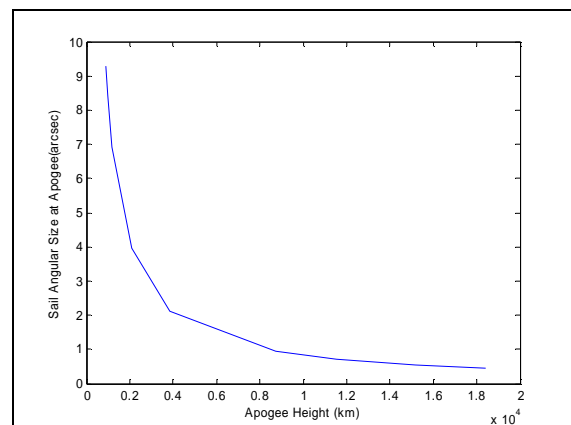


Figure 4. Angular Size of Sail at Apogee Passage

More than the tracking rate, the greater challenge will be contrast ratio between the bright solar sail and background stars. Several factors influence the visual magnitude: the angle of the sail with respect to the sun (“cone angle”), the angle of the sail with respect to the observer’s line of sight (“look angle”), the altitude of the sail, atmospheric seeing, and the sail’s optical properties, among others. For a 1500km circular orbit, Figure 5 shows the visual magnitude of a

sail with 60% reflectivity for various look angles and cone angles. Figure 6 shows the visual magnitude as a function of altitude for the elliptic orbits with the sail oriented perpendicular to the incident sunlight. Obviously this corresponds to the sail at opposition and all look angles are not feasible, but this represents a limiting case.

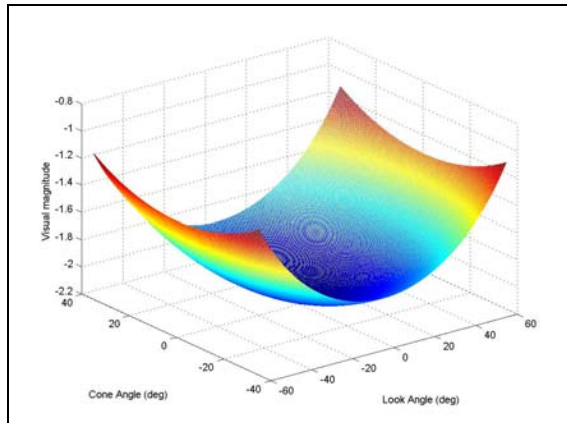


Figure 5. Visual Magnitude at 1500 km

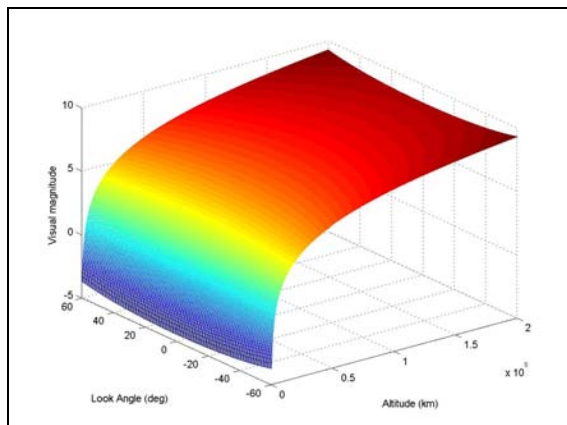


Figure 6. Visual Magnitude as a function of altitude and clock angle

5. Solar Sail Orbit Determination Methods

Several methods offer promise for the determination of the orbital elements for a spacecraft powered by solar sails. Each method is summarized in terms of the equipment and level of participation that might be required, organizational structures necessary and methods for mobilizing the required cadre of observers. We propose that these methods can be used to demonstrate the concept using various candidate objects such as the International Space Station.

5.1. Method 1: Still Photography, - Multiple Observers

This method employs multiple geographically separated observers with still cameras capable of 5 second to 60 second exposures.

5.1.1 Requirements

1. Precise knowledge of observer latitude and longitude. This can easily be determined with a GPS receiver or from many web sites where the street address is provided.
2. Precise knowledge of the time of the satellite passage at their location. This information is easily obtained from web sites such as www.heavens-above.com, or can be calculated with several freeware orbital calculators such as STS-Orbit available through NASA.
3. A tripod mounted still camera with a cable release.
4. A method for accurately determining time to ± 0.5 seconds. The accurate determination of time can be achieved in several ways:
 1. The participant can use a cell phone or cordless phone, if at home, and call the local time service or the NIST Boulder time service number and listen to the time signals.
 2. Tune a shortwave radio to WWV or WWVH.
 3. Synchronize a portable PC with the NIST atomic clock via a network connection using NISTTIME software supplied free by NIST and subsequently run the PC Clock or utilize readily-available software to generate an audio time code using the computer's sound card.
 4. Synchronize a portable PC with a GPS/NEMA signal via free geodesy software available from the web site www.sscorp.com (follow the Observatory link to Geodesy).

5.1.2 Observational Procedure

Each observer is instructed to take one daylight exposure to mark the start of roll and framing interval, and a second of a cue card containing the observer's name and the roll index number. The observers then take 30 15 second exposures of the satellite

on the start of each minute and half minute during their passes..

The film isse photographs are then subsequently processed to negatives. The negative and the observing journal page for that roll are submitted to the data reduction team. Users of digital still cameras can simply save their images in any uncompressed format, TIFF being the recommended standard, and can be transmitted on digital archival media to the data reduction team.

5.1.3 Data Reduction and Analysis

, each print is marked on the back with the exact (GPS lat/lon or street address) where the image was taken and the

exact time the image was made. These images are then emailed to the data reduction team. These images, taken with a normal 50mm lens will cover a field of view of approximately 45 degrees. The satellite should have transited about 20 10 degrees of the field. The exact start and end points of the arc can be determined from the image. Typical 35mm film, scanned at 1200dpi 2400dpi will resolve positions to about 1-2 arcminute accuracy. The background star field and local sidereal time and geodesy together will allow the satellite's azimuth and altitude to be solved. For more precise calculations atmospheric refraction can be used in the solutions. Off the shelf astrometric software such as "ASTROMET" can perform these reduction or IRAF scripts can be generated relatively easily. With this technique a moderate elevation pass (say 30 degrees for both observers) should allow observers on a 50km baseline to locate the satellite to within a 15km radio radius circle of error. The time standard is the critical value. If timing can be held to within ± 100 msec, the error circles diameter drops to 3km.

Method 2: Videography – Multiple Observers

This method employs multiple geographically separated observers with home video cameras.

Requirements:

- 1) Precise knowledge of latitude and longitude.(See above)
- 2) A modern video camera, preferable with a low light mode. The camera must be capable of recording stars down to magnitude 3.0
- 3) A method of accurately determining time. In addition to the above, many cameras have the ability to insert a time code in the image; however the clock chip in the camera must be precisely set with a standard time service.

Process:

These stock cameras are used to record satellite passes. The user is encouraged to use a wide field enough field of view so that several places in the video, several stars and the satellite may simultaneously be visible in the field of view. Since these cameras image at 30fps, but have a courser resolution, the camera will likely be the limiting factor on precision. Assuming 640pixels in a 45 degree field of view each pixel is about 0.07 degrees. This method also will located the satellite to an error circle of 6 km diameter for observers of a 30 degree elevation pass on a 50 km baseline assuming an 850km circular orbit and the time code inserted on the audio track accurate to 1/30 sec. Realistically, few observers will have the ability to reduce their own data. The tapes will need to be digitized and precisely time coded. The data reduction team will need to digitize the videos tapes and perform plate solutions on the fields containing at least two additional stars. The challenge is that background stars may be hard to locate with 1/30 second exposures of video cameras. It should be easy to test this technique by taking some night time videos of space station passes. With several observers triangulating the positions to generate the path should be possible.

5.2. Method 23: Still Photography, – Multiple Exposurees

ures

This method requires only a single observer, but more sophisticated math. The idea is that the observer makes photos as in the multi-observer method. The data reduction team computes the precise Az, El and Time of the start and end point of each track on several images from the same pass. To the first order, these passes are Keplarian orbits precessed by the Earth's gravitation field. Using an iterative method one can compute a least squares fit of the [Az, El, Time] observations to adjust to the initial NASA two-line elements to best match the observed pass. The most interesting method for adjusting the two-line elements is to treat the drag term as a vector rather than a scalarscalar. By allowing it to have a direction relative to the direction of motion, rather than treating it as a scalar against the direction of the motion, one effectively models the sum of drag and acceleration resulting from the sail. By adjusting only this quantity and fitting the observations, one directly solves for the acceleration of the sail.

It is then a simple process to look atuse the time elapsed time since the ephemeris time, and with knowledge of the spacecraft mass, determine the mean force vector generated by the sail. Any earth

orbit prediction program is capable can be modified to make this calculation.

Distribution of this program to participants allows to have observers to perform their own analysis, provided they would need to have the means to:

1. Get their images in digital format.
2. Perform the astrometric reductions on their image.
3. Convert [RA,DEC,Time] from their images to [AZ,EL,Time]
4. Obtain an initial orbital element set.

5.3. Method 3: CCD Multi-Observer

This method is similar in philosophy to the Photographic Multi-Observer Method, but instead of film this method utilizes an integrating CCD imager. Obtain the orbital solver program that will find best fit of their images to spacecraft acceleration.

Method 4: Videography – Single Observer

This is essentially similar to the Still Photography – Multi-Image method, but uses the video to generate the Az,El,Time sequence for analysis. Using an orbital prediction program, the project team predicts the approximate time and locations when the satellite will occult either the Sun or Moon. Observers are then requested to deploy across the path of occultation. During solar occultation pinhole or projection images of the sun are observed. It should be noted that many amateurs own safe full aperture solar filters that can allow direct viewing and imaging of the even. Lunar occultations are safe to watch directly.

Requirements:

- 1) Knowledge of observer location. (See above)
- 2) A precise timing source.
- 3) Observe the precise time of 1st contact and last contact.

The data reduction team can then take these observations along the path of eclipse and determine the exact trajectory of the spacecraft. This method will also produce some great photos and video.

with short focal length lenses mounted upon tracking telescopes.

5.3.1 Requirements

1. Precise knowledge of the observer's latitude and longitude.
2. Precise knowledge of the time of the satellite passage at their location.

3. A CCD Camera with imaging software equipped to image a FOV from 4 to 20 degrees mounted piggyback on a tracking telescope.
4. 4) A method for accurately determining the exposure time to ± 0.1 seconds.

5.3.2 Observational Procedure

Each observer slews his telescope to the center of the predicted satellite pass. Prior to the pass, the observer will make a long duration exposure of the field of view, assuring that at least 10 stars of sufficient S/N ratio are imaged to insure good astrometry of the images. During the pass, the observer will take a series of images of approximately 1-second duration during the pass until the satellite has transited the field.

Observers should submit these images in FITS format with their observing journals on archival media to the data reduction team. Among the challenges of this method is the recording of the image time with very high accuracy. Provided that the PC clock is synchronized with the NIST timeserver, it should be possible to get ± 0.1 second accuracy for exposure times.

5.3.3 Data Reduction

As with the Photo-Multi-Observer method, astrometry is performed on images and the potential accuracy of these measurements is again time limited, but can be within ± 3 km.

5.4. Method 4: CCD Multi-Pass

This method uses the same procedures as the CCD Multi-Observer method but measures the satellite position on successive passes. The same software and methodology as described for the Photo Multi-Exposure method can be used to solve for orbital acceleration.

6. Experimental Procedure Validation

We have begun tests to validate the experimental methods proposed above. To validate our method, we have been applying the proposed photographic and CCD imaging methods to bright satellites. Our imaging targets have been satellites making passes with apparent magnitudes of 2.5 brighter. Targets have included ISS, HST, TRMM and serendipitous targets occurring during other CCD imaging projects.



Figure 7: 15-second ISS Exposure at high air mass.

We have verified that satellites are easily photographed from suburban environments with the proposed setup. Even in the presence of significant light pollution, both the track and enough background stars are detectable to assure accurate astrometry.

Analysis of the image in Figure 7, scanned at 2400 dpi, yield a plate scale of 44.2"/pixel. FWHM of stars in the image averaged 7.8 pixels. This indicates a psf of 5.75'.

Performing precise astrometry on wide field images proved a challenge. It could not be performed with Astrometrica. The latest generation of the program is optimized for deep field minor planet work. As such, it uses USNO A.1, USNO A.2 and USNO B catalogs that do not include bright stars. Reversion to the older DOS based program succeeded in working with GSC 1.1 and ACT-GSC catalogs, but did not provide reasonable fits.

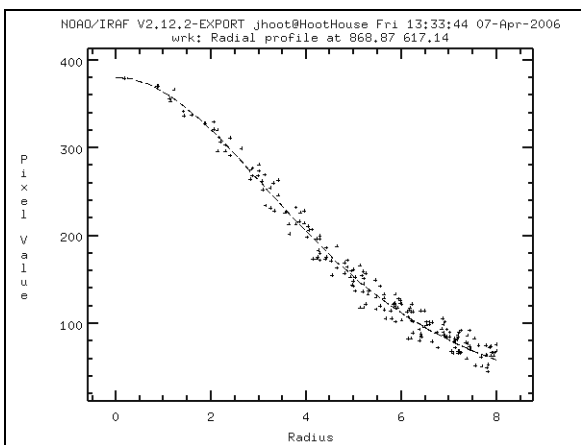


Figure 8: PSF Radial Profile

There are several factors that make photographic plate solutions challenging. First, the fields themselves are very large and the pixel scale, at 44", is atypical for most astronomy. The second challenge is that wide field photographic lenses suffer from not only field curvature, but also from barrel distortions

and astigmatisms as a result of their design for wide fields of view. Finally, additionally, the film scanning process can introduce additional distortions, notably skew. Finally, images taken in ALT-AZ with tripods always contain significant field rotations. These higher order corrections require more complex fitting than typical second-order plate scale solutions.

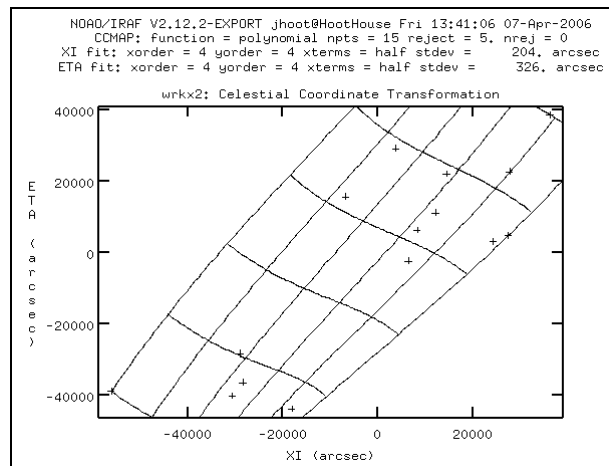


Figure 9: IRAF Plate Scale Solutions

After looking into several alternatives, acceptable results were obtained using IRAF, now available running in native mode under Windows using the Cygwin library. Using 4th order plate solution polynomials, fits were obtained with residuals compatible with PSF of the plates. The 1-sigma RA error was 3.4' and the Declination 1-sigma error was 5.4'. Both are smaller than the PSF of the image. A script to automate the IRAF fitting routine is under development.

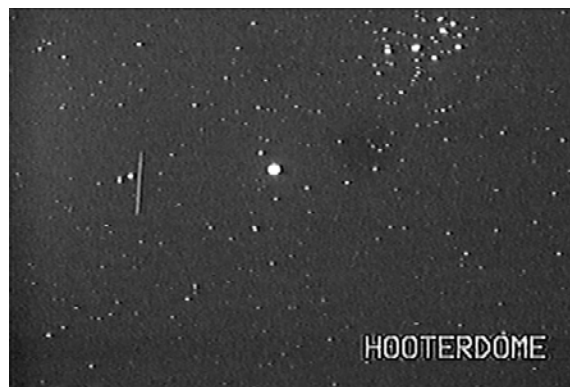


Figure 10: Wide Field 2 Second CCD Exposure

Similarly, wide field CCD images have proved the feasibility of their use. The image in Figure 10 was a 2-second exposure from a time lapse series that was produced during Mar's recent occultation of SAO76327. This 2-second exposure, and those

bounding it, shows the passage of a high inclination angle satellite through the frame. Analysis of the image shows a plate scale of $42.414''/\text{pixel}$ and a FWHM of 3.6, yielding a PSF of $2.55''$. This would indicate that short exposure, wide field CCD images should be able to provide about twice the positional accuracy of photography with comparable time resolution. With computer triggering of exposures and precision timing, even better results should be obtainable. Furthermore, flatter fields should also lead to better astrometry from all digital images.

These results have convinced us that the photographic methods are viable within the error ranges projected. These methods will reach the broadest audience of potential participants.

We are now in the process of taking further imagery and modifying SSC orbital prediction software to solve for satellite acceleration and orbits

6.7. Where We Go From Here

NASA, academia, and industry are working together to advance the technology of solar sail propulsion systems with the goal of validating the technology in flight. An important part of that flight validation will be the gathering of data to support the analysis for thrust estimation and model validation. A collaboration between the astronomical imaging community and the mission analysis team will be a synergistic effort that may advance the state of the art for both communities.

This proof of concept demonstration will add significant merit to the flight validation mission concept proposal. If selected, this concept will be implemented as part of a solar sail flight validation mission. In either event, the astronomical imaging community will have contributed substantially to the technology by demonstrating the feasibility of ground observations for solar sail low-earth orbit determination

7.8. References

Burke, Ch., *Cygwin IRAF Port*, <http://www-astronomy.mps.ohio-state.edu/~cjburke/> 2006

McInnes, C. R., *Solar Sailing: Technology, Dynamics, and Mission Applications*, Springer-Praxis, 1999.

Random Factory, *Open Source Astronomy for Win32/Cygwin*, <http://www.openastro.com> 2006

Statler, T, *Draft IRAF Astrometry Cookbook*, Private Communication, 2002.

Superhumps in Cataclysmic Variables

*Joe Patterson
Center for Backyard Astrophysics
Columbia University
Physics Laboratories, 1316 Pupin
New York, NY
jop@astro.columbia.edu*

Abstract

The individual telescopes of the CBA produce fast (<1 min) photometry of variable stars. With runs of >5 hours and spliced data from many longitudes, we aim to assemble long light curves with nearly continuous coverage. This is an ideal data base for period and other timing studies. I have found it to be many times more effective than one large telescope proudly performing its hijinks on one mountaintop. I'll give a brief account of how this enterprise has evolved from one CCD in a tuna fish can to the world's leading supplier of periodic signals in cataclysmic variables. The most interesting and productive research program has been the discovery and study of "superhumps", mysterious large-amplitude waves at a period slightly offset from the true orbital period of the binary. These result from the "precession" of the accretion disk. The disks appear to wobble and precess in a manner similar to the Moon's orbit, and we can use this as a tool for weighing the unseen secondary stars. I'll describe the superhumps, and their fascinating astrophysical uses. © 2006 Society for Astronomical Sciences.

Arecibo and Goldstone Radar Imaging of Near-Earth and Main-Belt Asteroids in 2005

*Lance A. M. Benner
Mail Stop 300-233
Jet Propulsion Laboratory
4800 Oak Grove Drive
Pasadena, CA 91109-8099
lance@reason.jpl.nasa.gov
<http://echo.jpl.nasa.gov/>*

Abstract

This talk will summarize radar imaging of near-Earth asteroids (NEAs) at Arecibo and Goldstone during 2005-2006. During 2005, 32 near-Earth and 21 main-belt asteroids (MBAs) were detected by radar, a rate of nearly one detection per week. Of these, 26 NEAs and 15 MBA were detected by radar for the first time. As of February 2006, 187 NEAs and 107 MBAs have been detected by radar, increases of factors of 3.7 and 2.7, respectively, since completion of the upgrade at Arecibo in January 1999. Highlights during 2005 include discoveries that 1994 XD and 1862 Apollo are binary systems, detections of 15 targets-of-opportunity, detailed images of 1992 UY4, a 2-km-sized object with a "lumpy" surface, and the first Mars-crossing binary asteroid detected by radar. Other highlights include the extraordinarily narrow Doppler-broadening of 2005 OE3, which may indicate extremely slow rotation, radar imaging of several main-belt asteroids, and new radar astrometry from 99942 Apophis in August 2005, which significantly reduced its orbital uncertainties and eliminated a low-probability impact in 2035. New radar observations of Apophis are scheduled in early May 2006 at Arecibo and preliminary results will be discussed at the meeting. © 2006 Society for Astronomical Sciences.

Radar Images and Shape Models of Asteroids 10115 (1992 SK), 23187 (2000 PN9), and 29075 (1950 DA)

M.W. Busch

*Division of Geology and Planetary Science, CalTech
and
Asteroid Radar Group, Jet Propulsion Laboratory
busch@caltech.edu*

S.J. Ostro, L.A.M Benner, J.D. Giorgini

Abstract

This talk will describe delay-Doppler radar imaging, spin vector estimation, and shape reconstruction of Near-Earth asteroids 1992 SK, 2000 PN9, and 1950 DA. For each object the radar data yield two pole directions and shape models that give comparable fits to the data. Inclusion of lightcurves greatly reduced the uncertainty in the spin states and was essential to break a degeneracy in the pole direction of 1992 SK. 1992 SK was observed at Goldstone in March of 1999. Inversion of the images and lightcurves reveals an elongated object with dimensions of 1.3 x 0.9 x 0.9km and prominent surface topography. 2000 PN9 and 1950 DA were observed at Arecibo and Goldstone in March of 2001. The two 2000 PN9 models are roughly spherical and approximately 2km in diameter. For 1950 DA, the pole direction degeneracy persists after inclusion of lightcurves and the two pole directions yield very different shape models. One model has distinctly angular surface features, low elongation, and a diameter of about 1.15km. The other model is oblate and roughly 1.4km in equatorial diameter. 2000 PN9 and 1992 SK will approach within 0.020 and 0.110 AU in March 2006, when they will be strong radar imaging targets. New observations are scheduled and will be used to improve the pole directions and shape models. Preliminary results will be reported at the meeting. © 2006 Society for Astronomical Sciences.

The Discovery and Initial Characterization of a New Eclipsing Binary with Peculiar Properties

Dale E. Mais

*Earth Sciences Department, Palomar College, San Marcos, CA
dmais@ligand.com*

Richard O. Gray

*Appalachian State University
Boone NC, 28608
grayro@appstate.edu*

David Richards

*Aberdeen and District Astronomical Society, UK
david@richweb.f9.co.uk*

Abstract

During the course of a general spectroscopic survey at the Dark Sky Observatory (Appalachian State University), a new eclipsing binary star, HD5501, was found. Photometric observations in the BVRI bands for nearly a year give a period of 7.53 days with a primary eclipse of 0.45 magnitude and a secondary of 0.3 magnitude. The system is constantly varying, suggesting an ellipsoidal variable with the stars in or near contact, perhaps with one or both Roche lobes filled. Spectroscopic examination (1.8Å/pixel) of the system at different phases show the Balmer lines (beta, gamma and delta) along with the important shell lines of FeII between 4900 and 5200 Angstroms are stronger in eclipse than at quadrature. This suggests differing orientation of gas around the system. Higher resolution spectra (0.9Å/pixel) shows slightly broader metallic lines in quadrature than in eclipse. This suggests the system is an SB2. A spectrum at H-alpha shows a classic wind signature, again suggesting the presence of mass transfer in the system. © 2006 Society for Astronomical Sciences.

1. Introduction

HD 5501 (= BD+59 154 = BSD 8-397) is a 9th magnitude star in the constellation of Cassiopeia in the field of the Cas OB1 association, which has attracted almost no attention in the astronomical literature. It has been observed once in the UBV system (Bigay & Lunel, 1965) and once in the Stromgren uvbyBeta system (Perry & Johnston, L. 1982). It was observed by Fehrenbach (1961) and by Barbier (1968) using objective prisms to measure its radial velocity (-46 ± 20 km/s). We do not have a parallax for the star. Spectral types given by Hardorp et al (1959) and Fehrenbach et al (1961), both based on objective prism plates, indicate an early, luminous, A-type star, not an unusual find in a rich Milky Way field. However, after these efforts, the literature is silent on the star.

On November 7/8 2004, one of us (ROG) obtained a slit spectrum of HD 5501 as part of a campaign to discover new A-type shell stars in Kapteyn

selected region #8. When the spectrum was reduced a few days later, it was noted that this star showed the spectra characteristics of an A-type shell star, in particular, enhanced absorption in the Fe II multiplet 42 lines at 4924, 5018 and 5169Å. Hence, another follow-up spectrum was obtained later that month (Nov 28/29 2004), and it was noticed that the strength of the shell lines had changed! We then checked the photometry in the TASS (The Amateur Sky Survey) database, and found that this star displayed photometric variability with an amplitude of nearly 0.5 magnitude. Analysis of the TASS data indicated a rough period of about 7.5 days, with a lightcurve that appeared to be that of an ellipsoidal eclipsing binary. We began obtaining photometry at the Dark Sky Observatory, but since ongoing programs did not permit a concentrated photometric study of this star with the phase coverage required to obtain a definitive light curve, ROG asked Dale Mais for help.

2. Methodology

Photometry was conducted with an Astrophysics 5.1-inch f/6 refractor using an ST-10XME camera, 2x2 binned pixels, and the Johnson BVR and I filters. Images were obtained in duplicate for each band and two reference stars used per variable star for analysis. Image reduction was carried out with CCDSOFT image reduction groups and specially written scripts for magnitude determinations, which allowed for rapid, nearly real time magnitudes to be found. Spectroscopy was carried out with a slit spectrometer and the 0.8m DFM reflector at Appalachian State University. Light curve analysis was carried out using Peranso software (Vanmunster, 2005).

3. Results and Discussion

Figure 1 shows the unanalyzed results of magnitude determination spanning greater than a 100 day observing session in the V-Band. The determinations have been controlled using 2 standard stars in the field. The B, R and I band results are very similar (data not shown).

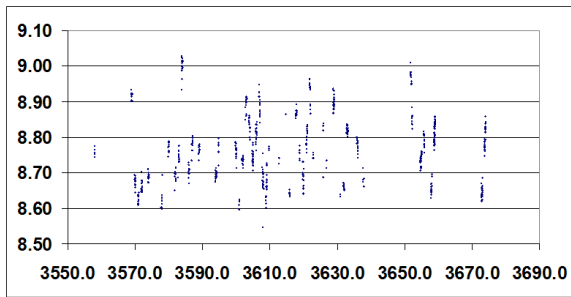


Figure 1. Corrected magnitudes in the V-band during a >100 day observing period. Multiple determinations were carried out during each evening of observing. Magnitude is indicated along the y-axis with Julian day number along the x-axis.

Clearly there is variation in this star that appears to span approximately 0.4-0.5 magnitude in the V-band. These results were imported into the software package Peranso for period determination and creation of a phase diagram. The period determination routine used within Peranso was the ANOVA method. Shown in Figure 2 is the phase diagram generated from analysis of the observations from Figure 1. The results favor a period of 7.53 days with a primary drop in magnitude of approximately 0.45 and a secondary drop of 0.3 magnitude. The result of the period determination is shown in Figure 3.

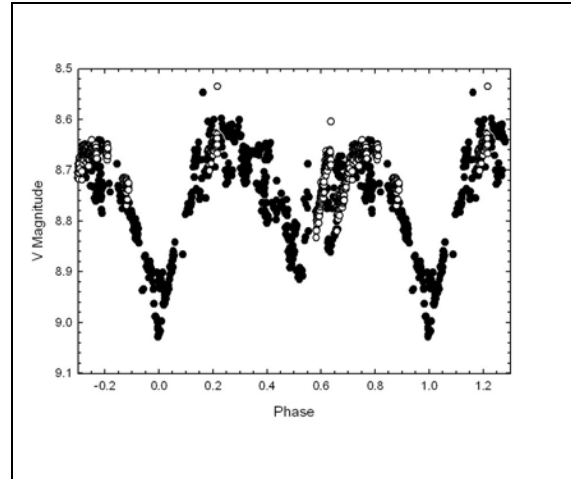


Figure 2.

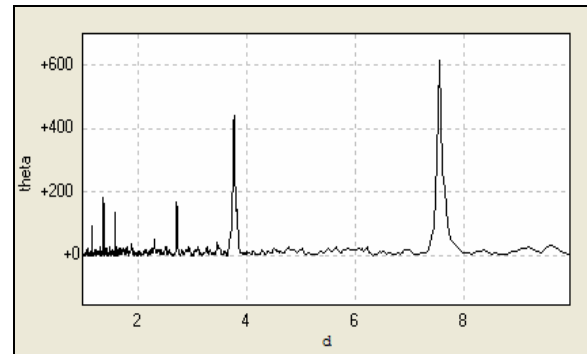


Figure 3.

While the period determination favors the 7.53 days as indicated by its greater theta value (a measure of the likelihood this is the correct period), a period corresponding to exactly half this value also has a reasonable theta value.

The fact that a “smoother” phase diagram is not produced would appear to indicate that HD5501 is a more complex system than a simple eclipsing binary. During the descent into the primary eclipse the curve appears better behaved but between primary and during secondary there seems to be a lot of flickering activity observed in the data.

At the same time that photometric observations were being carried out, the spectrum of the system was being determined. Figure 4 shows the spectrum obtained at different light curve phases in the blue part of the spectrum. The Balmer lines (beta, gamma and delta) along with the important shell lines of FeII between 4900 and 5200 Angstroms are stronger in eclipse than outside eclipse.

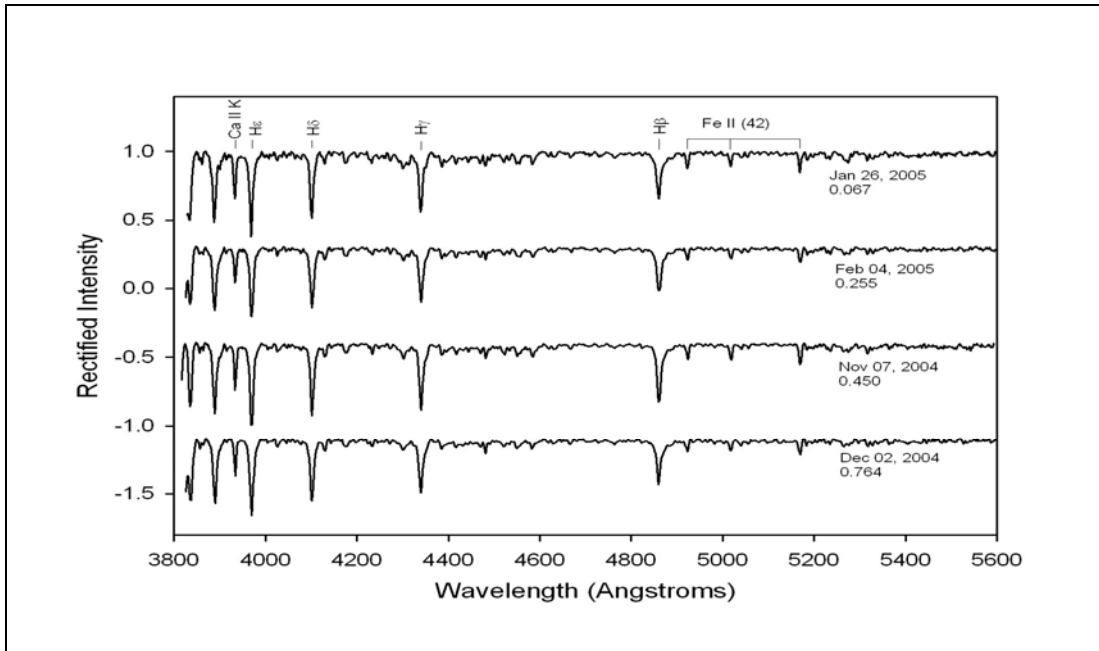


Figure 4 (above) shows the spectrum obtained at a resolution of 1.8 Angstroms per pixel in the blue region of the spectrum.

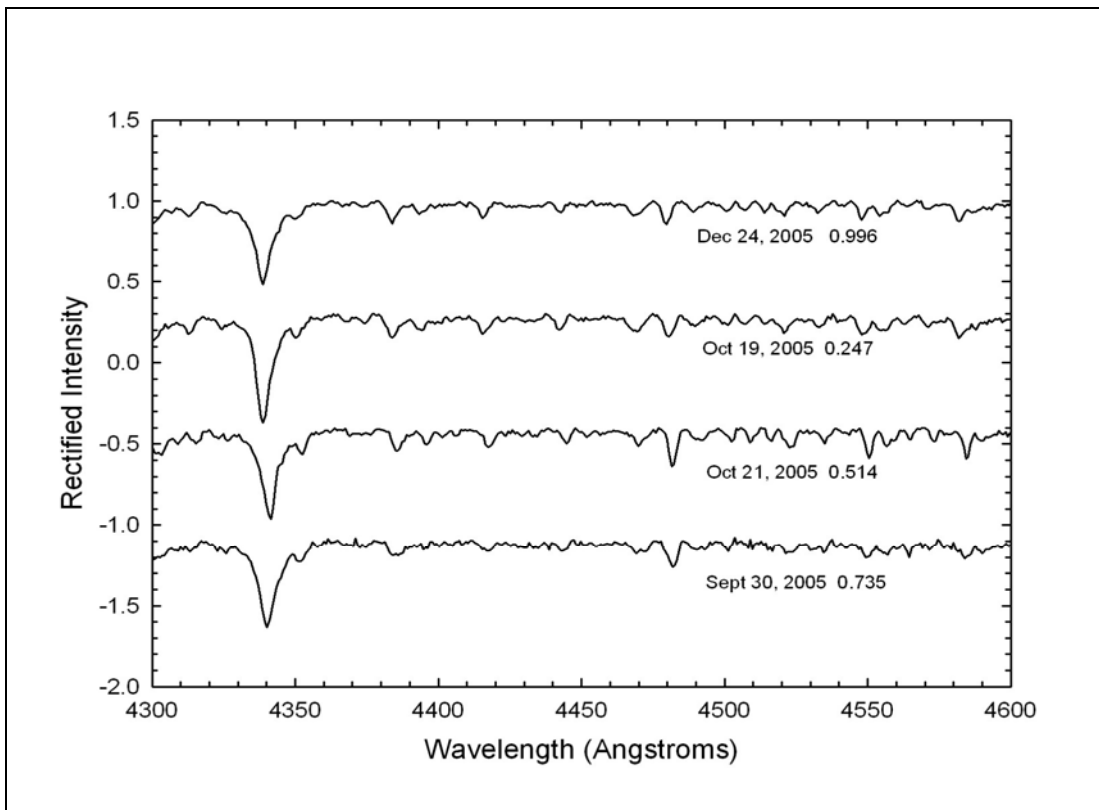


Figure 5 (above) shows the spectrum obtained at a resolution of 0.9 Angstroms per pixel. The strong line at approximately 4340 A is hydrogen-gamma

This can be seen by comparing the Fe and Hydrogen lines at phase 0.067 and 0.45 to the lines at phases 0.256 and 0.764. Indeed, the calcium K line exhibits the same behavior. In the higher resolution spectrum in Figure 5, various metal lines such as those at approximately 4480, 4550 and 4580 Å are broader at quadrature than during eclipse. In addition, spectra obtained in the hydrogen alpha region shows this line to have emission on top of the absorption line (data not shown).

Clearly this is a complex system. The spectrum of the system is indicative of an early A type star. This would suggest a temperature of the "system" to be ~9200 K. However, temperatures determined from the B-V photometry give temperatures which are relatively constant between 6800-7200K. (See Figure 6). Thus the system is significantly reddened. Cou-

pling the early A type spectrum to the rather dim apparent magnitude suggests that this star is at a great distance.

In addition, this star is within the galactic plane, so there is most likely significant reddening due to dust. Utilizing previous Stromgren photometry and temperature calibrations, we calculate, after de-reddening, a temperature for the system at 9220K (Gray, R., 1992).

Temperatures aside, clearly this star system is peculiar and warrants more work. Both the photometric and spectral we have thus far suggests that the system is constantly varying and may be an ellipsoidal variable with the stars in or near contact, perhaps with one or both Roche lobes filled.

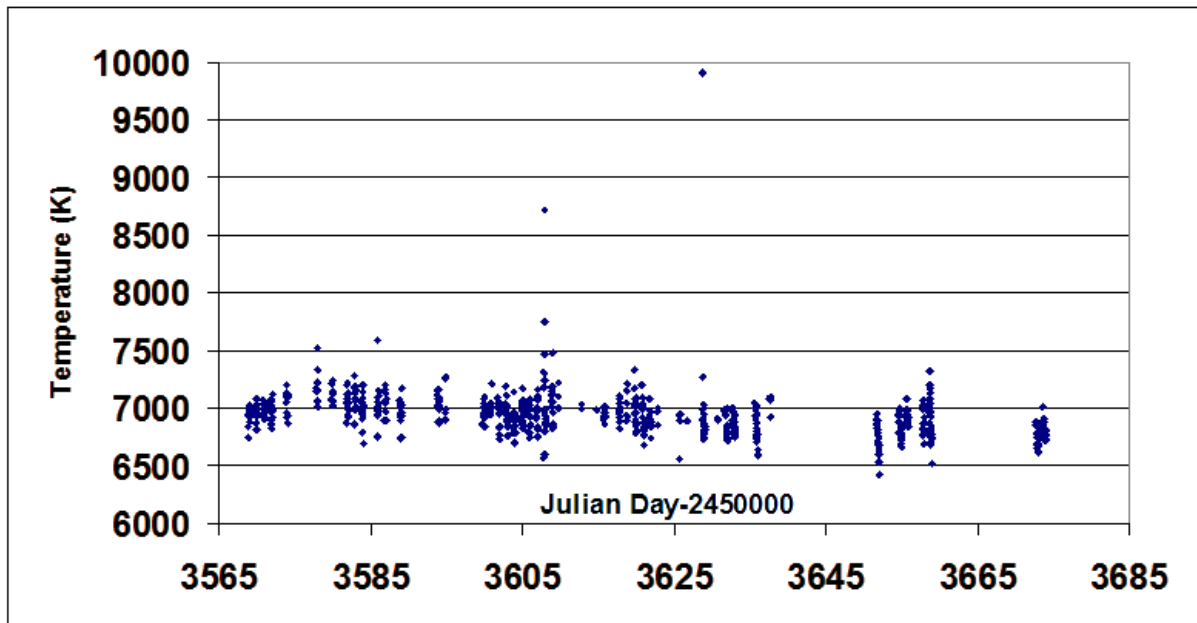


Figure 6. The B and V determined magnitudes were used to obtain B-V which was then converted to a first approximation temperature. Analysis of this data or the B-V vs. julian day data in Peranso produced no period. So the temperature of the system is independent of the light curve.

4. Conclusions

A new and unusual eclipsing binary system is described along with some of its initial photometric and spectroscopic characteristics. The system is clearly complex with a changing light curve noted. Further efforts will be directed towards refining the light curve and more detailed spectroscopic observations in an effort to better define this unusual system.

5. References

Barbier M. La mesure des vitesses radiales au prisme objectif XXI. Revision et resultats nouveaux dans la SA 8. Publ. Obs. Haute-Provence, 9, 38 (1968)

Bigay J.H., Lunel M.,J. Photometrie photoelectrique UBV de 263 etoiles B et A de la SA. 8. Obs., 48, 171, (1965)

Fehrenbach C. La mesure des vitesses radiales au prisme objectif. XII. 5eme liste de vitesses radiales

determinees au prisme objectif a vision directe. Publ. Obs. Haute-Provence, 5, 54 (1961)

Fehrenbach C., Petit M., Cruvellier G., Peyrin Y. J. La mesure des vitesses radiales au prisme objectif. XII. 5eme liste de vitesses radiales determinees au prisme objectif a vision directe. Obs., 44, 233, (1961)

Gray, R.O., The calibration of Stromgren photometry for A, F and early G supergiants. III - The A and early F supergiants. A&A 265, 704, (1992)

Hardorp J., Rohlfs K., Slettebak A., Stock J. Luminous stars in the Northern Milky Way. Part I. Hamburger Sternw., Warner & Swasey Obs., 1 (1959)

Perrt C.L., Johnston L. A photometric map of interstellar reddening within 300 parsecs. Astrophys. J., Suppl. Ser., 50, 451-515, (1982)

Vanmunster, T., 2005 <http://users.skynet.be/fa079980/peranso/index.htm>

An Amateur Astronomer’s Growth into Science

Cindy Foote
Vermillion Cliffs Observatory – Venus Building
4175 E. Red Cliffs Drive, Kanab, UT 84741
cindyf@scopecraft.com

Abstract

This paper will discuss the change of interest and progression of a visual observer to a participant in astronomical science. It will talk about the move from using a borrowed telescope to buying a telescope, building an observatory, automating the telescope, and buying a CCD camera. The importance of having a mentor to expedite the learning process will be stressed. After more than a year’s effort, the reward was a light curve showing the egress of HD209458b, which will be presented. © 2006 Society for Astronomical Sciences.

1. Introduction

As a visual observer for several years, my interest in astronomy took me to RTMC each spring to see and hear what was new, meet with old friends, and look through a variety of different telescopes. To this point, my contributions in astronomy had been sharing the night sky with the public outreach programs. At RTMC 2004, Tim Castellano (Castellano, 2004) gave a presentation that caught my attention. This discussion on detecting transiting exoplanets was something to get excited about. It was something I thought I could do and so make a contribution to science. Further reading (Castellano, 2004) (Laughlin et al. 2003) on the subject convinced me to move ahead.

The next course of action was to obtain a telescope, build an observatory, and automate the entire process.

With everything in place, the search for an exoplanet transit began. There were several nights of frustration, exasperation, and bad weather. However, the reward finally came in June 2005 when the telescope captured the egress of HD209458b.

2. Vermillion Cliffs Observatory – Venus Building

Desire to do research is one thing, but having the equipment to do the research is another. The current problem was that my husband, Jerry Foote, has one observatory (Vermillion Cliffs Observatory) on the property already. His observatory is focused on the measurement of Cataclysmic Variable stars in conjunction with the Center for Backyard Astrophysics.

You can readily see that sharing his telescope was not an option. There was no dedicated telescope of my own to work with for the extended periods of time that it would be needed to capture a transit.

At the RTMC 2004 meeting, circumstance led me to a person with a new Meade 14” LX200GPS that he was interested in selling. Over the next few days we negotiated a price and it was loaded into the RV headed for Utah.

2.1. Observatory

The next decision was where to build the new observatory. It was important that it didn’t interfere with the current observatory but allow each telescope to observe the full sky available from this location. A sandstone bluff blocks the horizon to the northwest, so the ideal location was to the northwest of the main observatory, in the shadow of this bluff and construction began (Figure 1).

The observatory is a roll off roof design. The building is nine feet square. Six piers support the building and the roll off outriggers that are north of the building. The powered roll off roof is mounted on four V-rollers that ride on inverted angle iron tracks. The telescope sits on a pier isolated from the building. The upper portion of the south wall hinges down to allow access to the southern horizon. Since local light pollution is minimal, windows were installed to allow light during the day, and to provide ventilation during the hot summer nights. Power to the observatory is via underground conduit with a separate data cable conduit that connects the observatory computer to the house computers.

The observatory construction began July 10, 2004 and was completed in August (Figure 2). First light was 8/27/04 at ironically 8:27 PM MDT.



Figure 1. Placing the first floor support beam.



Figure 2. Completed Vermillion Cliffs Observatory – Venus Building with Vermillion Cliffs Observatory in the background.

2. 2. Telescope

The telescope is a Meade 14” LX200GPS (Figure 3). Tests after polar alignment showed tracking to be very poor. After repeated PEC trainings, it was found that the telescope still wouldn’t track an object in RA throughout the night. Efforts to improve this included replacement of the nylon gears in both the RA and Dec drives with Petersen stainless steel gears and installation of Richard Seymour’s patch to the Autostar control system. With these changes, an object could be tracked for a few hours but still not an entire night. At this time, the only way to track a program star throughout the night is to guide the telescope. There are multiple forums on the Internet dealing with LX200GPS telescope problems that are invaluable. With this said, the telescope is a good working instrument with reasonable optics for the money spent.



Figure 3. Meade 14” LX200GPS with SBIG ST-7E Camera attached.

2. 3. CCD Camera and Other Equipment

The CCD Camera is a previously owned SBIG ST-7E. This camera was purchased from an astronomy friend who wanted to have a larger camera. The focal reducer was another used item purchased from a local astronomy amateur. Recently, a SBIG CFW-8 filter wheel has been installed, again a used item that contains LRGB filters.

2. 4. Software

In order for the telescope to operate scripted, the Meade Autostar needs to be controlled by a separate computer. The software used to control the telescope and the camera is MPO Connections. This software has extensive scripting capabilities allowing very complex observing programs.

Rather than build a warm room next to the observatories, it was decided to run the computers by remote operation from the house. The software used is Remote Administrator which provides full screen, mouse and keyboard access of the observatory computer.

For data reduction of the many images collected each night, AIP4WIN (Berry et al., 2005) is used. The reduction process results in a text file that is imported into Microsoft Excel for final analysis.

2. 5. Time Calculator

One of my most valuable tools is a time calculator developed by Edwin Sheridan, Crescent Butte Observatory in Kanab, Utah (Figure 4). This calculator relates Universal Time, Local Time, and Local Sidereal Time. It has an overlay that shows the available range of RA that can be viewed at any particular local time.

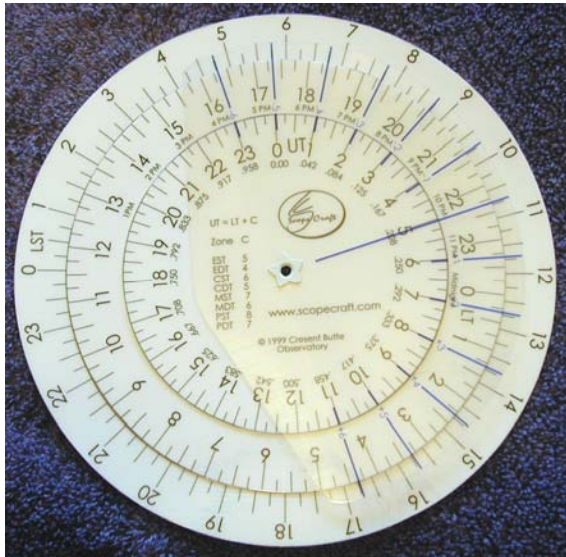


Figure 4. Time Calculator

3. HD 209458b

HD 209458 is a reasonably bright star located at RA 22:03:10.8 (J2000) Dec +18:53:04.0 (spectral class estimates F8V to G0V). It has a known Jupiter-mass planet that orbits every 3.52 days. The initial discovery was with spectroscopic radial velocity measurements. Later it was found by the STARE project that a photometric dip occurred at the expected time from the spectroscopic orbital parameters. This was confirmation of an exoplanet by photometric means (Transitsearch.org).

3. 1. Observations

A visit to the Transitsearch web site provided a list of possible times when HD 209458b would make a probable transit. The predicted central transit time was July 1, 2005, 05:29 UT, which was below the eastern horizon from this location. However, it was found that the egress would occur at 07:09 UT, making it possible to capture, but it would require making the initial measurements through a large air mass. The air mass range during the 500 observations was between 4.1 and 1.1.

Each observation was of five-second duration and was repeated with a 20-second delay between observations. With download time included, this resulted in a new observation every 32 seconds.

3. 2. Data Reduction

Previous to the night of observations, a master dark and a twilight master flat were created. The master dark is a median combination of 20 dark frames. The twilight master flat is the normalized median combination of 30 exposures with the telescope drive stopped.

AIP4WIN was used to reduce the data. Prior to the photometric measurement, each image was dark subtracted and flat fielded. The photometric process utilized an aperture of three times FWHM. A sky background measurement was made in an annulus around the star. Similar measurements were made of a comparison star and a check star in each image.

The differential photometric measurements from AIP4WIN were imported into a Microsoft Excel spreadsheet where the measurements could then be graphed.

3. 3. Results

There is considerable noise in the measurements due to the large air mass and scintillation from the short exposure times. However, it is clear that the egress was captured (Figure 5).

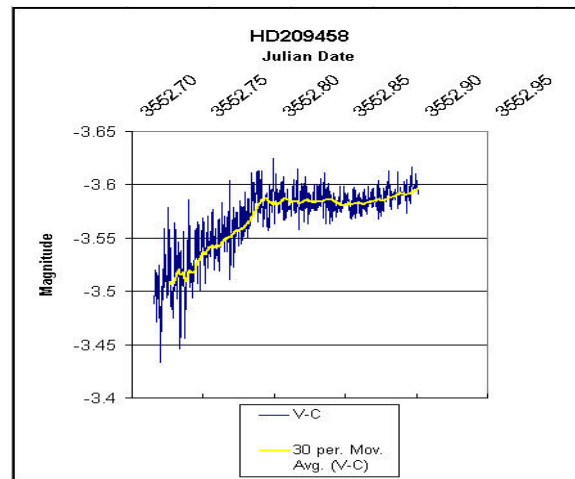


Figure 5. Light curve showing egress of HD209458b.

The trend line in Figure 5 is a moving average of 30 measurements. The general shape of the egress curve can be seen from this trend line. The predicted JD of egress was 3552.80 in close agreement with the light curve.

4. Importance of a Mentor

Enough cannot be said about having a mentor to expedite the learning process. Without one, the learning curve is great. Frustration sets in quickly and what you thought was going to be a satisfying progression into science contribution ends with failure.

A mentor provides a never-ending supply of knowledge about telescopes, software, observing techniques, data reduction, analysis, and terminology that a new astronomer gets lost in.

There are a number of mentors available in the SAS organization, both amateur and professional, to help you succeed. You just need to ask.

5. Conclusion

The intrigue of capturing an exoplanet transit was enough to lead me to find a telescope of my own and build an observatory that would facilitate the search. It involved learning a lot of new software and then finding an affordable camera and focal reducer. The learning curve was steep so a mentor was needed. Several other amateur astronomers as well as the SAS organization became valuable assets. Wanting to provide worthwhile contributions to astrophysics has been a journey of frustrations and successes, all worth the road traveled.

6. Acknowledgements

I would like to thank Ed Sheridan, Crescent Butte Observatory, for introducing me to the time calculation tool that helps me plan my observations

and for his suggestions in the design of my observatory.

Thanks to Brian Warner, Palmer Divide Observatory, for his considerable help with MPO Connections (www.minorplanetobserver.com) and his dedication to continued improvements to this software.

Many thanks to the SAS Committee, especially, Lee Snyder, Dale Mais, Robert Stevens, and Brian Warner for continued encouragement. Thanks might be in order for their persistence in convincing me to write this paper.

Last, definitely not least, many thanks to my husband Jerry Foote. His knowledge in this area is endless as well as his patience. I am grateful for his mentoring through all aspects mentioned in this paper and appreciate his continued commitment to my success.

7. References

Castellano, T., Presentation at RTMC Expo 2004.

Castellano, T., "Detecting Transiting Exoplanets", *Sky and Telescope* magazine, page 77, March 2004.

Laughlin, G., Castellano, T., "Join the Hunt", *Astronomy* magazine, page 54, January 2003.

Berry, R., Burnell, J., *The Handbook of Astronomical Image Processing*, Willmann-Bell, Inc., 2005.

Transitsearch website (2005), www.transitsearch.org.

Serendipitous Discovery of Variable Stars While Gathering Asteroid Lightcurves

Bob Buchheim
Altimira Observatory
18 Altimira, Coto de Caza, CA (USA) 92679
rbuchheim@earthlink.net

Abstract

Altimira Observatory is located in southern California and has primarily been used for asteroid photometry. Instrumentation consists of an 11-inch Schmidt-Cassegrain (Celestron NexStar-11) operating at F/6.3, a CCD imager (ST-8XE NABG), and filter wheel (CFW-8A) with Johnson-Cousins B, V, and R filters. A detailed description of the observatory, the calibration of the instruments, and some reported results, can be found at the author's website (http://www.geocities.com/oaca_bob), or by e-mail request (rbuchheim@earthlink.net). © 2006 Society for Astronomical Sciences.

1. Introduction

Most asteroid lightcurve projects start with a night-long series of images containing the asteroid – between 50 and 200 images (1-minute to 5-minute exposure, depending on the brightness of the target asteroid) of the same FOV. Differential photometry is used to detect variations in the asteroid's brightness. Since comparison-star brightness is assumed to be stable during the night, ensemble-photometry (i.e. up to 5 comp stars) is used to confirm the stability of the selected comp stars. Each comp star's brightness is checked relative to the average of the other four comp stars through the night, thereby identifying any significant change in the brightness of any selected comp star during the course of the night. The photometry program MPO Canopus simplifies this process.

During the past year, two interesting variable stars were discovered accidentally in this way – they just happened to have been selected as comp-stars for an asteroid.

2. GSC 0376-0596: A High-Amplitude Delta Scuti type Star in Hercules

In May 2005, during a photometric study of asteroid (6327) 1991 GP1, one of the “comparison stars” used for differential photometry was found to be a variable star. Identification data for this star are:

RA(2000) = 16:20:02
Dec(2000) = +4:28:41
Cross- identifications = UCAC2 3316055
= GSC 0376-0596

A search of references showed that it had not been previously reported as being variable.

The other comp stars in the field showed the expected trend of raw instrumental magnitude – brightness rising slightly as the star rose from the horizon, peaking at culmination, and fading again as they set. This trend is the signature of atmospheric extinction.

The raw instrumental (unfiltered) light curve of “comp star 4” was clearly unusual: its brightness varied by over 0.5 magnitude in a bit less than 3 hours.

Since I was providing my asteroid data to Brian Warner for this project, when we compared notes we were surprised to find that we had both discovered variable stars in this same field of view, on the same night – and that they were two different stars, both previously unrecognized!

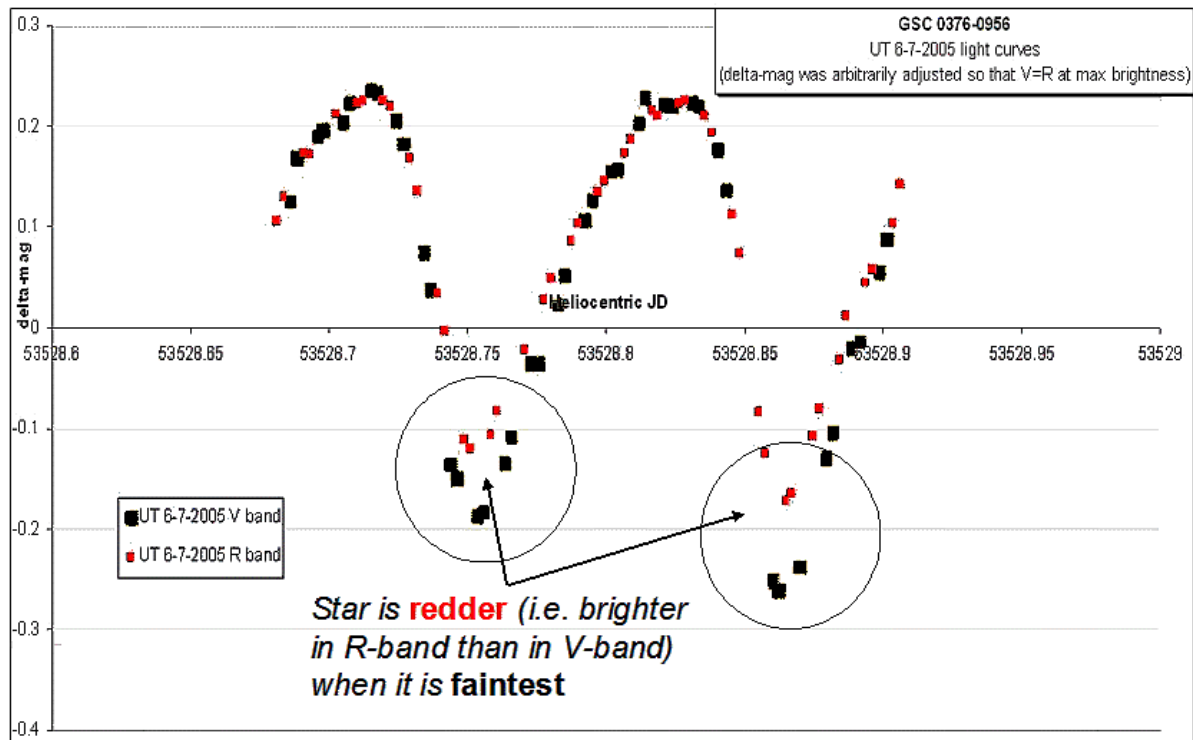
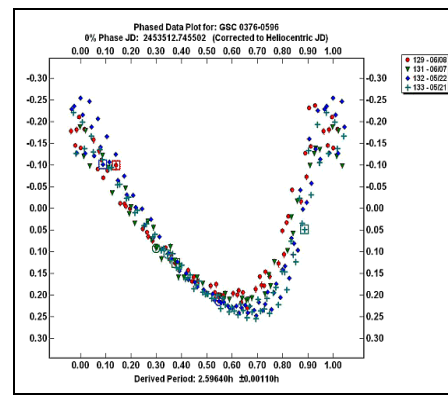
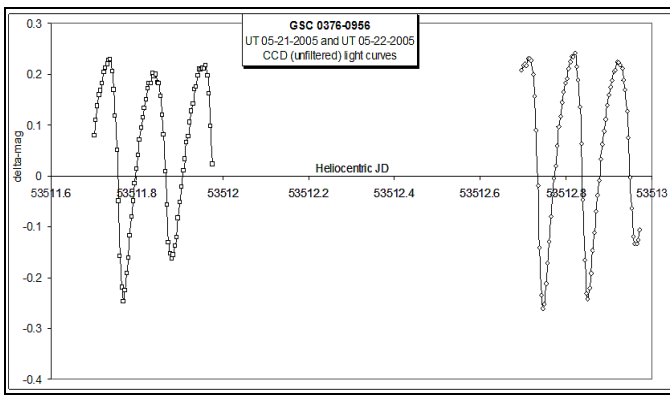
Differential photometry (unfiltered) for two nights confirmed the $\Delta m \approx 0.5$ mag (p-p) brightness fluctuation. I had the opportunity to show these two nights to Dr. Arne Henden at the 2005 SAS meeting, and he pointed out that this star displays many of the characteristics of Delta Scuti type variable stars:

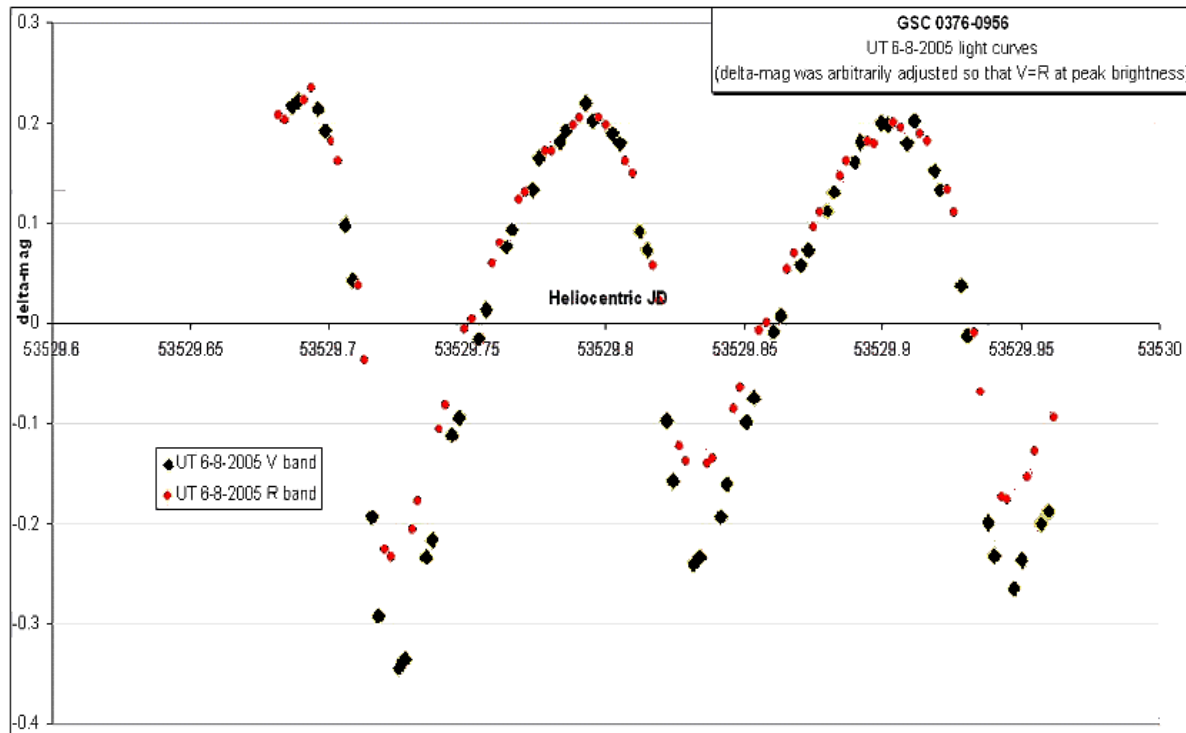
1. The period is quite constant
2. The amplitude of light variation is not constant (each cycle has a slightly different P-P amplitude, similar to an amplitude-modulated carrier).

A primary period $P=2.5964$ hours was determined from 4 nights of data (approximately 8 hours per night of continuous monitoring). A phased light-curve, wrapped to this period, is shown below.

Delta Scuti's are pulsating variable stars. The theory of stellar oscillations predicts that the temperature (and hence, the color) of the star should change as it pulsates. Specifically, when the star has expanded it will be cooler, redder, and fainter. When it has contracted, it will be hotter, bluer, and brighter. In order to investigate this, I took two nights of data through V and R band filters. The imaging sequence of V-V-R-R-... was continued all night, throughout both nights.

The filtered CCD photometry confirms that the star's color does, indeed, change slightly during its brightness fluctuation cycle. Displayed in the plots below are the instrumental V and R band lightcurves (from UT 06-07-2005, and UT 06-08-2005, respectively). In these plots, the R band curve has been adjusted downward by an arbitrary amount, so that it overlays the V band plot at maximum brightness. This makes it easier to see the color variation. The star is somewhat redder at minimum brightness than it is at maximum brightness, confirming the expected result for a pulsating variable star.





The V and R band data from these two nights was calibrated using Landolt standard stars as the primary reference. The characteristics of this star, on the standard Johnson-Cousins photometric system, are

Average (mid-point) brightness is $V \approx 12.87$

The peak-to-peak amplitude variation is about $\Delta V \approx 0.6$ magnitude

max brightness $V \approx 12.58$

min brightness $V \approx 13.14$

the P-P amplitude changes by up to 0.1 V-mag from cycle to cycle

The color changes with the brightness – it is about 0.12 magnitude redder at minimum brightness than it is at maximum brightness.

max brightness (V-R) ≈ 0.1

min brightness (V-R) ≈ 0.22

Absolute photometry accuracy is estimated to be ± 0.03 magnitude.

3. Acknowledgement

I am grateful to Dr. Arne Henden (Director, AAVSO) for his encouragement and advice.

Observing Visual Double Stars with a CCD Camera at the Palmer Divide Observatory

Brian D. Warner
Palmer Divide Observatory
17995 Bakers Farm Rd.
Colorado Springs, CO 80908
brian@MinorPlanetObserver.com

Abstract

One of the more frustrating times for observing is when the moon is near full, when the rising chorus of our natural satellite drowns out the diminutive voices of faint asteroids. This doesn't mean that telescopes and cameras must sit idle during this time, allowing valuable photons to hit the ground. There are many other targets available even during full moon. Among these are visual double stars, which – with the aid of an automated telescope/camera – can be quickly measured and so add valuable observations that can be used to compute binary star orbits.

1. Introduction

Observing visual double stars with a CCD camera is a relatively easy way to get involved in scientific research. While many doubles are not true binary stars, many are. By measuring the distance and position angle of the secondary star with reference to the primary, it is possible to determine the orbit of the binary star. Once the orbit is known, then the masses of the two stars can be determined. Combined with spectroscopy or multi-color photometry, the data can be combined to determine a wealth of important astrophysical information.

2. Equipment and Software Requirements

Relatively simple and inexpensive equipment is required to observe double stars with a CCD camera.

2.1. Telescope

Almost any telescope will do. Since the majority of stars being observed can be captured in 2-60 seconds, a high precision mount is not required but, obviously, is preferred.

2.2. CCD Camera

Almost any camera that, combined with the telescope, gives a good pixel scale will do. Double stars have separations from <1 arcsecond to >200 arc-

seconds, so the pixel scale will determine which pairs you can work with sufficient precision and accuracy.

2.3. Software

Any software that can perform accurate astrometry will do. It's better to work with derived astrometric positions than attempt to convert X/Y coordinates. Use the UCAC2 catalog exclusively when possible to get the most accurate astrometric positions. Some software packages, e.g., MPO Canopus, have special features specifically designed to store and generate reports of double star observations. Many observers record the derived positions in a spreadsheet and let the spreadsheet perform the calculations and generate a page that can be easily exported for publication.

3. Getting Started

The best place to start is with the Washington Double Star Catalog (WDS). The latest version is available on-line at

<http://ad.usno.navy.mil/wds/wds.html>

This web site includes not only the full catalog but also a selected list of "neglected" double stars, those that have not been measured for many years.

There is also an excellent Yahoo News Group for double star observers at

<http://groups.yahoo.com/group/binary-stars-uncensored/>

This group is monitored by Brian Mason, one of the principals at USNO in charge of the WDS.

4. Taking Images

The exposure time you'll use depends on the brightness of the stars in the pair and whether or not you're using filters. Take at least three or four images of the pair (per filter if using filters). Measure each image once and find the mean and standard deviation for the combined data set.

4.1. Short versus Long Exposures

To avoid apparent overlapping of stars, some observers use very short exposures of <1s. While this can appear to avoid overlapping, it also reduces the signal-to-noise (SNR) of the stars and the number of pixels involved for each star. This can lead to less precise astrometric solutions.

“Long” exposures, 2-20s depending on whether or not filters are used and the desired limiting magnitude, give a higher SNR. However, for very bright and close stars, the two images will overlap, making accurate astrometry difficult if not impossible without sophisticated techniques.

You'll need to experiment to see what works best for your system and observing goals.

4.2. Filters

If at all possible you should use at least two filters and reduce the raw instrumental magnitudes to standard magnitudes. The additional information of standard magnitudes and one or more color indices is very valuable and takes only a little extra time and effort to determine.

5. The Measure of Double Stars

Double stars are measured in terms of the distance and position angle of the secondary from the primary. The primary is usually the brighter star. The position angle is measured from North (0°), to East (90°), and so on. The distance is measured in arc-seconds.

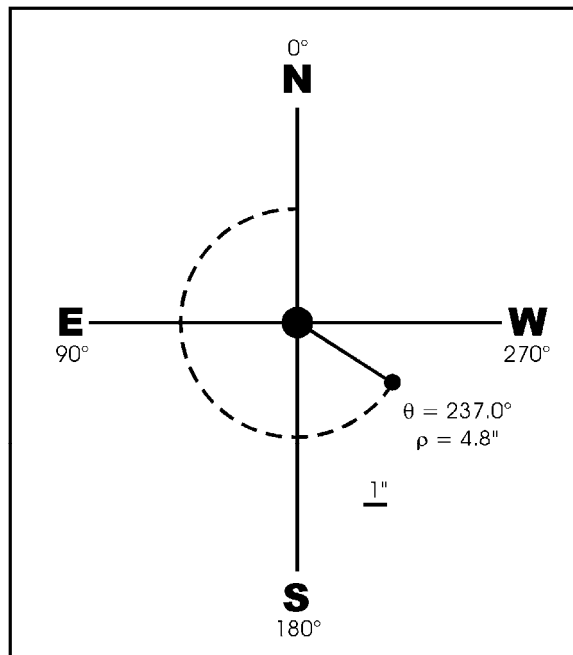


Figure 1. Measuring the distance and position angle of a double star.

To avoid problems with field rotation and pole precession, measurements are best determined by measuring the Right Ascension and Declination of the two stars in a standard epoch, e.g., J2000, with the UCAC2 catalog and then computing the distance and position angle from

$$\rho = \sqrt{(\alpha_b - \alpha_a)^2 \cos(\delta_a) + (\delta_b - \delta_a)^2}$$

$$\theta = \tan^{-1} \left(\frac{\delta_b - \delta_a}{(\alpha_b - \alpha_a) \cos(\delta_a)} \right)$$

Where α_a / δ_a RA / Dec of the primary
 α_b / δ_b RA / Dec of the secondary

6. Publishing Your Observations

You need to publish your observations if they are to be of any use. There are several possibilities. Two of the most prominent are:

6. 1. Journal of Double Star Observations

University of South Alabama


**Journal of
Double Star Observations**

VOLUME 1 NUMBER 2 SUMMER 2005

**Brian Mason Joins the
Journal of Double Star Observations**

In this second issue of the JDSO, we are excited to announce that Dr. Brian Mason, Director of the Double Star Program at the United States Naval Observatory, has joined us in the capacity of Advisory Editor.

Most of you will already be familiar with Dr. Mason, or at least know of him. If not, you will be if you continue observing double stars for long. In his position at the USNO, he is the main caretaker of the Washington Double Star Catalog, the primary database of double star data. Brian has been very helpful in encouraging and aiding amateur astronomer's observations of double stars. Of course he has an ulterior motive, because double star measurements made by



Brian Mason with the USNO speckle camera on the 26" telescope in Washington, D.C.

amateurs and published in some journal (including this one) will be incorporated into the WDS.

Brian is a frequent contributor to the binary stars newsgroup (<http://groups.yahoo.com/group/binarystars>), answering questions, offering tips, and issuing challenges ("can you measure μ and θ of the other companions of Polaris?"). You can request past measurements of double stars you are studying through the USNO web site at <http://ad.usno.navy.mil/peo7/WDS>. Also, check out his article in this issue. He regularly observes double stars himself, employing speckle interferometry and the 26" Clark refractor at the USNO in Washington, D.C.

We look forward to working with Dr. Brian Mason.

Inside this issue:

Double Stars Studied by LIADA in 2002 <small>Francisco M. Rico Romero</small>	24
New Common Proper Motion Pairs <small>Ross Stuart</small>	33
New Common Proper Motion Pairs Containing White Dwarfs from SDSS Data <small>John Greaves</small>	41
Investigation into the Motions of "Neglected" Double Star WDS 01477+6351 <small>R. Kent Clark, Jarrod Cunningham, Jessica Gundry, Jonathan Pearce, J.M. Sanders, Tiffany Scarborough</small>	44
LDS 968 AB-C: The Distant Companion of HD575 <small>Eduardo Ruben Mesa Martin</small>	49
On Line Double Star Resources at the U.S. Naval Observatory <small>Brian G. Mason</small>	57

This journal can be downloaded free off the Internet by visiting <http://www.jdso.org/>

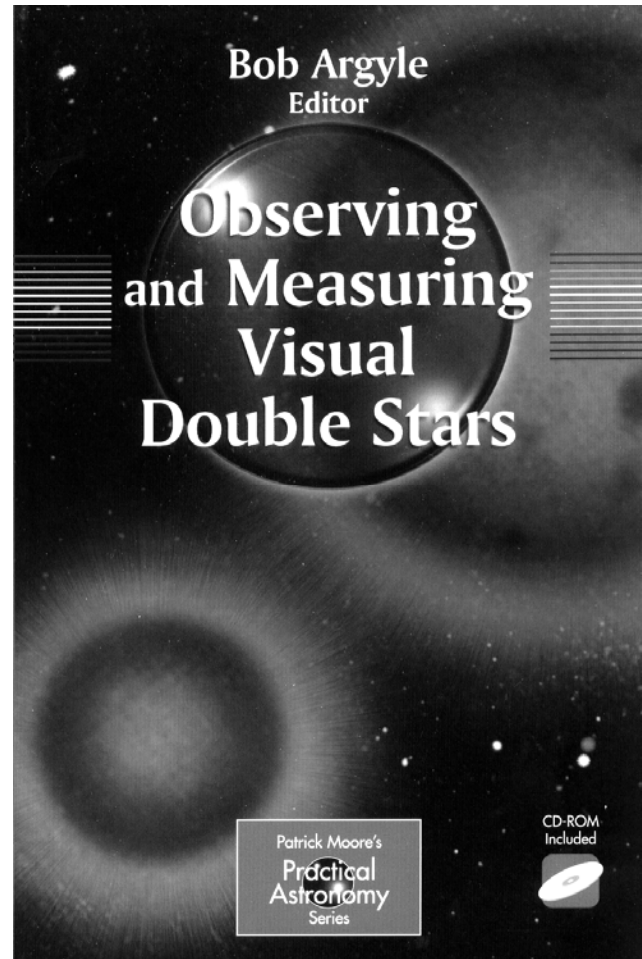
6. 2. The Webb Society Double Star Circulars

This is one of the journals published by the Webb Society. Visit:

<http://www.webbsociety.freemove.co.uk/notes/doublest01.html>

Contact the editors for these journals to get information on submission requirements.

7. Additional Reading



Bob Argyle's "Observing and Measuring Visual Double Stars" is a must read. Argyle is the head of the Double Stars Section of the Webb Society.

Sample Data for Publication

Table 1. Clear Filter Observations

Name	Comp	RA	Dec	Mags	PA	Dist	Epoch	N	Obs	Psd	Dsd	Mpsd	Mssd
SCA 26		0400.0	+2122	9.1,11.5	59.2	31.19	2006.115	3	BW	0.06	0.030	0.01	0.01
SCA 27		0400.2	+2127	10.9,11.4	118.2	17.32	2006.115	3	BW	0.07	0.028	0.01	0.00
PLQ 47		0400.8	+0838	8.2,8.8	150.3	39.52	2006.115	3	BW	0.03	0.014	0.00	0.01
STF 487	AB	0400.9	-1027	8.8,9.1	9.4	11.55	2006.115	3	BW	0.14	0.074	0.01	0.01
STF 487	AC	0400.9	-1027	8.8,9.7	229.2	20.21	2006.115	3	BW	0.25	0.092	0.01	0.00
STF 487	BC	0400.9	-1027	9.1,9.7	215.0	30.04	2006.115	3	BW	0.13	0.017	0.02	0.00
SCA 28		0401.8	+2140	7.7,11.4	155.7	28.04	2006.115	3	BW	0.30	0.077	0.01	0.01
POU 355		0402.5	+2353	12.1,12.9	92.8	18.26	2006.115	3	BW	0.13	0.075	0.02	0.02
POU 357		0402.9	+2405	10.7,11.9	101.6	12.20	2006.115	3	BW	0.21	0.018	0.00	0.01
POU 364		0403.8	+2402	12.3,12.9	217.6	17.71	2006.115	3	BW	0.11	0.103	0.01	0.01
POU 366		0403.8	+2509	11.8,13.6	111.7	15.25	2006.115	3	BW	0.23	0.181	0.00	0.01
GRV 201		0403.9	+2447	10.5,10.9	29.2	37.50	2006.115	3	BW	0.04	0.045	0.00	0.01
HJ 2223		0407.9	+0119	10.4,11.2	199.9	18.50	2006.115	3	BW	0.15	0.047	0.01	0.01
ST 499	AC	0410.1	+2407	8.8,10.4	280.6	30.18	2006.115	3	BW	0.08	0.058	0.00	0.01
AG 78		0410.4	+3618	9.4,10.0	198.1	18.01	2006.115	6	BW	0.09	0.024	0.01	0.01
STF 502	AB	0411.2	+2630	8.0,9.6	246.2	16.60	2006.115	3	BW	0.50	0.108	0.01	0.01
STF 502	BC	0411.2	+2630	9.6,9.6	303.7	10.75	2006.115	3	BW	0.73	0.212	0.01	0.00
CHE 76		0412.8	+1614	11.4,12.0	272.5	28.75	2006.115	3	BW	0.06	0.072	0.01	0.01
SEI 37		0413.5	+3201	10.8,12.0	120.3	25.67	2006.115	3	BW	0.15	0.021	0.00	0.02
GRV 208		0414.5	+2852	10.4,11.0	196.2	22.84	2006.115	3	BW	0.05	0.035	0.00	0.01

Table 2. V and R Observations

Name	Comp	RA	Dec	Mags	PA	Dist	Epoch	N	n	Obs	V-Rp	V-Rs	PAsd	Dsd	Mpsd	Mssd
HLD 14	AC	1300.8	+0252	9.5,11.6	100.6	49.86	6.138	8	4	BW	0.337	0.329	0.06	0.089	0.01	0.01
HLD 14	AC	1300.8	+0252	9.2,11.2	100.6	49.86	6.138	8	4	BW	0.337	0.329	0.06	0.089	0.01	0.03
STF 1705		1300.8	+1423	8.9,9.9	187.8	26.77	6.138	8	4	BW	0.360	0.458	0.05	0.047	0.01	0.00
STF 1705		1300.8	+1423	8.5,9.5	187.8	26.77	6.138	8	4	BW	0.360	0.458	0.05	0.047	0.00	0.01
GRV 860		1300.9	+2135	12.5,12.6	231.7	30.40	6.138	8	4	BW	0.480	0.417	0.19	0.085	0.03	0.01
GRV 860		1300.9	+2135	12.0,12.2	231.7	30.40	6.138	8	4	BW	0.480	0.417	0.19	0.085	0.02	0.02
STF 1708		1302.1	+0717	9.0,10.1	294.1	10.53	6.138	6	2	BW	0.351	0.321	0.27	0.320	0.02	0.05
STF 1708		1302.1	+0717	8.6,9.8	294.1	10.53	6.138	6	4	BW	0.351	0.321	0.27	0.320	0.05	0.03
HJ 2632		1302.9	+4643	9.7,13.5	336.4	44.59	6.138	8	4	BW	0.275	0.772	0.09	0.077	0.01	0.05
HJ 2632		1302.9	+4643	9.4,12.7	336.4	44.59	6.138	8	4	BW	0.275	0.772	0.09	0.077	0.01	0.03
POU 3132		1303.1	+2412	13.6,14.1	291.5	10.88	6.138	8	4	BW	0.468	0.484	0.69	0.196	0.03	0.03
POU 3132		1303.1	+2412	13.1,13.6	291.5	10.88	6.138	8	4	BW	0.468	0.484	0.69	0.196	0.03	0.04

It's important to include error estimates whenever possible. This allows those computing orbits to give proper weight to your data.

Magnet Loader for Schmidt-Cassegrain Mirror Flop Reduction

Gary A. Vander Haagen
Stonegate Observatory
825 Stonegate Rd, Ann Arbor, MI 48103
garyvh2@att.net

Abstract

The struggle with mechanical and optical issues in most commercially available Schmidt-Cassegrain amateur telescopes is exacerbated by the random flop of the primary mirror as it progresses beyond the meridian. Several retrofit techniques are available to reduce this problem, including lock-down screws and collars. Such approaches all require some modification to the optical tube. This paper discusses “work-in-progress” on a Magnetic Loader for the popular C14 optical tube that locates a rare-earth magnetic assembly on the primary mirror collar thereby continuously loading the sleeve bearing assembly. This technique requires no machined modifications or parts, can be accomplished by removal of the secondary mirror, and requires no operator intervention during focusing. While the initial data looks favorable, additional development and testing over a wider range of conditions is necessary. ©2006 Society for Astronomical Sciences.

1. Introduction

The ever-present problem of mirror flop in most Schmidt-Cassegrain optical tubes creates some major limitations to the serious amateur. This mechanical problem arises largely from the necessary clearances between the inner stationary guide tube and the mating outer sleeve bearing that supports primary mirror. Secondary issues such as flexure and thermal instability in the mirror supporting structure also affect performance.

Expensive research optical tubes go to great length to eliminate this problem with more complex loaded bearing assemblies and/or locking schemes to eliminate the mechanical play and use of more thermally stable materials. Some newer amateur or research grade optical tubes offer built in mirror locks and at least one after-market locking collar is available to solve this problem. The latter requires some machining and modification to the tube assembly.

Without attention to this problem the amateur is continually frustrated by variations in pointing, tracking, and difficulty in holding collimation across the full sky. Software approaches such as T-Point cannot correct for this problem since its magnitude and position are not predictable from run to run or night to night. The technique described in this paper was designed around the popular C14 optical tube but should be adaptable to other manufactures and mirror sizes where the secondary access hole is large enough to gain access to the inner support tube or, the corrector plate is removable.

2. Approach

The design objective was to find a method of substantially reducing mirror flop that could be accomplished without disassembly or modification of the optical tube and would accommodate some movement of the primary mirror using a remote focusing system.

Reviewing other references, it was decided to try a magnetic loading approach using very powerful rare-earth magnets^{1, 2}. The magnets are available inexpensively in a wide variety of shapes and flux levels. This approach could potentially meet the design objectives and be compact enough to eliminate light shadowing issues. The initial concept was to place a narrow-strip steel pole piece within the central stationary tube and locate bar magnets on the outer movable tube. This technique was found to provide inadequate force between the sleeve bearing assembly. The separating tubes’ permeability and air gap significantly reduces the force between the inner and outer tube.

Figure 1 shows a technique that provided substantially more force and could be scaled to higher force levels.

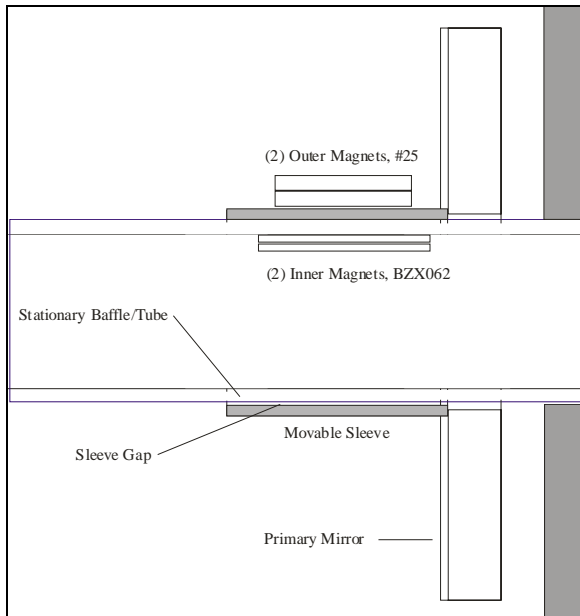


Figure 1, Magnetic Circuit Using Two Pair of Rare-Earth Magnet Assemblies.

Note that the inner and outer magnet’s attracting force pulls the sleeves together along a line in the plane of the magnetic force. It is estimated that a force between 15 and 30 pounds is required to adequately load the sleeve bearing. An exact minimum value would require disassembly of the optical tube, which was not undertaken.

Changing magnet type, size, and number in the stack can easily scale the approach shown. For this study the internal assembly has two stacked, BZX082, 100x12x3mm magnets³ each rated at 140 lbs force and two external, #25, 75x25x12mm magnets each rated at 150 lbs force⁴. The internal magnet projection into the light path is at its maximum for this optical setup. Scaling of this technique is easy: with one internal and one external magnet as the base force level, adding a third internal or external magnet doubles the force. Adding a fourth magnet doubles the force again. The four-magnet assembly was used for all experimentation in this paper.

3. The Performance Data

A major issue with the existing C14 was holding collimation across the sky and 30+ arcseconds of random pointing error that could not be compensated by T-Point. Quantifying the amount of mirror flop proved to be a real challenge. The Software Bisque T-Point model of the non-loaded C14 was investigated to quantify mirror flop. Patrick Wallace had suggested terms PZZ0 and HZCH0 as candidates for isolation of the mirror flop magnitude. Analysis of the model was not conclusive due the interaction of

un-modeled DEC axis flexure, HA gear errors, and other variables.

A new program by CCDWare, CCDInspector (CCDI), was tried to see if it could quantify the collimation level with the full optical train in place⁵. CCDI proved useful for measurement of both the level of collimation and the direction and magnitude of the resultant optical misalignment.

Figure 2 shows a sketch of the CCDI graphical output for each image. The output for each image includes the range of FWHM across the image, curvature, tilt of the X and Y image axes, collimation level, and the number of stars used for the calculation. Finding areas in the sky with adequate and uniform star counts that are about to cross the meridian proved a real challenge. The most reliable method was to follow an open star cluster for several hours as it passed through the meridian.

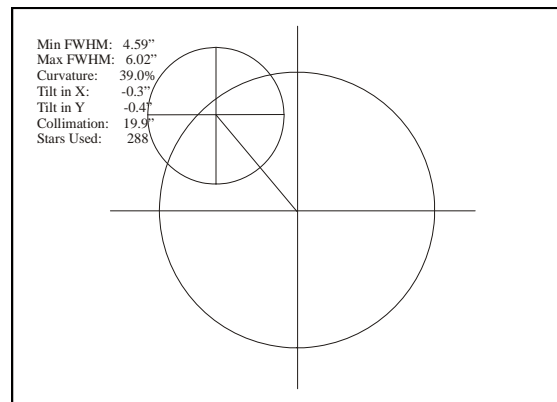


Figure 2, Drawing of the CCDInspector Output Showing the Mechanical and Optical Centerline Misalignment

Figure 3 shows collimation as the standard C14 approaches and crosses the meridian. The meridian crossing occurred at image 14. East of the meridian the collimation was misaligned and averaging about 20 arc-seconds. The flop resulted in an increased collimation error of approximately 15 arcseconds. The data scattering in all cases is due to the poor Michigan sky conditions. Collimation deterioration for the later images is due to focusing shifts and mechanical shifts from temperature change.

The most useful data for assessing performance proved to be the X-Y optical tilt data. Collimation was useful but you could have mirror flop and still have the same collimation level when the misalignment moved same amount to another quadrant.

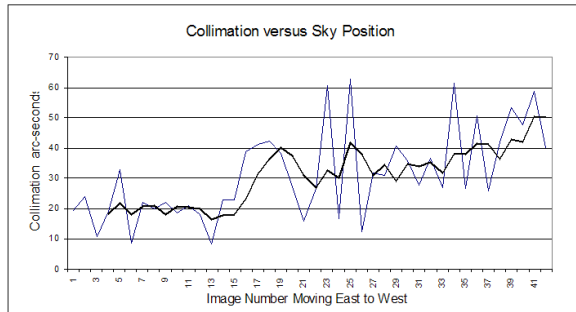


Figure 3. Standard C14, Collimation as the Telescope Crosses the Meridian.

Figure 4 shows an example of tilt as the telescope passes through the meridian using the same images as Figure 3. In this graph the X-tilt shifts approximately 1.1 arc-seconds (black curve) and the Y-axes approximately 0.9 arc-seconds. In all the graphs a rolling average line for analysis purposes augments the scattered data lines. It is important to note that the flop is highly variable; it does not always occur near the meridian and its magnitude varies with sky position, temperature, etc.

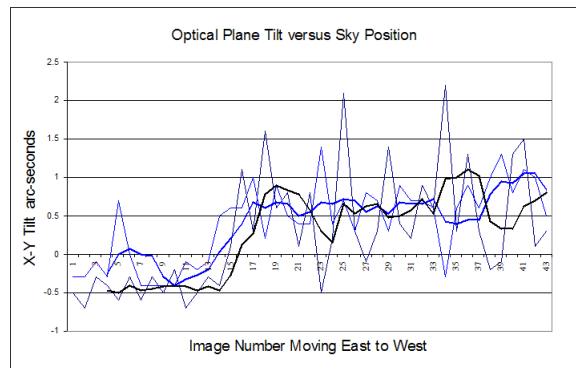


Figure 4. Tilt Each Side of the Meridian for the Same Image Data of Figure 3. No Magnetic Loader. Black is X-axes.

The two-pair Magnetic Loader was attached per Figure 1 with the magnetic force vector in the DEC plane. Figure 5 shows the X-Y tilt following an open cluster for 267 minutes passing the meridian at image 111. This graph shows that the total flop magnitude was reduced substantially with no obvious step changes. The gradual shift in tilt is likely thermal instability, deteriorating focus, and other mechanical instabilities. Figure 6 shows an additional run with the loader attached. Here there is very little change versus sky position with a total lapsed time of 107 minutes.

Other runs were conducted and a few showed some residual flop. It is likely that the estimated 15 plus pounds force provided by the two-pair Magnetic Loader is still marginal. Additional trials will utilize

the same two internal magnets and 3-external magnets to provide approximately a 30% force increase. Other circuits for trial are the same two internal magnets with a two to four stack of larger 100x12x6mm BZ084 series magnets.

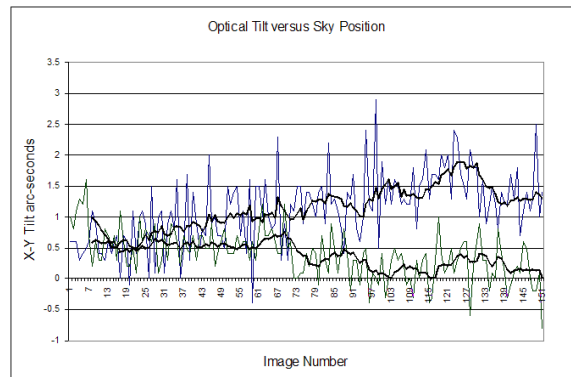


Figure 5. X-Y Tilt with Magnetic Loader as the Telescope Crosses the Meridian. Black is X-axes.

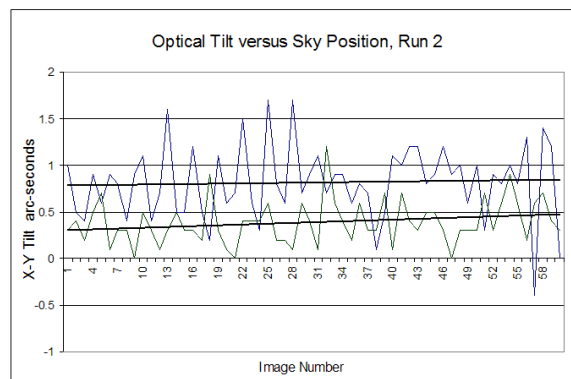


Figure 6. Run 2, X-Y Tilt with Magnetic Loader as Telescope Crosses the Meridian at Image 30. Black is X-axes.

4. Some Practical Considerations

This paper is provided as a “work-in-progress” report and idea starter. Numerous other magnetic circuits are possible and may work even better. Additional experimentation is the key.

A few notes on how to proceed. The references note two good sources for the rare-earth magnetic material. Be extremely cautious in working with these materials. The forces involved are very high and you can be easily pinched or hurt. Experiment on a bench with all ferromagnetic materials removed. To checkout various configurations use an aluminum tube about 1 inch square with 1/8 inch wall, clamp it over the edge of the bench, and tape one magnet set to the bottom and place the other on the top. This allows testing of various configurations with forces that are scaled down to less than you’ll experience

inside the optical tube. Also, be extremely careful when mating two magnets. Slide them together being careful not to pinch you or allow them to snap together since they are extremely brittle and will fracture.

Second, once you are familiar with the magnets, remove the optical tubes' secondary mirror. If your arm is not small enough you may have to solicit help or build a wooden placement tool to allow entry and placement. Identify any ferromagnetic materials that you will want to avoid when introducing the magnet assembly into the optical tube. Next, set the primary mirror to the nominal focus position for your setup. It is not a problem with plus or minus several knob turns from this position. The C14 configuration used for testing had a second external Optec TCF-S for fine focusing with the primary mirror focus used during large temperature changes and setup modifications.

Third, before installing the magnets, spray with a flat black paint or cover the non-contact areas with black masking tape. The latter works better due to poor paint adhesion to the magnetic material. The setup described had the Magnetic Loader installed so the direction of force was in the mounts DEC plane. Other mounting configurations were not tried.

To install, be sure you know the magnet surfaces that will attract. Place the inner magnet into the stationary tube using a stiff wire or long thin screwdriver and center along the movable sleeve. The magnet will slide using the outer magnet to properly center. With the second magnet's polarity identified, move the magnet through the secondary mirror hole, keeping away from the central tube until the correct position is reached. Keep fingers away from contact and place against the tube. The assembly can now be wiggled to its final position. If the mirror is going to be moved more than three or four turns attach the outer magnet to the tube to keep it stationary. A Ty-Wrap works well for this purpose. Figure 7 shows the external magnet pair of the Magnetic Loader installed on the C14.

5. Conclusion

From the initial data of the two-pair Magnetic Loader in a C14 application, the approach looks promising as a technique for substantially reducing mirror flop. However, the loader's force is still insufficient for the wide range of operating conditions experienced. A 50-100% increase in force is necessary. An additional number, more powerful, and longer external magnets will be tried to improve the robustness of the approach. Application to additional C14 optical tubes and other manufacturer tube types will be needed to confirm the full effectiveness of

this technique. Ideas and results from others interested astronomers will also help solve this illusive problem.

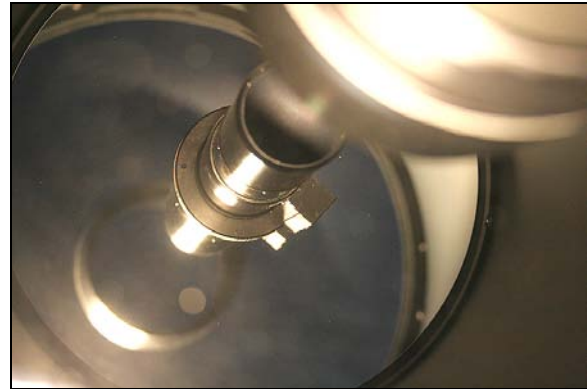


Figure 7, Two-Pair Magnetic Loader Installed on C14 Optical Tube

6. Acknowledgements

Paul Kanevsky, Designer/Writer of CCDInspector, for continuous assistance in using the software and techniques for gathering data.

Patrick Wallace, Tpoint Software, for his assistance in identifying mirror flop within existing T-Point models and general encouragement on the subject.

7. References

- 1) Schmidt-Cassegrain Mirror Stabilizer, Chris Vedeler, www.isomedia.com/homes/cvedeler/scope/mirrorlock.htm.
- 2) Software Bisque, C-14 Locking Collar and Installation Service, <http://www.bisque.com/Products/Collar/Default.asp>.
- 3) K&J Magnetics Inc., 2110 Ashton Dr. Suite 1A, Jamison, PA 18929, www.kjmagnetics.com. Inner Magnets: (2) BZX082, 100x12x3mm, N42, #140 force each.
- 4) Gaussboys Super Magnets, PO Box 55401, Portland, OR 97238-5401, Tel: 866-840-4400, www.gaussboys.com/default.php?cPath=3. Outer magnet: (2) Block #25, 75x25x12mm, N38, #150 force each
- 5) CCDWare, CCDInspector v1.1.4, www.ccdware.com/products/ccdinspector/